16552-6007-R0-00
CR 114350

STUDY OF A COMMON SOLAR-ELECTRIC-PROPULSION UPPER STAGE FOR HIGH-ENERGY UNMANNED MISSIONS

VOLUME II
TECHNICAL

PREPARED FOR NASA/OART
ADVANCED CONCEPTS AND MISSIONS DIVISION
MOFFETT FIELD, CALIFORNIA

UNDER CONTRACT NAS2-6040

14 JULY 1971

TRW SYSTEMS GROUP

16552-6007-R0-00

STUDY OF A COMMON SOLAR-ELECTRIC-PROPULSION UPPER STAGE FOR HIGH-ENERGY UNMANNED MISSIONS

VOLUME II
TECHNICAL

PREPARED FOR NASA/OART
ADVANCED CONCEPTS AND MISSIONS DIVISION
MOFFETT FIELD, CALIFORNIA

UNDER CONTRACT NAS2-6040

14 JULY 1971

TRW
SYSTEMS GROUP

The final report of this study
is presented in three volumes:

I Summary Report
II Technical Report
III Appendix

ABSTRACT

The results of this study show that the multi-mission solar-electric stage concept is a practical, economical, and versatile approach to space exploration. A vehicle designed for repeated use in a variety of missions permits amortization of development and reduction of recurring cost. The upper stage concept affords additional cost savings because new development for any mission is largely restricted to payload engineering.

The selected configuration consists of a center body and two rollout solar arrays developing 17.5 kw at 1 AU. The vehicle, launched by a Titan class booster, has an injected mass ranging from 1500 to 2500 kg and carries up to 500 kg of attached or separable payload packages. A large payload stowage volume is provided.

High-energy missions to be performed by this stage starting in the mid-70's are those where solar-electric power can be used most effectively, namely a Mercury orbiter, a close approach solar probe, asteroid and comet rendezvous missions, and a high-inclination extra-ecliptic probe. Alternate missions to which the stage can be adapted are high-data-rate Mars and Venus orbiters, and outer planet flybys and orbiters. Still more advanced missions such as surface sample return from Mars or the asteroid Eros, and the very difficult rendezvous with Halley's comet in 1986 have also been suggested.

TRW Systems has analyzed mission characteristics, scientific objectives and payload requirements, performed design tradeoffs and interface studies, and defined a conceptual stage configuration that meets the specified wide range of mission objectives. The study also includes program plans and cost estimates and identifies advanced technology development that will be required for implementing the electric stage program.

TABLE OF CONTENTS

TABLE OF CONTENTS (Continued)

TABLE OF CONTENTS (Continued)

TABLE OF CONTENTS (Continued)

TABLE OF CONTENTS (Continued)

TABLE OF CONTENTS (Continued)

LIST OF ILLUSTRATIONS

LIST OF ILLUSTRATIONS (Continued)

LIST OF ILLUSTRATIONS (Continued)

LIST OF ILLUSTRATIONS (Continued)

LIST OF ILLUSTRATIONS (Continued)

LIST OF ILLUSTRATIONS (Continued)

LIST OF TABLES

LIST OF TABLES (Continued)

1. INTRODUCTION

The technology of electric thrusters, power conditioners, and large lightweight solar arrays has progressed to the point where plans for application of solar-electric propulsion to interplanetary missions should receive serious consideration. The SERT-2 test mission in 1970 demonstrated the desired performance characteristics and almost all of the projected mission life. Ion engines of the type flown in SERT-2 provide the basic technology for any projected electric propulsion spacecraft to be developed and flown in the 1970s.

The multi-mission application of an electric propulsion vehicle and its use as a high-energy upper stage are of paramount interest at this time. By designing a vehicle for multi-mission use, the initial development cost can be amortized through repeated use of the vehicle, permitting a lower recurring cost per flight. The upper stage concept suggests a multiple use for which each new application requires development only in the payload engineering area, also with the object of cost savings.

The primary missions for which the electric stage is intended are all of the type that can exploit solar-electric propulsion most effectively by remaining reasonably close to the sun. Since these missions require the propulsion capabilities of the stage at least up to and sometimes after arrival at destination, separation of the stage proper from the payload is not required and actually often undesirable. However, the stage can carry and eject smaller probes.

In addition to these primary missions in which the stage is performing as a payload bus, alternative missions have been investigated for which the stage's propulsion capabilities are not useful at destination, such as outer planet orbit missions. In this alternate application, the stage is jettisoned after it completes the propulsion phase, and a separable spacecraft continues to destination.

In this study we have made extensive use of the results of earlier design studies by TRW, JPL, North American-Rockwell, Hughes and Marshall Space Flight Center (Ref. 1-1 through 1-5) and have incorporated from this prior work many applicable design features to the

stage concept. As aresult, we adopted a configuration consisting of a vehicle center body and two large lightweight solar arrays of the roll-out type. This vehicle is shown in Figure 1-1 in two nearly identical configurations for the two types of applications mentioned. Launched by a Titan 3D/Centaur booster the vehicle has an injected mass ranging from 1500 to 2500 kg, depending on the mission, and a propulsion power of nominally 15 kw. Permanently attached payload packages or a separable payload spacecraft are stored in the upper portion of the stage center body. This design concept resembles that of the earlier studies (Ref. 1-1 and 1-2), being distinguished by the provision of a large payload stowage volume and a minimum of electrical interfaces between the stage and the payload components. We have established compatibility of the payload bay dimensions with those of existing spacecraft that might be carried by the stage, such as the TOPS and PIONEER outer planet probes and examined the feasibility of stowage of these vehicles on board the stage and their separation at the end of the thrust phase.

Flexibility of mission application was a major objective of the design effort. The concept of a standardized stage configuration that can be used with minimum design modification to perform a series of different missions is appearing because of reduced cost and risk factors. These advantages have to be weighed against weight penalties, mission constraints and other limitations that must be accepted by the user of a standardized transportation system. This tradeoff was considered during all phases of the study and influenced the design decisions.

In sum, the objectives of this study have been as follows:

- Define a solar-electric upper stage concept for multiple high-energy unmanned missions.
- Establish characteristics of five primary missions to be performed by the electric propulsion stage.
- Establish characteristics of alternative missions to which the stage also can be adapted.
- Determine scientific mission objectives and payload complements.

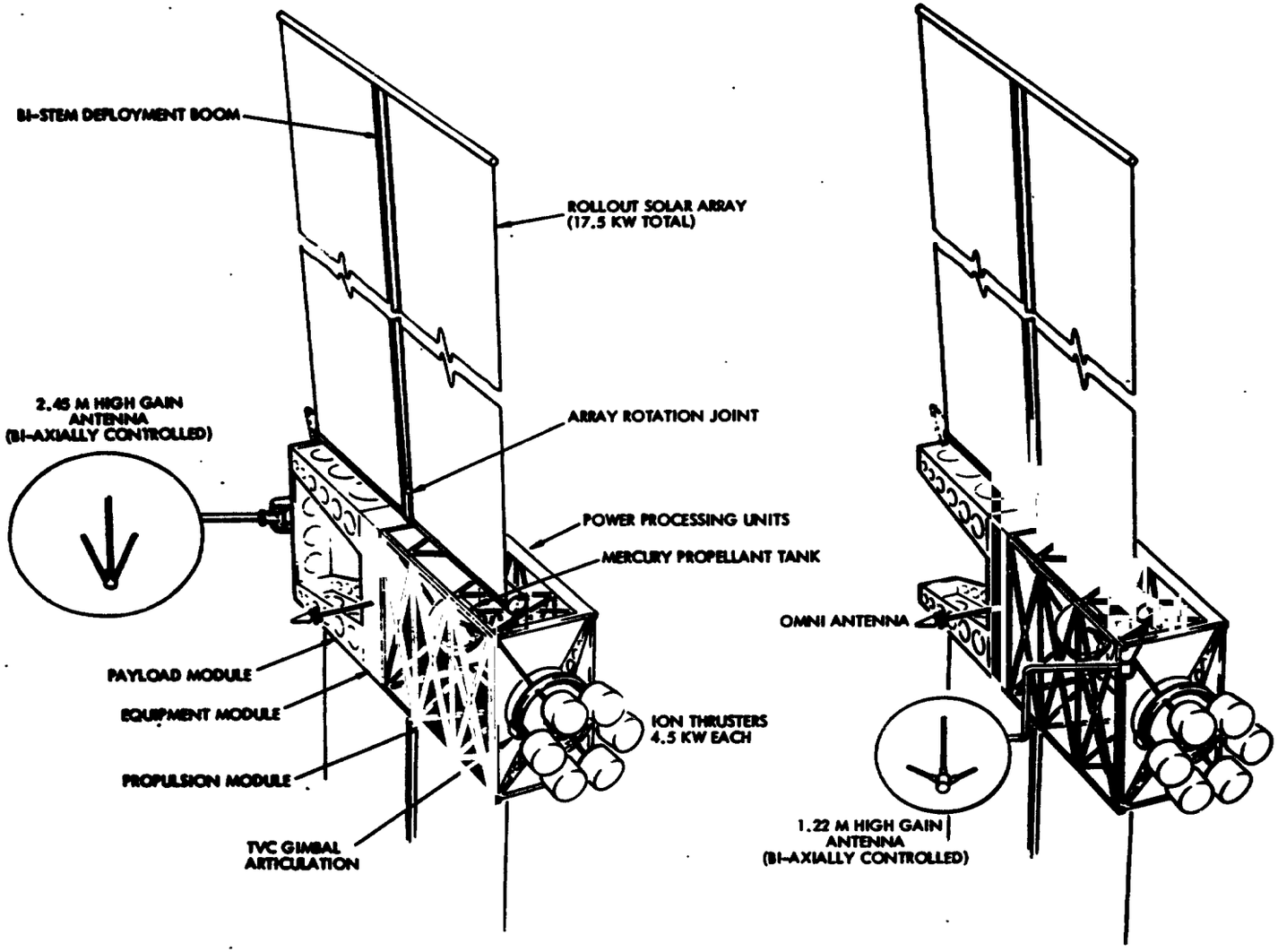

Figure 1-1. Two Versions of Multi-Mission Electric Stage. Left, Baseline Configuration for Primary Missions, Right, Alternate Configuration

- Design a baseline stage configuration and interchangeable modules required for multi-mission adaptation.
- Define subsystems and alternate design approaches.
- Establish a development plan and cost estimates for the total program and recommend an orderly sequence of program evolution.
- Identify advanced technology needs to implement the program.

The study effort was allocated as diagrammed in Figure 1-2, with emphasis placed on electric stage and subsystem design (40%) and on system engineering, tradeoffs and interface studies (20%). Analysis and design of the primary missions was a necessary initial task absorbing about 10% of the effort. Trajectory analysis was performed jointly by TRW and the Advanced Concept and Mission Division (ACMD) of NASA/OART. To assist TRW in proceeding to the principal task of the study, Mr. A. C. Mascy, the technical contract monitor at ACMD, provided a comprehensive set of trajectory data and furnished the new trajectory simulation programs CHEBYTOP and QUICKTOP developed under his direction. NASA also furnished the results of concurrent trajectory studies by Horsewood et al (Ref. 1-6), which served to verify and complement trajectory data used in this study.

Development planning and cost studies were emphasized during the final phase of the study utilizing the extensive data bank of previous scientific spacecraft flown by TRW and our previous multi-mission electric spacecraft study (Ref. 1-1). The results establish the viability of the multi-mission stage concept as an economical approach to the overall future space exploration program. The total number of missions that can be reasonably assigned to the electric stage amounts to about 30 distributed over 12 different mission categories, including growth missions. This count largely reflects different mission objectives rather than backup missions. With this scope of applications in mind, and the initial development cost of the three flight units, approximately $96 million, and the relative low recurrent stage cost of about $15 million, the economic advantage of this concept appears firm.

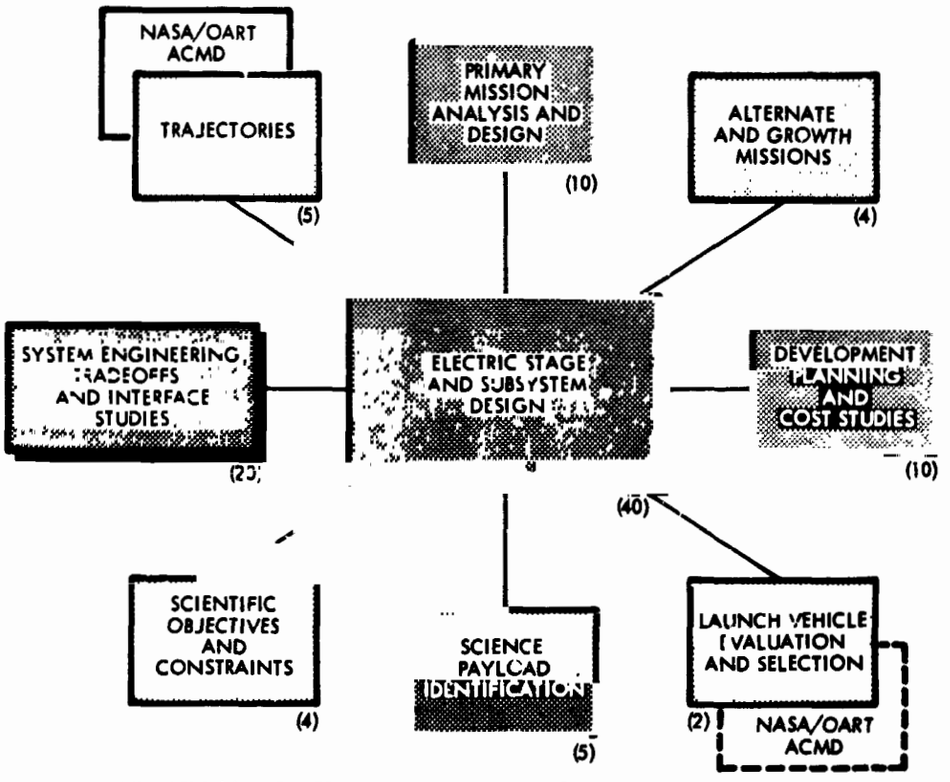

Figure 1-2. Relative Distribution of Effort

As shown in Figure 1-2, the definition of scientific objectives and identification of science payloads have received limited attention during this study. The crucial question of how compatible and advantageous the stage concept is with various types of payloads, not as yet defined, requires comprehensive study that was not within our scope here. Further work is needed covering more detailed definition of payload elements for the specified missions, definition of mission phases and exploration strategies, and a quantitative evaluation of the scientific data return anticipated.

2. MISSION TYPES

2.1 MISSION CATEGORIES

The high-energy missions for which the solar-electric upper stage is being considered are grouped into primary and alternate mission categories as specified in the contractual work statement. Their mission profiles are illustrated schematically in Figure 2-1. The primary missions are those which derive unique performance advantages from the solar electric propulsion technique and, in fact, cannot be performed as effectively by conventional, chemical propulsion means alone. These missions are largely confined to the inner part of the solar system. Included in this category are these mission types:

- Asteroid rendezvous
- Comet rendezvous
- High inclination out-of-ecliptic probe
- Mercury orbiter
- 0.1 AU solar probe

Alternate missions, to be considered with less priority, are those that could be performed advantageously once the solar-electric stage has been developed, but that do not, as such, justify its development since they would also be feasible by means of chemical propulsion. Performance characteristics would be improved by using the electric stage. Included in the second category are these missions:

- Mars and Venus high data rate orbiters (using the large power capacity available after the thrust phase is completed).
- Outer planet flyby and orbiter missions (having payload mass or flight time advantages over ballistic missions, particularly if a major planet swingby maneuver is excluded).
- A high data-rate deep space communications relay for the support of other missions.

The electric stage is to be designed specifically for compatibility with all of the primary mission types such that only a minimum of modification of the basic configuration is necessary from mission to mission.

PRIMARY MISSIONS

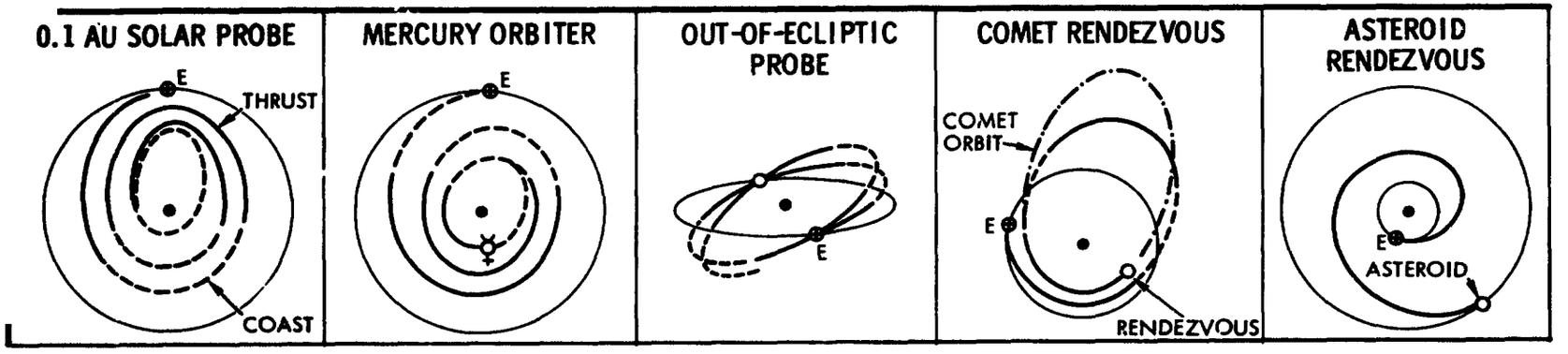

ALTERNATE MISSION SAMPLES

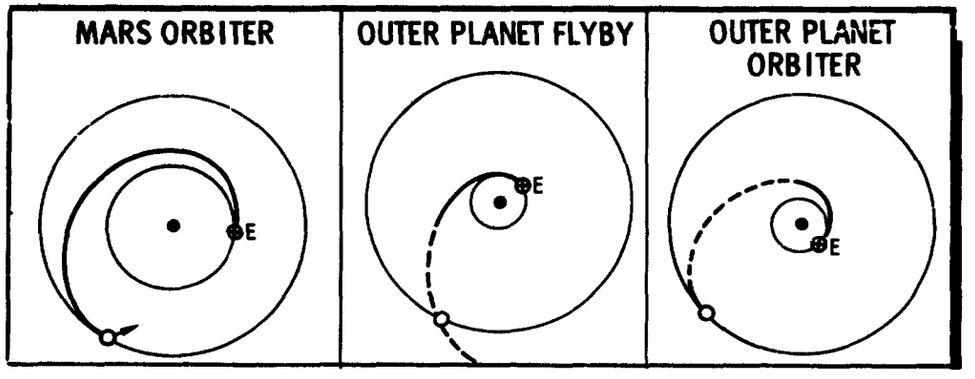

Figure 2-1. Mission Types

Adaptability to alternate missions is desirable and would be a major economic incentive, but is not a design requirement. Obviously, the greatest benefit of the multi-mission electric stage development will accrue if all primary and as many alternate mission types as possible can be carried out by the same basic vehicle configuration. We therefore have contemplated additional mission types of an advanced nature such as:

- Asteroid rendezvous and sample return
- Comet rendezvous and sample return
- Mars landing and sample return
- Rendezvous with Halley's comet

to strengthen the economic argument in favor of the electric stage development. Since we may anticipate rendezvous missions to several asteroids and comets, not counting backup missions, plus a series of individual outer planet flyby and/or orbiter missions plus several "growth" missions such as those listed above, the number of missions that would advantageously use the electric upper stage exceeds a total of 20 in the decade following the first successful stage flight. Characteristics of the various missions profiles are briefly summarized below as introduction to the more detailed discussions to follow in Sections 4 and 5.

2.2 PRIMARY MISSIONS

2.2.1 Asteroid Rendezvous

Rendezvous and orbit insertion require high propulsion energy at destination because of the extremely small gravity of the target body which provides virtually no assistence in capturing the probe. However, once orbit insertion has been attained the additional velocity increment for soft landing is quite small, therefore a landing should be considered as a reasonable additional mission objective. Electric propulsion can provide the equivalent velocity of many thousand m/sec with an affordably small propellant mass, and thus achieves a high net payload ratio. There will be enough solar power left at asteroid belt distances to provide adequate maneuver capability in the terminal approach phase

both for the primary rendezvous maneuver to achieve zero relative velocity and for guidance corrections.

The electric stage can also carry out the orbit insertion maneuver and perform maneuvers in orbit as desired for greater flexibility of observations. Therefore it should not be jettisoned at the time of arrival at the target but can serve as bus vehicle from which the scientific payload instruments can perform the desired measurements. It may however eject a lander capsule which relays its measurements to earth via the orbiting stage. The high payload capacity of an electric propulsion vehicle is essential in providing the weight margin for the separable lander probe. Once in orbit the large unused power of the stage is a natural asset in its use as relay link. Conceivably the stage can depart from the asteroid after completing local observations and continue exploring the asteroid belt, achieving multiple asteroid fly-by's etc.

2.2.2 Comet Rendezvous

As in the case of an asteroid, the large velocity increment required to achieve rendezvous with a near-massless target such as a comet can be readily supplied by an electric stage. For the highly eccentric and often highly inclined orbits of many comets the rendezvous velocity requirement is often higher than with asteroids and the advantage of using electric propulsion is therefore accentuated.

In missions to the comets Encke and D'Arrest the stage first travels to a large solar distance, 2 to 3 AU, to gain the angular momentum and energy required to match the comet's orbital velocity and inclination. Recovery of the comet by observers on earth generally will only occur late in the mission such that major terminal guidance maneuvers become necessary. These orbital corrections can be executed during the last 50 to 100 days as part of the terminal thrust phase required to match the comet velocity.

One of the outstanding advantages of the electric propulsion vehicle is its ability to carry out large successive maneuvers in the vicinity of the comet to explore nucleus, coma and tail. In addition it can deploy a daughter probe for more effective exploration of the very large region

of interest and serve as relay link to earth applying its otherwise unused large electric power.

2.2.3 Out-of-Ecliptic Probe

The stage makes continuous out-of-plane maneuvers during those portions of its orbit around the sun where out-of-plane thrusting is effective in raising the orbital inclination, i.e., within 60 to 70 degrees from the ascending and descending nodes. Between thrust periods the vehicle must be reoriented 180 degrees by rotating around the sun line, in order to reverse the thrust orientation in each successive thrust phase as required for cumulative inclination build-up.

A large inclination (45^{o}) out of the ecliptic is clearly unattainable for a direct ballistic probe, requiring a hyperbolic departure velocity of 22.6 km/sec, or an injection velocity of 82,500 ft/sec. On the other hand, an indirect ballistic mission via Jupiter swingby, while much less demanding in propulsion energy (typically $V_{\infty} \approx 12$ km/sec), requires several hundred days of additional flight time, must traverse the asteroid belt on the outbound leg and must pass Jupiter at a close distance, thereby being exposed to significantly greater risks than the low thrust out-of-ecliptic probe which remains largely at a fixed solar distance of 1 AU through its mission life. The mission profile of a low-thrust probe which increases its inclination gradually at nearly fixed solar distance permits systematic coverage of physical phenomena as functions of heliocentric latitude only. This is not possible in a ballistic probe via Jupiter where large radial changes occur simultaneously with latitude changes.

2.2.4 Mercury Orbiter

The trajectory sprials inward and leads to rendezvous with Mercury by a continuous expenditure of retrograde thrust. A substantial orbit inclination change is executed as part of the thrust phase. The preferred time of arrival at Mercury from the standpoint of thermal control, solar array protection, and electric propulsion system operation is at a point of the planet's eccentric orbit where it approaches aphelion. Orbit insertion can be achieved by a chemical or electric propulsion maneuver; the latter option saves propellant mass without causing more

than a few days of mission time extension. The vehicle enters a highly eccentric orbit around Mercury which conserves propellant and has the advantage of reducing the exposure to intense thermal radiation from the hottest part of the planet.

Because of Mercury's low gravity, orbital capture during a fast flyby would demand an extremely high retro velocity increment which makes a ballistic orbiter mission prohibitive. The low thrust mission mode permits reduction of the hyperbolic approach velocity almost to zero at an affordable propellant cost and thus minimizes the orbit insertion maneuver requirement.

2.2.5 0.1 AU Solar Probe

Two mission profiles will be considered: (a) an elongated spiral (as illustrated in Figure 2-1) with successively closer approaches to the sun, attaining a 0.1 AU perihelion during the third passage. Thrust phases, centered around the aphelion passages alternate with coast phases. The trajectory is confined to the region inside the earth's orbit. (b) an indirect trajectory which first swings inside 1 AU, then outside to gain greater thrust effectiveness, attaining a 0.1 AU perihelion on the second approach to the sun.

The repeated close solar approaches of the first mission profile are advantageous from a data gathering standpoint but also increase the survival risk. The second profile permits only one close solar approach at substantially higher relative velocity after which the probe does not return. Thus the opportunity for repeated sampling and extended data collection is eliminated, but the risk factor is lower. Payload performance is somewhat better than in the first case.

Both low thrust mission modes compare favorably with a ballistic mission via Jupiter swingby that would have at least twice the flight time, and would introduce the risk of asteroid belt crossing and a close Jupiter encounter. A direct ballistic mission to 0.1 AU would be prohibitively costly requiring an injection velocity of 67,000 ft/sec (V_∞ = 17.2 km/sec).

2.3 ALTERNATE MISSIONS

2.3.1 Mars and Venus High Data Rate Orbiters

Mars and Venus orbiters do not require high mission energies and a ballistic Mars orbiter is currently in preparation To justify use of electric propulsion we postulate the use of the available large unused power for scientific purposes after arriving in orbit.

2.3.2 Outer Planet Flyby and Orbiter Missions

These missions are generally regarded to be feasible with future Titan class launch vehicles, although a swingby of either Jupiter or Saturn is required to gain flight time or payload advantages. The electric stage would carry a separable payload spacecraft to be ejected after the propulsion phase is completed. The payload would then continue the mission as in a ballistic launch.

Since the mission can be completed without the benefit of an outer planet swingby a major launch time and targeting constraint would be eliminated through use of the electric stage. However low-thrust missions that include Jupiter or Saturn swingby will also be considered.

In order to derive the greatest payload advantage for the most energetic outer planet missions (Uranus, Neptune) we anticipate that the indirect low-thrust mission mode will be preferred where the vehicle first swings inside 1 AU for increased solar power and thrust effectiveness at the expense of longer thrust time.

2.3.3 Deep Space Communication Relay

A 4 AU deep space communications relay station originally postulated as one of the alternate missions has very limited usefulness because it can serve only those space probes which are at relatively close distance i.e., within about 1.3 AU, in order to compete with direct signal transmission to an 85-foot DSIF antenna on the ground. This assumes a 30-foot antenna diameter for the relay station. To compete with direct transmission to the 210-foot DSIF antenna the space probe-to-relay station distance must be less than 0.6 AU. This constraining geometry indicates the limited value of a relay station at 4 AU.

A much greater advantage can be gained by a relay stationed permanently at 1 AU from the sun and about 160 to 170 degrees away from earth. This stationary vehicle can relay to earth signals from space probes that are temporarily unable to communicate directly due to sun obscuration (i. e., at positions near superior conjunction or syzygy). In addition, any space probes within 0.6 AU of the relay can use the relay link to advantage in transmitting to the 85-foot DSIF antenna even if not at syzygy. This relay station can serve probes inside 1 AU such as Venus, Mercury, solar and cometary probes, as well as those to the distance of Mars. If the stationary 1 AU relay is used in addition for the second purpose of monitoring solar phenomena not observable from earth to provide advance warning of severe solar activity a potentially very valuable mission concept might be defined. Propellant requirements for attaining stationary position at longitudes 90 to 180 degrees from earth have been determined. The vehicle does not require a very high-propulsion energy for this mission, but it can use the large solar array effectively in the relay mode.

2.4 ADVANCED MISSIONS

In addition to the mission specified in the work statement we anticipate utilization of the stage, once developed, on various high energy missions that would otherwise require carrying substantial chemical propellant masses for maneuvering in deep space.

Round trip missions to Mars, some small asteroids, and some comets appear feasible with a growth version of the electric stage. However, these missions are outside the scope of this study.

A very promising concept of electric stage application involves missions that will be launched by the Earth Orbital Shuttle. An upper stage such as Centaur, that will perform the interplanetary injection maneuver will also have to be carried, but the payload bay of the E.O.S. has adequate space for both the chemical and electric stage. Principal advantages of shuttle launch are the following:

- With the addition of the Centaur upper stage the total injected mass performance from low earth orbit would be significantly increased over that of Titan 3D/Centaur.
- The projected cost per sortie including a Centaur stage is up to $12 million smaller than that of a Titan 3D/Centaur launch.
- The shuttle crew can check out the electric stage after deploying it from stowage and erecting the solar array. Thus malfunctions not detectable in earth-based checkout can be detected and possibly corrected.

The mission profiles after shuttle launch would in principle be the same as for unmanned launch operations. This launch concept is outside the scope of the present study but merits early attention by those planning electric propulsion missions for the next decade.

3. THE MULTI-MISSION ELECTRIC STAGE CONCEPT

3.1 INTERPRETATION OF ELECTRIC UPPER STAGE CONCEPT

As a first step in the selection of a preferred design approach it is important to interpret the concept of an electric upper-stage more clearly and to review alternate design options that are consistent with the contractual work statement outlined in Section 1 and meet the mission objectives discussed in Section 2.

The vehicle must be able to perform the five specified primary missions which are confined largely to the inner solar system, but should also be adaptable to a variety of alternate missions such as missions to the outer planets. Design options that would meet this spectrum of mission requirements include stage configurations where payload instruments are either permanently attached to the stage throughout a mission and are operated within the environment of the stage, or are part of a separable autonomous payload spacecraft carried by the stage. The stage can thus be used alternately as a "payload bus" or as a "pure stage".

With the concurrence of NASA/OART, Advanced Concepts and Mission Division, we have formulated a design concept compatible with both options and have carried out the design study on this basis. We feel that this concept offers the greatest multi-mission flexibility.

In our interpretation the term "electric propulsion upper stage" thus designates a bus vehicle, or delivery system, that propels, carries and accommodates permanently attached or separable payload packages for extended periods, typically from two to three years. It must be designed for compatibility with the propulsive, environmental, and payload accommodation requirements of a large number of different mission applications. Of principal concern is the design of the interfaces, both mechanical and electrical, between the vehicle and the scientific payload, and in particular, the question of the weight and cost effectiveness and practical usefulness of a stage design in which electrical interfaces are minimized or fully eliminated.

A recent NASA technical memorandum by E. A. Willis, et al (Reference 3-1) gives a definition of the term electric upper stage that agrees very closely with our interpretation.

One of the principal objectives of making the electric propulsion vehicle a "stage" is to permit its procurement under a program funded and administrated similar to the procurement of launch vehicles or conventional chemical upper stages. Hence the requirements for a mission-independent baseline configuration and maximum commonality with diversified mission and payload characteristics. At the same time, we envision that the utilization of an electric stage, once developed and placed in the inventory, imposes on the user the burden of adapting a candidate payload complement to the weight and volume capacity, available resources, and mounting and environmental constraints of the stage.

An analogy that illustrates the use of a versatile "payload bus vehicle" is provided by the multi-purpose Convair 990 used at Ames Research Center to carry a variety of instruments under an ongoing airborne research and test program. Users of the aircraft become accustomed to accepting the accommodations provided for, and constraints imposed on, their instruments as the condition under which the test vehicle is made available to them, instead of expecting a vehicle tailored specifically to their experimental objectives.

The cost-savings achieved by the multi-mission versatility of a standardized transporation system should outweigh the cost penalty placed on the user. The incremental cost of a new mission, when viewed from a standpoint of the entire space exploration program could thus be appreciably reduced.

3.2 COMPARISON OF BASIC DESIGN AND INTERFACE OPTIONS

Figure 3-1 illustrates schematically some prinipcal design options for electrically propelled spacecraft or stages. The vehicle includes a center body consisting of a structure and required subsystems, a power and propulsion module, and a payload package. Option A defines an electric spacecraft where the three parts are fully integrated. Options B, C, and D show the payload package attached to but not integrated with the center body. These options meet the definition of the term "stage". In Option B the payload has a limited complement of

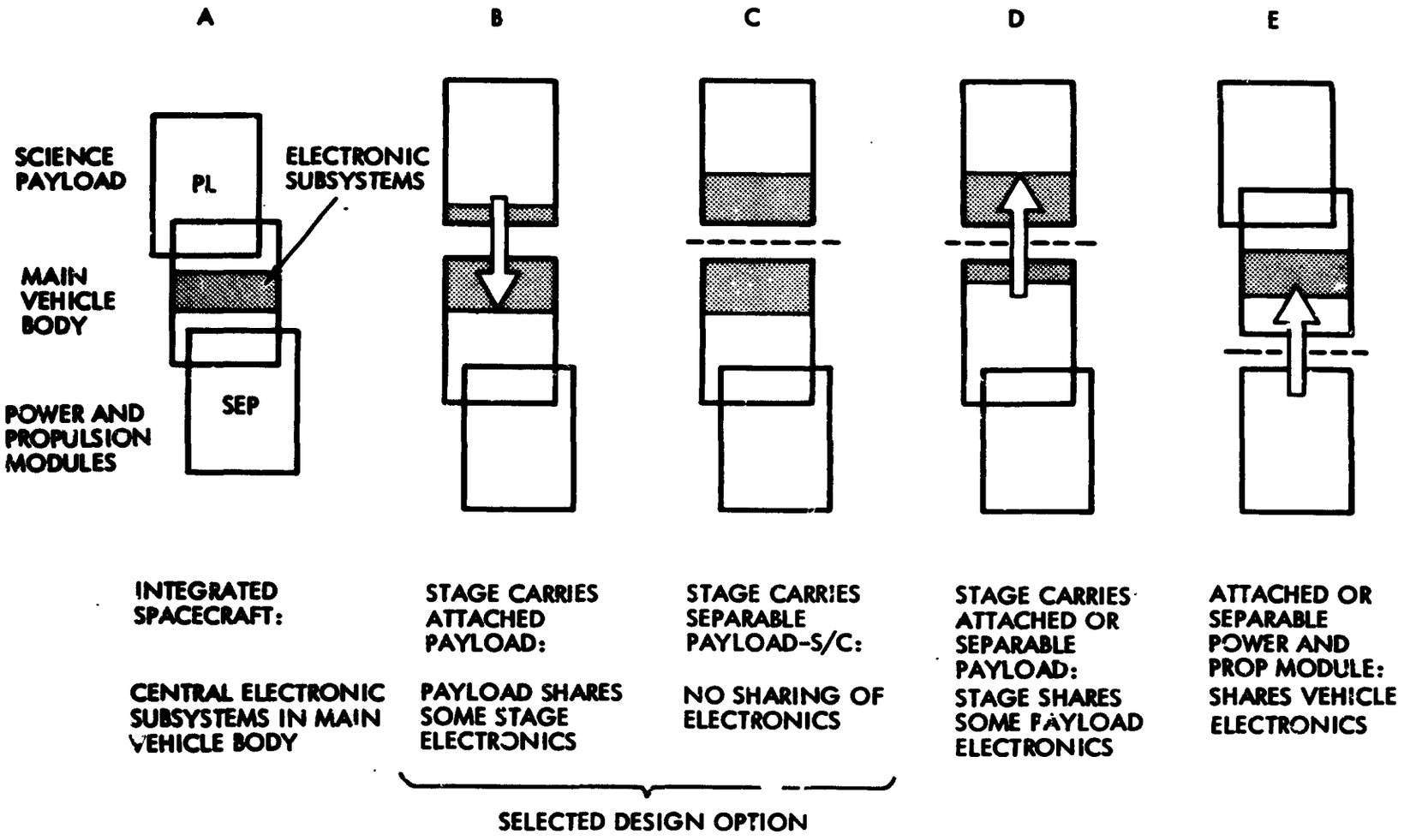

Figure 3-1. Principal Subsystem Interface Options

electronic subsystems (see shaded block) and shares some subsystems with the rest of the vehicle, as symbolized by the arrow. In Option C which requires stage separation there is no sharing of subsystems, hence duplication of electronics is required. The interface is exclusively mechanical. In Option D the stage depends on the payload package for subsystem functions, carrying only a minimum of electronics. Option E is the extreme case where the propulsion and power modules are building blocks that depend on the remaining vehicle for structure and subsystem support. By reducing the "stage" into a separate propulsion module which must be integrated with the center body to function as required a configuration is obtained which has again some characteristics of the integrated spacecraft design Option A.

The baseline stage configuration selected in this study is of Type B where the payload package shares the communication system with the stage. The payload is permanently attached to the stage in all specified primary missions, some of which require communication ranges up to 3.5 or 4 AU. Hence a duplicate telemetry system for the payload package would be more costly and weight consuming and would unnecessarily require a second high-gain antenna with a possible conflict of mounting, articulation, and field-of-view requirements. The CC&S and data subsystem can also be shared in this design by placing a remote acquisition unit on the payload side of the electrical interface. This unit is connected to the electrical integration assembly which is a principal subsystem element of the stage proper. This type of electrical interface is simple and versatile, and is commonly used in other spacecraft applications.

In missions where the stage is to be jettisoned (outer planet missions using a TOPS type autonomous spacecraft/payload) the electrical interface is eliminated, which converts the stage design adopted in this study to Option C. Thus both stage design options are represented by the selected configuration. The necessary weight penalty for duplication of subsystems must be accepted in this case.

Option D could conceivably also be used for these types of missions. However this has been ruled out because of the dependence of the electric

stage on the payload package and because of the higher cost of developing a new subsystem complement for each new mission compared to a standardized multi-mission subsystem complement integral with the stage proper.

3.3 STAGE PROCUREMENT

The economic advantage of the multi-mission electric stage program, i.e., amortization of the large initial development cost through many repeated missions, can only be realized if the procurement cycle assures a continuous production effort, and costly stop and restart cycles are avoided.

It is reasonble to anticipate that the procurement of such a program will not occur in large blocks but rather on a mission-by-mission basis, perhaps on an annual or biannual schedule. This schedule will be consistent with the projected cost savings of the multi-mission stage concept, as long as the production, integration and test facilities are used continuously. This is illustrated in Figure 3-2 for the case of a year-by-year procurement cycle.

The top of the chart shows staggered project spans of 3 years each. The development effort of each project is shown by a curve which first rises, then tapers off as the project progresses into the assembly and test phase (shaded area). The projects could be separated over a larger time span than shown in the chart without interrupting the work load in the contractor's assembly and test facilities. The bottom of the chart shows the cumulative effort for the first six projects over a 9-year span, with only minor deviations from an average level of effort that represents about three times the individual project effort at any given time. Assumptions made in this procurement plan are summarized as follows:

- 2-3 year project duration for each mission
- New procurement each year; with incremental funding flexibility
- 12 mission types achieved by annual new procurement
- 2 to 3 stages used per mission (launch rate per year is 2 to 3 stages)

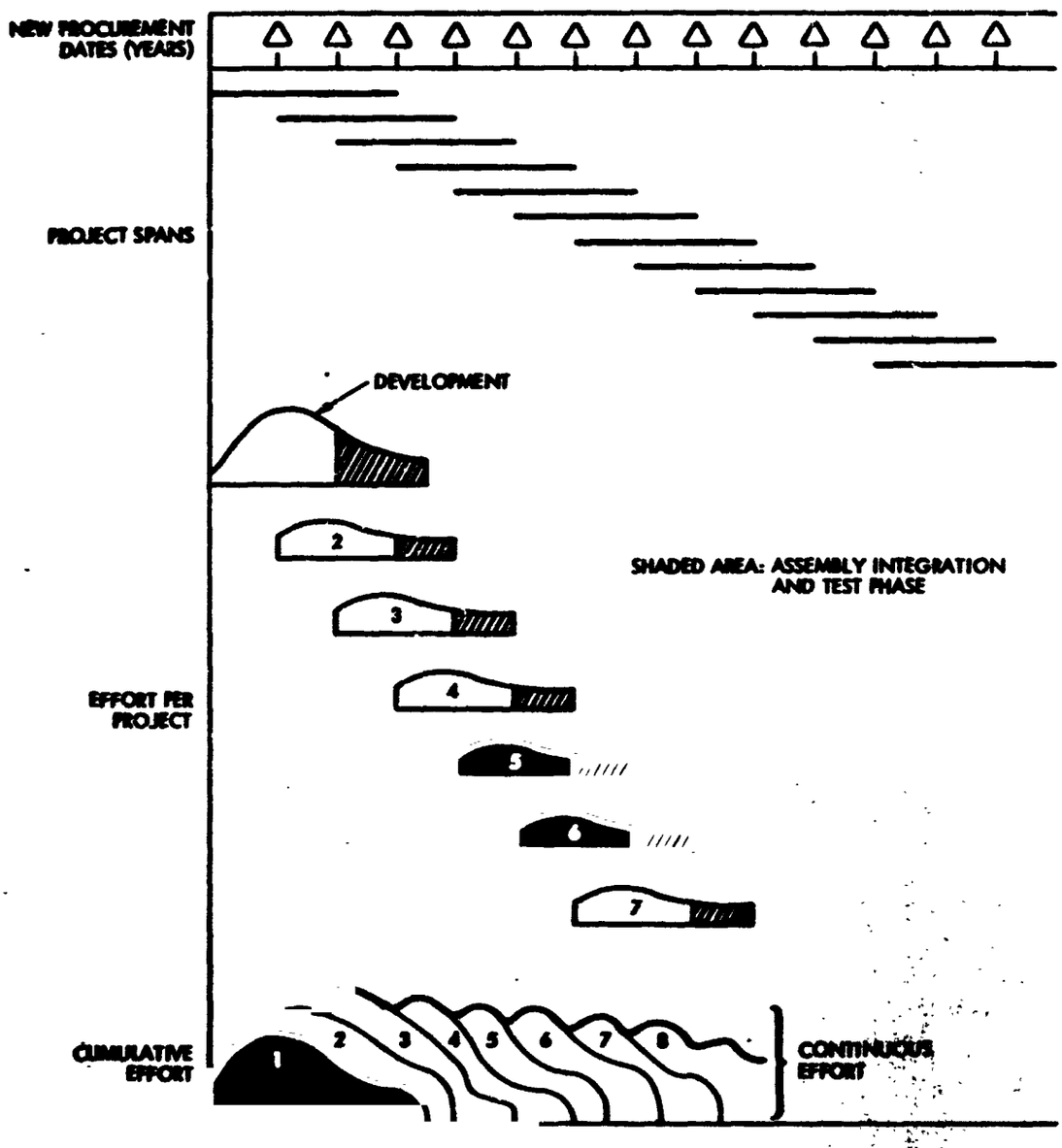

Figure 3-2. Procurement Plan (Assumes New Procurement Each Year)

- Plan on stage improvement (update), at 10-15% of unit cost. This prevents premature obsolescence. Stage should be good for at least 12 mission types over a 10-15 year period.

3.4 QUESTIONS REGARDING STAGE UTILIZATION

The following questions and problem areas are to be investigated as part of the multi-mission stage design and analysis effort:

- Does the vehicle provide adequate weight effectiveness despite weight penalties inherent (a) in multi-mission design and (b) in duplication of some structural and subsystem functions?
- Do cost advantages of the approach outweigh weight penalties?
- How much greater is the initial development cost required to provide acceptable multi-mission commonality?
- How much burden is placed on the user in adapting his payload instruments or the mission sequence to the constraints imposed by a standardized stage?
- Can a procurement method be adopted that achieves the full cost benefit of continuous production?
- Does the vehicle provide adaptability to technology growth? (Time span of keeping it in the inventory and rate of technology growth are critical factors.)

These questions will be covered in the remainder of this report and will be answered in terms of cost and weight effectiveness, performance characteristics, performance limitations, mission evolution and expected technology growth.

Questions that are beyond the scope of this study include detailed science payload definition for the specified missions, evaluation of stage effectiveness in accommodating selected payload instruments and specified mission objectives, and detailed comparison of performance characteristics and cost of the stage compared to the competing concept of an integrated multi-mission electric spacecraft such as SEMMS. It is recommended that these questions be addressed in a separate study.

4. SCIENTIFIC MISSION OBJECTIVES AND PAYLOAD

The scientific objectives of the specified primary missions are reviewed in this section (a) to provide a rationale for the selection of mission characteristics, operating modes and exploration strategies, and (b) to establish a basis for preliminary estimates of payload composition and desired electric stage payload weight capacities in each of these missions. The missions will be examined from the perspective of NASA's overall program of solar system exploration and the physical phenomena of principal interest in each mission will be discussed.

The implementation of the multi-mission stage concept demands that some compromises be made between potentially conflicting requirements and constraints imposed by different missions and science objectives. With the science objectives in mind the vehicle designer can use his best engineering judgement in making tradeoffs between weight capacity, payload mounting and field-of-view capability, system reliability and cost economy. In making these design choices the practical constraints of the present state of technology and reasonable projections of advances in technology by the mid-seventies must be taken into account, and the overall criteria of multi-mission commonality and operational feasibility of the design must be applied at every step. This process will be governed by the scientific objectives that are outlined in this section and by the conceptual payload complements synthesized as a result of this preliminary study.

An iterative process is envisioned where the multi-mission electric stage design concept developed in this study (Section 6) must be re-evaluated with regard to effectiveness of payload accommodation and mission performance after specific payload complements have been defined in greater detail. These tasks which are beyond the scope of the present study are strongly recommended as part of a follow-on effort of studying the most effective utilization of the multi-mission stage with regard to primary missions discussed in this section as well as alternative and growth missions that are being contemplated but have not been covered here.

4.1 ASTEROID RENDEZVOUS

First priority is given to the asteroid rendezvous mission because of the central importance accorded the asteroids in theories of formation of the solar system and because any experimental study of asteroids is practically non-existent. Almost nothing is known about any of the asteroids except for their trajectories, and even these are of generally limited accuracy. Presently tabulated asteroid sizes, albedos, and masses are inferential and require improved data for verification. A program of spectroscopic observation of the largest asteroids for the purpose of assaying their surface composition is presently under way, but results have just recently been reported for only a single body, namely, Vesta.

The electric multi-mission stage concept makes possible the actual landing of a substantial payload on an asteroid, and may present an opportunity to return with a sample from the asteroid's surface. Moreover, most of the instrumentation needed for the scientific objectives of such a mission is already available. The ratio of potential scientific return to present scientific knowledge is therefore extremely high for the asteroid mission described in this study.

Background. There are two principal theories of asteroid origin: one postulates that existing asteroidal bodies are the fragments of one or more shattered, larger planetoids; the second holds that planetary accretion accounts for the formation of the asteroids more or less as they now are. In either case, the structure and composition of an asteroid may tell much about the material from which the planets were formed and the state of the material at an early stage in the life of the solar system. The chief interest in a mission to an asteroid lies then in obtaining and analyzing an actual sample of asteroidal material rather than in mere observation from a distance (Reference 4.1).

Of secondary, but by no means unimportant, interest is the interaction of an asteroid or its magnetosphere with the solar wind plasma. The small diameters and small probable magnetizations of even large

asteroids make them candidates for marginal interaction processes, such as standing whistler wave fronts, which may be unique in the solar system (Reference 4-2). Observation of such phenomena, however, would only be accomplished very close to the target body (within 1-2 radii), for remote sensing of an asteroid influence on the solar wind is improbable (Reference 4-2).

Clearly, an important goal of asteroid exploration would be contact with the body. An ordinary flyby mission with a closest approach of perhaps several thousand kilometers would fall far short of the objective stated earlier. A rendezvous including orbiting and landing therefore is the preferred approach to an asteroid mission. Although the following discussion stresses the desirability of a lander capsule it would also apply (with appropriate deletions) to a rendezvous and orbit mission where no lander is carried.

Mission Profile. The postulated rendezvous and landing mission is best accomplished with a combination parent vehicle and separable lander module. The parent serves as bus for the journey and as data relay and environmental monitor during the surface operation phase. The lander measures the surface environment, transferring its data to the parent spacecraft.

Operations would consist of the following phases:

1) Cruise. Standard interplanetary fields and charged particle measurements and dust measurements are made.

2) Reconnaissance. The target asteroid is located precisely and surveyed. Physical properties of the body as a whole, such as size, shape, albedo, physiography, spectral reflectivity, magnetization, are measured using optical and environmental sensors; the landing site and mode are established, if necessary, by circling the asteroid.

3) Landing. The lander is detached and sent to its landing site; environmental sensors monitor ambient conditions during descent, similar measurements being made simultaneously by the parent vehicle.

4) Surface observation and sampling. The lander observes and analyzes the properties of its site, telemetering its data to the parent; the parent relays the data to earth, together with its own continued measurements of the space environment.

Measurements. Specific measurements serving the scientific objectives are as follows:

1) Plasma particles. Two plasma regimes should be measured, the solar wind, and a possible asteroidal wake or even magnetotail, in which a low energy plasma might be present. Velocity, temperature, density, and energy distribution functions would be measured by two analyzers, one optimal for each regime.

2) Magnetic and electric fields. Interplanetary magnetic and electric fields would be measured by a dc magnetometer. An ac loop, or coil, magnetometer, and an electrostatic plasma wave detector, would cover the range of electromagnetic and electrostatic waves from a few Hz to 100 kHz. The interaction, if any, at the asteroid should be covered adequately by the same instruments, but could occur very close to the surface. The lander would then need to make these measurements during Phase 3 and, would, of course, need a dc magnetometer at the landing site to detect local magnetizations. Since it would still be desirable to monitor the solar wind's EM input functions during phases 3 and 4, duplicate instruments are assumed on both spacecraft. Proper mounting of the two sets of instruments far apart before separation of the lander might allow comparison of simultaneous observations and correction of engine interference during Phase 1.

3) Cosmic Rays. It is assumed that the usual interplanetary cosmic ray telescopes would be included to measure galactic and solar cosmic ray properties, so long as the instruments could be accommodated by the spacecraft without jeopardizing the main mission objectives.

4) High energy trapped radiation. A simple device to detect trapped electrons and protons would observe ionizing particles which might be caught in a small asteroidal magnetosphere.

5) Dust. Since the target asteroid would be located in the asteroid belt, a device, or devices, to monitor the ambient micrometeroid flux is desirable. Optical meteroid sensors, such as the 4-beam Sisyphus developed by G. E., and penetration sensors developed by

Langley Research Center, would be logical candidates both instruments being included in the payload of Pioneer F for launch in 1972. A simpler and lighter weight penetration sensor with unlimited counting capacity (TRW's retractable foil penetration sensor concept MIMOSA) would be an effective addition to the micrometeroid instrumentation. In addition, the lightweight impact mass spectrometer developed by TRW (Cosmic Dust Analyzer) would be carried. A zodiacal light detector might be included.

6) Electron density and ultrafine orbital determination. A dual frequency transponder would serve the purposes of both measurements, the latter useful in fixing parameters distinguishing among cosmological models in general relativity. Integrated electron density is measured along the link path length, and two instruments are assumed, one on the parent vehicle for the earth-spacecraft path, the other on the lander for local electron density over the lander-parent communication path.

7) Gas envelope. An asteroidal atmosphere, possibly caused by charge exchange between the solar wind and the surface, would be detected and characterized by a group of optical and mass measuring devices: UV, visible, and IR spectrometers, and neutral and ionized mass spectrometers.

8) Geometry and physiography. Optical image devices would provide pictures of the asteroid's body and its surface features. It is assumed that a telescope of variable focal length would examine the target in Phase 2 and, being mounted on the lander, would record progressively greater detail in Phases 3 and 4.

9) Surface texture and composition. A group of devices such as those used on Surveyor and the Viking lander would make on-site measurements of surface properties: scraper, mass analyzer, α-scattering detector, and seismometer.

We note that the full instrumentation of a lander discussed here may be beyond the payload capacity of an early asteroid rendezvous mission. However, even a simple soft-landing capsule of the type first landed on the moon by the Russians (Luna 9) which primarily provides panoramic views of the surface would be very useful to enhance the scientific value of the mission.

Instrument Complements. Two separate instrument complements are required, one for the parent bus and one for the lander. Most instruments are assigned to the lander, since they can serve all phases of mission operations, both before and after separation, and are not needed by the parent after separation. Table 4-1 lists the scientific objectives of the asteroid rendezvous mission, the phases in which the various objectives are accomplished, the instruments applied to each objective, and the vehicle assignment of the instruments.

4.2 COMET RENDEZVOUS

A cometary body, like an asteroid, is of interest for the information it may yield on the origin of the solar system. It is believed that the cometary heads, or nuclei, may be composed of "primeval" matter, whose composition will yield key data on the conditions affecting formation of the planets. The actual sizes of comet nuclei are conjectural, known only within broad limits, but they are small, generally only a few kilometers in diameter, and generally unobservable from the earth, being enveloped in their comas of radiating, ionized gases. The gases emitted by the comet interact with solar radiation and the solar wind to form the coma, tail, and bow shock. The processes of interaction are fundamental to plasma physics and of great interest in themselves.

An ideal cometary probe would make close observations of a comet's nucleus, even to contacting it and obtaining a sample for analysis, measure the composition of coma and tail, and monitor the processes of plasma interaction occurring in the region between the bow shock and the coma. Since the cometary interaction processes are dynamic, with varying effects probably depending on continual fluctuations in solar wind parameters, separation of space and time phenomena would be a necessary capability for an ideal probe.

Fulfillment of all of the foregoing requirements is a rigorous burden for a cometary mission. The cometary rendezvous by a stage with high payload capacity and extensive low thrust maneuvering capability at destination can come close to the ideal, however. Although landing on, or contacting, the nucleus appears to be ruled out, the electric stage concept offers an opportunity for separating spatial and temporal effects by releasing a secondary probe into the coma and tail so that the functions of

Table 4-1. Asteroid Rendezvous Mission - Scientific Instrument Complement

Objective	Phase	Instruments	Vehicle Assignment: Stage	Vehicle Assignment: Lander	Note
Monitor interplanetary medium	1, 2, 3, 4	Solar wind plasma analyzer	•		
		dc magnetometer	•	•	
		ac magnetometer	•	•	
		Plasma (electric) wave analyzer	•	•	
		Cosmic ray telescope	•		
		Optical (micrometeroid) detector	•		
		Cosmic dust analyser (impact mass spectrometer)	•		
		Penetration detector	•		
		Photopolarimeter	•		
		Zodiacal light meter	•		
		Electron density detector (dual frequency transponder)	•	•	
Determine solar wind interaction: bow shock, magnetosheath, magnetosphere, wake	2, 3, 4	Same as above, with exception of dust detector,	As above		
		Trapped radiation analyzer	•		
		Low energy plasma analyzer	•		
Determine gas envelope	2, 3, 4	Neutral gas analyzer		•	
		Ionized gas analyzer		•	
		Electron density detector	As above		
		UV spectrometer		•	
		IR spectrometer		•	
		Visible spectrometer		•	
Observe physiography	2, 3	TV imaging telescope	•		
Observe surface features	4	TV imaging telescope		As above	
Determine surface texture and composition	4	Scraper		•	
		Mass chromatograph	•		
		X-ray spectrometer	•		
		α-scattering analyzer		•	
		Seismometer		•	

improved observation and close ambient monitoring can both be accomplished with a single mission. Much of the instrumentation would be adapted from existing devices.

Background. The scientific benefits of intercepting a comet have been discussed for almost a decade (Ref. 4-3 to 4-5). The principal interest in comets, as in asteroids, arises from the belief that cometary nuclei represent the primeval material of the solar system, so that close examination of a comet might reveal fundamental information on the origin, structure, and composition of the planets. Unlike the asteroids, comets exhibit a spectacular appearance which, in addition to commanding attention, permits enough remote observation and measurement from the earth to encourage partial understanding of their nature, thus making the unknown part doubly intriguing. Also unlike the asteroids, comets have very definite, visible, rather than speculative, interactions with the solar wind. Theoretical explanations for these can only be verified by direct measurement. Like the asteroids, on the other hand, comets are unlikely to reveal their most important secrets unless approached very closely or perhaps even contacted, because the nuclei are estimated to be very small, i.e., no more than a few tens of km in diameter, or no larger than small to medium sized asteroids.

The objectives of a cometary probe include observation of the nucleus and measurement of its dimensions, examination of its plasma interaction region, sampling of the neutral and ionized coma and tail gases, including transient rings, rays and other structures, and measurement of the dust components of the coma and tail.

The most distant upstream plasma interaction probably consists of a magnetosonic bow shock, together with some associated upstream waves. The shock may be 10^6-10^7 km ahead of the nucleus, and the interface between solar wind and ionized cometary gas 10^4-10^5 km ahead of the nucleus (Ref. 4-6). The coma may be 10^4 10^5 km in diameter and the tail the same, but on the order of 10^6 km long. These dimensions determine the distances within which a comet should be sampled in various directions. The closest approach distance to the nucleus should be no more than a few thousand km, and the greatest distance along the tail at least several hundred thousand km to achieve essential mission objectives.

The time varying appearance of a typical comet imposes an important requirement on a properly designed cometary probe. It is desirable to sample the materials of coma and tail both in and out of the structural inhomogeneities that propagate through these regions. The only way to tie local measurements in, say, the coma, to the passage of some feature through it, for example, an expanding ray, is to know the position of the point of measurement with respect to the ray as the latter progresses through the coma. This can best be accomplished by observing the comet from outside, with one probe recording the ray's appearance optically, while a second probe monitors its properties inside. An ideal comet rendezvous mission should then have separable mother and daughter spacecraft. This arrangement also allows the determination of cometary response to interplanetary transients, such as solar flare shocks, by having an interplanetary monitor outside the comet at all times.

As in the case of asteroid missions we have stressed the desirability of including a daughter probe in this mission. The following discussion, with appropriate deletions, also applies to the more austere concept of a comet mission where no daughter probe is carried.

Mission profile. The comet rendezvous mission is performed preferably by the stage and a daughter probe. They are joined until the rendezvous, when the daughter probe separates and proceeds independently through the various regions of the comet. Mission phases are:

1) Cruise. Standard interplanetary field and charged particle measurements and dust measurements are made.

2) Approach. The dimensions and appearance of the target comet are examined and the best route for the daughter probe determined. The daughter probe instruments are checked out against the possibility that in case of important failures, the stage can enter the comet in its place.

3) The daughter probe is separated and sent into a trajectory of close passage, less than $\approx 5 \times 10^3$ km, from the nucleus. Its velocity relative to the comet should be on the order of 1 km/sec. Data recorded by the daughter probe are telemetered to the mother vehicle for relay to earth. In the event of failure of key daughter probe instruments, the stage can carry out this phase.

Measurements. Specific measurements appropriate to a cometary probe are:

1) Plasma particles. The solar wind would be monitored in the interplanetary region by a standard plasma spectral analyzer. Solar wind modified by the cometary bow shock and low energy plasma leaking into the cometary tail would be measured by a separate plasma detector, mounted on the daughter probe.

2) Magnetic and electric fields. A dc magnetometer, ac loop, and electrostatic plasma wave detector would measure fields from 0 to 100 kHz in the solar wind, the comet's interaction region, and the cometary environment (coma and tail). Duplicate groups of instruments are assumed on mother and daughter vehicles.

3) Dust. Determination of the characteristics of dust particles in the cometary environment, particularly in the tail, would be made to investigate directly the origin of meteor showers and the structure, perhaps even composition, of the comet nucleus, from which these small solid particles are emitted.

4) Electron density and ultrafine orbital determination. A dual frequency transponder would serve the purposes of both measurements, the latter useful in fixing parameters distinguishing among cosmological models in general relativity. Integrated electron density is measured along the link path length, and two instruments are assumed, one on the stage for the earth- spacecraft path, the other on the daughter probe for local electron density over the stage-daughter communication path.

5) Neutral gases. It is the emissions from ionized products of the interactions of solar illumination and solar wind with the neutral gases emitted by the comet nucleus that are observed from the earth. The original neutrals are not detected and their exact identifications are unknown. These neutral gases are ionized as they expand from the nucleus through the coma and some neutral gas may survive in the interplanetary region around the comet. A neutral mass spectrometer would seek to identify these gases outside the coma and in the coma as close to the nucleus as feasible.

6) Ionized gases. The ionized gases themselves would be analyzed by an ion mass spectrometer. These would include, most importantly, those constituents which are presently unknown because their emissions are absorbed by the earth's atmosphere.

7) Physical appearance. The dimensions and appearance of the nucleus would be prime objectives for determination, using a straightforward imaging telescope from as close a vantage as possible. Overall appearance of the coma and tail, especially showing formation and propagation of various cometary forms, would also be essential; for this, a wide angle imaging system is assumed.

8) Optical spectrum and photometric properties of coma and nucleus. Observations of the principal emission bands and of photometric properties such as albedo and polarization would be made by UV, IR, and visible light spectrophotometers. In addition, high resolution spectrographs of the inner coma closer to the nucleus than the daughter probe would be appropriate.

Instrument complements. Two separate instrument complements, one on the stage proper, one on the daughter probe, would enable the mission to carry out its objectives. These are listed in Table 4-2.

4.3 OUT-OF-ECLIPTIC MISSION

Only about eight percent of the undisturbed solar wind flows through the region observed by space probes whose trajectories are confined to the ecliptic plane. It follows that exploration of interplanetary space can never be considered complete without a three-dimensional sampling of the solar wind off the ecliptic at high solar latitudes. A mission to high solar latitude can also serve as a valuable contributor to the study of solar-terrestrial relations by providing an over-the-horizon view of solar activity on the side of the sun opposite the earth. Such a function, however, imposes restrictions on the launch time of an out-of-ecliptic probe, if the best view of far-side activity is to be obtained. Since out-of-ecliptic solar wind measurements would be most meaningfull in comparison with simultaneous measurements nearer the ecliptic at the same longitude, an out-of-ecliptic mission which provided a separate monitor, or daughter probe, at an intermediate orbit inclination would have great scientific value. Measurements made at earth generally do not meet this objective if the out-of-ecliptic probe departs significantly from earth's longitude during the mission. The electric stage has sufficient payload capacity to accommodate a small daughter probe in addition to carrying a sufficiently large payload to perform both ambient solar wind and over-the-horizon solar activity observations. All necessary scientific instrumentation is available.

Table 4-2. Comet Rendezvous Mission - Scientific Instrument Complements

Objective	Phase	Instruments	Vehicle Assignment: Stage	Vehicle Assignment: Daughter Probe
Monitor interplanetary medium	1, 2, 3	Solar wind plasma analyzer	●	
		dc magnetometer	●	●
		ac magnetometer	●	●
		Plasma (electric) wave analyzer	●	●
		Dust (micrometeroid) analyzer	●	●
		Electron density detector (dual frequency transponder)	●	●
Determine solar wind interaction: bow shock, transition region, magnetosphere, tail formation	2, 3	Same as above, with exception of dust detector,	As above	
		Low flux plasma analyzer		●
Observe configuration and constitution of comet	2, 3	TV imaging telescope	●	●
		TV wide angle telescope	●	
		UV spectrophotometer		●
		IR spectrophotometer		●
		Visible spectrophotometer		●
Observe configuration and constitution of nucleus and inner corona	3	TV telescope, as above		As above
		UV, IR, visible spectrophotometer, as above		As above
Determine neutral and ionized gas constitution of coma and tail	3	Neutral gas mass spectrometer		●
		Ionized gas mass spectrometer		●

Background. No deep space probe has yet been placed on a trajectory that carried it away from the ecliptic more than a few million kilometers. Consequently, experimental space physics of the interplanetary region has remained almost entirely two-dimensional. However, in regard to the physics of solar emissions it must be kept in mind that the solar equator, rather than the ecliptic, is of fundamental importance. Since the sun's rotational axis is tilted some 7° from the ecliptic pole, interplanetary measurements, having been made within $\pm 7^{\circ}$ to 9° of the solar equator, have been less planar than figures of absolute distance from the ecliptic suggest. Nevertheless, the range of heliocentric latitude samples has been extremely limited, especially considering that solar wind properties proportional to the cosine of solar latitude will differ within the sampled region by no more than around 1 percent from their equatorial values. Such a small geometrical effect is lost amid a host of temporal and other geometrical factors. A three-dimensional characterization of the solar wind and its convected magnetic field cannot be achieved, then, without planned measurements well away from the ecliptic.

Solar astronomy, like space physics, has also been hampered by a perspective of the sun confined essentially to the solar equator. In particular, the configurations of coronal features, such as extended streamers, are not visible, and the history of coronal formations cannot be followed when they disappear against the disk. Although recent combined observational and theoretical work has made great strides in determining coronal structure, the results are necessarily inferential. A high latitude view of the corona would provide the direct observations needed to complement what can be done from earth.

Scientific interest in out-of-ecliptic observations does not reside exclusively in heliocentric phenomena. Large scale inhomogeneities in galactic properties may have sufficient gradients to be detectable by spacecraft leaving the ecliptic. For example, the galactic magnetic field may have a gradient transverse to the ecliptic which would affect cosmic ray rigidities differentially, producing a transverse variation in cosmic ray flux. Only an out-of-ecliptic mission could determine the existence of such an effect.

The field of solar-terrestrial relations would benefit from off-ecliptic observations. There are mysterious, but rare, magnetic storms and associated phenomena which have no apparent source on the visible disk. Solar-terrestrial researchers have long wished for spacecraft to monitor solar activity on the anti-terrestrial solar hemisphere. An out-of-ecliptic probe is not ideal as a far-side monitor, but it can partially serve the purpose by providing an over-the-horizon view of either the northern or southern sunspot zones, at least when these are at their maximum heliographic latitudes early in a fresh sunspot cycle. A far-side solar monitor on the ecliptic in contrast, cannot provide any off-ecliptic measurements of solar wind or cosmic ray properties.

Mission profile. An out-of-ecliptic mission would depend heavily for its value on comparisons between measurements at progressively increasing latitudes and simultaneous measurements on or near the ecliptic at the same longitude. A daughter probe may be deployed that would continue to travel at the orbit inclination at which is was ejected, to provide simultaneous measurement at similar longitude as the parent vehicle, but at lower latitude. The mission would be planned so that the parent would reach the greatest northern or southern off-ecliptic position at the longitude to which the solar axis is tilted. This would add the 7^{o} solar tilt to the probe-sun-ecliptic angle, giving the probe a maximum possible heliographic latitude. The mission would also be timed such that the culmination point or "apecliptic" occur early in the sunspot cycle, preferably before the end of the third year, so as to take advantage of the relatively high latitude (20^{o}-30^{o}) of early activity centers for the best over-the-horizon view. Table 4-3 gives the way in which visibility of the sun is improved at various heliographic latitudes λ, for an observer at 52^{o} heliographic latitude. This value ($52^{o} = 45^{o} + 7^{o}$) is the maximal solar latitude attainable at an apecliptic of 45^{o} if the timing permits addition of the full solar tilt angle. The table indicates that with this mission geometry the probe can observe solar activity at 20 to 30^{o} latitude 66 to 76 percent of the time.

Table 4-3. Gain in Visibility of High Solar Latitudes for 45° Out-of-Ecliptic Mission

Heliographic Latitude of Observed Phenomena	Heliographic Longitude of Disappearance, Measured from Central Meridian	Net Gain	Time of Visibility Per Solar Rotation
0°	±90°	0°	50%
10°	±104°	28°	58%
20°	±119°	58°	66%
30°	±137°	94°	76%

The out-of-ecliptic mission can be thought of as having two phases:

1) Cruise. Solar wind properties, cosmic ray flux, and dust measurements are monitored concurrently by a probe at low latitude and by the parent spacecraft as it gains latitude.

2) Apecliptic. The parent spacecraft records white light and spectral images of the corona and monitors UV and X-ray emissions from activity centers on the far-side limb. It also continues to make ambient measurements.

Measurements. Out-of-ecliptic measurements would include the following:

1) Plasma particles. These would be measured by solar wind plasma spectral analyzers.

2) Magnetic and electric fields. Standard dc and ac magnetometers and ac plasma wave detectors would monitor ambient electromagnetic conditions.

3) Cosmic rays. A cosmic ray telescope experiment would monitor both solar and galactic cosmic ray flux.

4) Electron density. A dual frequency transponder would provide this measurement over the probe-earth link.

5) Dust. Latitude dependence of micrometeroid flux would be measured. A zodiacal light detector would be included.

6) Coronal structure. Images of the corona beyond 2-3 $R_\odot$ would be recorded by a coronascope.

7) Solar activity. An imaging coronagraph would monitor far-side solar activity in the X-ray and UV region of the spectrum.

8) General solar conditions. It may be anticipated that if mission parameters were to permit it, high-resolution scanning spectroheliographs would be included for a general investigation of solar physics. Temperature profiles of the sun across the pole could be made, for example.

Instrument Complements. Table 4-4 lists the instruments assigned to the mother and daughter spacecraft for the out-of-ecliptic mission.

4.4 0.1 AU SOLAR PROBE MISSION

Background. The sun being the source of most physical processes in interplanetary space is a prime object of investigation and its observation at close range is of enormous scientific interest. If existing optical instruments developed for earth orbiters were transported to 0.1 AU, the resolution with which solar features could be delineated would be improved by an order of magnitude, and new details of sunspot activity regions, flares, and prominences, would be visible.

Measurements of ambient physical conditions would also have great significance. This is best discussed by thinking of heliocentric distance in solar radii, $R_\odot$, where 0.1 AU $\approx$ 21 $R_\odot$. Acceleration of the solar wind takes place between 5 and 40 $R_\odot$, with little change of velocity thereafter. Plasma measurements at 20 $R_\odot$ would therefore be made right in the region where the solar wind is significantly different from its steady state condition. Direct measurement of solar transient phenomena may also be accomplished for the first time. The material of coronal streamers, eruptive prominences and flare surges, and magnetic loops from individual activity centers, together with trapped radiation on the loops, may be detectable at 20 $R_\odot$.

Questions of solar wind abundance of various ion species may be accessible to a close approach solar probe. One barrier to establishment of these abundances is the unknown cross section of certain highly ionized species with respect to galactic neutral hydrogen. Comparison of measurements at 0.1 AU with neutral hydrogen measured simultaneously at 1 AU might determine not only a true abundance distribution, but some of the unknown cross sections as well.

Table 4-4. Out-of-Ecliptic Mission - Scientific Instrument Complements

Objective	Phase	Instruments	Spacecraft Assignment: Stage	Spacecraft Assignment: Daughter Probe
Monitor latitude dependencies of solar wind properties, interplanetary dust	1, 2	Solar wind plasma analyzer	●	●
		dc magnetometer	●	●
		ac magnetometer	●	●
		Plasma (electric) wave detector	●	●
		Dust (micrometeoroid) analyzer	●	●
		Cptical micrometeroid detector	●	●
		Micrometeroid impact sensor	●	
		Electron density detector (dual frequency transponder)	●	●
		Zodiacal light meter	●	
Determine transverse gradient of galactic cosmic rays	1, 2	Cosmic ray telescope	●	●
Monitor solar cosmic rays	1, 2	As above	As above	
Observe high latitude solar features, including corona	2	Coronagraph	●	
Monitor far-side solar activity	2	UV-coronameter	●	
		X-ray spectrophotometer	●	
Observe high latitude solar characteristics	2	Scanning spectroheliograph	●	

Finally, hydromagnetic and plasma wave processes contributing to the particle distribution functions of the solar wind, co-rotation of the solar wind, and solar neutron emission would be determined by examining the radial dependence of all the solar wind properties.

Mission Profile. Once again, this mission is best served by a mother/daughter spacecraft combination: the daughter probe designed to provide normalization measurements would be deployed at first perihelion in the vicinity of 0.4 to 0.5 AU while the parent vehicle would continue its mission toward the sun. This arrangement automatically provides the advantage of two spacecraft in the interplanetary region halfway to the sun, thus permitting space-time separation of variations in solar wind parameters.

Strictly speaking, all measurements are more or less continuous, so that distinct phases are not readily assignable in this mission. The objectives do, however, suggest a rather loose division, as follows:

1) Early cruise. Parent and daughter spacecraft are separated and monitor the space environment, taking advantage of vehicle separation to differentiate space and time contributions to fields and particles variations.

2) Cruise. The interplanetary environment is monitored. Radial dependencies of mean fields and particles parameters are determined by comparison of measurements at mother and daughter spacecraft.

3) Perihelion. The environment, consisting of inner solar wind and outer corona, is monitored at closest approach to the sun. Solar features are observed in detail.

Measurements. Basic environmental measurements would be much the same as in the out-of-ecliptic mission described previously. These are:

1) Plasma particles
2) Magnetic and electric fields
3) Cosmic rays
4) Electron density
5) Dust.

Radial, rather than latitudinal, dependencies would, of course, be sought for the above group of phenomena, and extensions of local solar fields would be measured. The frequency range of the electric wave detector would extend to MHz frequencies to monitor solar radio noise. Additional measurements would include:

6) High energy radiation. Ionizing radiation, should any be trapped in high altitude solar magnetic loops, would be detected.

7) Neutron flux. Solar neutron radiation, most of which decays rapidly, would be sought near perihelion.

8) Gas species. Ion and neutral atom mass spectrometers would investigate solar wind abundances. A neutral hydrogen detector at 1 AU would monitor galactic background for comparison.

9) Coronal structure. The appearance of coronal features, and their spectral emissions would be recorded.

10) Solar disk features. Telescopic images would provide glimpses of details of the solar surface in general, and of activity centers in particular. UV, IR, and visible light measurements would all be included. This type of observation presents special thermal problems and might be too ambitious an objective to be regarded as part of a basic payload.

Instrument Complements. The daughter probe would be relatively simple in this mission, most experiments being assigned to the parent stage. Table 4-5 lists the instruments and their assignments.

4.5 MERCURY ORBITER

The scientific benefits anticipated at present from a mission to place an orbiter around Mercury will undoubtedly be affected by data returned from the forthcoming Mariner Mercury flyby mission, which may greatly increase the interest of planetologists and other investigators of the evolution of the solar system, considering the unresolved mysteries of Mercury.

Background. Very little is presently known about Mercury, and interpretations of some of the measurements that have been made are still problematical (Reference 4-7). The Mariner Mercury mission,

Table 4-5. Solar Approach Mission - Scientific Instrument Complements

Objective	Phase	Instrument	Vehicle Assignment: Stage	Vehicle Assignment: Daughter Probe
Monitor interplanetary medium	1, 2	Solar wind plasma analyzer	●	●
		dc magnetometer	●	●
		ac magnetometer	●	●
		Plasma (electric) wave and radionoise detector	●	●
		Dust (micrometeoroid) detector	●	
		Zodiacal light detector	●	
		Cosmic ray telescope	●	●
		Electron density detector (dual frequency transponder)	●	○
		Zodiacal light meter	●	
Monitor solar wind acceleration region and outer corona	3	Same as above, plus	As above	
		High energy radiation (trapped particle) detector	●	
Detect solar neutron emission	3	Neutron flux detector	●	
Analyze ambient gases	2, 3	Neutral mass spectrometer	●	
		Neutral hydrogen detector	●	●
		Ion mass spectrometer	●	
Observe corona	3	Coronascope	●	
Observe disk features characterizing disk and coronal emissions	3 Supplemental objectives	UV spectrophotometer	●	
		IR spectrophotometer	●	
		Visible spectrophotometer	●	

moreover, will make its flyby so rapidly that conclusive data may still be unavailable afterward. From the standpoint of postulating a scientific payload, the best procedure is simply to assume that the electric stage mission will provide the first source of comprehensive data on the planet. The paragraphs below reflect this approach.

The objectives of a Mercury orbiter would be principally to learn as much as possible about the planet itself. Surface features and texture are of primary interest as they may provide evidence of planetary evolution in very close solar proximity. In addition to an optical image system a radar system could therefore be desirable. Some kind of wake or "plasma shadow" in the solar wind is certainly expected, so plasma field and particle measurements behind the planet would achieve definite results. Interplanetary measurements would be of interest, as would also observations of the sun from the closer vantage of Mercury's orbit. The latter would be of particular value to studies of solar-terrestrial relations because during a large part of the time while anchored in orbit around Mercury the vehicle can monitor solar activity invisible from the earth, i. e., around the limbs of the sun. This would be useful for understanding the origin of magnetic storms having no apparent source on the visible disk.

The composition and properties of Mercury's atmosphere, if any, are completely unknown. The atmosphere is likely to be tenuous enough in any case to make rapid measurements by any flyby difficult to interpret. An orbiter provides a statistical advantage in allowing repeated measurements of, say, UV absorption and emission. Extended observations would eliminate a major concern, namely that emissions caused by sporadic solar activity might inject ambiguity into measurements made during a single, brief pass by a flyby probe.

Mission Profile. Two mission phases can be defined:

1) Cruise. Interplanetary measurements would be made.

2) On station in planetary orbit. Mercury's surface features, atmospheric properties, magnetospheric characteristics, and solar wind shadow would be detected and the solar disk would be monitored.

Measurements. Interplanetary environmental measurements would include:

1) Plasma particles.
2) Magnetic and electric fields.
3) Cosmic rays.
4) Electron density.
5) Dust.

Measurements specific to Mercury would be:

6) Plasma particles. In addition to solar wind measurements, low energy, or thermal, plasma detection in Mercury's wake would be provided for.

7) Magnetic and electric fields. The interaction between the solar wind and a prospective planetary field or ionosphere would be sought. The wake would be detected.

8) Trapped radiation. Ionizing particles trapped in a possible planetary field would be detected.

9) Gas properties. Neutral and ionized constituents of a possible atmosphere would be detected with appropriate mass spectrometers if the orbiter could be moved to low altitude. Composition would also be estimated from gata gathered by UV, IR, and visible light spectrophotometers.

10) Surface features. Physiography and texture of the surface would be recorded by an imaging telescope and a radar sounder.

Measurements related to solar-interplanetary and solar-terrestrial relations would be:

11) Solar activity monitoring. UV and X-ray imaging spectrophotometers and radionoise detectors would sense solar flare emissions.

Instrument Complement. Table 4-6 lists the instruments postulated for the Mercury orbiter mission.

4.6 SCIENCE INSTRUMENTATION WEIGHT ESTIMATES

On the basis of the payload complement selections made in Sections 4.1 - 4.5 we have obtained first estimates of the instrumentation weight

Table 4-6. Mercury Orbiter Mission - Scientific Instrument Complement

Objective	Phase	Instruments
Monitor interplanetary medium	1, 2	Solar wind plasma analyzer dc magnetometer ac magnetometer Plasma (electric) wave analyzer Dust (micrometeoroid) detector Electron density detector (dual frequency transponder) Cosmic ray telescope
Determine solar wind interaction	2	Same as above with exception of dust detector Low flux plasma analyzer
Determine planetary envelope	2	Trapped radiation detector Neutral gas mass spectrometer Ionized gas mass spectrometer UV spectrophotometer IR spectrophotometer Visible spectrophotometer
Observe surface properties	2	Imaging telescope Spectrophotometers, as above Radar sounder
Observe solar activity	2	Radionoise detector, part of extended range of plasma wave analyzer, above UV imaging spectrophotometer X-ray imaging spectrophotometer

requirements of the five primary missions, for payload packages that remain permanently attached to the stage and for those that will be ejected on a lander or other daughterprobe. Since a detailed definition of instruments exceeded the scope of the present study we supported these estimates by reference to the previous SEMM-1 study and other interplanetary mission studies performed by TRW.

The resulting estimates are given in Table 4-7. Included in the estimates are the sensors and supporting electronics but not the mounting provisions and other payload integration equipment that complete the payload package and are needed for attachment to the stage. In the case of the separable daughter probes, no weight elements are included

Table 4-7. Preliminary Instrumentation Weight Estimates for Primary Missions: Sensors Plus Electronics (KG)

INSTRUMENT TYPE (PHENOMENA MEASURED)	ASTEROID RENDEZVOUS		COMET RENDEZVOUS		EXTRA ECLIPTIC		SOLAR PROBE		MERCURY ORBITER
	STAGE	LANDER	STAGE	DAUGHTER	STAGE	DAUGHTER	STAGE	DAUGHTER	STAGE
INTERPLANETARY AND AMBIENT MEDIUM									
SOLAR WIND PLASMA PROBE	3		3	3	3	3	3	3	3
MAGNETOMETER	5	3	5	5	5	5	5	5	5
ELECTRIC FIELD METER	1	1	1	1	1	1	1	1	1
COSMIC RAY TELESCOPE	2		2		2	2	2		2
OPTICAL MICROMET-DETECTOR	11		11		11	11			11
PENETRATION DETECTOR	20		20		15				
COSMIC DUST ANALYZER	4		4	4	4	4			4
PHOTO POLARIMETER	5		5		5				
ZODIACAL LIGHT METER	4		4		4				
ELECTRON DENSITY EXPERIMENT	3	3	3	3	3	3	3	3	3
TRAPPED RADIATION	2		2				2		2
LOW ENERGY PLASMA ANALYZER	3			3					3
TARGET OBJECT									
NEUTRAL GAS ANALYZER		10	10	10			10	10	10
IONIZED GAS ANALYZER		10	10	10			10		10
UV-SPECTROMETER									
IR-SPECTROMETER	10			10			10		10
VISIBLE SPECTROPHOTOMETER									
TV IMAGE SYSTEM	10	8	10	10					10
SURFACE EXPERIMENTS		20							
RADAR SOUNDER									(75-100)*
NEUTRAL HYDROGEN DETECTOR							10		
SOLAR FEATURES									
NEUTRON FLUX							4		
UV EMISSION							45		15
X-RAY EMISSION							55		15
VISIBLE IMAGE					20		20		20
RADIO NOISE							6		6
CORONA GRAPH					40		20		20
SPECTRO HELIOGRAPH					(100-150)*				
HORIZON ACTIVITY MONITOR					20				
TOTAL ESTIMATED	78	55	90	49	133 (233-283)*	29	206	22	150 (225-250)*

*IF PAYLOAD CAPACITY AVAILABLE

that represent the structure and subsystems needed for an autonomous payload spacecraft. Even for the simplest, spin-stabilized configuration an increase by at least a factor of 3 is needed to arrive at an estimate for the gross weight of the daughter probe.

Table 4-8 converts these data into upper and lower brackets of overall payload capacity required for the five missions. These figures will be referred to in Section 5 as "net payload". Since no practical limits were placed on the estimated instrumentation weights it will obviously be necessary to update the payload selection after the actual weight capacity of a preferred stage configuration has been narrowed down. This means that priorities may have to be reevaluated so as to match payload weight requirements with stage capacity, if the former exceeds the latter. A better definition of payload instruments will have to be obtained as a first step.

Table 4-8. Upper and Lower Weight Estimates for Payload Packages (KG)

S = STAGE (MOTHER) D = DAUGHTER

PAYLOAD ITEM		ASTEROID		COMET		EXTRA-ECLIPTIC		SOLAR		MERCURY
		S	D	S	D	S	D	S	D	S
PROPOSED INSTRUMENTATION	UPPER	100	60	100	60	250	50	200	40	250
	LOWER	50	25	50	30	80	25	90	25	100
PAYLOAD PACKAGE ATTACHED TO STAGE	UPPER	150	--	150	--	300	--	250	--	300
	LOWER	90	--	90	--	120	--	130	--	140
SEPARABLE (DAUGHTER) SPACECRAFT	UPPER	--	210*	--	230*	--	150	--	120	--
	LOWER	--	100*	--	120*	--	75	--	75	--
COMBINED WEIGHT (NET PAYLOAD)	UPPER	360		380		450		370		300
	LOWER	90		90		120		130		140

*INCLUDES CHEMICAL PROPULSION SYSTEM

5. MISSION AND SYSTEM ANALYSIS

5.1 OBJECTIVES AND GUIDELINES

Mission and system studies have been performed to define basic mission and system parameters for the electric stage. The objective has been to identify a single basic vehicle design concept that will be compatible with all primary and some alternate missions without significant modifications. Some performance compromises are required in meeting the wide variety of specified mission objectives. Thus, it is necessary to study representative characteristics of the entire mission spectrum and to make judicious choices between available alternatives. The following criteria were applied in selecting mission characteristics and design parameters:

- Achievement of ample payload capacity to meet the scientific objectives of all specified missions.
- Selection of simple mission profiles and vehicle operating modes
- Achievement of system economy by holding propulsion power levels within limits consistent with adequate payload capacity and reasonably short flight duration.
- Selection of system characteristics that facilitate practical implementation, minimizing new technology requirements
- Attention to cost-effective use of launch vehicle performance capability
- Provision of vehicle growth capability to more advanced missions which will evolve once the electric stage becomes operational.

Guidelines for adequate payload capacity are not readily available. From the discussion of scientific objectives and candidate payload instruments in Section 4 first estimates of desired weight capacity can be derived. Typically, for permanently attached payload complements in the primary missions we estimate a required capacity of 100 to 250 kg. If a separable daughter spacecraft is to be carried in addition, we estimate a desired total capacity of 200 to 350 kg, and even much larger capacities in missions such as the Venus or Mars orbiter missions.

System simplicity and economy place a limit on the desirable propulsion power. Ideally, an optimal match between the large injected mass capability of the Titan class of boosters and the electric propulsion upper stage in high-energy missions is reached at propulsion power levels upward of 40 kw with net spacecraft mass often in excess of 1500 kg. A lower limit of power exists below which the Titan boosters would not be effectively utilized. This limit is about 10 kw. Our analysis will be concerned with finding a common power level that will provide adequate payload capacity for all primary and as many alternate missions as possible, but allowing a potential growth capability to larger power for more demanding future missions (e.g., a rendezvous with Halley's comet in 1986).

A detailed evaluation of mission options and parameter tradeoffs was a major objective of our mission and system analysis effort. In accordance with provisions of the contractual work statement, our effort in trajectory analysis was limited to those areas where available trajectory data did not cover the specified missions adequately for purposes of our study. Mission characteristics derived by other investigators were used wherever applicable. A comprehensive set of trajectory data of the primary missions and several alternate missions were furnished to TRW by Mr. A. C. Mascy of NASA/OART at the beginning of the study along with the new low-thrust trajectory simulation programs (CHEBYTOP and QUICKTOP) for our use in deriving additional trajectory characteristics.

From the results of these evaluations and tradeoffs we selected a set of nominal mission characteristics, common propulsion system design parameters and a common power level as a basis for the multi-mission electric stage design, so as to provide the desired performance capability and to minimize design penalties inherent in the choice of a compromise set of vehicle parameters. We determined cost saving mission options by making use of a reduced power level and/or a smaller than the nominal Titan 3D/Centaur launch vehicle. We derived new mission modes for the basic multi-mission stage and determined its growth capability to alternate missions not originally specified, namely an asteroid and Mars lander and sample return mission and a rendezvous mission to Halley's Comet. We also evaluated techniques for improving

the navigation and guidance accuracy of asteroid and comet missions using onboard navigation sensors.

5.2 ENGINEERING ASSUMPTIONS, REQUIREMENTS AND CONSTRAINTS

The following engineering characteristics and constraints were specified by NASA/OART at the beginning of the study:

1) Solar array specific mass:

Roll up array	15 kg/kw
Fold up array	21 kg/kw

The single boom deployed roll up array of the type being developed by General Electric under JPL contract has a nominal power level of 2.5 kw per panel. An increase of panel size to larger power levels is consistent with G. E.'s design approach. The fold-up array is the rigid panel type developed by Boeing.

2) Power conditioning:

Specific mass	5 kg/kw
Efficiency	91 percent

3) Ion thrusters:

Mercury electron bombardment thrusters; maximum propulsion period on any one thruster shall be limited to 10^4 hours as function of specific impulse. Thruster efficiency was specified by NASA as shown in Figure 5-1.

4) Total specific mass:

Values of the total specific mass of the solar array plus electric propulsion hardware were assumed as 25 to 30 kg/kw in trajectory data furnished by NASA/OART (a larger specific mass may be required in inbound missions).

5) Propellant tankage:

As specified by NASA/OART for preliminary mission analysis, the tankage mass is assumed to be three percent of the maximum propellant load.

6) Solar array power output:

As specified by NASA/OART, the solar array output power as function to solar distance (for distances above 0.66 AU) is assumed to be as shown in Figure 5-2.

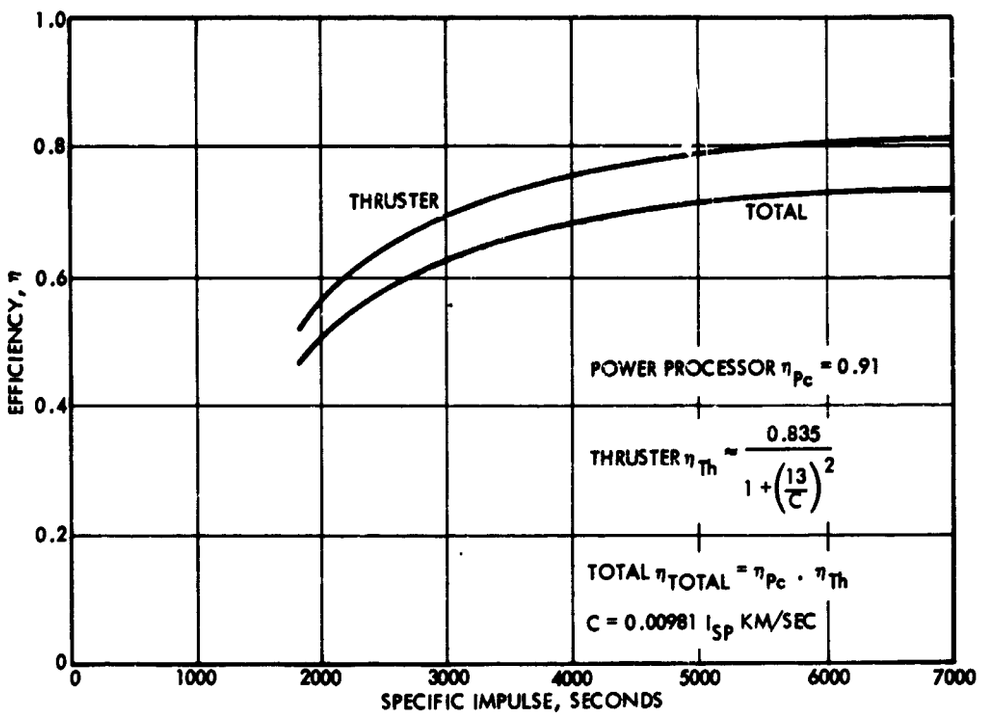

Figure 5-1. Mercury Electron Bombardment Thruster Efficiency (Nominal Technology)

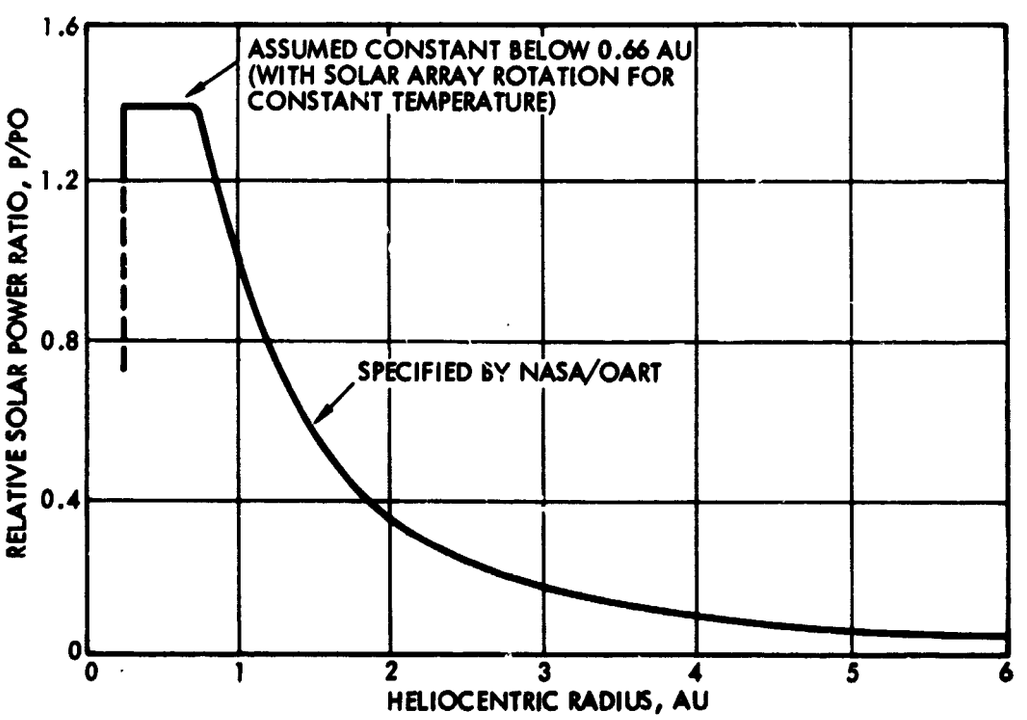

Figure 5-2. Relative Solar Power Ratio

For values below 0.66, we assume a constant power output for constant temperature achievable by array rotation away from the sun. This output is assumed valid between 0.66 and 0.3 AU.* (No thrust power will be needed for distances smaller than 0.3 AU).

5.3 CANDIDATE LAUNCH VEHICLES

The missions will be launched by boosters of the Titan family. Titan 3D/Centaur (5 segment solid strap-on version) will be considered as the prime booster for purposes of this study. If it is found that a smaller launch vehicle would be adequate to ensure the multi-mission aspects of the stage, the Titan 3B/Centaur (Core/Centaur), the Titan 3C/Burner 2 (with transtage) and Titan 3D/Burner 2 may also be considered. The latter two booster candidates were added to the list after the start of the study when it became apparent that the Titan 3B/Centaur gave insufficient performance. Booster performance curves as specified by NASA/OART are shown in Figure 5-3.

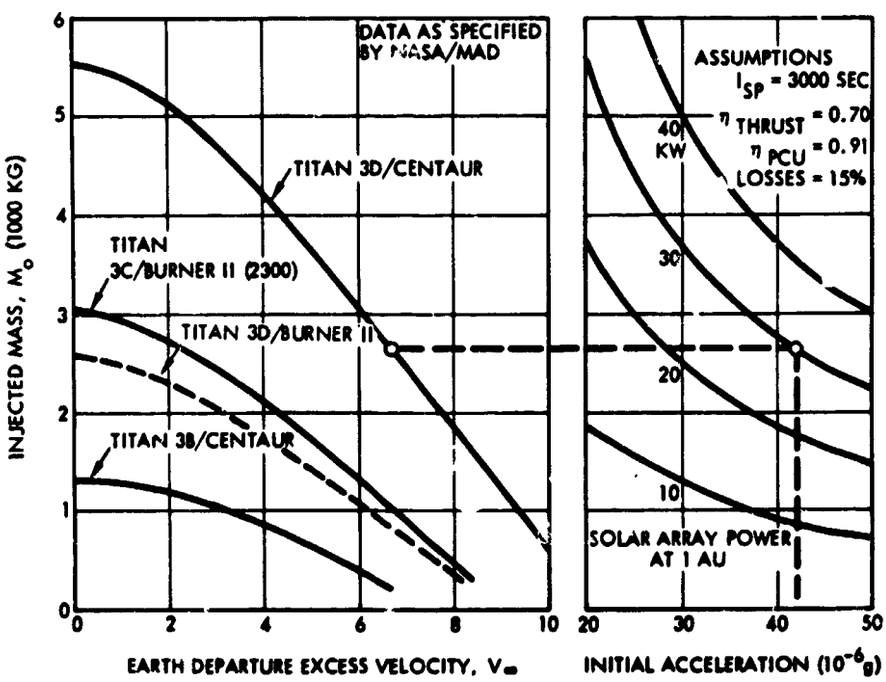

Figure 5-3. Injection Performance of Titan Family Boosters

*See also Section 7.1

The most recent cost estimates for the four Titan class boosters obtained from NASA/OSSA are given in Table 5-1. These estimates include all cost elements including launch support. The table also lists payload mass at a commor reference point (V_{∞} = 2 km/sec) and cost per kg of payload for the four boosters. The last column gives cost effectiveness figures expressed in payload mass per unit cost, in percent compared to Titan 3D/Centaur (100). The much larger cost-effectiveness of the two intermediate boosters compared to the Titan 3B/Centaur is apparent from these data. We note that Titan 3D/Burner 2 delivers about twice as much injected mass as Titan 3B/Centaur at a cost increase of only about $1.3 million and only about 20 percent less payload than Titan 3C/Burner 2 in the velocity range of interest at a cost saving of almost $5 million. Thus for certain lower energy missions the Titan 3D/Burner 2 is the most attractive intermediate cost, and intermediate performance booster alternative. According to information received from Martin-Marietta Co. integration of the Burner 2 with either Titan 3C or 3D would require the expenditure of $3.5 million of non-recurring cost. Neither of these booster options have active project status at present.

Table 5-1. Projected Cost Figures for Candidate Titan 3 Class Boosters (Revised Preliminary Planning Data from NASA/OSSA)

Launch Vehicle	Cost ($\$x10^6$)	Payload to V_{∞} = 2 km/sec (kg)	Cost-Effectiveness ($/kg)	(%)
Titan 3D/ Centaur	25.146	5130	4,900	100
Titan 3C/ Burner 2	22.340	2650	8,430	58.3
Titan 3D/ Burner 2	17.420	2200	7,920	61.9
Titan 3B/ Centaur	16.166	1180	13,700	35.8

The graph on the right in Figure 5-3 relates the injected mass M_o to the gross solar array power required at earth departure for a range of initial thrust accelerations, assuming representative values of specific

impulse, propulsion system efficiency and losses in gross power due to solar radiation effects, etc. Typical thrust acceleration requirements run from 30 to 50 micro-g in the specified missions, hence the solar array power for a Titan 3D/Centaur-launched electric stage falls in the 15 to 40 kw range. For the Titan 3C/Burner 2 and Titan 3D/Burner 2 the power requirement ranges between 8 and 25 kw.

In the launch vehicle performance curves we note a prounounced trend of proportionality such that the Titan 3C/Burner 2 has about 46 to 50 percent, Titan 3D/Burner 2 about 42 to 45 percent and Titan 3B/Centaur about 20 to 24 percent of the injection capability of the Titan 3D/Centaur for a given V_∞ in the velocity range of interest. This property is very useful in deriving electric stage payload performance data for the intermediate boosters by scaling from the precise data obtained for Titan 3D/Centaur and Titan 3B/Centaur.

5.4 PAYLOAD PERFORMANCE OF SOLAR ELECTRIC STAGE IN PRIMARY MISSIONS

5.4.1 Stage Launched by Titan 3D/Centaur

Based on the above booster and electric propulsion data the payload performance of the electric stage with optimal thrust pointing angles and specific impulse was obtained for the five primary missions as a function of mission time and propulsive power, as shown in Figures 5-4 and 5-5. The total specific mass of solar array plus electric propulsion hardware was assumed to be 25 and 30 kg/kw, respectively. The launch vehicle assumed here is Titan 3D/Centaur. These data were furnished by NASA/OART (Mr. A. C. Mascy) at the start of the study. Payload is expressed in terms of net spacecraft mass, i.e., the mass remaining after deducting solar array, electric propulsion and propellant mass. The disposable net payload mass to be carried by the stage is from 300 to 400 kg smaller than the net spacecraft mass to allow for structural and engineering subsystem mass allocated to the stage proper. (This initial estimate was subsequently substantiated by the design study; i.e., in the baseline stage design the weight difference is 340 kg.) The larger value of total specific mass, α = 30 kg/kw, assumed in this preliminary mission analysis was confirmed as realistic by the design study.

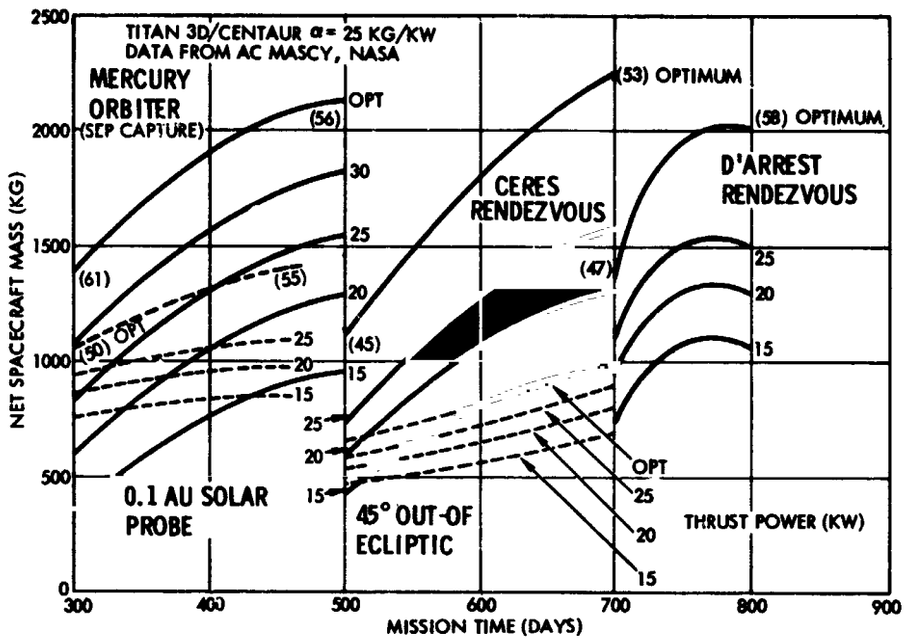

Figure 5-4. Net Spacecraft Mass vs Mission Time - Primary Missions (Specific Mass α = 25 kg/kw)

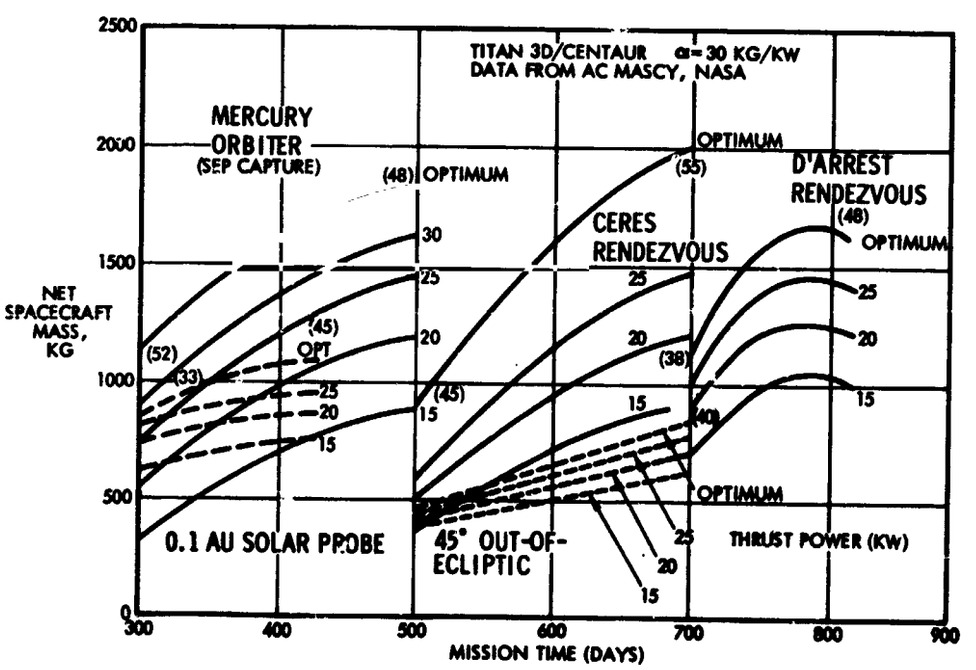

Figure 5-5. Net Spacecraft Mass vs Mission Time - Primary Missions (Specific Mass α = 30 kg/kw)

The results show that in all primary missions ample payload capacity is provided by power levels significantly lower than the "optimal" power level which falls in the 40 to 60 kw range. The largest values of payload obtainable for optimum power level are greatly in excess of what is needed for any of the primary missions. Hence the preference for the more economical and manageable power level in the 15 to 25 kw range.

The general trend of the curves shows a large increase in payload as mission time is increased. For the longest mission times in each category a power level of 15 kw provides a range of payload values from 600 to 1200 kg. For the missions with highest energy requirements, the solar probe and out-of-ecliptic mission, the net spacecraft mass ranges from 600 to 800 kg for this power level; for the three other, less demanding missions the payload range is between 900 and 1200 kg. These data correspond to theoretical optimum values of specific impulse that are in some cases below those attainable by foreseeable electric thruster technology development. The actual net spacecraft mass for the currently available specific impulse of 3000 sec is typically 10 percent lower than the data shown in the chart. Other weight reductions due to effects not reflected in this analysis, such as launch penalties, solar array degradation and nonoptimal thrust pointing must also still be taken into account (see Section 6). These add up to about 10 percent of further net payload loss.

Figure 5-6 through 5-8 show payload as function of propulsion power (referenced to 1 AU) for several primary missions, and indicate the effect on payload of operating at a fixed specific impulse I_{sp} = 3000 sec rather than at the theoretical optimum value which varies with power level. The payload difference can become appreciable in the lower range of power levels where the theoretical optimum I_{sp} values are very low, particularly in rendezvous missions with a target far from the sun. In these missions the very low theoretical I_{sp} value indicates that the system would operate more effectively if more thrust per unit power were available, i.e., if the specific impulse could be lowered. For area missions such as the 1 AU extra-ecliptic probe the I_{sp} influence on payload is negligible. A more detailed explanation of these factors will be given in Appendix A.

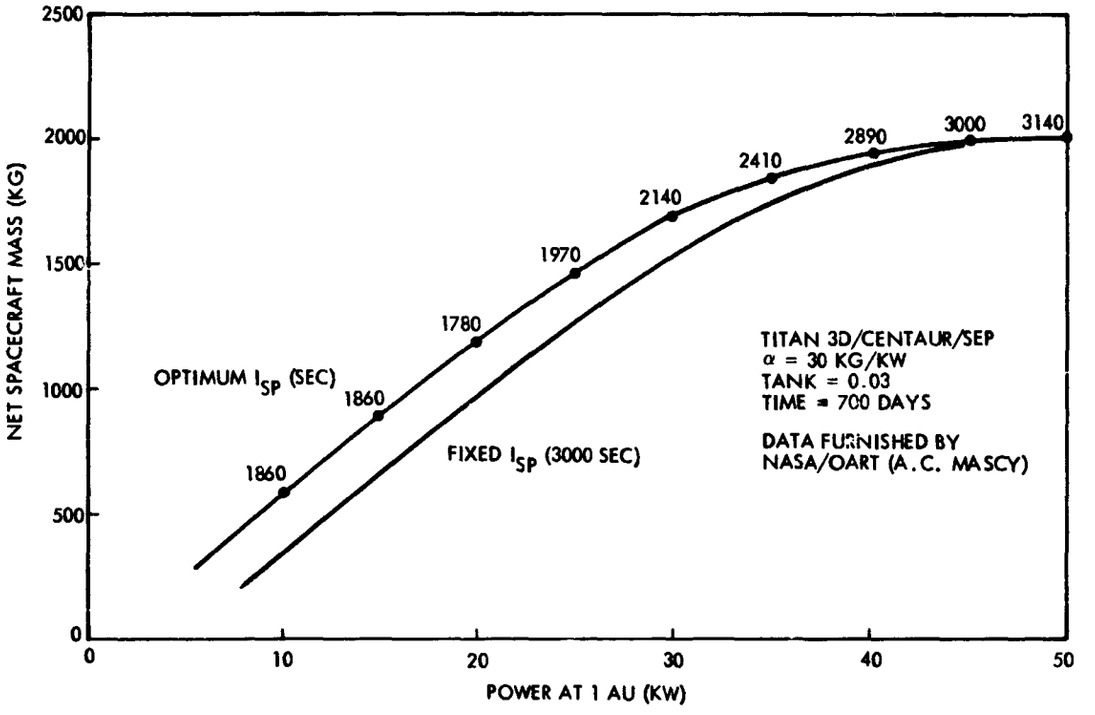

Figure 5-6. Net Spacecraft Mass vs Propulsion Power for 700-Day Ceres Rendezvous (1978)

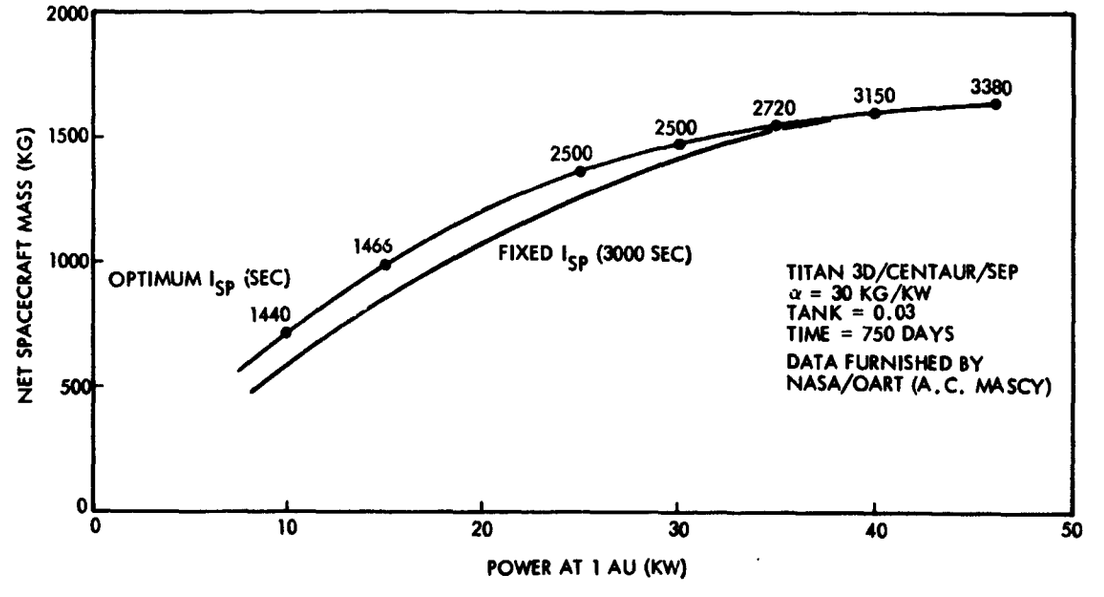

Figure 5-7. Net Spacecraft Mass vs Propulsion Power for 750-Day D'Arrest Rendezvous (1982)

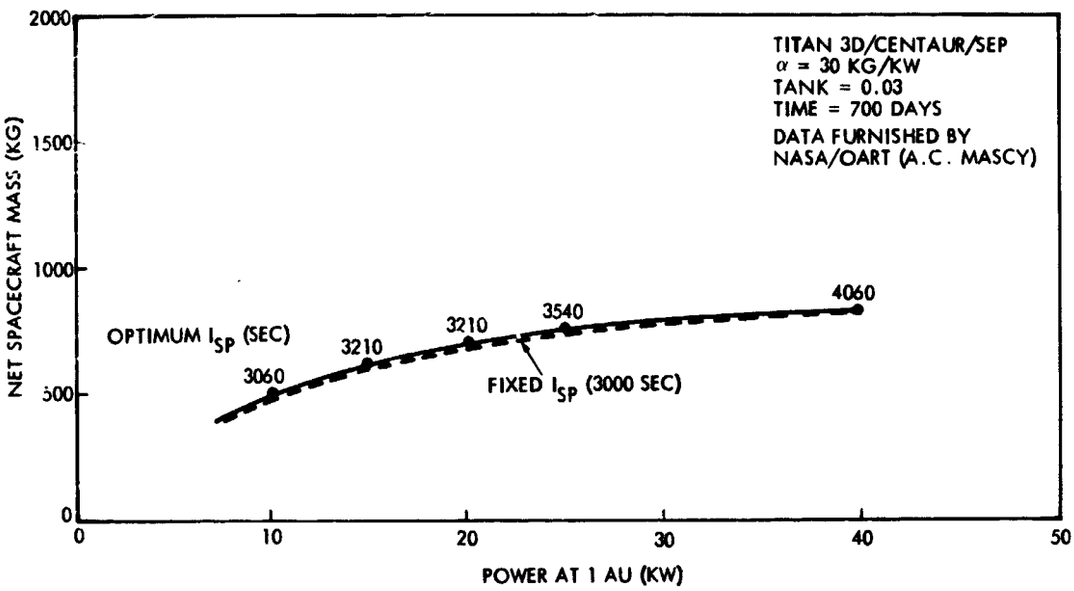

Figure 5-8. Net Spacecraft Mass vs Propulsion Power for 700-Day Extra-Ecliptic Mission (45°)

5.4.2 Stage Launched by Alternate Boosters

The payload performance achievable with the smaller launch vehicles Titan 3B/Centaur and Titan 3C/Burner 2 is shown in Figures 5-9 and 5-10. A specific mass of 30 kg/kw was assumed. Results for Titan 3D/Burner 2, not shown here, are very similar to those for Titan 3C/Burner 2, the payload mass being about 10 percent lower as a result of the slightly lower injection capability of Titan 3D/Burner 2. The payload mass obtained from a Titan 3B/Centaur launch is marginal in most primary missions, even with a near-optimal power level of 12 kw, Figure 5-9. However launch by the intermediate booster Titan 3C/Burner 2 gives an adequate payload capacity at least in the less critical missions to D'Arrest, Ceres, and Mercury, Figure 5-10. The upper power level of 15 kw indicated in the graph is nearly optimal with this booster/stage combination. We note that the payload data shown here are again reference values for theoretical optimum I_{sp}. The actual payload mass for I_{sp} = 3000 sec is about 5 percent lower.

From these results we conclude that the 15 kw electric stage provides adequate to excellent net payload capacity in all specified primary missions when launched by Titan 3D/Centaur, but at best only adequate capacity in some missions when launched by the medium class Titan.

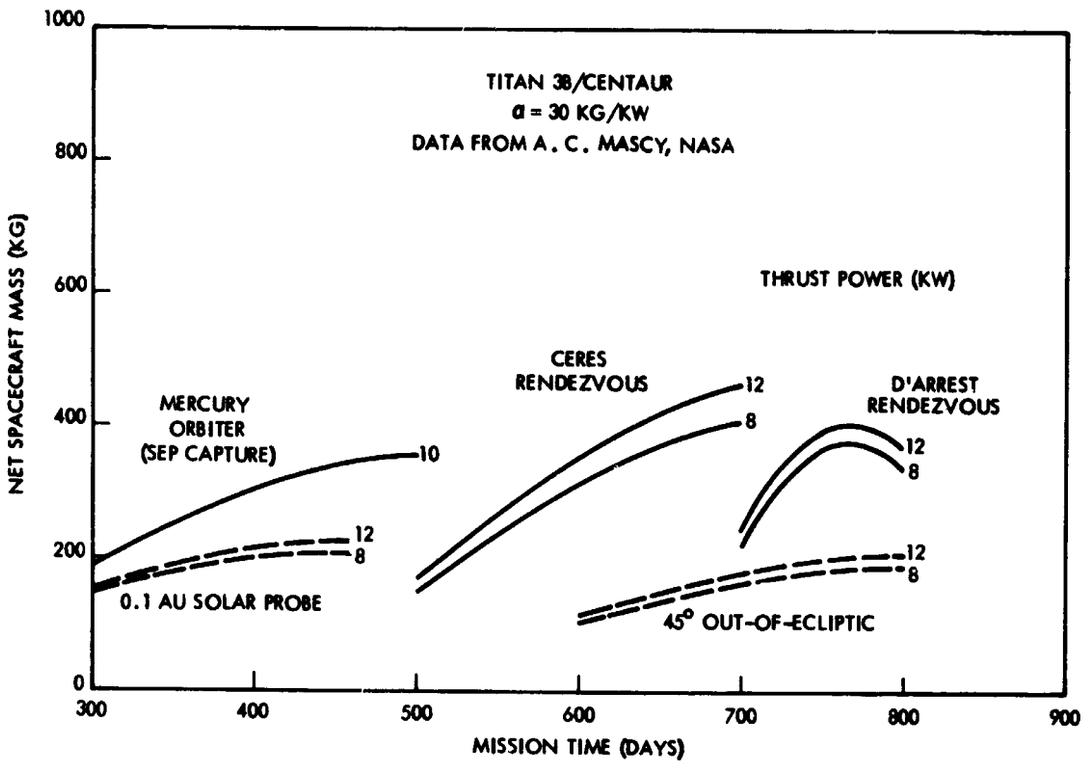

Figure 5-9. Net Spacecraft Mass vs Mission Time in Primary Missions (Titan 3B/Centaur)

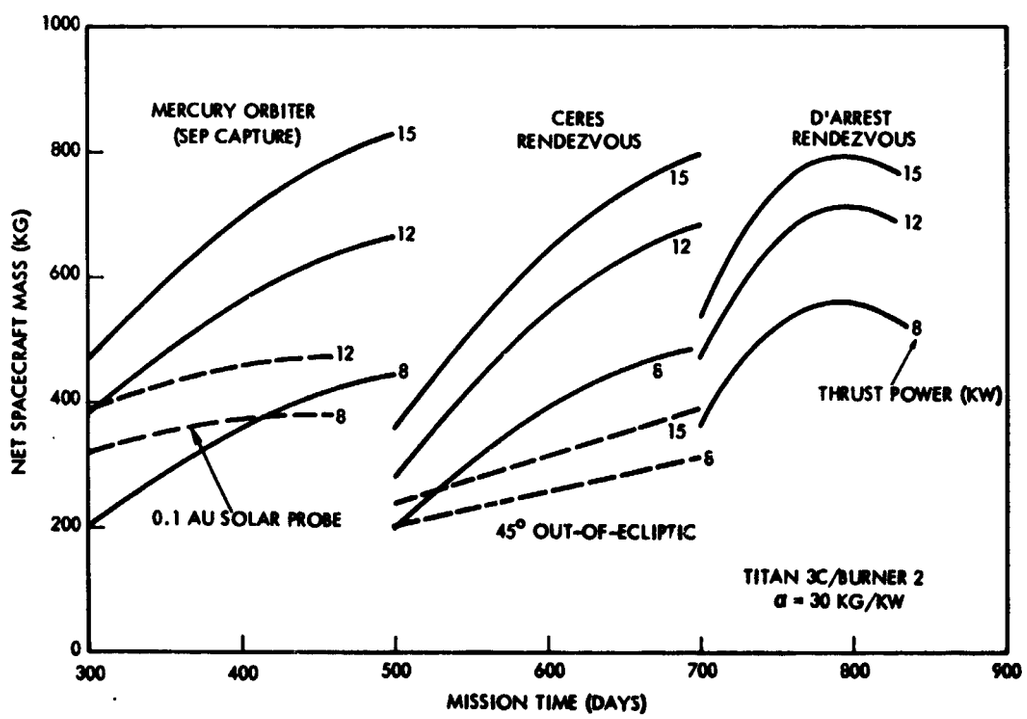

Figure 5-10. Net Spacecraft Mass vs Mission Time in Primary Missions (Titan 3C/Burner 2)

The payload capacity of a 10 to 12 kw stage launched by Titan 3B/Centaur would be marginal even in the less critical mission types. In order to obtain the best multi-mission capability plus the growth potential desired for advanced missions we selected the Titan 3D/Centaur as primary booster, but with the option of considering one of the intermediate Titans as candidates for the less energetic missions, pending a decision by NASA in regard to the possible acceptance and integration of Burner 2 as an upper stage. The Titan 3B/Centaur was eliminated from further consideration in this study.

5.5 PAYLOAD PERFORMANCE IN SOME ALTERNATE MISSIONS

Alternate missions considered for the electric stage include outer planet flyby and orbiter missions, Mars and Venus high data rate orbiters, and a deep space communications relay. In this section the adaptability and mission performance of the stage will be evaluated based on a nominal propulsion power level of 15 kw but with some possible alternate power options.

5.5.1 Outer Planet Missions

In outer planet flyby and orbiter missions the electric stage is jettisoned after completing the thrust phase, and the payload package continues the mission independently as an autonomous spacecraft. Because of the rapidly decreasing solar-electric power in these outbound missions the stage would not provide any useful function at destination except possibly in a Jupiter flyby or orbiter mission.

One of the principal advantages of this concept is the relatively short mission life required of the stage, commensurate with typical mission life in the primary missions which does not exceed 2 to 3 years. An integral electric spacecraft intended for outer planet missions would have to survive for 8 years or longer in some cases.

The payload spacecraft could be a vehicle such as the TOPS or Pioneer outer planet probe which will be available and flight-proven prior to the development of the stage (References 5-1, 5-2). Design compatibility of the stage with these vehicle types will be discussed in Section 6. In the case of orbiter missions the payload spacecraft must carry its own retro-propulsion system. A major objective of this analysis is to

determine whether the electric stage is capable of providing the additional mass for retro-propulsion required in critical outer planet missions. These are the orbiter missions to Uranus and Neptune which cannot be performed with an adequate payload by the TOPS vehicle using even the most advanced Titan class booster currently being contemplated.

Figure 5-11 shows the stage payload delivery capacity versus flight time for TOPS and Pioneer-type vehicles in missions to Jupiter, Saturn, Uranus, and Neptune based on data from Horsewood and Mann (Ref. 5-4). The assumed power level is 15 kw. Each curve shows a discontinuous slope at a point designating the cross-over of direct and indirect low-thrust mission characteristics (Ref. 5-5). The indirect mode represented by the upper branch of each curve, uses an initial inward maneuver toward the sun to gain performance. This mode out-performs the direct mode when flight time is sufficiently extended. In this diagram the upper curves (solid lines) indicate net spacecraft mass for each of the four planetary targets, the lower curves (dashed lines) indicate net payload, which, in this case, actually means the entire payload spacecraft. The shaded area represents an allowance for structural and subsystem mass, assumed conservatively as 400 kg.

Mass brackets for Pioneer and TOPS type flyby and orbiter vehicles are shown, based on data from Refs. 5-1, 5-2 and 5-3. We note that the 15 kw stage gives ample payload performance for all planetary targets except in TOPS orbiter missions to Uranus and Neptune. A higher power level than 15 kw might be indicated here.

Actually a more detailed investigation of orbiter missions would be required taking into consideration approach velocities and orbital parameters which is beyond the scope of this study. For simplified analysis we have assumed a nominal orbit insertion maneuver capability of 1500 to 1800 m/sec, sufficient to establish the vehicle in a highly eccentric orbit at the target planet assuming approach velocities of 8 to 10 km/sec.

As an alternative we have also considered electric stage missions that would take advantage of Jupiter or Saturn swingby maneuvers. Figure 5-12 shows the increased payload capacity versus flight time achievable with the aid of a Jupiter swingby maneuver. Jupiter would be reached by an indirect low-thrust trajectory. The curves represent

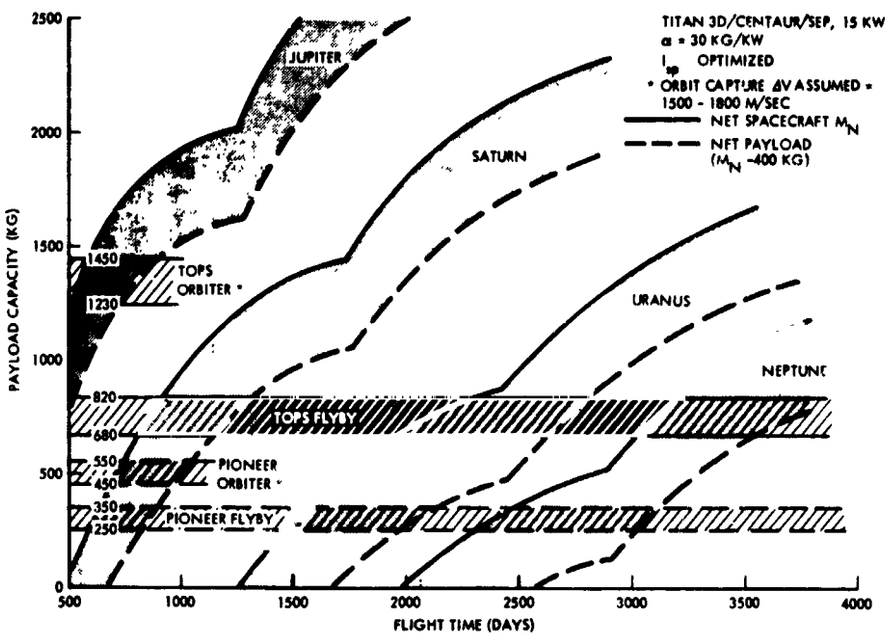

Figure 5-11. Electric Stage Delivery Capacity for TOPS and Pioneer Vehicles

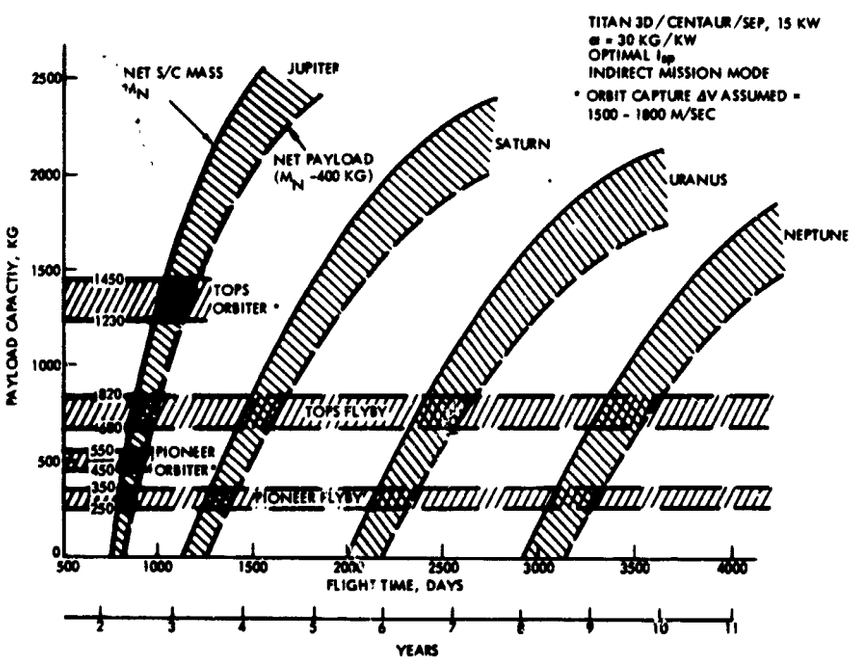

Figure 5-12. Payload Capacity vs Flight Time for SEP Outer Planet Missions via Jupiter (Extrapolated Data)

average performance conditions, extrapolated from Refs. 5-1 and 5-7. The results indicate that adequate payload capacity is obtainable even for reasonably fast Uranus and Neptune missions. However in the latter case the approach velocities are very large (on the order of 15 to 20 km/sec) requiring orbit insertion maneuvers of at least 4 km/sec. The available payload capacity indicates that a vehicle of the Pioneer class (300 to 350 kg) could be placed into Uranus orbit with flight times of 8 to 9 years, and into a Neptune orbit with flight times of about 11 years.

It is interesting to compare these low-thrust mission characteristics with ballistic missions that use either the Titan 3D(5 segment) / Centaur/Burner 2 (1440 lbs) or the Titan 3D(7 segment, Stretched First Stage) /Centaur/Burner 2 (2336 lbs). The latter booster is the largest Titan-class booster currently being considered. Its injection capability at V_∞ = 10 km/sec is 1500 kg, or about 600 kg larger than that of the standard vehicle plus Burner 2. Figure 5-13a shows the payload delivered to Saturn, Uranus and Neptune by the SEP stage (solid curves) and by ballistic launch (dashed curves). Figure 5-13b shows a similar comparison but for missions with Jupiter swingby.

In the first case the cross-over point where the SEP stage payload exceeds the ballistic payload occurs at 2.5 and 4 years for Saturn, at 5.7 and 7.1 years for Uranus and at 8 and 8.4 years for Neptune. The maximum SEP stage payload exceeds that achievable with the growth version of Titan 3D/Centaur by more than 500 kg. In the second case the SEP performance curves show longer mission times than the ballistic curves in all cases, but achieve at least 800 kg more payload than the large Titan.

On this basis we conclude that the mass penalty associated with the electric stage concept (generally less than the 400 kg allowance mentioned before) reduces the large overall performance potential of the SEP missions but leaves a sufficiently large performance margin compared to the purely ballistic missions to permit the achievement of advanced flyby, entry probe and orbiter missions to Uranus and Neptune, with and without the aid of a Jupiter swingby. The fundamental question as to the weight-effectiveness of the electric stage concept in missions where it operates in the "pure stage" mode can thus be answered affirmatively.

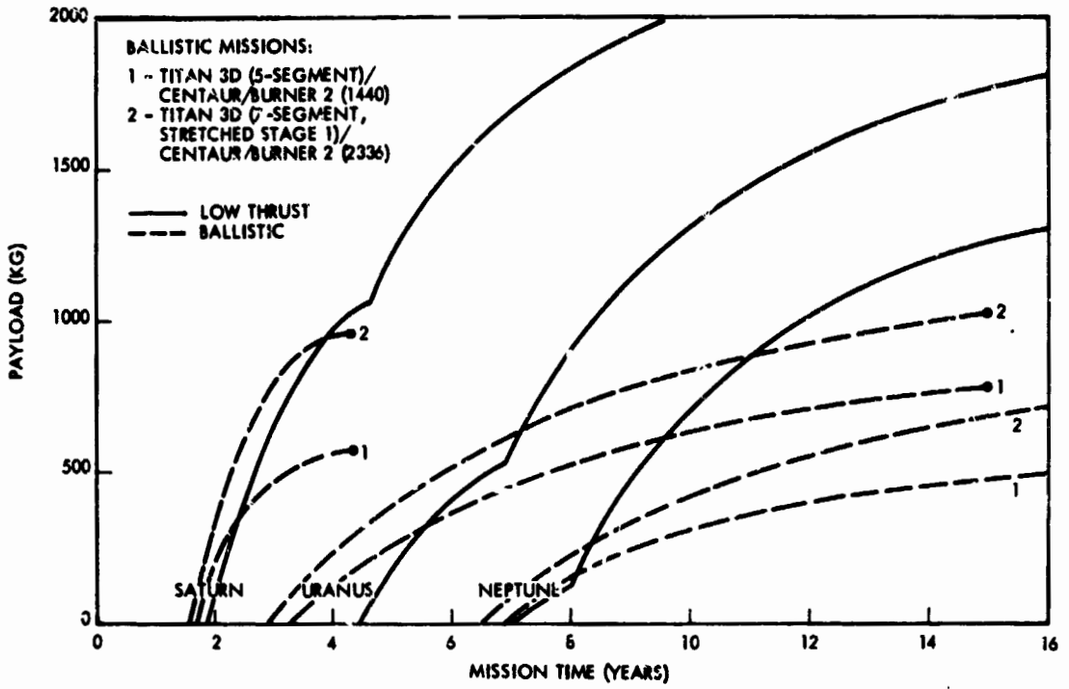

Figure 5-13a. Comparison of Low-Thrust and Ballistic Outer Planet Missions

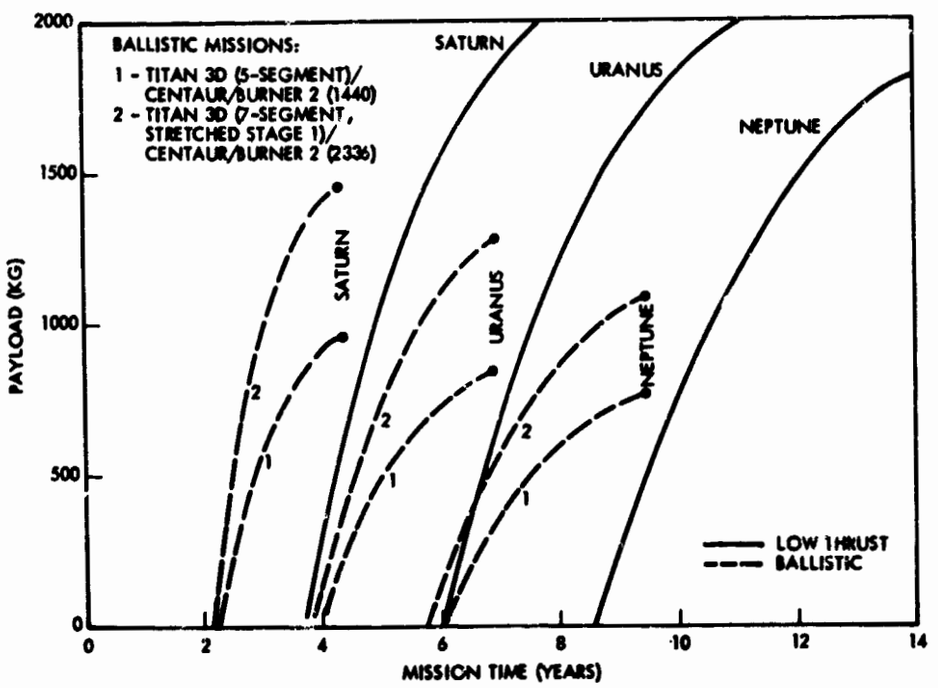

Figure 5-13b. Comparison of Low-Thrust and Ballistic Outer Planet Missions with Jupiter Swingby

The electric stage facilitates relatively fast, weight-effective missions to the outer planets without necessarily requiring a Jupiter swingby with its time constraint, complexity and potential hazard. However, more comprehensive comparisons of these mission capabilities are still required.

5.5.2 Mars and Venus Orbiter

In this class of missions the electric stage is used to achieve rendezvous with the planet at nearly zero velocity to minimize the orbit capture velocity requirement. A small retro velocity increment of only a few hundred meters/sec suffices to establish an eccentric initial orbit, assuming dimensions of 2 by 38 planetary radii. As in the case of the Mercury orbiter low-thrust capture could also be achieved, at least in the case of Venus where the thrust acceleration is about 35 percent larger than at departure from earth. After orbit insertion the stage is used for orbit control to lower the apoapsis, to change the apsidal orientation or the orbital inclination as dictated by scientific objectives. The large unused power level can be used in the case of the Venus orbiter to operate a synthetic array, side looking radar for enhanced ground resolution. In both Mars and Venus missions the large power level also is useful to operate at high transmitter power for high-data rate telemetry of planetary images. These objectives justify the retention of the stage through the orbital phase of the mission. (Refs. 1-5, 5-8.)

Figure 5-14 shows the payload performance versus mission time for both targets, based on data from Horsewood and Mann (Ref. 5-4). Since the net spacecraft mass is extremely large for the primary launch vehicle, Titan 3D/Centaur, we have also considered a smaller stage power of 10 kw and a smaller launch vehicle, Titan 3C/Burner 2. Even in this case both missions can be performed with a net spacecraft mass of about 2000 kg or a net payload of 1600 to 1700 kg. The extra payload capacity could be employed to carry an entry and/or lander probe of nearly 1500 kg in the case of a Titan 3C/Burner 2 launch, or nearly 3000 kg with Titan 3D/Centaur. We note that mission time has relatively little influence on payload mass. In the Venus orbiter case the indirect mission mode (Mode B) would increase the payload by 500 kg while doubling the mission time to 400 days or more; this trade is therefore not warranted.

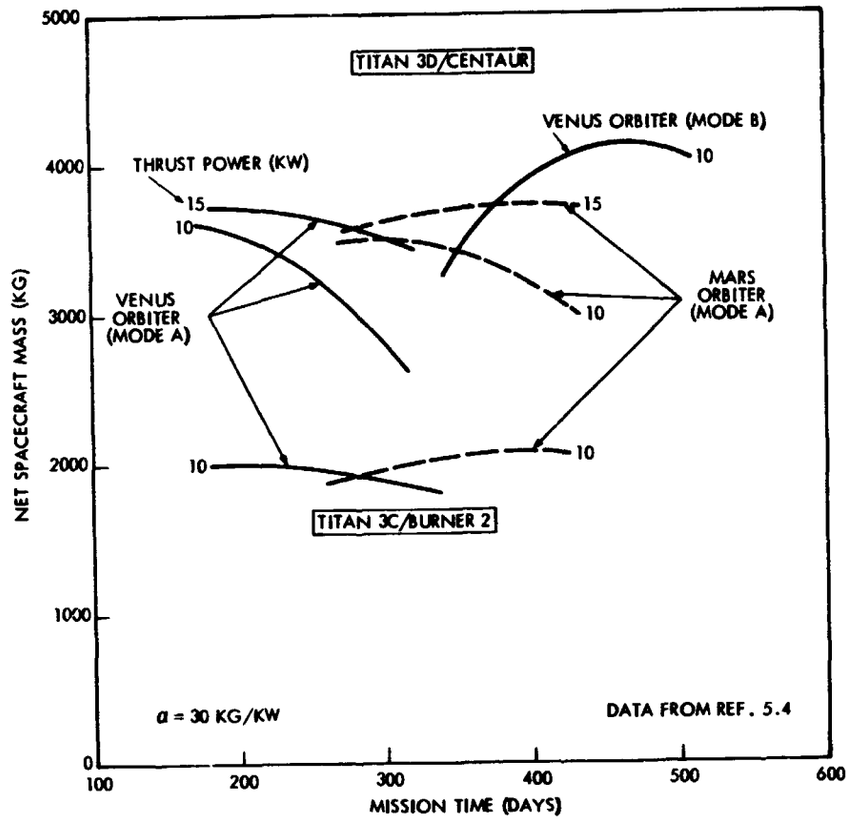

Figure 5-14. Net Spacecraft Mass vs Mission Time - Mars and Venus Orbiters

5.5.3 Deep Space Communications Relay

A 4 AU deep space communications relay station originally postulated as one of the alternate missions has limited usefulness because it can serve only those space probes which are at relatively close distance i.e., within about 1.3 AU, in order to compete with direct signal transmission to an 85-ft DSIF antenna on the ground. This assumes a 30-ft antenna diameter for the relay station. To compete with direct transmission the 210-ft DSIF antenna the space probe-to-relay station distance must be less than 0.45 to 0.7 AU depending on earth's position relative to the two vehicles.

A much greater advantage can be gained by a relay stationed permanently at 1 AU from the sun and about 160 to 170 degrees away from earth. This stationary vehicle can relay to earth signals from space probes that are temproarily unable to communicate directly due to sun obscuration (i.e., at positions near superior conjunction or syzygy).

In addition, any space probes within 0.4 to 0.7 AU of the relay can use the relay link to advantage in transmitting to the 85-ft DSIF antenna even if not at syzygy. This relay station can serve probes inside 1 AU such as Venus, Mercury, solar and cometary probes, as well as those at the distance of Mars. If the stationary 1 AU relay is used in addition for the second purpose of monitoring solar phenomena not observable from earth to provide advance warning of severe solar activity a potentially very valuable mission concept might be defined.

A preliminary analysis of propulsion requirements shows that for a relay station at 1 AU between 170 and 180 degrees from earth the propellant ratio is about 22 percent. The vehicle uses low thrust on leaving earth and in station acquisition. The time to station acquisition is 1.80 years. A 10 kw version of the stage launched by the lowest performance booster candidate, Titan 3B/Centaur, would have a net spacecraft mass of about 720 kg or 350 kg of net payload. Even this capacity appears excessive for the purpose of the mission. If the extra payload capacity is used to increase the receivng antenna from the initially assumed 10 m size the additional complexity of high-precision vehicle and/or antenna pointing must be resolved.

5.6 SELECTION OF LAUNCH VEHICLE AND NOMINAL PROPULSION POWER

On the basis of the foregoing discussion and the results obtained on payload capacity in the various primary and alternate missions we have selected the Titan 3D/Centaur as the primary launch vehicle and designed the stage for a net propulsion power of 15 kw at earth departure. With a net spacecraft mass range starting at about 500 kg for the more demanding missions, and a corresponding net (science) payload capacity of at least 100 to 150 kg we have an ample growth margin for as yet undefined payload instruments. In addition the stage can carry a small daughter probe on missions where the scientific value will be enhanced by measurements made at separate observation points as discussed in Section 4 e.g., comet probes, asteroid probes, out-of-ecliptic probes, etc.

Table 5-2 lists typical ranges of net spacecraft mass and net payload capacity obtainable with this choice of a nominal launch vehicle and

Table 5-2. Range of Available Net Spacecraft Mass and Net Payload Capacity Compared to Desirable Payload Capacity in Six Primary Missions

(TITAN 3D/CENTAUR; α = 30 KG/KW; PROPULSION POWER 15 KW; I_{SP} = 3000 SEC)

ITEMS \ MISSIONS	1 CERES RENDEZVOUS	2 D'ARREST RENDEZVOUS	3 ENCKE RENDEZVOUS	4 EXTRA-ECLIPTIC 45°	5 MERCURY ORBITER (SEP)	6 SOLAR PROBE 0.1 AU
FLIGHT TIME (DAYS)	700	750	950	700	402	400
DEPARTURE VELOCITY (KM/SEC)	8.5	8.0	8.0	7.5	8.0	8.0
NOMINAL INJECTED MASS (KG)	1590	1860	1860	2143	1860	1860
NET SPACECRAFT MASS (KG)	660	810	927	564	572	823
NET PAYLOAD CAPACITY* (KG)	260	410	427	164	172	373
DESIRED INSTRUMENTATION**						
- ATTACHED TO STAGE (KG)	50	50	50	80	100	90
- ON DAUGHTER PROBE (KG)	25	30	30	25	—	25
INSTRUMENTATION PLUS SUPPORT **						
- ATTACHED TO STAGE	90	90	90	120	140	130
- DAUGHTER PROBE (TOTAL)	100	120	120	75	—	75
TOTAL DESIRED CAPACITY (MIN)**	90	90	90	120	140	130
TOTAL DESIRED CAPACITY (MAX)***	360	380	380	450	370	300

*ASSUMES 390 KG FOR STAGE STRUCTURE + SUBSYSTEMS IN ALL CASES EXCEPT IN ENCKE (400 KG) AND SOLAR MISSION (450 KG)

**MINIMUM VALUES FROM TABLE 4-8.

***MAXIMUM VALUES FROM TABLE 4-8.

nominal power level and indicates estimates of the desired minimum instrumentation mass including supporting equipment, mounting and articulation platforms and payload mass contingencies. In view of the limited investigation devoted during this study to payload definition additional effort is still required to determine the best utilization of the stage in various missions and the best allocation of its payload carrying capacity.

Figure 5-15 shows a bar graph of estimated payload capacity in the primary and alternate missions, assuming 15 kw of net propulsion power, a nominal specific impulse of 3000 sec and a specific mass α = 30 kg/kw. In some missions, such as the solar probe mission, Mercury orbiter and comet Encke rendezvous a somewhat higher value of α may be necessary to account for spare power conditioning equipment. An increase of the number of thrusters for inbound missions is not considered necessary since the thruster module will be designed for the largest thrust power available in any mission, in the interest of multi-mission commonality.

In selecting the nominal power level of 15 kw the option of providing either a larger or smaller power level in some missions is retained. A truncated solar array provides 10 to 12 kw of propulsion power in missions such as the lower-energy Mars orbiter, Venus orbiter, and the 1 AU communications relay and solar monitor mission. For growth missions such as Halley's comet rendezvous and Mars sample return an increase to 20 kw of propulsion power may be required for adequate payload capacity, as will be discussed below. A change of power level upward or downward from the nominal by a comparably small increment can be accomplished more readily and at lower cost than a large increase from a smaller nominal value of say 10 kw to an extended capability of 20 kw for growth missions. We believe that the larger initial development cost and recurrent costs associated with a 15 kw stage permit long-term cost savings by making the nominal stage compatible with a larger number of high energy missions without power level modification, and by providing a better baseline for adaptation to future growth requirements.

The possibility of major cost savings per mission either by recourse to a smaller booster (Titan 3D/Burner 2) and truncated power level in

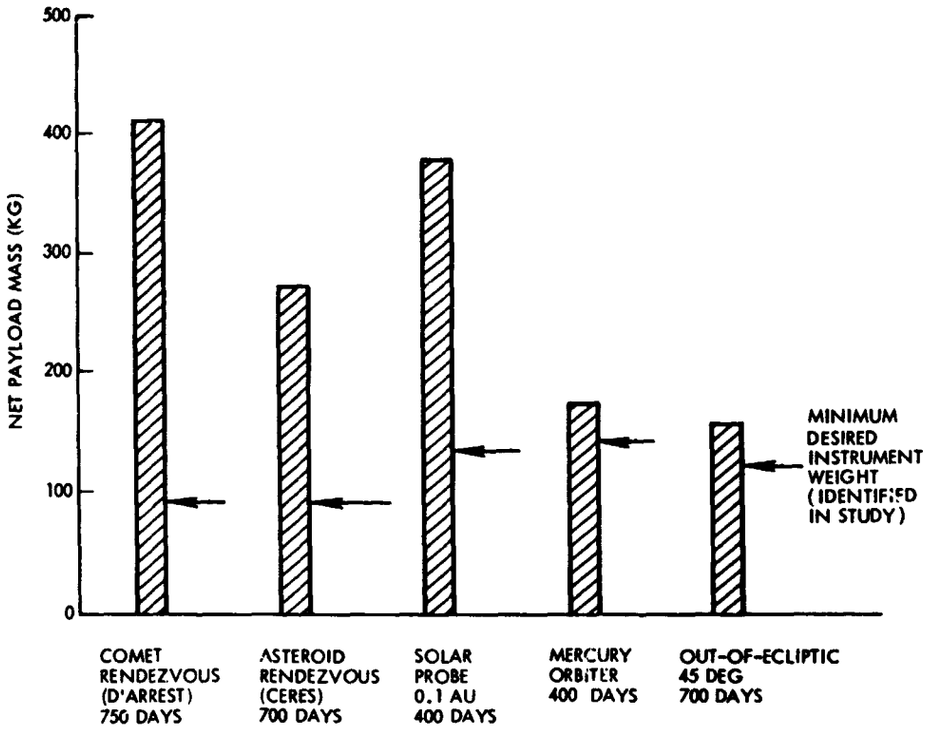

Figure 5-15a. Payload Capacity by Mission at 15 kw Power Level (Primary Missions)

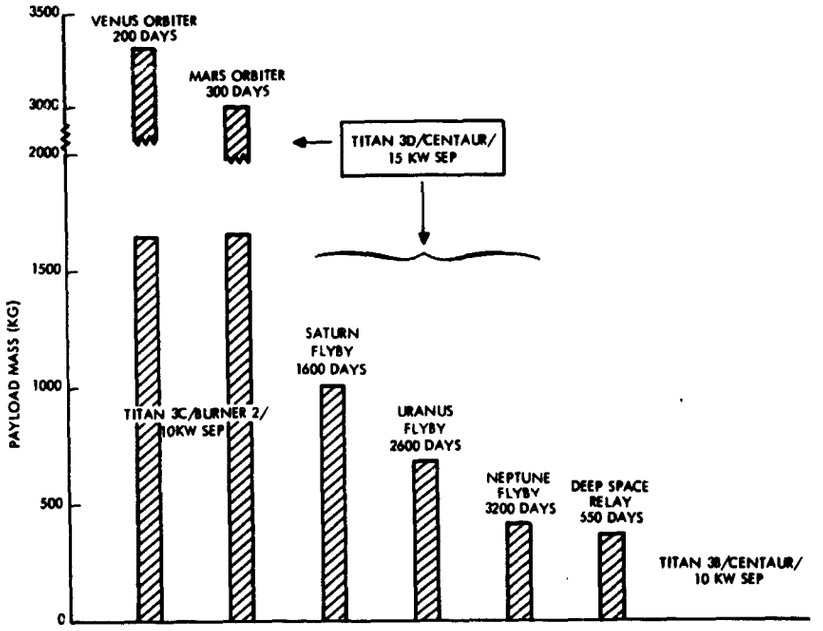

Figure 5-15b. Payload Capacity by Mission at 15 kw Power Level (Alternate Missions)

lower energy missions, or by a dual launch of the nominal 15 kw stage from a Titan 3D/Centaur has been explored and will be discussed in a subsequent section.

5.7 NOMINAL MISSION CHARACTERISTICS FOR PRIMARY MISSIONS

A complete set of nominal mission characteristics, including the trajectory profile, and time histories of solar radius, longitude, latitude, propulsion power, thrust acceleration, steering angles, communication distance and antenna pointing angles were obtained (using the QUICKTOP trajectory optimization program furnished by NASA) for these primary missions:

- Asteroid Ceres rendezvous (1978)* - 700 days
- Comet D'Arrest rendezvous (1982) - 750 days
- Comet Encke rendezvous (1980) - 950 days
- 45° Extra-ecliptic mission (1980) - 700 days
- Mercury orbiter (1981) - 400 days
- 0.1 AU solar probe - 400 days

The mission years were selected for favorable mission performance. The nominal booster Titan 3D/Centaur and a nominal power level of 15 kw at 1 AU was assumed. Allowance for a non-optimal specific impulse of 3000 sec was made in payload performance.

Principal characteristics of the 6 missions are summarized in Table 5-3. Trajectory plots are presented in Figures 5-16a through 5-16f and time histories of solar distance, power variation, and thrust acceleration in Figures 5-17 through 5-21. Other mission profile characteristics are given in Appendix B.

The results are in good agreement with initial data furnished by A. C. Mascy of NASA/OART and with data contained in the comprehensive

*Arrival years in parenthesis.

Table 5-3. Nominal Mission Profile Characteristics of Primary Missions

		CERES RENDEZVOUS	D'ARREST RENDEZVOUS	ENCKE RENDEZVOUS	EXTRA-ECLIPTIC	MERCURY ORBITER	SOLAR PROBE
Mission Time	(days)	700	750	950	700	402	400
Thrust Time	(days)	671	704	914	521	311	252
Departure Date t_o		Oct. 8, 76	Aug. 28, 80	Mar. 7, 78	Sept. 21, 78	Jun 9, 80	Open
Arrival Date t_1		Sept. 8, 78	Sept. 17, 82	Oct. 12, 80	Aug. 25, 80	July 14, 81	Open
Arrival Relative to Perihelion	(days)	--	0	-50	--	--	--
Departure Asymptotic Velocity	(km/sec)	8.5	8.0	8.0	7.5	8.0	8.0
Arrival Asymptotic Velocity	(km/sec)	0	0	0	--	0	--
Solar Distance, Maximum	(AU)	2.92	2.27	3.35	1.0	1.07	1.0
Solar Distance, Minimum	(AU)	0.93	1.0	(1.0)*	0.78	0.37	0.1
Solar Distance at t_1	(AU)	2.92	1.30	1.10	1.0	0.37	0.1
Earth Distance, Maximum	(AU)	3.6	3.25	4.0	1.72	1.54	1.95
Earth Distance at t_1	(AU)	2.4	0.8	0.4	1.66	0.85	0.95
Heliocentric Travel Angle	(deg)	282	340	233	810	810	900
Maximum Heliocentric Latitude	(deg)	-6.5	+18.2	+11	+45	+6.8	0
Orbit Inclination at t_1	(deg)	10.61	19.61	12.4	45	7.0	0
Maximum Variation of Thrust Cone Angle	(deg)	20	94	156	42	90	0
Approximate Average Thrust Cone Angle	(deg)	85	~90	~90	93	96	0
Maximum Variation of Thrust Cone Angle	(deg)	147	170	>360	305	158	0

*Minimum distance during extended mission = 0.34 AU

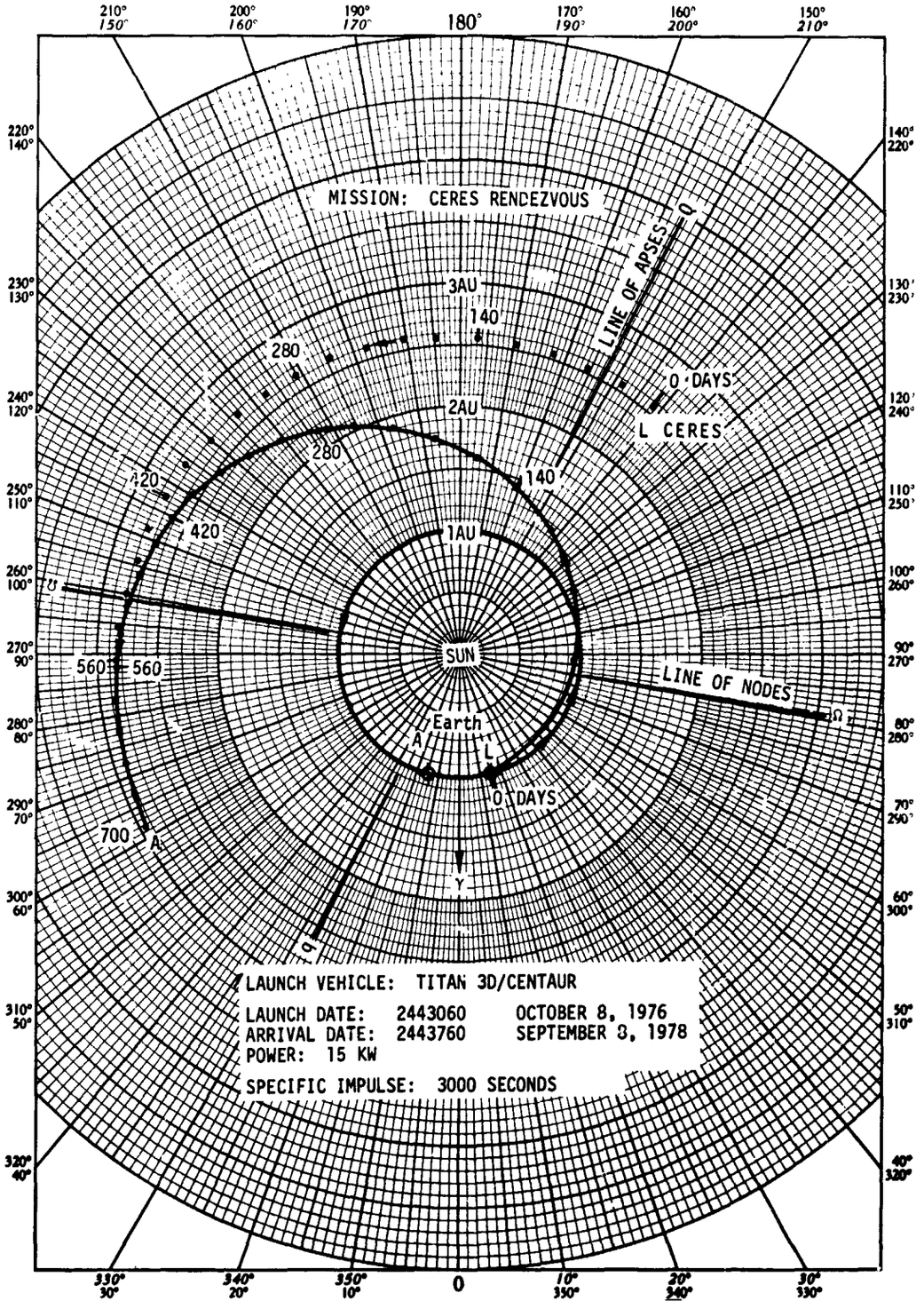

Figure 5-16a. Trajectory Profile - Ceres Rendezvous

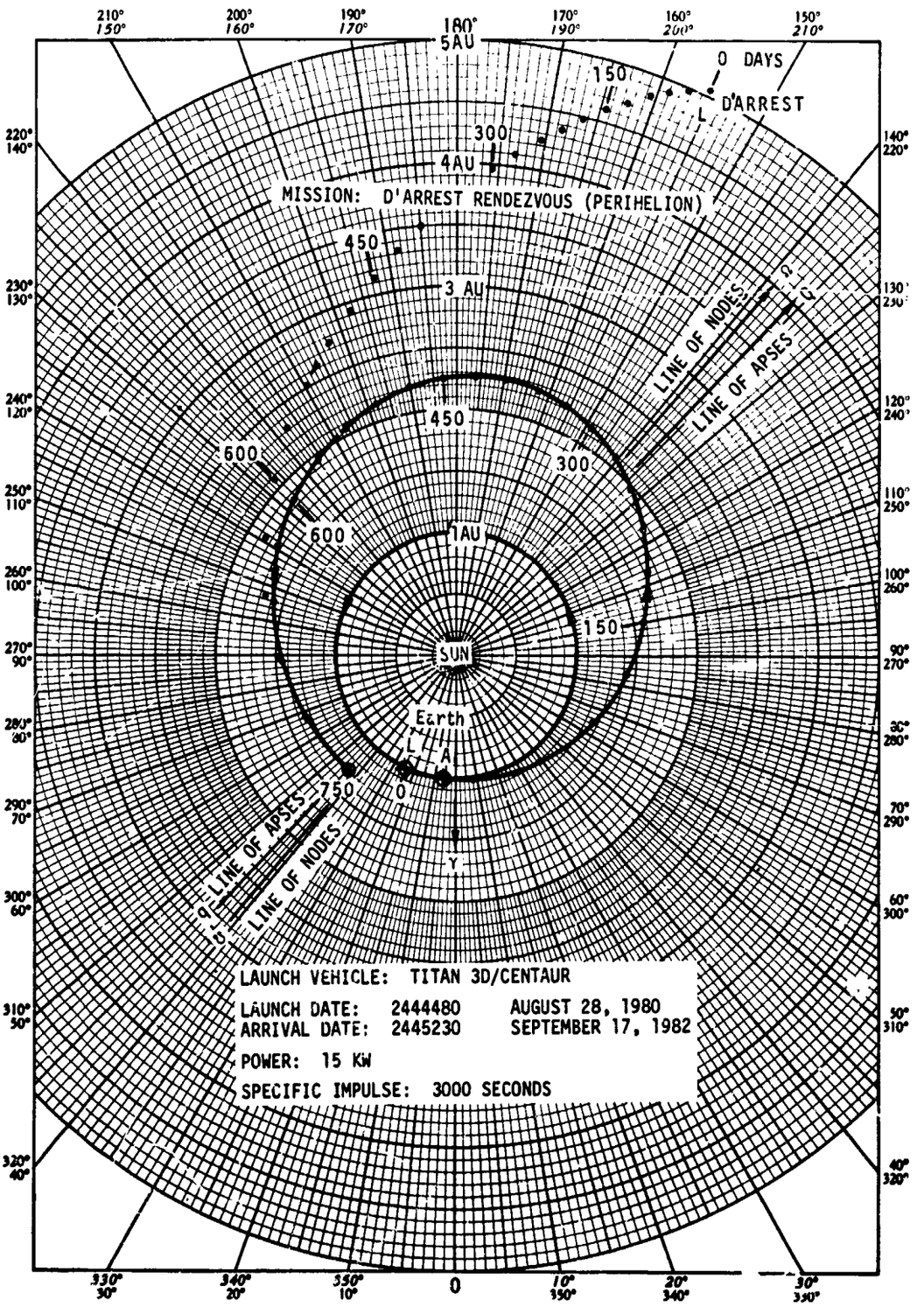

Figure 5-16b. Trajectory Profile - D'Arrest Rendezvous (Perihelion)

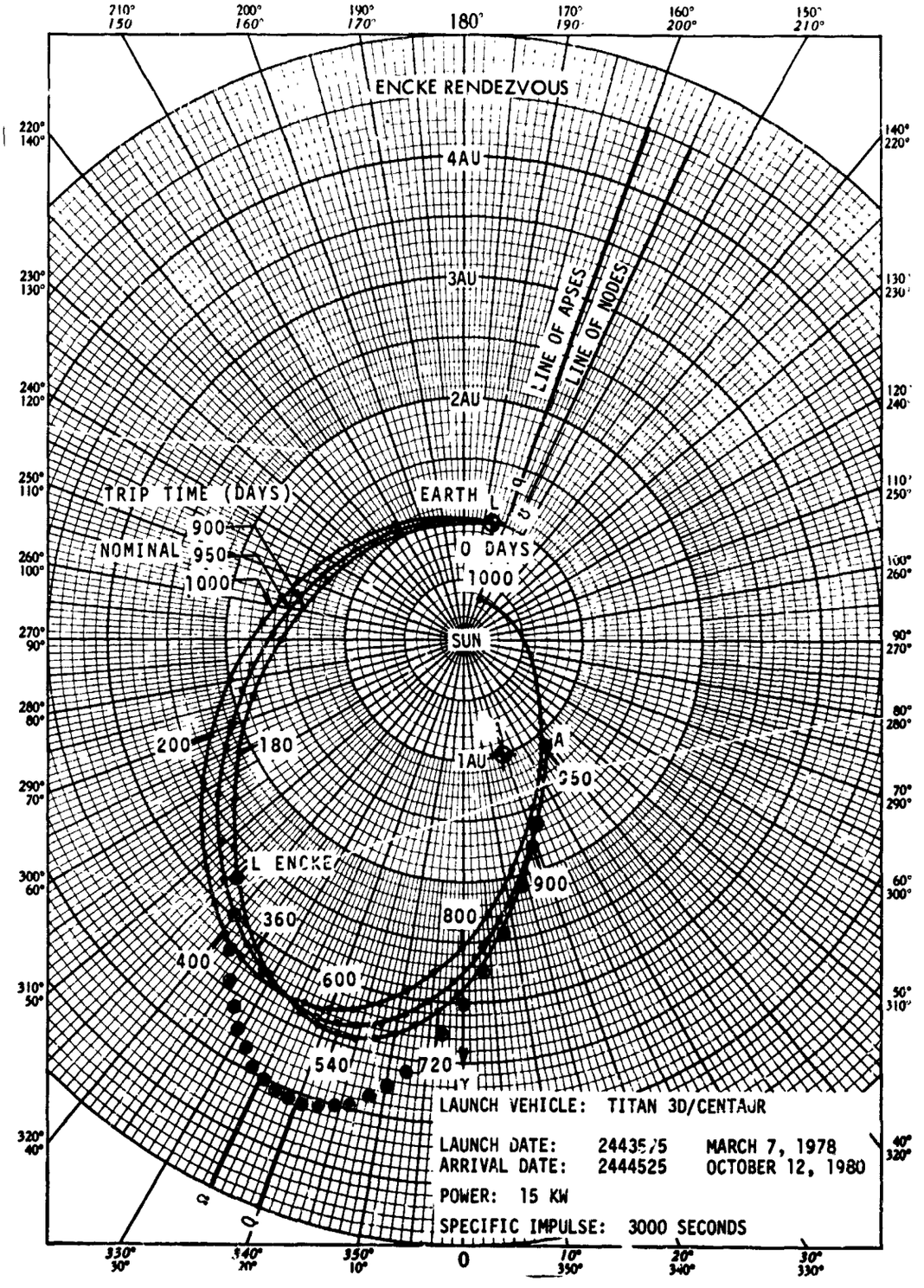

Figure 5-16c. Trajectory Profile - Encke Rendezvous

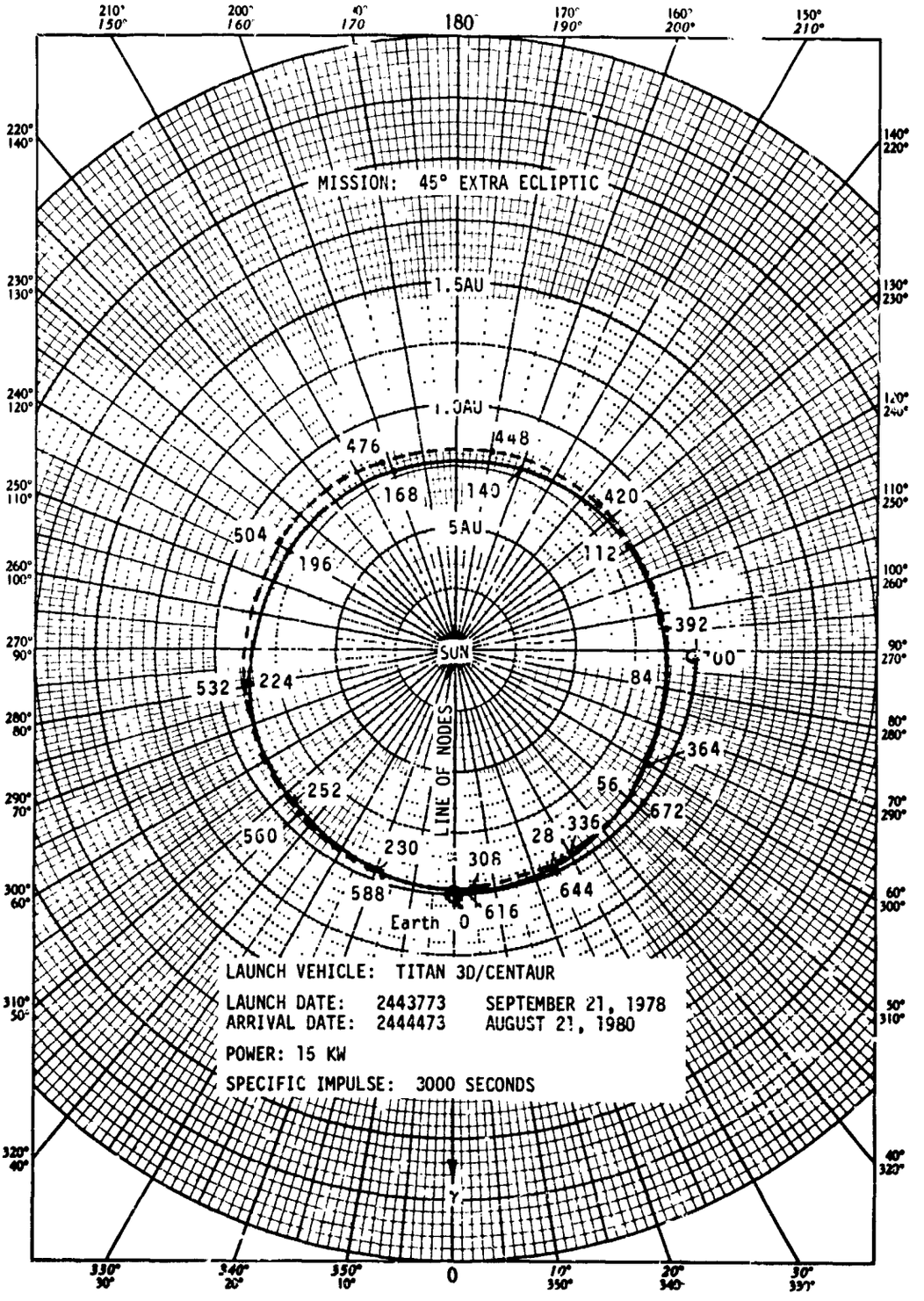

Figure 5-16d. Trajectory Profile - 45° Extra Ecliptic

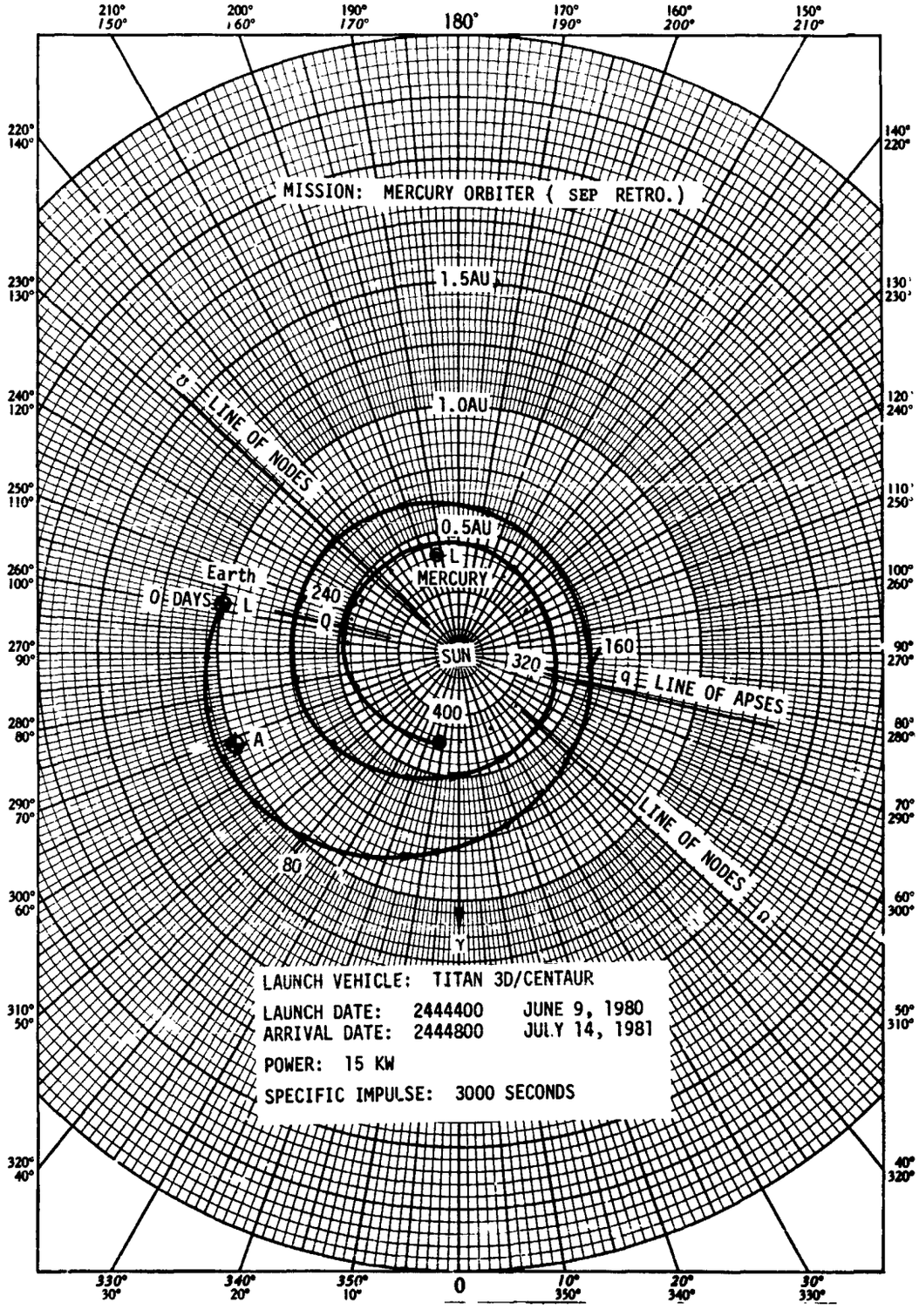

Figure 5-16e. Trajectory Profile - Mercury Orbiter (SEP Retro)

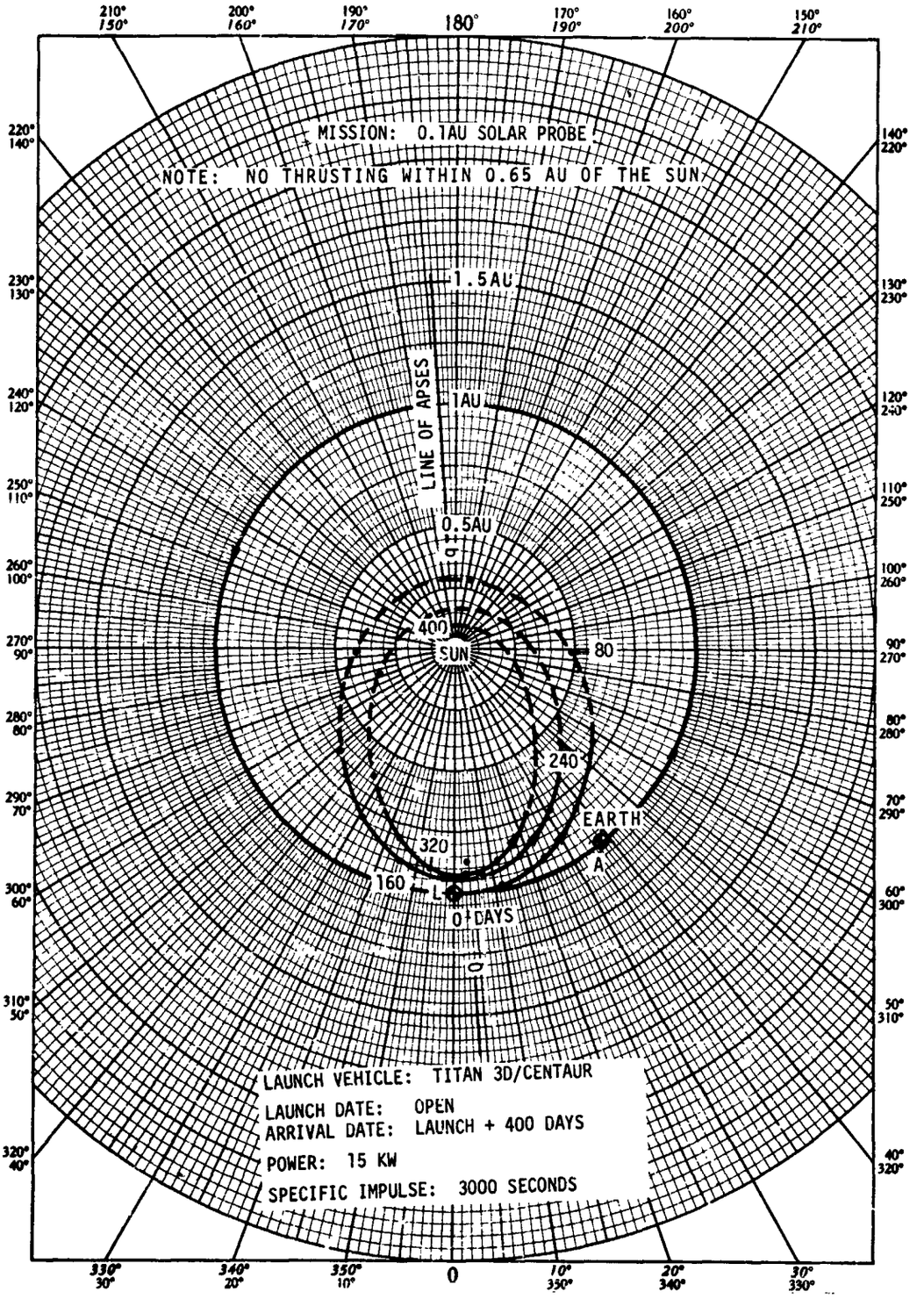

Figure 5-16f. Trajectory Profile - 0.1 AU Solar Probe

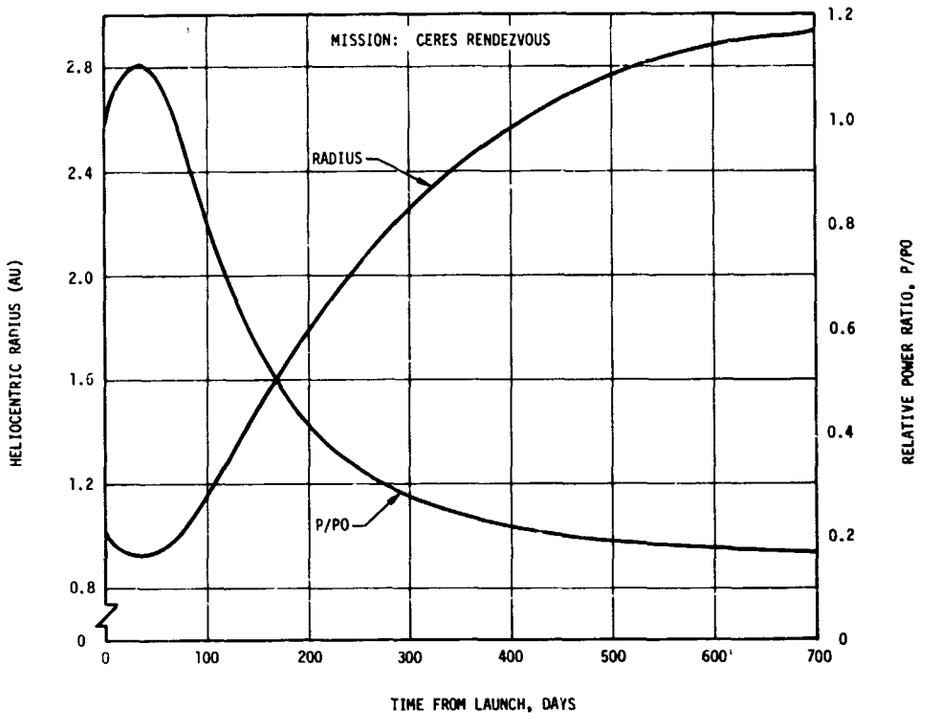

Figure 5-17a. Heliocentric Radius and Relative Power Histories - Ceres Rendezvous

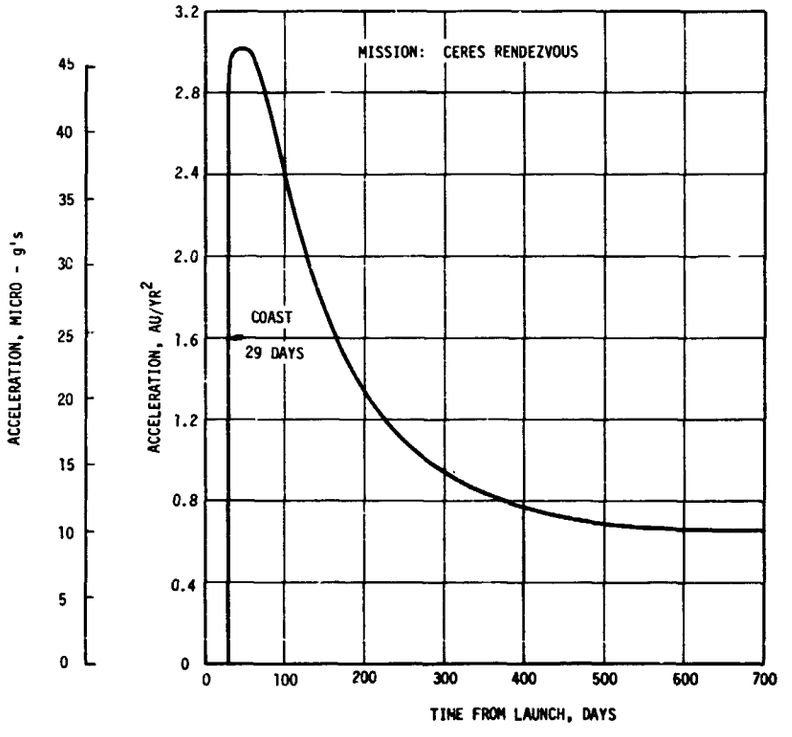

Figure 5-17b. Thrust Acceleration - Ceres Rendezvous

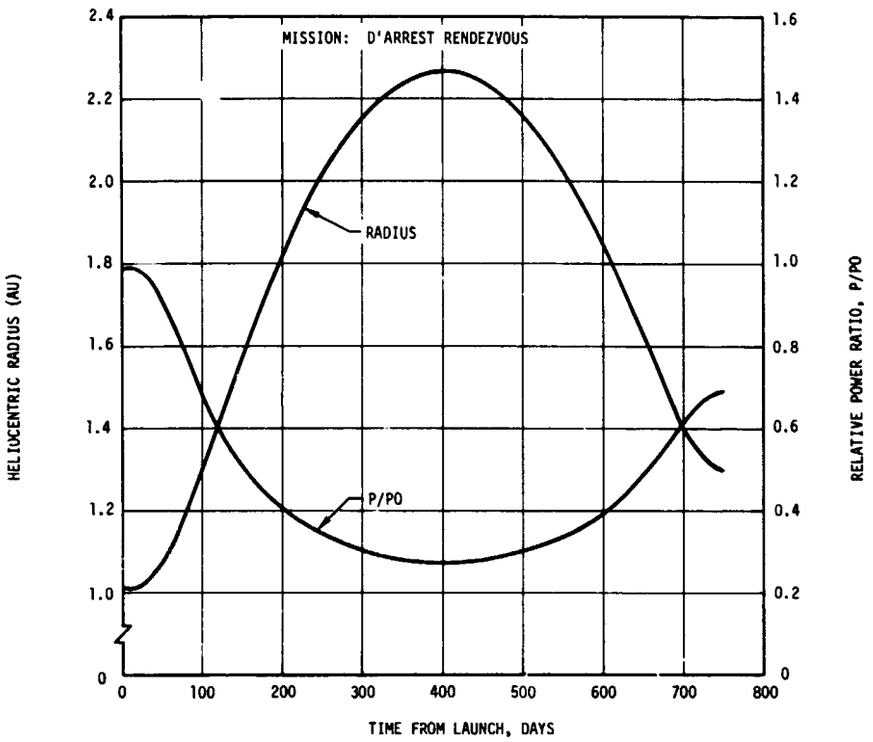

Figure 5-18a. Heliocentric Radius and Relative Power Histories - D'Arrest Rendezvous (Perihelion)

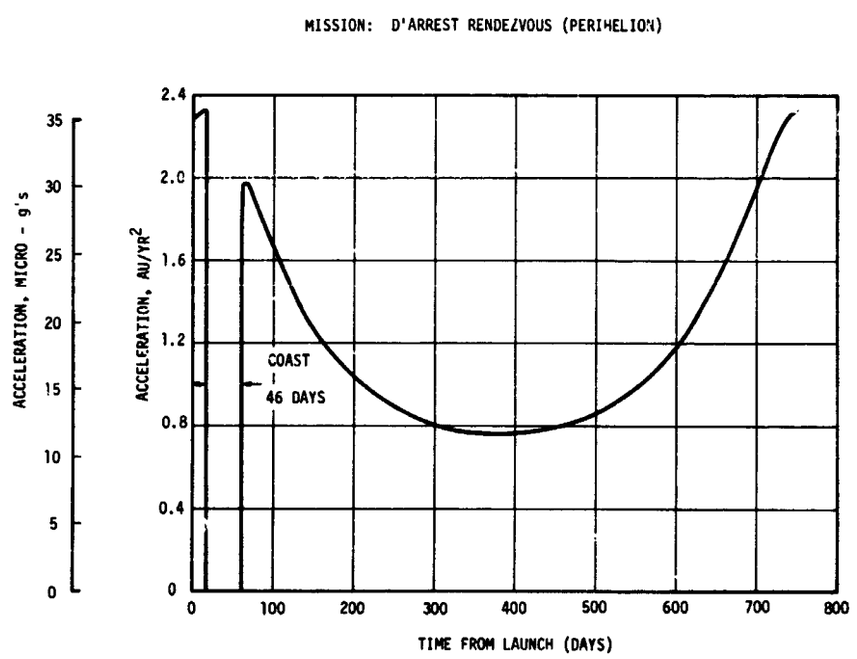

Figure 5-18b. Thrust Acceleration - D'Arrest Rendezvous (Perihelion)

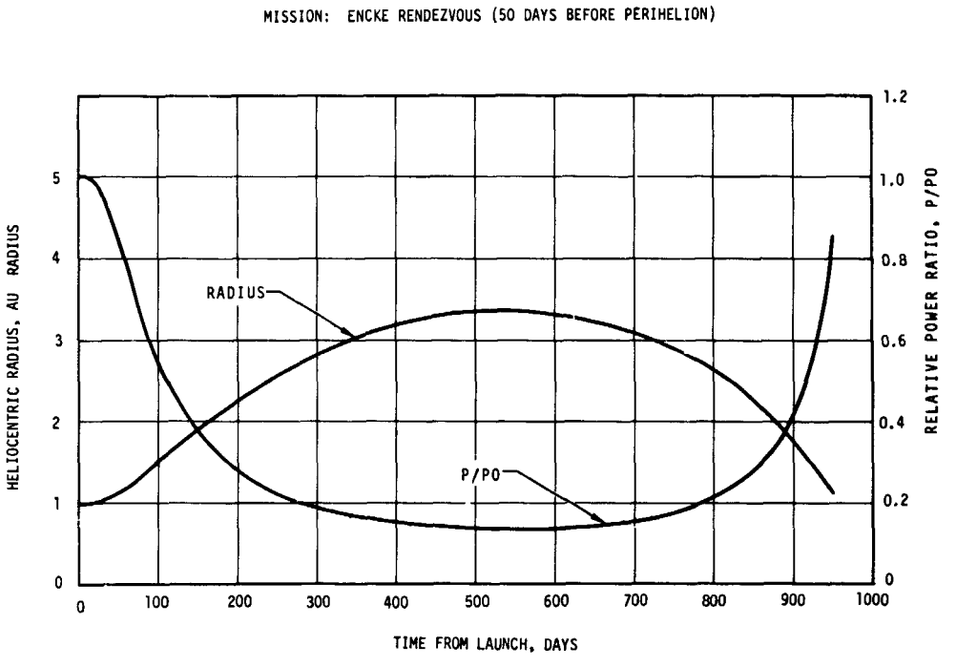

Figure 5-18c. Heliocentric Radius and Relative Power Histories - Encke Rendezvous (50 days before Perihelion)

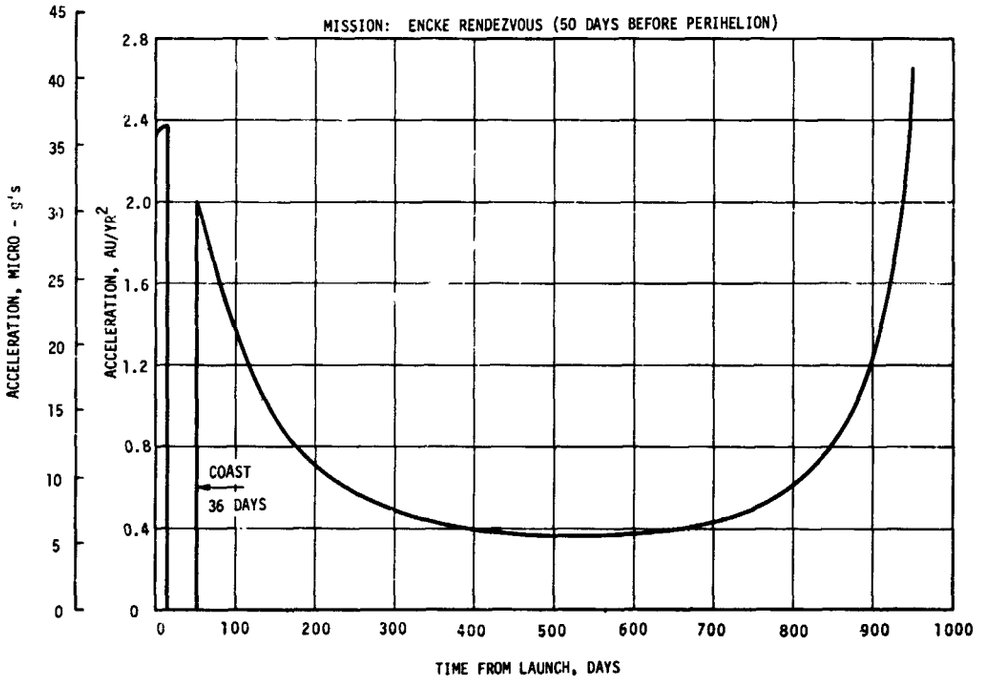

Figure 5-18d. Thrust Acceleration - Encke Rendezvous (50 days before Perihelion)

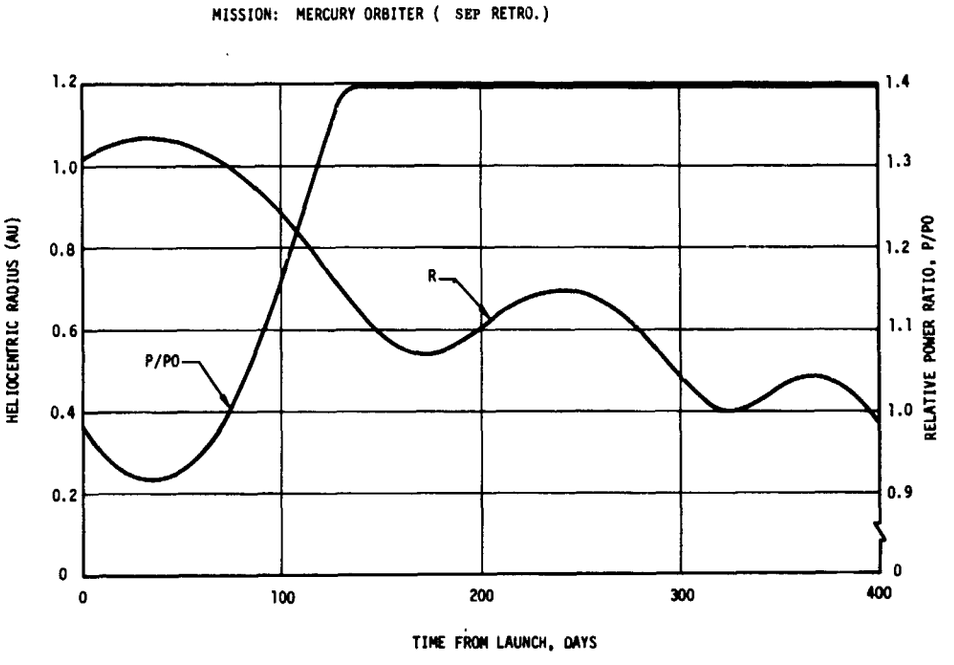

Figure 5-19a. Heliocentric Radius and Relative Power Histories - Mercury Orbiter (SEP Retro)

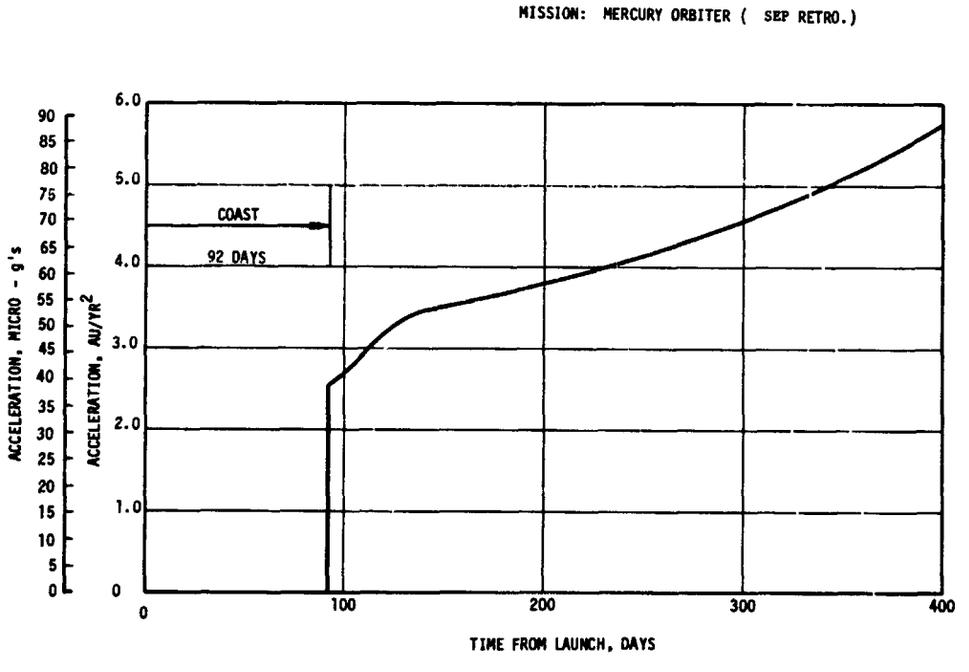

Figure 5-19b. Thrust Acceleration - Mercury Orbiter (SEP Retro)

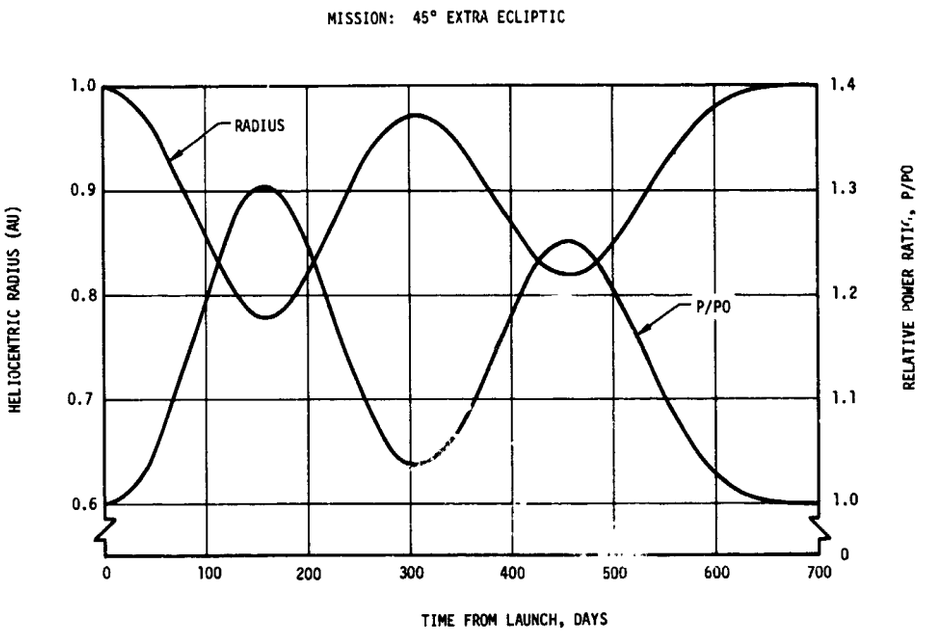

Figure 5-20a. Heliocentric Radius and Relative Power Histories - 45° Extra Ecliptic

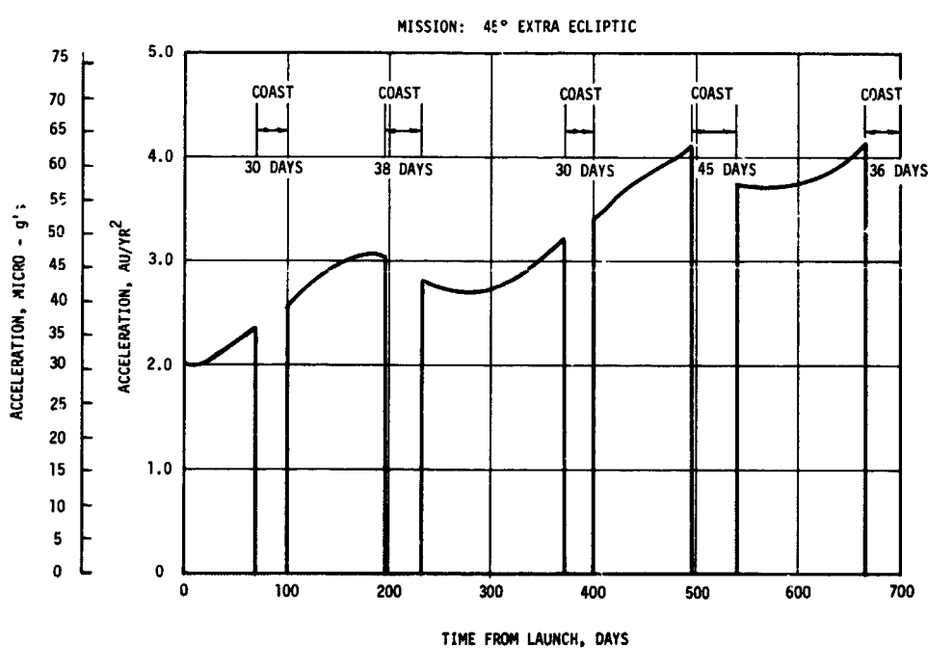

Figure 5-20b. Thrust Acceleration - 45° Extra Ecliptic

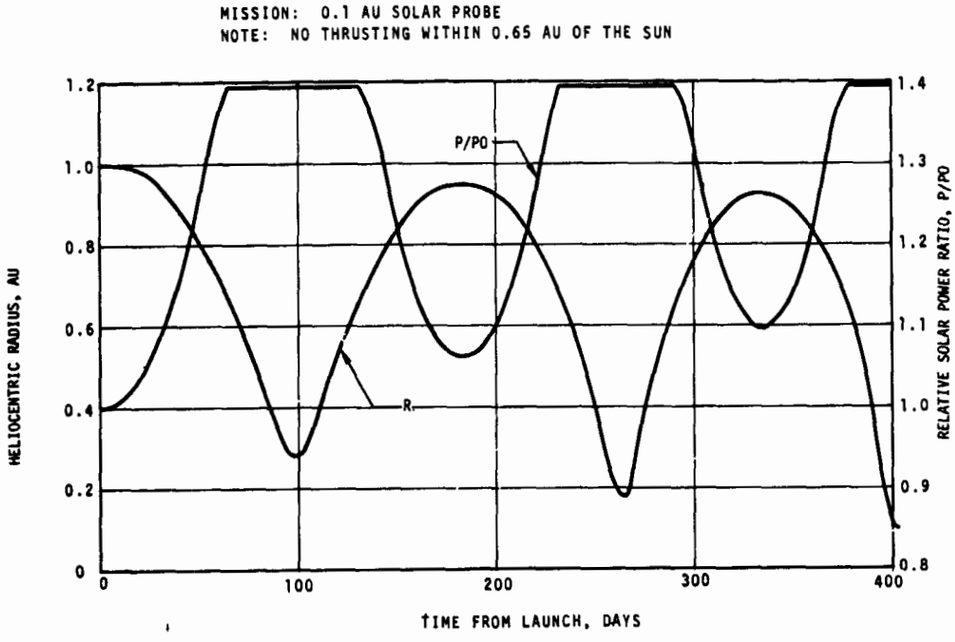

Figure 5-21a. Heliocentric Radius and Relative Power Histories 0.1 AU Solar Probe

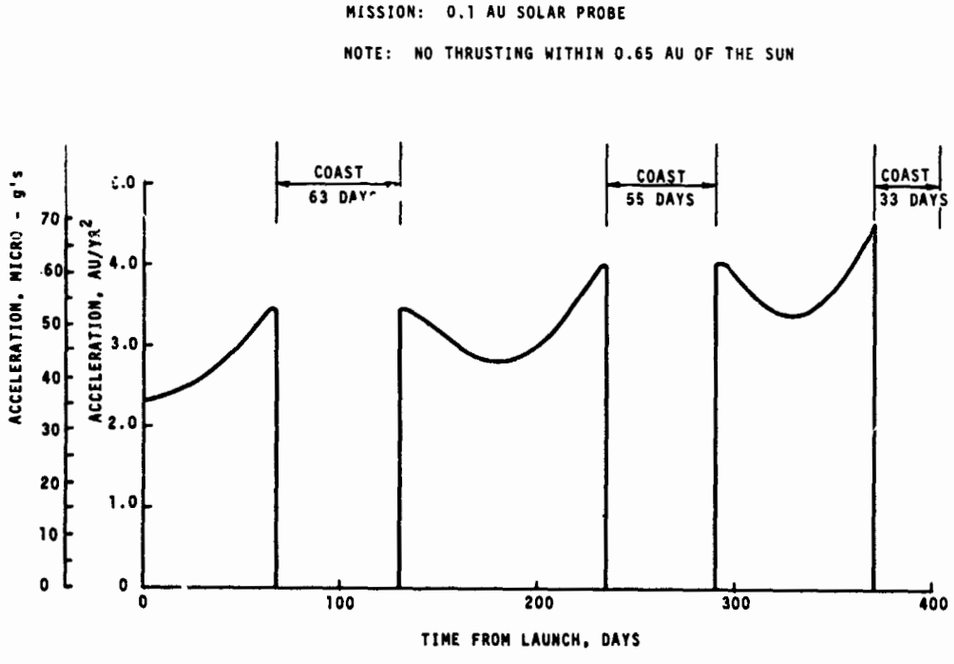

Figure 5-21b. Thrust Acceleration - 0.1 AU Solar Probe

mission performance charts by Horsewood, Mann and Flanagan (Ref. 5-6)* The nominal flight times were selected by a compromise between desired payload performance and reasonable commonality of mission and thrust duration. Other flight times and mission characteristics can be selected and performance tradeoffs obtained with the aid of the above-mentioned reference document.

The following aspects of the nominal mission profiles are worth noting:

- In the comet Encke rendezvous we selected an arrival 50 days prior to perihelion to enhance the value of the mission from a scientific standpoint; to obtain a favorable propulsion and power profile for the rendezvous maneuver and guidance corrections; to allow sufficient time after comet acquisition for navigational updating and guidance corrections; and to obtain a favorable communication range at rendezvous. Earlier or later arrivals would be less favorable as discussed in the Appendix E.

- In the extra-ecliptic mission we imposed no constraint on the solar distance in order to obtain a mission profile which minimizes flight time and yields adequate payload. The resulting trajectory includes two approaches to perihelion distances of about 0.8 AU. The increase in propulsion power at this distance outweighs the additional maneuver effort that is required as path velocity increases.

- The Mercury orbiter mission is based on low thrust orbit insertion. It was found that only few days of increased mission time are required in return for an appreciable payload increase by avoiding the use of a chemical retro system.

- The solar probe mission shown here uses a spiral-shaped trajectory with successive perihelion distances of 0.28, 0.17 and 0.1 AU. This mission profile permits repeated solar observations at close distance which has advantages from a scientific standpoint but at increased risk. An alternate mission profile which permits only one close solar approach after initially swinging inward to 0.4 AU and then outward to 1.48 AU is also being considered Figure 5-22). Thrust termination occurs at 0.55 AU after continuous thrusting for 384 days. This mission profile eliminates the risks of, and potentially severe solar array degradation due to

*These data were received toward the end of the study, after we had made a selection of nominal characteristics for system design purposes.

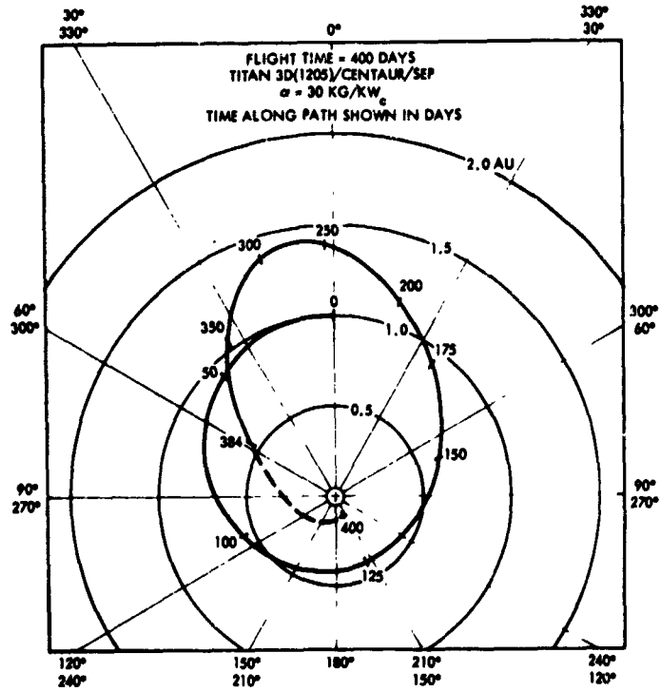

Figure 5-22. Alternate Mission Profile for 0.1 AU Solar Probe

several successive close solar approaches but also tends to diminish the total scientific data yield. Payload performance in both mission types is similar.

5.8 THRUST POINTING OPTIONS

Variation of the thrust vector pointing angles in three dimensions in accordance with an optimum steering program that maximizes the payload delivered for a given flight time and power level is a principal element of the trajectory simulation studies performed by NASA, AMA and TRW, and is reflected in the nominal mission profiles summarized in the preceding section. The required thrust pointing variations in cone and clock angle are shown in detail in Appendix B. We find that in some missions, especially the untargeted missions, and Ceres and Mercury missions a large cone angle variation from a fixed 90° angle is not critically required. This permits a simplification of the stage design.

Payload characteristics resulting from pointing the thrust vector in accordance with an optimal time-varying cone angle program or at fixed cone angles are compared in Figure 5-23 for four primary missions. A diagram that defines the geometry of cone and clock angles as used in this discussion is inserted in the graph. We note that the net spacecraft mass is only slightly penalized by the much simpler non-optimal pointing mode. Secondly, the payload reduction resulting from thrusting at other than the optimal fixed cone angle is also quite small, except in the case of the D'Arrest mission.

These results show that the much simpler, non-optimal fixed cone angle implementation of thrust vector pointing can be adopted in all primary missions, including the solar probe missions where previous studies have shown similar characteristics. If the payload loss is more than a few percent a compromise vehicle reorientation away from the sun line can be used to trade power against propellant penalties (see Figure 5-23). It should be noted that optimal out-of-plane thrusting is not compromised because the optimal clock angle variation can be accomplished simply by vehicle rotation around the sun line.

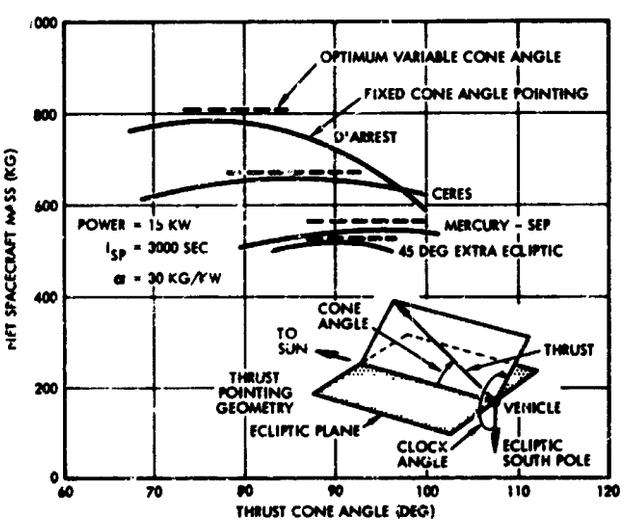

Figure 5-23. Thrust Pointing Mode Comparisons

Figure 5-24 illustrates the point that the propellant penalty of non-optimal thrust pointing is an integrated effect of a "cosine-loss", expressed by the term 1-cos ϵ. This explains the fact that departure from the optimum fixed orientation is governed approximately by a square-law function and imposes small penalties over a considerable angular range. Variation of $\pm$ 10 degrees from the optimal fixed orientation corresponds to less than 2 percent propellant penalty. See also Appendix C.

In summary, the spacecraft designer can choose between the thrust pointing options listed below:

1. Optimal variable thrust angle - Requires steering mechanization, e.g., solar array rotation. (Complexity and weight).

2. Non-Optimal variable thrust angle - Small thrust change by body rotation; small power penalty traded against propellant penalty.

3. Optimal fixed thrust angle - Fixed body offset or fixed thruster offset, requiring weight tradeoff. Simple and effective.

4. Non-Optimal fixed thrust angle - Simplest, often fully satisfactory.

5. Combination modes, e.g., several distinct fixed thrust angles to approximate optimal profile - Takes advantage of low cosine-loss penalties.

For the baseline stage configuration we have selected a rotatable solar array such that the thrust vector can be oriented by relative rotation of the center body to point in accordance with the optimum cone angle. (Option 1). Thus the baseline configuration meets the more demanding thrust pointing requirements of missions such as Encke and D'Arrest comet rendezvous. In missions that do not require a relative rotation of the solar array such as the extra ecliptic probe and outer planet missions, the rotation joint can be eliminated to save weight. The principal objectives of including the rotation capability on the baseline is the freedom of center body (or solar array) orientation which is desired for terminal guidance corrections, maneuvers in immediate vicinity of the target and in orbital operations, as will be discussed in Section 6.

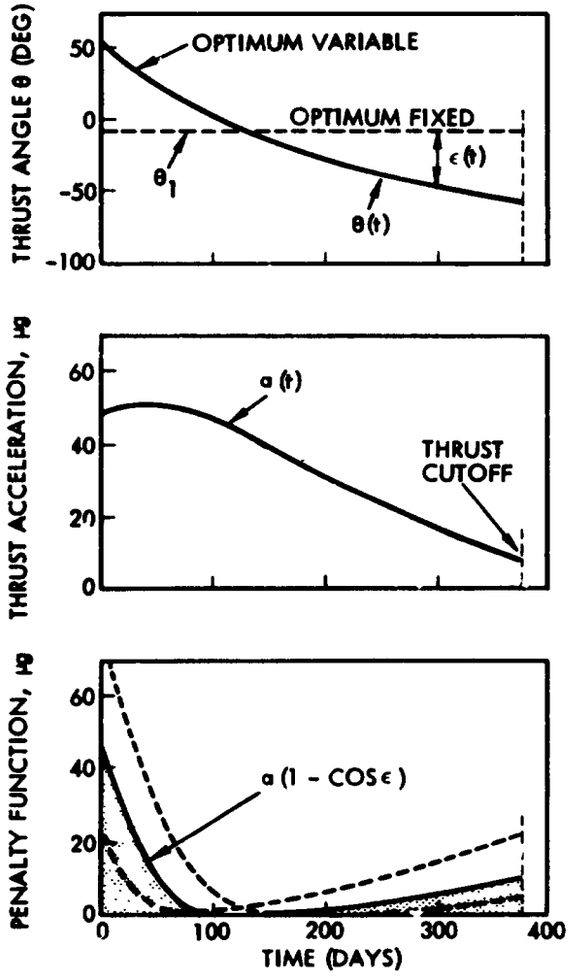

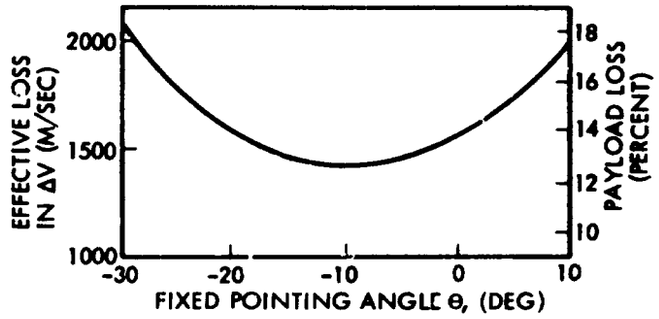

- DEPARTURE FROM OPTIMUM: $\epsilon = \theta(t) - \theta_1$
- OPTIMUM FIXED POINTING ANGLE IS A WEIGHTED AVERAGE OF OPTIMUM VARIABLE THRUST ANGLE. (t) IS WEIGHTING FUNCTION.
- PAYLOAD PENALTY MINIMIZED IF

$$\Delta V_{LOSS} = \int_o^T a\,(1 - \cos\epsilon)\,dt = \text{MIN}$$

i.e. SHADED TRIANGULAR AREAS ARE EQUAL.

Figure 5-24. Propellant Penalty Due to Fixed Thrust Orientation

5.9 ALTERNATE LAUNCH MODES, LAUNCH VEHICLES AND POWER LEVELS

As noted earlier, the electric propulsion power level that would yield maximum payload capacity for a Titan 3D/Centaur launched stage is in the 40 to 50 kw range. Figure 5-25 illustrates this for Ceres rendezvous. Restriction to a power level of 15 kw means that the injection performance of the booster is far from being fully utilized. Two options that would allow operating nearer the point of maximum payload have been studied:

1) Tandem launch of two 15 kw electric stages from a single Titan 3D/Centaur booster, which is equivalent to launching one 30 kw stage.

2) Use of a lower performance booster such as Titan 3D/Burner 2. The propulsion power of 15 kw is closer to the payload optimum in this case.

In the 700-day Ceres mission the tandem launch mode yields a total payload capacity of 1480 kg, or 740 kg for each 15 kw stage, nearly identical to the 750 kg payload capacity for single launch of the same stage as shown in Figure 5-25. The solid line extending to the origin of the graph represents Titan 3D/Centaur in an off-loaded condition for improved payload performance at low power level. (See Section 5.10). The fully loaded booster would actually yield only 650 kg of net spacecraft at 15 kw, as shown by the dashed curve. Other missions, except the extra-ecliptic probe, show the same trend: in the 750-day D'Arrest mission a single launch yields 860 kg at 15 kw, while tandem launch would yield 680 kg each. In the 400-day Mercury orbiter mission the payload capacities are 650 and 625 kg, respectively.

The cost advantage of a tandem launch, which would save a $25 million booster, must of course be weighed against added risks, more complicated scheduling and launch operations and the question of whether procurement of two missions at the same time can be assumed. The missions can actually be targeted to different destinations owing to the flexibility of low thrust trajectories.

A parametric study of risk versus gain involved in the tandem launch mode was conducted. On one hand, tandem launch reduces the

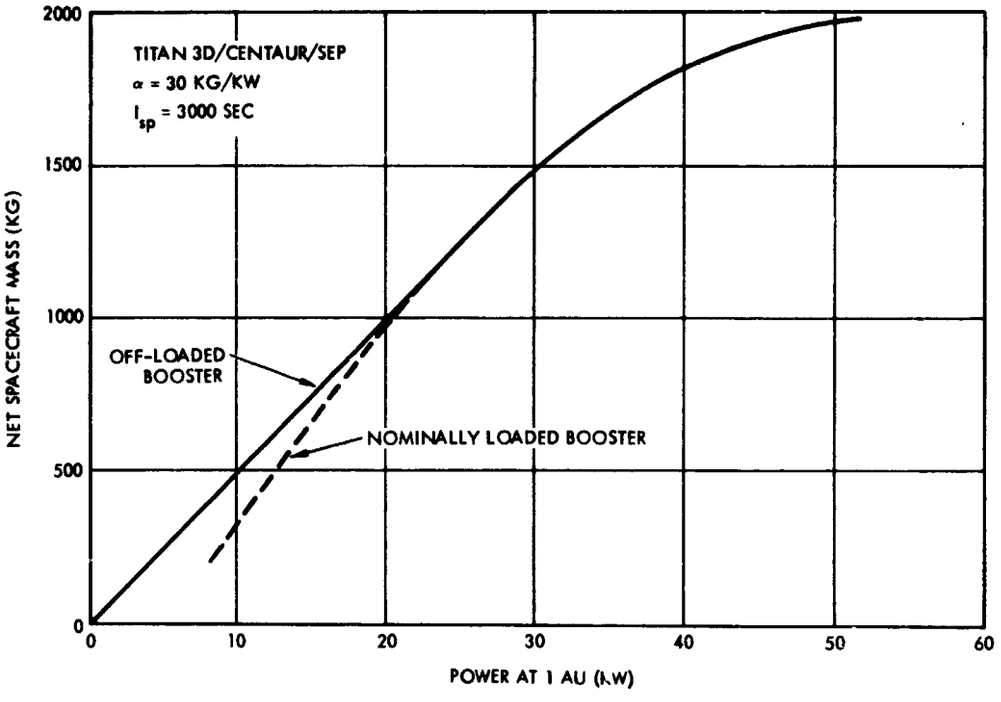

Figure 5-25. Net Spacecraft Mass vs Propulsion Power for 700-Day Ceres Orbiter with Nominally Loaded and Off-Loaded Booster

risk of having wasted a booster in the event of a subsequent failure of the electric stage. Since booster reliability, typically 85 to 90 percent, is much higher than that of the stage (assumed to be 50 to 70 percent), the dual-launch increases the probability of launching at least one successful mission. On the other hand, there is always the risk of losing two tandem-launched stages due to a single booster failure.

As a figure-of-merit to determine the net advantage of the dual launch mode we use the term "expected payload mass delivered per unit cost" where total cost includes launch vehicle, electric stage and estimated science instrumentation cost. A very preliminary science payload cost model was postulated, assuming cost to increase linearly from $5 million for 100 kg to $20 million for 1000 kg of science instruments.

Figure 5-26 shows the resulting figure-of-merit for a Ceres rendezvous mission versus power level and cost, with the stage reliability (R_s) as parameter, ranging from 0.50 to 0.85. This shows that

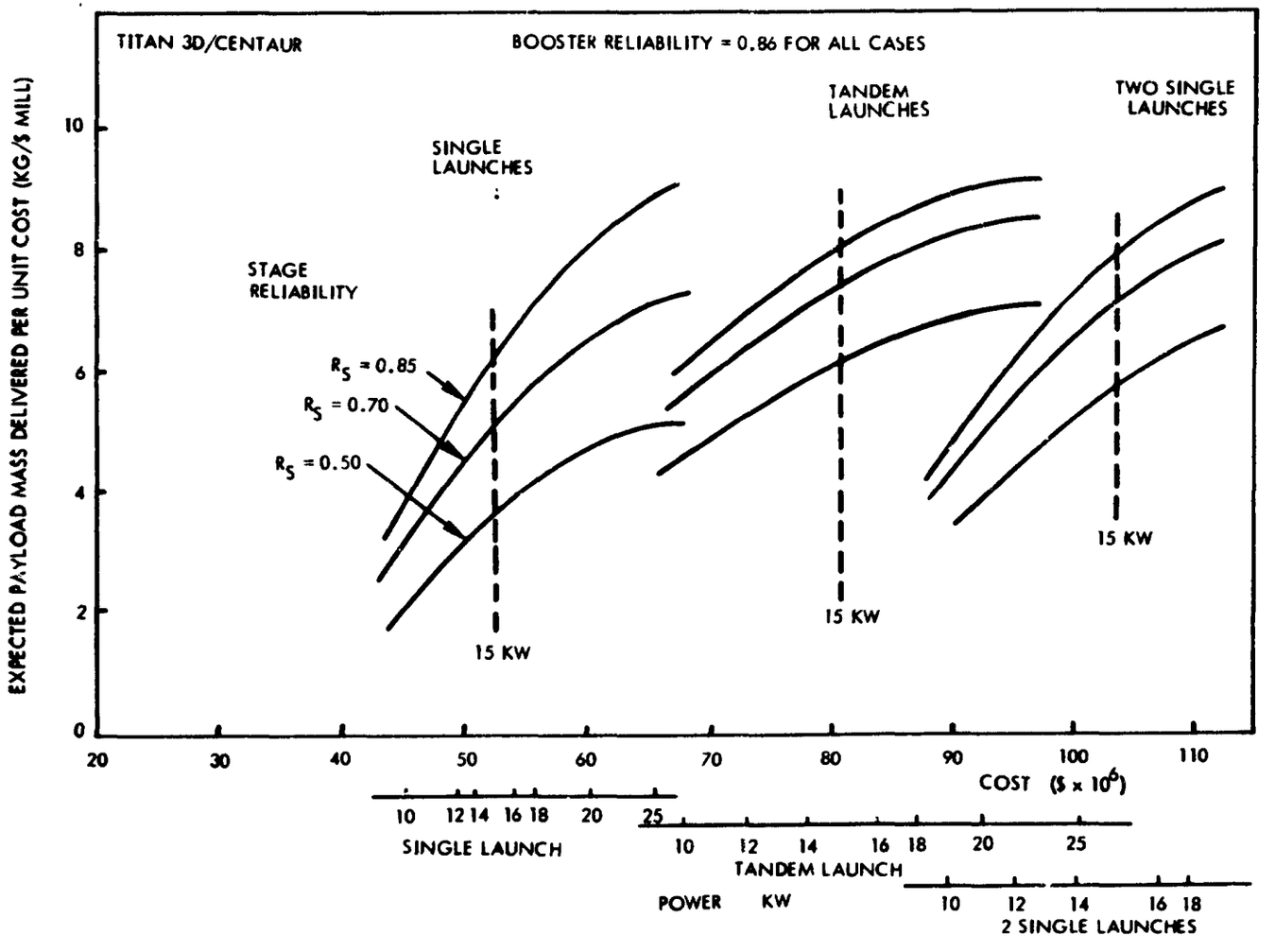

Figure 5-26. Expected Net Payload Mass Delivered per Unit Cost for Ceres Rendezvous Mission

tandem launch is more cost-effective i. e., has the highest expected payload delivery per unit cost, typically 2 times greater than that of single launch if the stage reliability is assumed significantly smaller than the booster reliability. The cost-effectiveness of two single launches is between that of the single and tandem launch.

The actual cost advantage that can be realized also depends strongly on the feasibility of pairing missions with different destinations which must be further investigated. Some possible pairing options are listed below:

1.	Solar probe/Mercury Orbiter	Inbound missions
2.	Out-of-Ecliptic/ Out-of-Ecliptic (Via Earth Swingby)	Cover North and South solar latitudes at same time
3.	Asteroid probe/outer planet probe	Outbound missions
4.	Comet probe/outer planet probe	Outbound missions (wide launch windows)
5.	Comet probe/ Communication relay	Outbound missions
6.	Asteroid probe/Out-of-Ecliptic (via Earth swingby)	Out-of-plane angle of asteroid accommodated
7.	Outer planet probe/ Out-of-Ecliptic	Performance gain through swingby mode

Note: Pairing particularly convenient if untargeted and targeted missions are combined

Electric propulsion makes it feasible, in principle, to launch two missions on divergent trajectories and achieve two different mission objectives if the launch window constraints are sufficiently flexible. The earth swingby mode discussed in Appendix D adds further flexibility to the tandem launch concept.

A study of the second option, use of a lower performance booster for greater cost-effectiveness shows that in the 700-day Ceres mission

Titan 3D/Burner 2 would yield a payload capacity of about 650 kg compared to 750 kg for the off-loaded Titan 3D/Centaur. In the 750-day D'Arrest mission the two boosters would yield 550 vs 850 kg; the 400-day Mercury mission 500 vs 650 kg, respectively.

Reduction of propulsion power to 10-12 kw reduces payload mass in about the same proportion and should not be considered except in those missions where the 15 kw baseline power level provides more than sufficient payload capacity. A truncated solar array configuration would serve this purpose.

These results show that there exist interesting and potentially very cost-effective variations from the nominal launch mode, the nominal booster, and nominal power level that should be further explored.

5.10 PERFORMANCE IMPROVEMENT THROUGH BOOSTER OFF-LOADING

Further analysis of payload performance at low power leads to the result that below a characteristic power level an improvement in net spacecraft mass can be achieved by offloading or otherwise reducing the injection capability of the booster below the nominal. This is illustrated in Figure 5-27. In this operating regime the full capacity of the booster would yield a gross injected mass M_o which would be larger than desirable for the available thrust level, hence the initial acceleration would be unfavorably small and the total required propellant mass too large, leading to a drastic reduction in net spacecraft mass. The shaded region in Figure 5-27 contains operating points where a derated booster can, in some cases, deliver a larger net spacecraft mass.*

Figure 5-28 shows net spacecraft characteristics for 1.0, 0.75, 0.50, and 0.25 of the nominal booster capacity, for the case of a 700-day Ceres rendezvous mission. At P_o = 15 kw a small performance gain could be achieved by offloading the booster to about 75 percent of nominal injection capacity. At 10 kw of propulsion power the Titan 3D/Centaur

*A recent NASA/Lewis Research Center Report, TMX-52980 by C. Zola, dated February 1971, has come to our attention which covers the same subject and uses essentially the same method of analysis yielding identical conclusions.

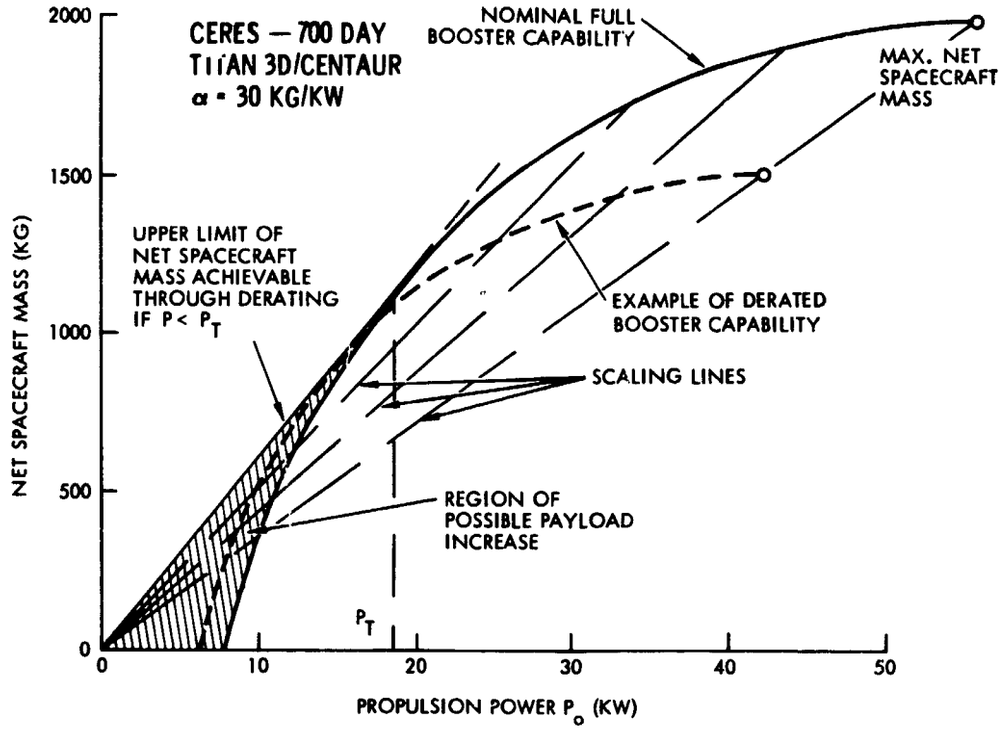

Figure 5-27. Effect of Booster Off-Loading on Net Spacecraft Mass

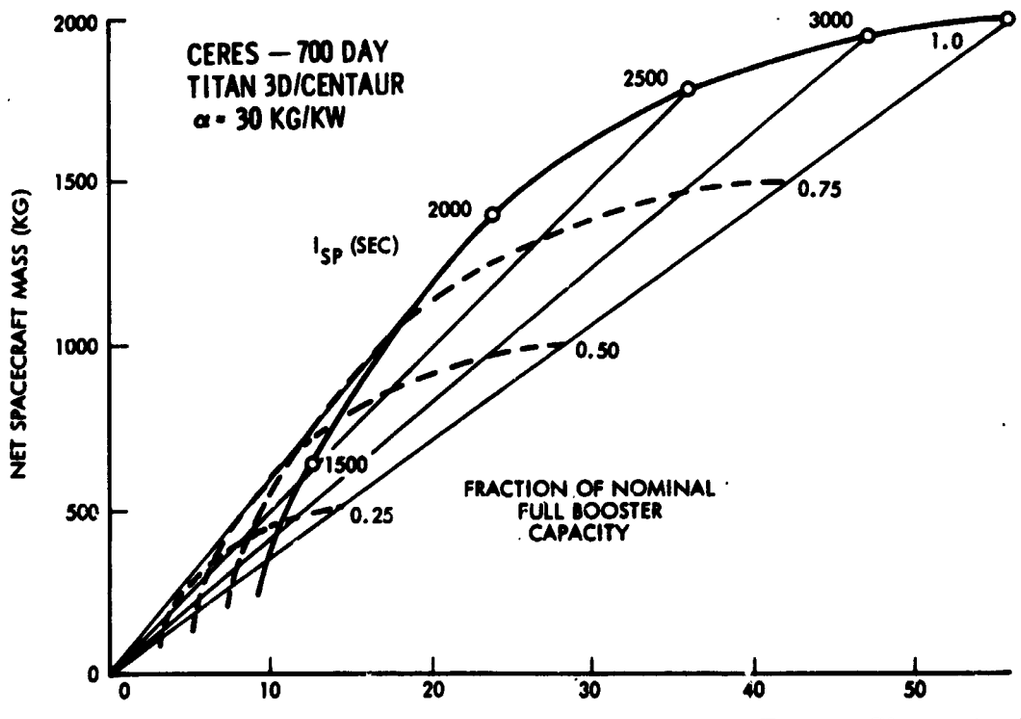

Figure 5-28. Scaling of Nominal Net Spacecraft vs Power Characteristics

would be used quite ineffectually, and a lower performance booster such as Titan 3D/Burner 2 at 45 percent injected weight capability of the Titan 3D/Centaur is preferable, as discussed before.

Referring to Figure 5-28, each scaling line that connects a point on the nominal booster performance curve to the origin of the graph is a locus of identical trajectories performed with the same departure velocity, thrust-to-weight ratio and specific impulse. Along such a line the mass and power parameters always vary in the same proportion.

5.11 EXTENDED USE OF STAGE CAPABILITIES IN SOME PRIMARY MISSIONS

In some of the primary missions the propulsion capabilities of the electric stage can be used advantageously beyond the principal task of delivering payload at destination. Examples include asteroid orbit insertion, asteroid belt cruise with successive asteroid flyby encounters, and exploratory maneuvers in the vicinity of a comet, especially along its tail. These applications will be discussed in the following paragraphs.

5.11.1 Ceres Orbiter and Lander Mission

A rendezvous mission to Ceres or any of the other major asteroids should logically include an exploratory phase with maneuvers in the vicinity of the asteroid and insertion into a low altitude orbit. The required velocity increments are small by virtue of the low asteroid gravity and can be provided by the electric propulsion system at a rate of about 10 m/sec per day of thrust. Direct insertion into low altitude orbit during the approach phase is also possible. Since the sphere of influence of the asteroid is about 50,000 km (using the asteroid radius of 383 km and lunar density of 3.3 gm/cm^3 as a basis of mass and gravity estimates) high or low altitude orbits would be feasible, but a low altitude orbit is preferable for higher resolution of surface features and in connection with landing capsule operation.

Deployment of a soft-landing capsule is envisioned after a period of orbital reconnaissance and determination of the asteroid's gravity with sufficient accuracy to compute the capsule's deorbit and landing retro-maneuver requirements. The alternative of deploying the lander prior to orbit insertion is less desirable since it involves greater risks of

hard landing and gives less accurate definition of the landing area. Typical maneuver requirements are as follows: Assuming a nearly parabolic approach velocity, an impulsive capture maneuver of about 40 m/sec for a 5000 km altitude circular orbit, and 100 m/sec for a 500 km circular orbit would be required. A low thrust orbit insertion is feasible and would be preferred with a hydrazine system serving as backup.

The deorbit and landing retro-maneuver for the soft-lander deployed from a 500 km altitude orbit would be 55 and 450 m/sec, respectively, requiring a small solid rocket with a propellant ratio of only about 0.15. The capsule would be similar to the first lunar soft-landing vehicle, Luna 9, with an initial mass of about 100 to 125 kg (Ref. 5-9). The orbital period at 500 km altitude is 6.2 hrs. This permits the stage to serve as relay link to earth with frequent capsule-to-stage contact periods of relatively long duration.

In summary, this mission concept makes the fullest use of the payload delivery capability as well as the maneuvering and communication capabilities of the stage at destination. To achieve rendezvous without also including the orbit and landing objectives would be a much less effective application of the stage in terms of the total scientific value of the mission.

5.11.2 Asteroid Rendezvous Followed by Multiple Asteroid Flyby

An attractive mission objective of an asteroid belt cruiser is observation of more than one asteroid by choice of a trajectory that demands relatively small maneuvers between encounters. (See Figure 5-29). A computerized search of favorable constellations of known asteroids is required to determine feasible mission opportunities. Such a mission is of the type where solar-electric propulsion can be used to good advantage, although solar distances of 2 to 4 AU tend to restrict the maneuverability. Closest approach distances in the range of 10^3 to 10^5 km are required, depending on asteroid size, to yield a detectable velocity perturbation of greater than 1 cm/sec to permit mass and density determination, as shown in Figure 5-30. This mission can also be achieved as continuation of an asteroid rendezvous mission by using low thrust for the departure maneuver.

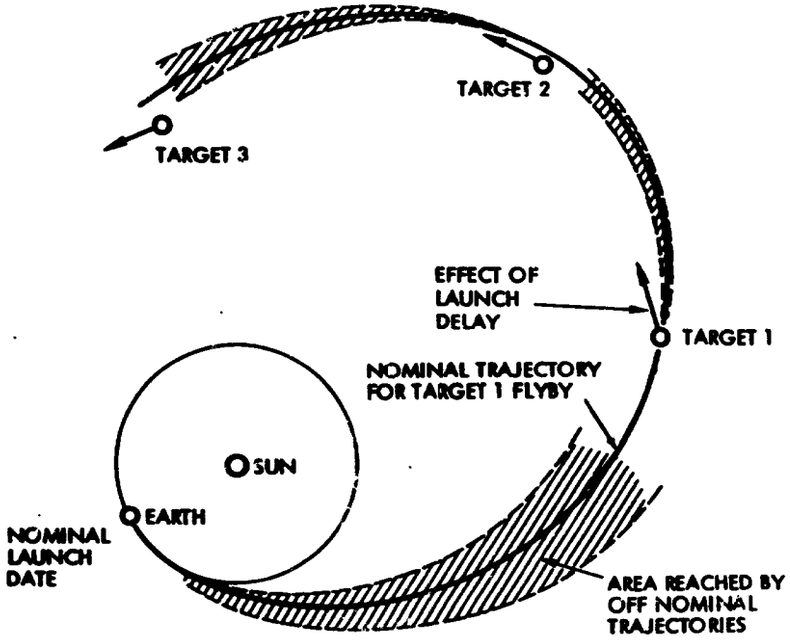

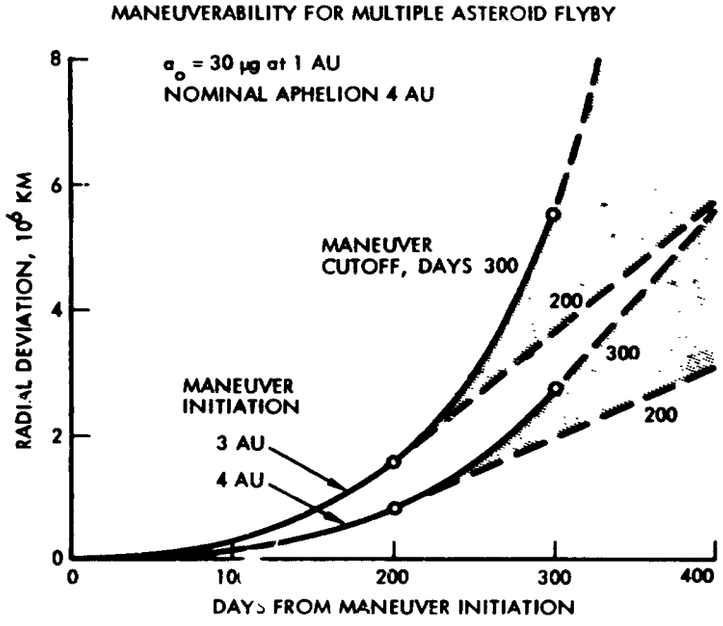

Figure 5-16. Asteroid Belt Cruise and Multiple Target Flyby

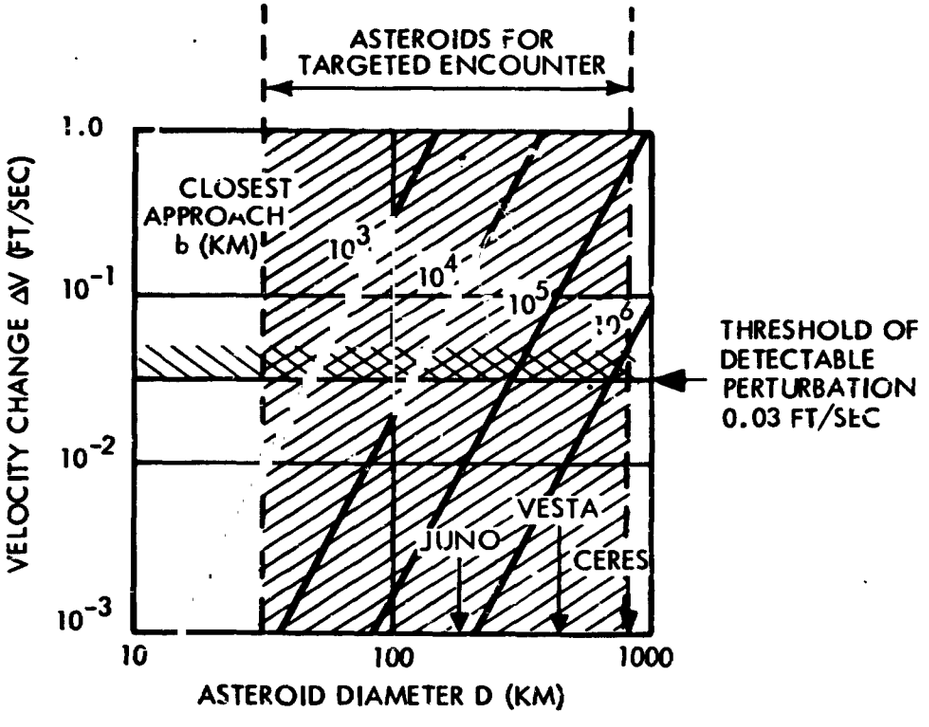

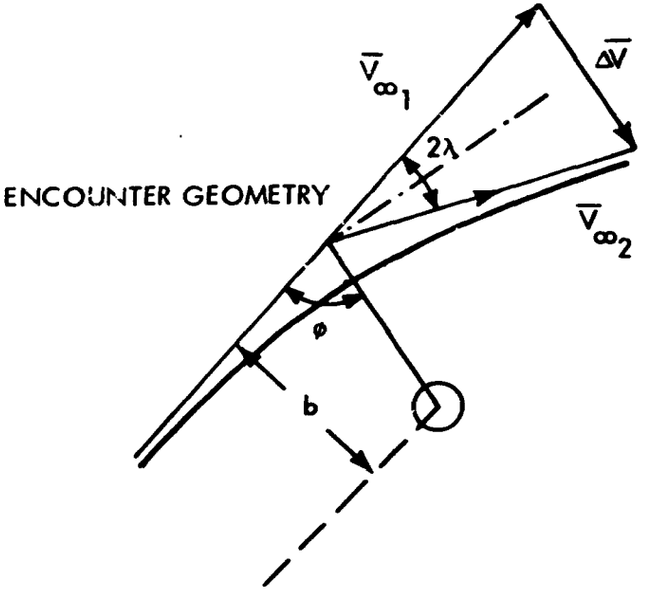

Figure 5-30. Perturbation by Asteroid Encounter

5.11.3 Exploratory Maneuvers in the Head and Tail Regions of a Comet

An attractive strategy for exploration of a comet as part of a rendezvous mission consists in the combined use of the electric stage and a ballistic daughter probe which is ejected after achieving rendezvous. This strategy makes use of the high-payload capacity of the spacecraft which permits a sizeable weight allocation to a daughter probe as well as to proepllant for exploratory maneuvers in order to increase the overall scientific data gathering capability and hence, mission effectiveness.

Figure 5-31 is a schematic diagram of systematic mapping excursions that can be made by the mother vehicle after performing stationary observations outside the comet's atmosphere for some time after arrival. The diagram shows a number of traverses of the coma and close approach to the nucleus on the sunlit side and subsequently on the dark side. A passage across the coma leads into the transition zone between coma and tail and is followed by a number of traverses of the tail at increasing distance from the nucleus. The spacecraft makes repeated exits and reentries of the tail to map the interaction effects of the comet with the solar wind at points of the contact surface at increasing distance from the nucleus. This mapping strategy is facilitated by the tendency of a coast trajectory to curve backward, in opposite direction of the comet's velocity, when plotted in coordinates relative to the comet. This means that propulsion need only be applied at intermittent times, as indicated in the diagram. Thus sensitive fields and particles measurements can be performed undisturbed by side-effects of electric propulsion during most of the mapping phase. Other observations not affected by thrust operation, such as mass spectrometry, visual, infrared and ultraviolet spectroscopy, photopolarimetry, dust particle detection and analysis, can be continued throughout this mission phase.

Extension of the mapping path from the gaseous tail which is expected to be predominant in comet Encke into the dust tail (if such a tail does exist) can be achieved by a modification of the trajectory shown in Figure 5-31. Dust tails are generally to be found behind, and curving away from, the trailing edge of the gaseous tail. The transition region between the two tails is expected to exhibit interaction phenomena of

(a) EXPLORATION PATTERN TO NUCLEUS, COMA AND TAIL

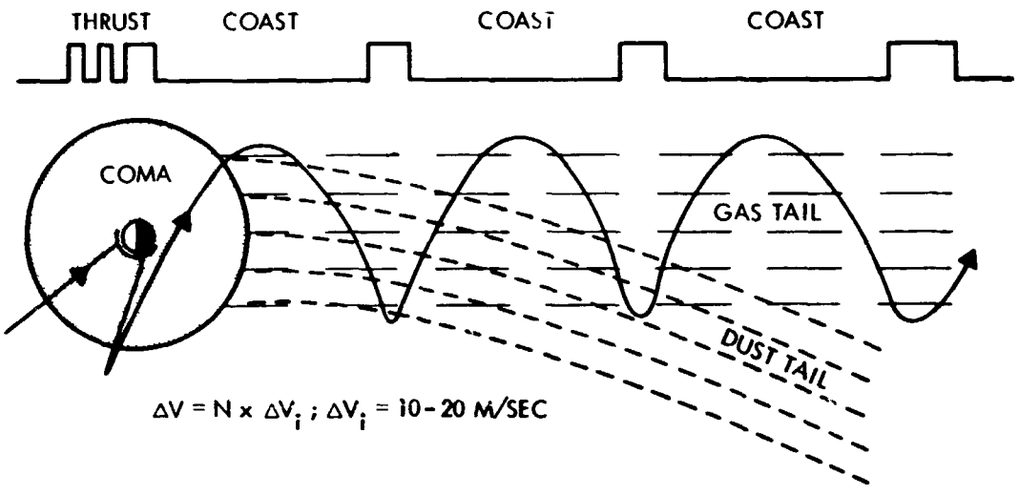

(b) THREE TAIL CROSSINGS BY BALLISTIC PRECURSOR PROBE

(c) PRECURSUR TO DISTANT TAIL REGION

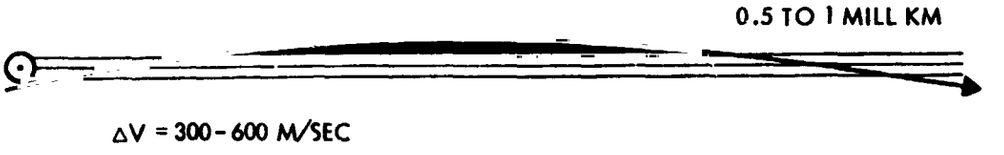

Figure 5-31. Samples of Relative Trajectories for Comet Exploration

special interest between the cometary plasma, charged and neutral dust particles and the solar wind. The maneuverability of the vehicle is particularly useful in exploration of this area, since changes in exploration tactics by ground command in response to unforeseen phenomena are feasible and should be included in mission planning.

If a daughter probe is being carried its separation soon after arrival is desirable, while the mother vehicle remains stationary outside the comet. The daughter probe serves as a precursor. In the initial phase, after entry into the coma and tail (Figure 5-31) it makes measurements of the comet's atmospheric environment (and possible hazards) transmits particles and fields data and samples the dust particle distribution prior to entry by the mother vehicle. A dual frequency transponder on the daughter probe can be used to determine electron densities, particularly in the later phases of the daughter probe excursion where the transmission path to the mother vehicle is along the tail at distances of 0.5 to 1.0 million kilometers. Findings by the precursor probe in the most distant region of the tail help determine the tail exploration strategy to be used by the mother spacecraft, e.g., permitting an assessment of the relative importance of proceeding along the tail at an early time rather than expending time and propulsion capacity nearer the nucleus.

As indicated in Figure 5-31 the daughter probe's relative trajectory can be shaped, by appropriate choice of the departure velocity, to curve in a gentle arc toward a second crossing of the tail at 0.5 to 1 million km distance. Halfway to this distance the probe exits and reenters the tail at a lateral distance of 50×10^3 km from the tail centerline. Probe separation velocities of 250 to 500 m/sec are required to achieve this relative trajectory. Supporting data and mission tradeoffs involving this exploration strategy are presented in a more detailed discussion of the Encke rendezvous mission (see Appendix E).

5.12 GROWTH CAPABILITY TO FUTURE MISSIONS: EROS AND MARS SAMPLE RETURN, HALLEY'S COMET RENDEZVOUS

Preliminary analysis of several future missions characterized by very high propulsive energy shows that the electric stage has sufficient growth capability to meet these requirements and to deliver substantial

amounts of payload. These missions include landing on and surface sample return from the asteroid Eros and from Mars, and rendezvous with Halley's comet in 1986, objectives which are being viewed with increasing interes by the space science community and are the subject of several recent NASA funded studies (Ref. 5-10, 5-11). Applicability of the multi-mission electric stage to these missions underscores the important role that it can assume as an economical transportation system for space exploration in the '70s and '80s.

5.12.1 Eros Sample Return, 1978

Preliminary studies of this mission by Mascy and Niehoff (Ref. 5-12) and Meissinger and Greenstadt (Ref. 5-13) show that the electric stage with a power level of 10 to 15 kw, suitably modified by the addition of a chemical retro system, landing gear and a landing radar can carry out a 1050 day round-trip mission to Eros, using a flight profile as illustrated in Figure 5-32. Typical mission and system characteristics and weight estimates for a vehicle launched by Titan 3D/Burner 2 are given in Table 5-4.

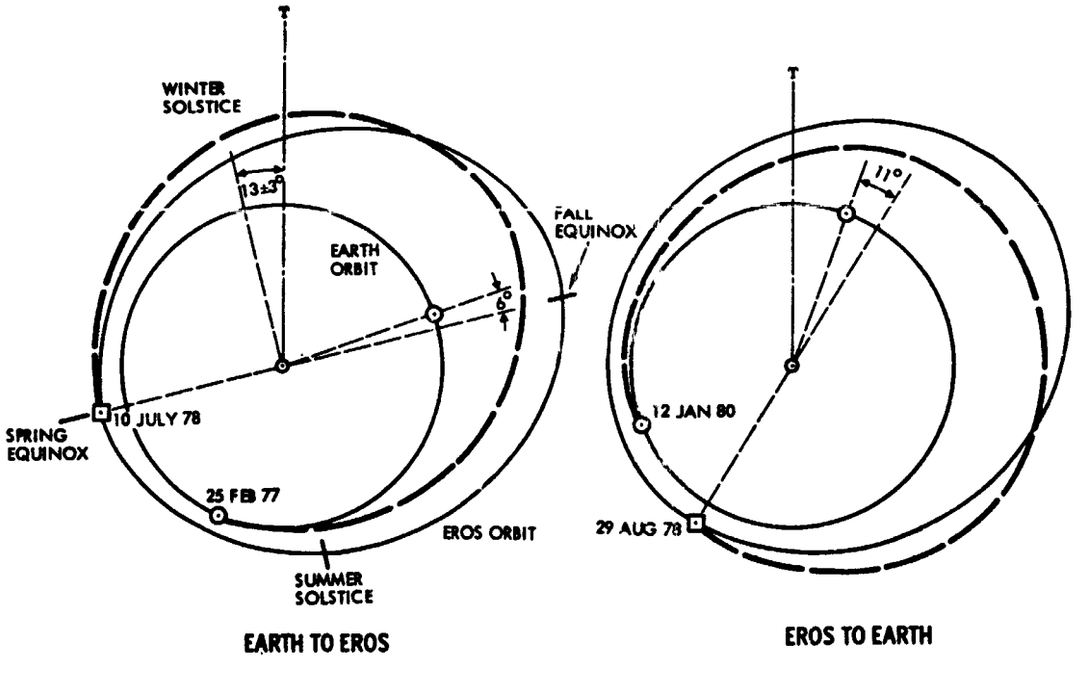

Figure 5-32. Eros Round Trip Trajectory from Mascy (Ref. 8)

Table 5-4. Eros Sample Return Mission: System Characteristics and Weight Estimates

LAUNCH VEHICLE	TITAN 3D/BURNER 2
LAUNCH DATE	25 FEBRUARY 1977
ARRIVAL AT EROS	10 JULY 1978
RETURN TO EARTH	12 JANUARY 1980
ROUND TRIP TIME	1050 DAYS
STAY TIME	50 DAYS
PROPULSION POWER AT 1 AU	10 KW
MERCURY ION THRUSTERS	5 (2 PLUS 3 SPARES)
SPECIFIC IMPULSE	3000 SEC
PEAK POWER TO THRUSTER	4.6 KW
MAXIMUM THRUST FORCE PER THRUSTER	48 MILLIPOUNDS
GROSS WEIGHTS	ESTIMATES (KG)
VEHICLE MASS AT EARTH DEPARTURE	2190
AT EROS ARRIVAL	1740
AT EARTH APPROACH	1400
SAMPLE RETURN CAPSULE IN EARTH ORBIT	400
SAMPLE MATERIAL	100
WEIGHT BREAKDOWN	
BUS VEHICLE PLUS CAPSULE AT EARTH DEPARTURE:	
SOLAR ELECTRIC PROPULSION	300
LOW THRUST PROPELLANT	750
HYDRAZINE PROPELLANT	40
STRUCTURE AND SUBSYSTEMS	455
SCIENCE INSTRUMENTS	200
RETURN CAPSULE (INCLUDES RETRO PROP., MINUS SAMPLE)	445
TOTAL	2190
CAPSULE (INCLUDING SAMPLE):	
STRUCTURE + MECHANISMS	80
SUBSYSTEMS AND SAMPLE STORAGE	220
RETRO PROPELLANT	145
SAMPLE MATERIAL	100
TOTAL BEFORE RETRO	545
TOTAL AFTER RETRO	400

The return capsule carrying between 50 and 100 kg of sample material is ejected from the stage on approach to earth. It uses a chemical retro system to enter earth orbit. Retrieval of the sample material from the return capsule can be made by Earth Orbital Shuttle or through atmospheric entry and recovery on the ground.

A brief description of the mission phases and operations at the asteroid and of the stage configuration adapted for landing and return is given in Appendix F. This mission can be carried out at opportunities

in 1974, 1977, 1979, and 1981 with relatively small variation of the mass of the sample material returned to earth, as discussed in Reference 5-12.

5.12.2 Mars Sample Return

A study performed by IITRI on solar electric propulsion capabilities for Mars surface sample return* shows several alternate mission concepts that require either one or two launches to perform a single mission, the latter using a Titan 3D/Centaur for launching a Mars orbiter/return vehicle and one for the lander vehicle. Titan and Saturn class boosters were considered for these mission m es. The results show the most effective use of solar electric propulsion to be in a 950-day round trip mission with 40 days of Mars stay time, using a single Titan 3D/Centaur booster and low thrust propulsion for Earth-Mars transfer, Mars capture, Mars escape and Mars-Earth transfer. Sample recovery is achieved in Earth orbit. The returned sample size varies between 6 and 20 kg depending on stage propulsion power ranging from 19 to 23 kw.

This example shows that the mission falls within the growth capability of the stage. The spiral capture and escape maneuvers at Mars required for greatest weight effectiveness demand full rotational capability of the solar array to ± 180 degrees or for compatibility with the designconcept adopted by us, ± 90 degrees plus a roll reorientation of the vehicle by 180 degrees once every Mars orbit revolution. This mode of thrust vector steering avoids the thermal control problem that would arise with full $\pm$ 180 degree thrust angle change relative to the solar array. Additional study of stage utilization in this mission is required. It appears to be the growth mission of highest scientific priority to which the stage may have to be adapted.

5.12.3 Halley's Comet Rendezvous

A rendezvous mission with Halley's comet at the 1986 opportunity has been studied by several authors in recent years. Direct ballistic missions, and ballistic missions which include a Jupiter swingby have been proposed, but they require a Saturn 5 class booster (Ref. 5-14).

*Preliminary results dated December 16, 1970 were received through NASA/ACM Division; final report in preparation.

Nuclear-electric propulsion would offer a more weight effective mission concept with total flight time of 3 years, requiring a Titan-class booster (Ref. 5-15). In view of the uncertainty surrounding the operational availability of a nuclear electric stage by the early 1980's new efforts have been extended to apply solar electric propulsion. Friedlander et al (Ref. 5-16) have studied this mission concept and found that with careful choice of the mission profile, including Jupiter swingby on the outbound leg, a Titan-class booster would be sufficient to achieve a minimum mission capability. A representative mission profile is shown in Figure 5-33.

Results of a current study by IITRI* indicate that a 16 kw stage launched by Titan 3D (7 solids) /Centaur can achieve rendezvous at Halley with a 7 to 8 year flight time and deliver a net spacecraft mass of 470 to 485 kg. The best launch year would be 1977. The above case was obtained for the slightly less favorable launch year 1979. Total mission time is 3040 days, with a total thrust time of 1222 days. The injected mass is 1350 kg at V_∞ = 9.5 km/sec.

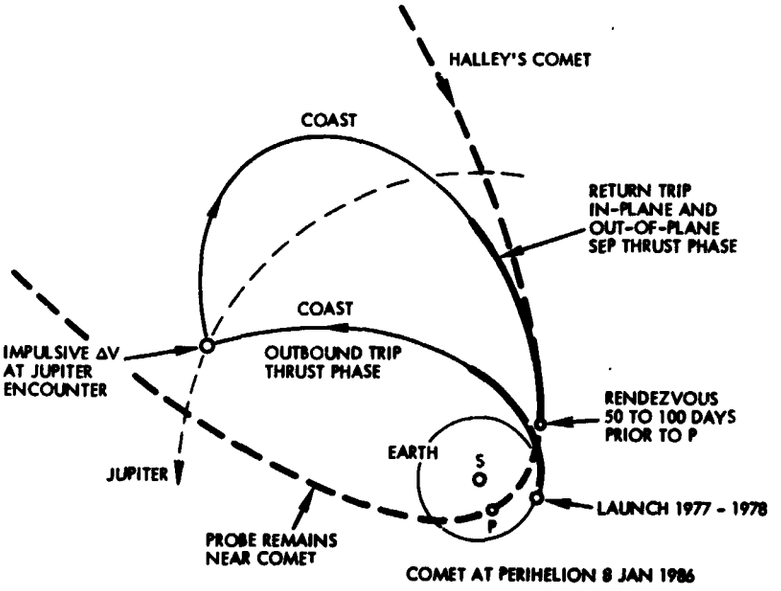

Figure 5-33. Hybrid SEP/Chemical Halley Comet Rendeavous (Qualitative Only)

*Being performed under JPL contract (final report in preparation), Ref. 5-17.

Preliminary consideration has been given by TRW to possible improvements of the mission profile to achieve a higher payload. We found that the inclusion of a powered swingby at Jupiter with an impulsive maneuver of about 1500 m/sec and an effective 2:1 magnification of the propulsive velocity increment due to Jupiter's gravity field tends to improve the net payload mass. This research is outside the scope of the present study, but additional effort is warranted.

5.13 NAVIGATION AND GUIDANCE

Navigation and guidance studies concentrated on problems inherent in missions to targets of poorly defined ephemeris such as asteroids and comets and approaches to their solution. The problem areas addressed included the following:

- Effect of continuous random perturbations during the thrust phase as a result of thrust vector magnitude and pointing uncertainty.
- Updating of position and velocity information available from DSIF orbit determination in the presence of continuous random thrust perturbation.
- Upgrading of DSIF tracking accuracy by addition of interferometry.
- Use of an on-board terminal navigation sensor to improve guidance accuracy in missions to asteroids and comets.
- Definition of a guidance technique which makes effective use of continuous and inexpensive low thrust course corrections.
- Use of high thrust in combination with low thrust and as back up for terminal guidance.

5.13.1 Brackets of Navigational Accuracy for Typical Mission

The relative severity of navigational errors representative of different navigation schemes in three types of missions is indicated in Table 5-5 by upper and lower brackets.

Errors in the transfer phase are referenced to an earth-based coordinate system, while errors in the approach phase must be referenced to a target-centered system. This means that even for a highly accurate

Table 5-5. Low-Thrust Guidance and Navigation Accuracy (Preliminary Brackets)

ONE-SIGMA NAVIGATION ERROR (IN KM)

NAVIGATION DATA TYPE	TRANSFER PHASE (RELATIVE TO EARTH)	APPROACH PHASE (RELATIVE TO TARGET)		
		NEAR PLANETS	FAR PLANETS	COMET/ASTEROIDS
DSN ONLY	1,000 - 10,000	1,000-10,000	5,000-10,000	10,000-100,000
DSN + ON BOARD ANGLE DATA	SAME AS ABOVE	10 - 1,000	10 - 1,000	10 - 1,000
DSN + ACCELERO-METERS	100 - 1,000	100 - 1,000	SAME AS DSN ONLY	
DSN + THRUST AND ATTITUDE PARAMETER TELEMETRY	200 - 2,000	200 - 2,000	SAME AS DSN ONLY	
BEST COMBINATION	100 - 1,000	10 - 1,000	10 - 1,000	10 - 1,000

ASSUMPTIONS:

1) Observed errors controllable: Guidance Error = Navigation Error
2) Continuous thrusting to target: Asymptotic errors quoted
3) Approach phase = 10^6 - 10^7 km from target
4) Target error = $[(\text{error rel to earth})^2 + (\text{ephemeris error})^2]^{1/2}$

navigation scheme during the transfer phase terminal errors will be as large as the uncertainty of the target ephemeris. This uncertainty ranges from several thousand km for small asteroids to several ten-thousand km for comets that are subject to large gravitational and non-gravitational (e.g., loss of mass) perturbations from one solar passage to the next.

It is apparent that the first two methods listed in the table are the only ones of interest in connection with the primary missions of the stage. Accelerometers are not expected to operate reliably for the long thrust durations involved, and even the highest resolution devices cannot give an accuracy that is at least an order of magnitude better than the typical thrust uncertainty of 1 percent of minimum full-scale acceleration which is about 10^{-8} g in outbound missions such as Ceres or Encke rendezvous. Telemetry of thrust and attitude parameters can help in identifying major deviations from the nominal thrust magnitude and orientation profile but cannot reduce the uncertainty of continuous small random thrust vector variations. It will be available as part of engineering telemetry with the beneficial side effect of improving DSIF's orbit determination accuracy capability.

5.13.2 DSIF Based Navigation

Past studies of the degradation of DSIF based navigational accuracy due to random thrust perturbations (Ref. 5-18) have shown the error to be increased by about two orders of magnitude for representative thrust perturbation levels (2×10^{-4} cm/sec^2). Figures 5-34a and 5-34b illustrate low-thrust guidance techniques for flyby missions and rendezvous missions. Results from previous studies at JPL and TRW indicate that high guidance accuracy can be achieved for flyby missions by performing main thrust pointing corrections on command from the ground (Phase I) plus a vernier coorection after a short coast period which upgrades navigation accuracy (Phase II a). The method proposed for rendezvous missions, where the low-thrust phase must be extended until arrival at the target, uses several successive coast intervals to upgrade navigational accuracy, followed by thrust periods which include steering corrections commanded from the ground (Phase II b). The achievable guidance accuracy is lower in this case. Table 5-6 lists advantages and disadvantages of these guidance methods. Alternative methods for terminal corrections possibly using onboard target sensing must be investigated to define a guidance technique with sufficient accuracy for critical rendezvous missions.

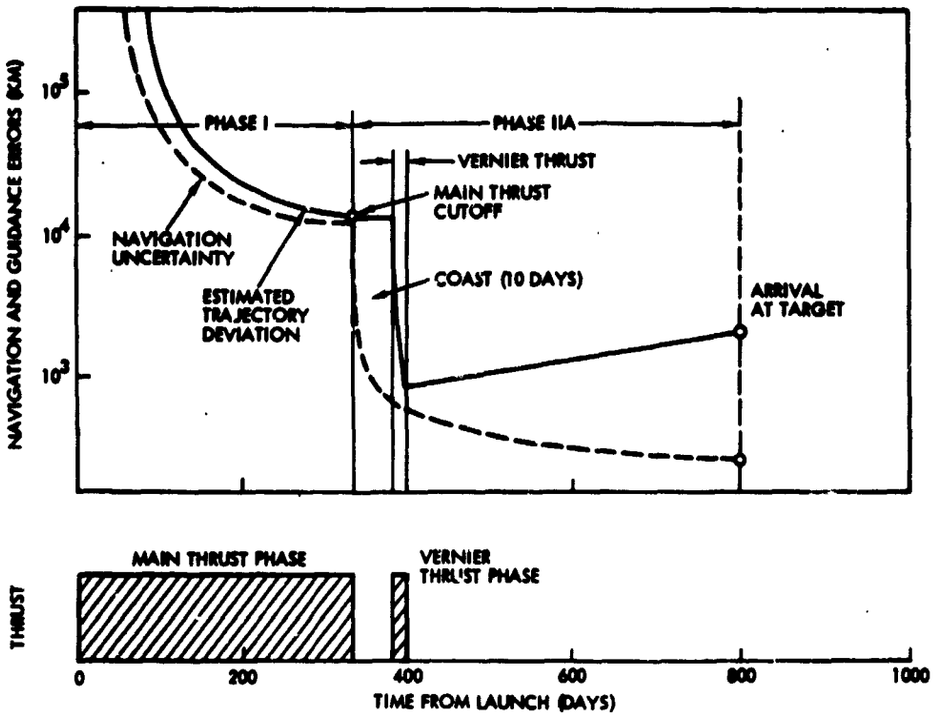

Figure 5-34a. Low Thrust Guidance for Flyby Missions (Qualitative)

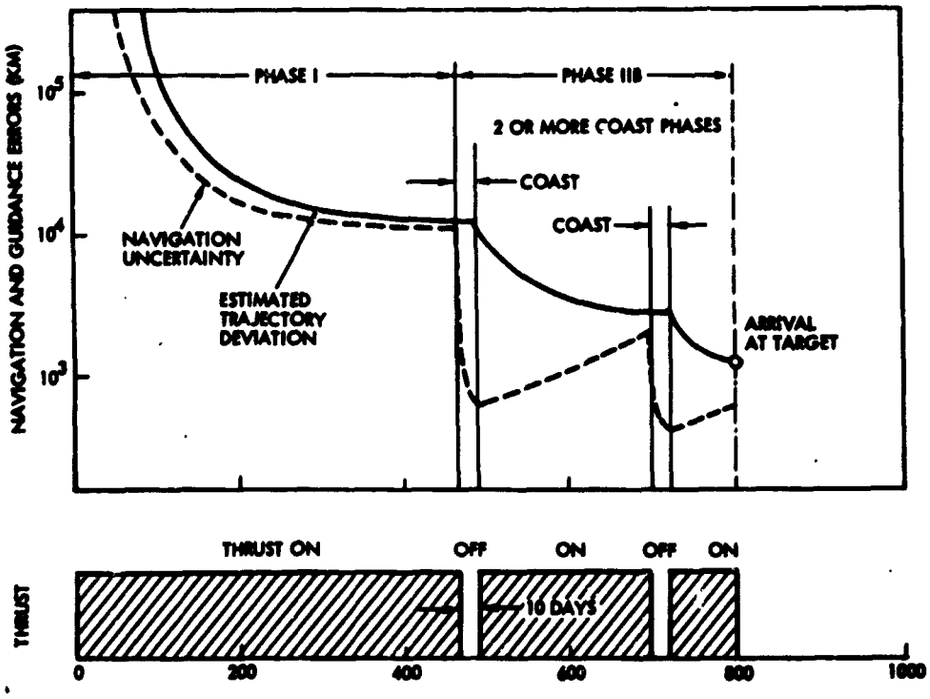

Figure 5-34b. Low Thrust Guidance for Rendezvous Missions (Qualitative)

Table 5-6. Comparison of Guidance Techniques

TECHNIQUE	ADVANTAGES	DISADVANTAGES
PHASE I ONLY (ONE CONTINUOUS THRUST PERIOD WITH PERIODIC STEERING CORRECTIONS SENT FROM GROUND)	SIMPLE AND MOST RELIABLE (DOES NOT REQUIRE ENGINE ON/OFF SWITCHING)	LIMITED GUIDANCE ACCURACY (60,000-10,000 KM AT TARGET)
PHASE I AND PHASE II A (PHASE II A CONSISTS OF A SERIES OF VERNIER CORRECTIONS)	ACCURACY COMPARABLE TO BALLISTIC FLIGHT WITH CHEMICAL MIDCOURSE CORRECTION SYSTEMS (2,000-500 KM AT TARGET)	REQUIRES REPEATED ENGINE RESTARTS. HIGHER COMPLEXITY FROM AN OPERATIONAL STANDPOINT. NOT APPLICABLE, AS SUCH, TO RENDEZVOUS TRAJECTORIES
PHASE I AND PHASE II B (PHASE I PLUS A SERIES OF TRACKING COASTS NEAR THE END)	APPLICABLE TO RENDEZVOUS TRAJECTORIES. ACCURACIES APPROACHING THAT OF PHASE I PLUS PHASE II A AND MUCH BETTER THAN PHASE I ALONE	SAME AS ABOVE, EXCEPT IS APPLICABLE TO RENDEZVOUS. ACCURACIES NOT QUITE AS GOOD AS PHASE I AND PHASE II A
PHASE I AND CHEMICAL MIDCOURSE	SIMPLER FROM A MISSION OPERATIONS STANDPOINT THAN PHASE I AND PHASE II. EXCELLENT FOR SUCH MISSIONS AS A CERES ORBITER	WEIGHT PENALTY. MORE COMPONENTS, HENCE GREATER COMPLEXITY
PHASE I, PHASE II AND CHEMICAL	HIGH ACCURACY AND FLEXIBILITY	WEIGHT PENALTY. RELIABILITY PENALTY. GREATER MISSION COMPLEXITY

5.13.3 Improved DSIF Capabilities

Analysis of the asymptotic behavior of the orbit determination error due to thrust noise shows that the asymptotic error of extended tracking can be derived from the error resulting from a single pass of tracking data by a DSIF station. It was further found that inclusion of range data in the orbit determination process rather than doppler data only greatly reduces the asymptotic error and the time constant of settling to the asymptotic value. The inclusion of angle measurements from an interferometer tracking system improves the accuracy still further. Thus the orbit determination error obtained with doppler data only can be reduced by at least one order of magnitude by addition of range data, and another order of magnitude by the addition of angle tracking data.

At present the DSN net is in the process of including the equivalent of a long-baseline interferometer system by correlating range measurements obtained at two widely separated stations, such as Goldstone and Woomera. The resulting accuracy of angle measurements is needed for the forthcoming Mariner Venus-Mercury flyby mission, in view of the critical guidance accuracy required at Venus swingby.

This improved DSN tracking capability will be extremely useful in refining the guidance accuracy of future SEP missions such as those of the electric stage. A simple calculation shows that for a spacecraft at 1 AU distance and a range error of 10 m at two stations 10,000 km apart an angle error of 2.0×10^{-6} rad and a cross range error of 300 km is obtained. By using the interferometer measurement to augment the orbit determination program, the cross range error should be greatly improved even in the presence of thrust noise.

5.13.4 Onboard Terminal Sensor

To improve on terminal navigation accuracy in the presence of large ephemeris uncertainties there can be no substitute for a precise onboard terminal navigation sensor. Such sensors have been under investigation at JPL (Ref. 5-19) and elsewhere, and at present the simplest and most effective system appears to be an image system that determines the subtended angle between the target (center of mass) and a convenient reference star at successive observation points. For a small target that appears as a point source at the time of measurement the use of this principle is particularly attractive. Angular accuracies of 0.1 millirad (1σ) have been assumed by JPL for this technique, based on an image system projected for TOPS. For large targets such as major planets it is found preferable to select a natural satellite with a well defined relative ephemeris as the reference point rather than to attempt to locate the center of mass from the irregularly-shaped and not fully illuminated disk of the planet itself.

For cometary targets, the small 3 to 10 km nucleus would be desirable as a point source, but there is some uncertainty as to the ability of the onboard sensor to detect the nucleus, because in some instances it cannot be observed from the ground. In this case the diffuse, nearly spherical shape of the coma will have to be used initially until the nucleus comes into view on closer approach. For a coma with 10,000 km diameter the subtended angle at 10 million km distance is about 0.06 degrees (1 milliradian) which should permit a navigational fix of at least an accuracy of 2000 to 5000 km for the center of the coma from this distance. Subsequent measurements would tend to improve this accuracy until the nucleus itself can be picked out.

Figure 5-35 illustrates the method of terminal navigation by successive optical fixes of the target with respect to a selected reference star. Rotation of the line of sight between fixes is essential to provide a measure of distance in addition to the angular (cross range) fix obtained by a single observation.

Three factors inherent in the orbital characteristics of low-thrust rendezvous are helpful in making the technique simple and accurate:

- The closing rate is slow, permitting many successive fixes after acquisition of the target;
- Continuing low-thrust operation until encounter permits execution of substantial guidance corrections at negligible extra propellant cost;
- The major axis of the navigational error ellipse, roughly along the line of sight between stage and target, is nearly perpendicular to the major axis of the ellipse of the target's positional uncertainty. Thus even a few consecutive fixes greatly reduce the initial navigation error (see Figure 5-36).

An asteroid of 100 km diameter at a distance of 10 million km has a visual magnitude of about 3, extrapolating from data available for Ceres, and can be readily detected, compared to the star background. A rotating irregularly shaped asteroid of significantly smaller dimensions facilitates detection by its modulated brightness characteristics. First estimates of terminal navigation accuracies based on the conservative assumption of angular measurement errors of 0.1 milliradian are shown in Figure 5-37 for three values of line-of-sight rotation between fixes. This shows that terminal guidance accuracies in the range of 10 to 50 km would be achievable.

One principal problem is the very slow rate of rotation of the line of sight on approaching rendezvous which has the effect of making the position uncertainty in the line-of-sight direction (range direction) much larger than in cross-range direction, typically by 1 to 2 orders of magnitude. A representative example is the 960 day Encke rendezvous mission where the positional uncertainty is about 400 x 10,000 km (1σ) in cross-range and range respectively at a distance of 4×10^6 km, or 60

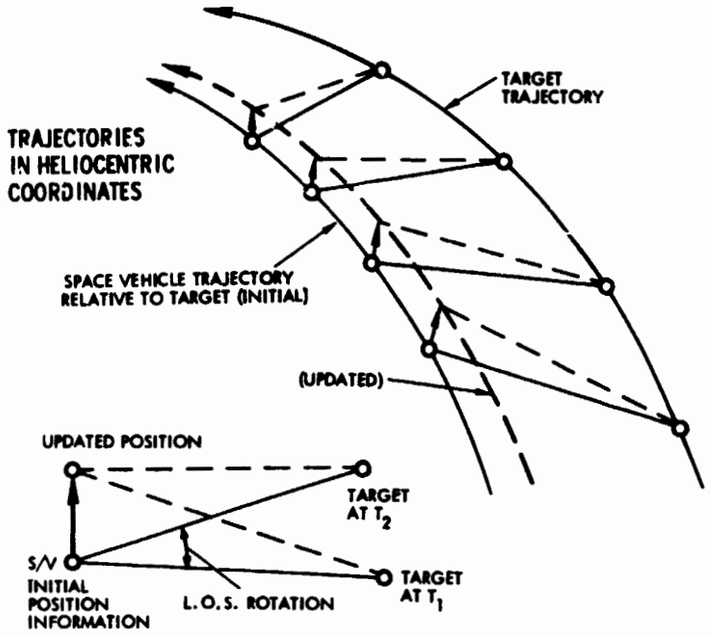

Figure 5-35. Terminal Navigation Fixes by Onboard Target Sensing

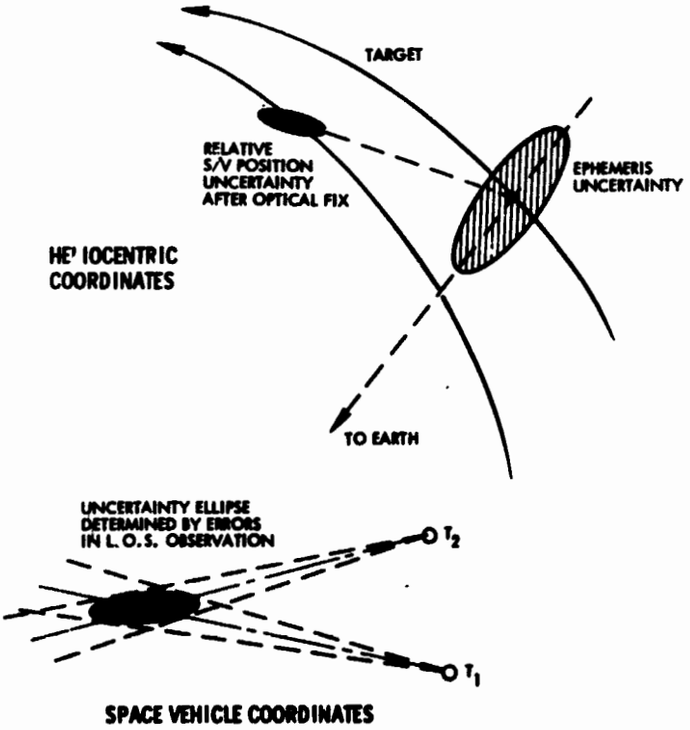

Figure 5-36. Geometry of Positional Uncertainty After Two Fixes

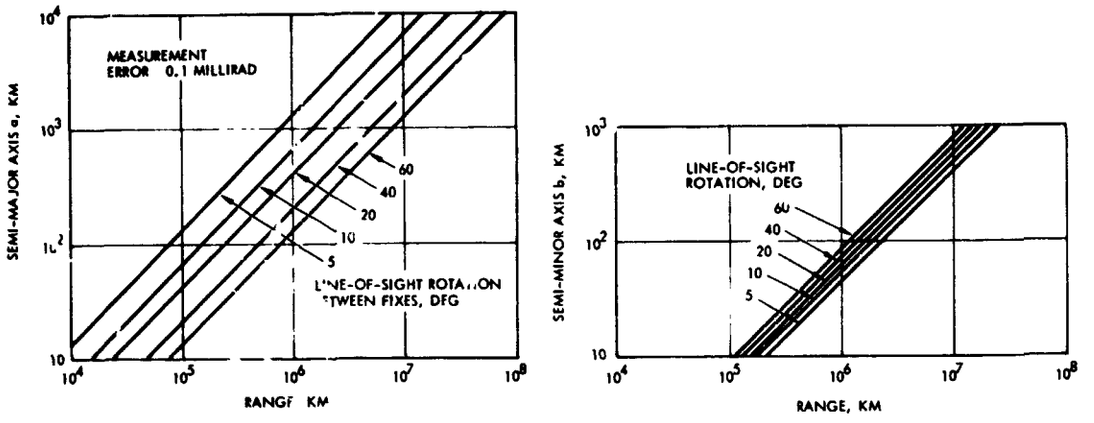

Figure 5-37. First-Order Approximation of Navigation Errors After Two Optical Fixes

days before rendezvous, assuming an observation error of 0.1 milliradian.* In the case of comet rendezvous the terminal line of sight rate tends to be larger than in asteroid rendezvous missions and the accuracy of navigational fixes tends to be greater except in the case of poor visual definition of the target object, i.e., when no nucleus is visible at time of acquisition.

An interesting concept for improvement of the range accuracy achievable in a terminal approach with a very small line-of-sight rate is the use of a deliberate change in the vehicle's approach velocity by insertion of a coast phase of several days. During this period and immediately after resumption of the thrust phase a substantial improvement of the range determination is possible since LOS-angle changes of about 10 degrees are obtained over a 10-day interval at a range of 10^6 km. This is an application of the maneuver-ranging technique employed in air-to-air combat.

*These results are from the current comet mission study by IITRI and were provided by Dr. A. L. Friedlander, (Ref. 5-17).

6.0 STAGE DESIGN

6.1 DESIGN APPROACH

Exploratory studies of several design concepts for the electric stage have led to the selection of the baseline configuration that will be described in Section 6.2. In keeping with the study guidelines, a baseline design was adopted that provides multi-mission versatility with little or no change in configuration.

Referring to the five basic design options A through E that were identified in Section 3 only the options B and C (see Figure 3-1) meet the study objectives and were considered as candidates for the multi-mission stage configuration. Option B calls for sharing of some of the stage subsystems by the payload package. This option is used in the configuration selected for the primary missions. Since the payload package remains permanently attached to the stage during these missions the communication and power subsystems of the stage can be used to support payload operation without requiring a complex interface. The stage serves as a "payload bus" in this case.

This design approach can be changed in missions where the payload package forms an autonomous spacecraft that will be ejected by the stage after completion of the propulsion phase as in an outer planet orbiter mission. No significant sharing of the stage subsystems by the payload is envisioned (Option C), i.e., the payload spacecraft must actually duplicate some stage subsystems. The stage serves as a "pure stage" in this case.

The design descriptions given in Sections 6.2 and 6.3 will show that the selected stage design concept can be readily converted from the former to the latter application as dictated by the type of mission to be carried out.

The outstanding advantage of using the vehicle as a separable stage in outer planet missions, notwithstanding the weight penalty of this approach, is the much shorter life time required of the stage versus an integral electric spacecraft. The long mission life requirement, 8 years in some missions, can thus be shifted to the payload spacecraft.

The multi-mission stage itself can therefore be designed with much less stringent reliability specifications, since the majority of its multi-mission objectives requires a mission life of only 2 to 3 years.

In selecting the baseline design concept we included only those design features that are required in a majority of the specified missions with room for adaptability to the special needs of more demanding mission types. Thus, the majority of stage users will not be burdened by weight, complexity and cost penalties of special features required by only a few mission types as for example the special thermal protection features of the 0.1 AU solar probe mission. The same criterion was also applied in the selection of subsystem design approaches.

The Ceres rendezvous mission was used as an illustrative example to provide representative mission profile data, design requirements, and constraints to guide the design approach for the baseline vehicle. Reasons for selecting the Ceres mission for this purpose are these:

- The mission is more typical for operations and environmental conditions of the majority of primary missions than would be the solar or extra-ecliptic probes.
- From a scientific standpoint the asteroid missions are of great interest.
- From a technology standpoint the asteroid rendezvous presents design and operational problems of intermediate complexity which should be resolved in the basic stage design concept.

Thus the illustrative mission example is representative of the most likely early mission application of the stage. However, the requirements of other mission types were taken into consideration throughout the design effort to assure multi-mission flexibility of the stage. Application of the selected baseline design concept to the various mission profiles and environmental conditions will be discussed in Sections 6.3 to 6.9. A conceptual adaptation to the "worst case" environment of the solar probe mission will be illustrated in Section 6.7.

A tentative payload complement was selected for the Ceres mission to illustrate its accommodation on the baseline stage configuration. However, detailed consideration of payload characteristics, operation

modes, and stage/payload interactions that would be required in such a design are outside the scope of this study.

Table 6-1 summarizes principal design features of the baseline configuration that were selected from various alternatives on the basis of system analysis, design tradeoff, and engineering judgement. Design experience from previous solar-electric multi-mission spacecraft studies by TRW, JPL, North American Rockwell and others is reflected in the choices made. The selected stage configuration will be discussed in detail in Section 6.2, and alternate design approaches in subsequent sections.

6.2 SELECTED BASELINE CONFIGURATION

The baseline stage configuration is shown in Figure 6-1. It consists of a long, narrow and flat center body and two boom-deployed, rollout solar array panels of the type being developed by G. E. under JPL contract. The solar arrays with a total deployed span of 43.0 m by 4.2 m width have a total cell mounting area of 162 m^2 and generate 17.5 kw of gross power at earth departure. The center body consists of the electric propulsion module, the stage equipment module and the payload stowage bay. Its structure is primarily an open truss work of aluminum tubing plus a U-shaped payload support superstructure which uses light-weight aluminum sheet and angles. The two structural members are tapered toward the upper end at which solar array retention brackets are attached to support the upper portion of the solar array storage drums during launch. Similarly the lower portion of these drums is supported during launch by a second pair of retention brackets attached to the lower part of the center body.

The solar array assembly is supported at the center by the rotation joints that permit reorientation of the extended array panels by $\pm$ 90 degrees from the nominal position parallel to the center line of the stage structure. A torque tube connects each panel to the centrally mounted drive mechanism which also includes a flexible, low-friction cable-wrap assembly for solar array power transfer into the stage proper, as shown in detail at the upper left of the design drawing. This cable-wrap design was developed and flown in OGO satellites.

Table 6-1. Principal Design Features Selected for Baseline Stage Configuration

	Feature		Option Selected	Selection Criterion or Rationale
1.	Vehicle Orientation	•	3-Axis controlled	-Provides multi-mission versatility -Freedom of orientation of thrust, solar panels and high gain antenna
2.	Center Body	•	Long and narrow	- Dictated by desired solar array width
3.	Payload Storage	•	As close as possible to center of stage	-Simplifies center-of-mass control of stage for large payloads -Shorter shroud -Reduces dynamic loads at launch
4.	Solar Array Configuration	•	Two paddles	-Avoids thrust beam impingement problem -Versatile and unobstructed payload storage
		•	Roll out model	-Rigid panel foldout too heavy and non-retractable
		•	$\pm 90^{\circ}$ articulation	-Necessary in many missions for thrust angle variation, orbital operations, etc. -Desired for thermal protection
5.	Thrust Vector Control	•	Gimballed thruster array	-Simpler and lighter than translation system
6.	Propulsion Module	•	Removable module	-Ease of assembly and test
		•	Switchable power processors	-Weight savings
		•	Standardized thruster array in all missions	-Avoids mission-to-mission modification at small w eight penalty
7.	Attitude References	•	Rotatable star sensor	-Multimission versatility; circumvents F. O. V. obstruction by solar array
		•	Gyro references	-Redundancy -Pointing mode versatility -Ease of reacquisition -Needed in planetary missions
8.	Antenna Size & Placement	•	Large dish, top mounted	-If desired for communication of science data
		•	Small dish, bottom mounted	-If not needed for science data -If larger antenna would obstruct payload mounting -If forced by environment (solar probe heat protection)

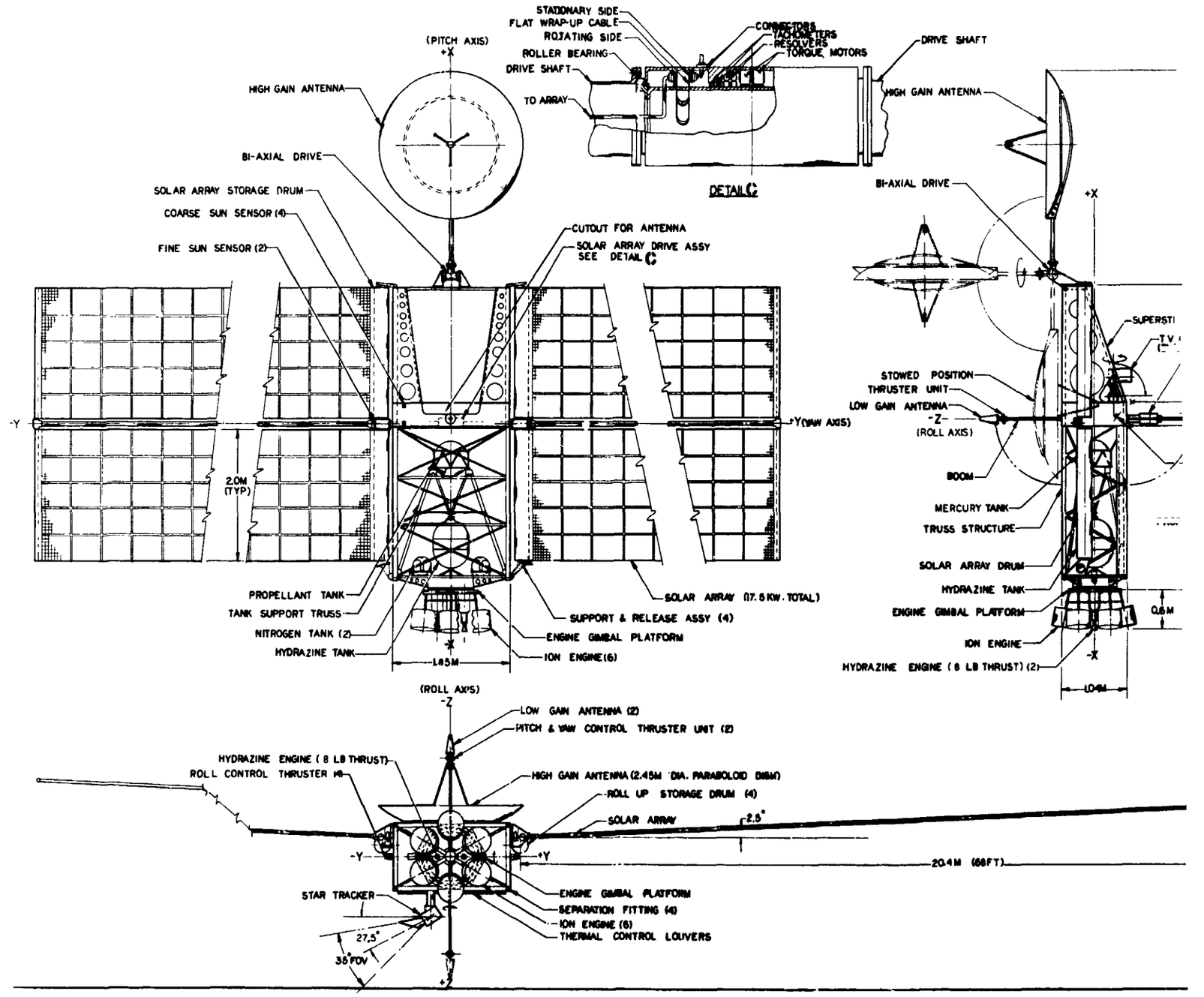

FOLDOUT FRAME 1

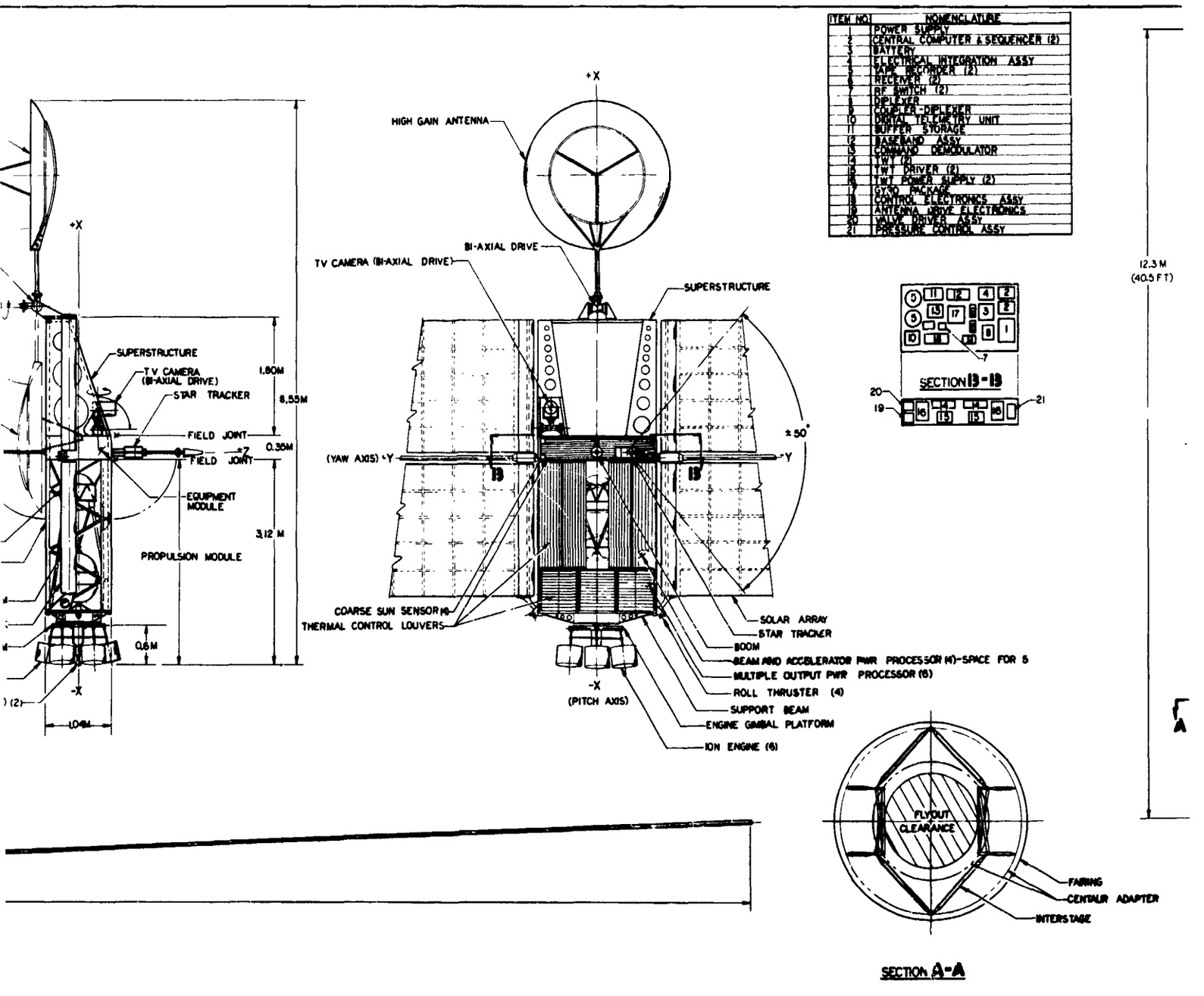

ITEM NO.	NOMENCLATURE
1	POWER SUPPLY
2	CENTRAL COMPUTER & SEQUENCER (2)
3	BATTERY
4	ELECTRICAL INTEGRATION ASSY
5	TAPE RECORDER (2)
6	RECEIVER (2)
7	RF SWITCH (2)
8	DIPLEXER
9	COUPLER-DIPLEXER
10	DIGITAL TELEMETRY UNIT
11	BUFFER STORAGE
12	BASEBAND ASSY
13	COMMAND DEMODULATOR
14	TWT (2)
15	TWT DRIVER (2)
16	TWT POWER SUPPLY (2)
17	GYRO PACKAGE
18	CONTROL ELECTRONICS ASSY
19	ANTENNA DRIVE ELECTRONICS
20	VALVE DRIVER ASSY
21	PRESSURE CONTROL ASSY

FOLDOUT FRAME 2

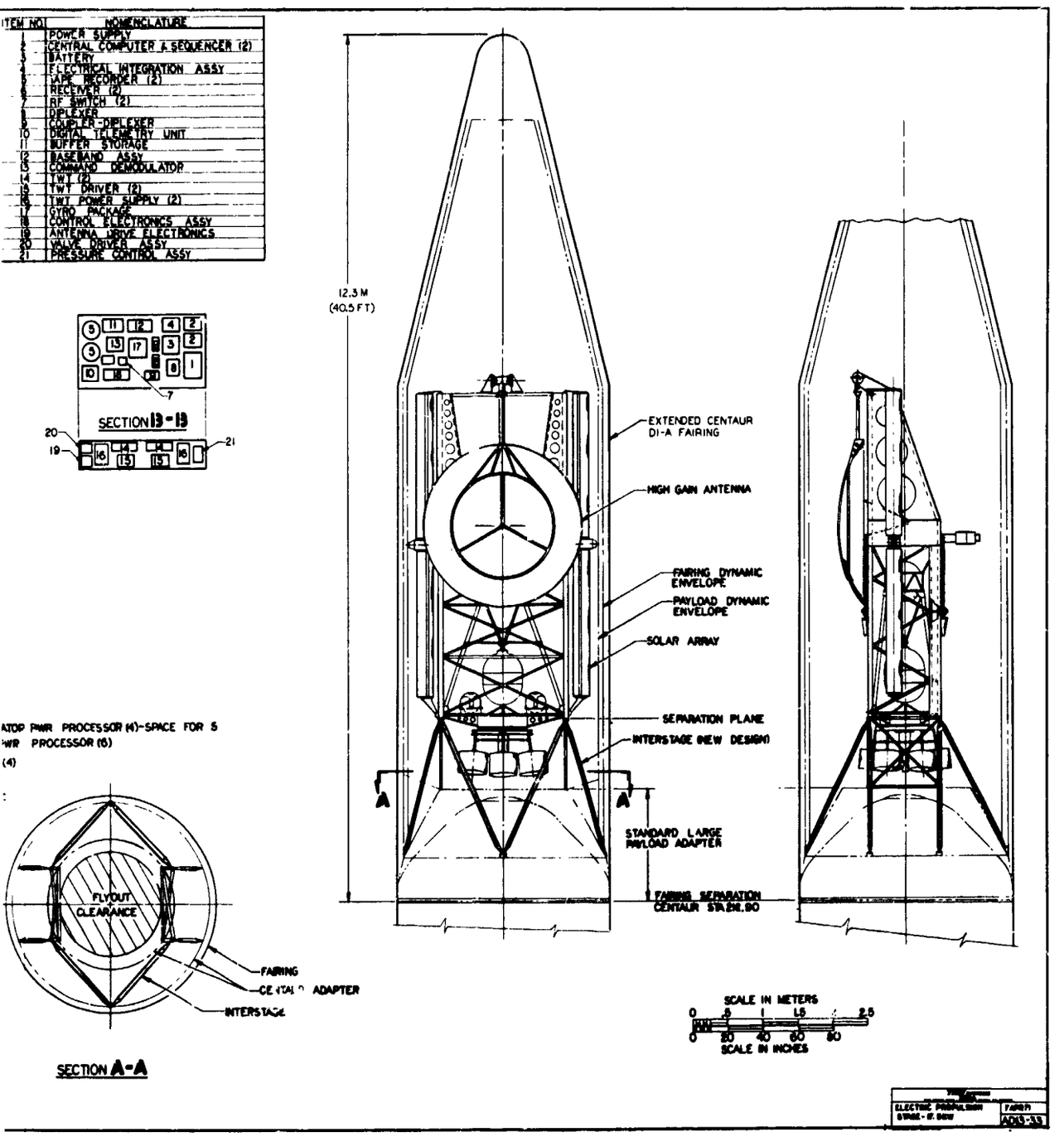

Figure 6-1. Baseline Electric Stage Design

FOLDOUT FRAME 3

The solar array rotation capability is included in the baseline configuration.

(a) to permit optimal thrust vector pointing in those missions where non-optimal (fixed) pointing would impose a significant payload penalty;

(b) to permit greater freedom for terminal guidance corrections and maneuvers near the target (e. g., orbit insertion without constraint of a fixed sun orientation of the stage);

(c) to permit body reorientation as required in planetary orbit missions, comet exploration, etc;

(d) to permit thermal protection of the solar cells in mission where the stage approaches the sun closer than 0.65 AU (Mercury, solar probe, and Encke mission) by reorienting the array away from full sun orientation; and

(e) to reduce solar pressure unbalance torques that can occur during intermittent coast periods when the center of mass and center of pressure do not coincide, thereby saving significant amounts of attitude control propellant.

This rotation capability is desired in the interest of greater flexibility of the stage in multiple mission applications. However, as was previously mentioned, solar array rotation is not necessary in all missions, and can be omitted by removing the articulation joint and drive assembly to save weight and simplify the configuration.

The 8-ft parabolic high-gain antenna dish is mounted on a long deployment arm and can be rotated for full coverage of the front and rear hemisphere by means of a biaxial rotation joint. It is mounted on the upper end of the center body in the center of a cross bar attached to the end points of the payload support superstructure. During launch the antenna is stowed against the front (sun illuminated) side of the center body with the feed structure protruding into a recess of the equipment module. The hinge axis drive of the biaxial rotation joint serves to deploy the antenna from, and to swing the antenna arm into a position relative to, the center body from which earth pointing is achieved by a second rotation around the shaft axis. The biaxial drive thus provides

full 4π -steradian coverage for the antenna. This arrangement eliminates the need for a second hinge for deployment purposes. Care has been taken to avoid shading of the solar array and obstruction of optical sensor fields of view by any pointing position of the high-gain antenna. There are alternate options of mounting the antenna in case the upper end of the payload support structure must be left open, as for example in the solar probe configuration of the stage where a solar heat shield must be mounted at the upper end, or in the case of outer planet missions where a large detachable spacecraft is stowed in this area. A simple departure from the baseline configuration accommodates these missions as will be discussed below.

Three-axis attitude control of the vehicle is provided either by gas jets mounted on a pair of deployed 1.2 m long outrigger booms in front and rear and at the bottom of the center body, or by the thrust vector control (TVC) mechanism of the electric propulsion module to be discussed below. In addition to the ACS nozzles the front and rear outrigger booms carry omni-directional antennas which provide command and downlink capability prior to high-gain antenna deployment and uplink communication to the stage when the high-gain antenna is not pointing at the earth.

A set of four coarse sun sensors are used for initial sun acquisition or reacquisition, and a fine sun sensor mounted on the center body provides the pitch and yaw reference. A second fine sun sensor, mounted on the solar array deployment structure is used at times when the solar array but not the center body maintains sun orientation. A pair of redundant gas-bearing integrating rate gyros provide an inertial roll reference (rotation around the sun line, or clock angle) with periodic updating by a rotatable star tracker, which is mounted at the rear of the center body with a field of view unobstructed by the solar array paddles. The articulated star tracker can be used during any mission phase to acquire and lock on to a bright reference star, based on a star pointing program stored aboard the vehicle. The inherent flexibility of the star tracker facilitates multiple mission use. Many bright reference stars can be conveniently found in the southern celestial hemisphere, such as Canopus; Sirius, α-Centauri and Achernar. The movability of the

star tracker has the advantage of providing a flexible choice of reference stars as the mission progresses without interference by the long solar arrays and other obstructing appendages.

The electric propulsion module forms the lower half of the center body placing the heavy mass concentration of propulsion hardware and propellant storage close to the launch vehicle adapter. A conceptual drawing of this module is presented in Figure 6-2. For convenience of assembly, handling and test the propulsion module is detachable from the remainder of the stage structure by a field joint. The power processor units which dissipate a maximum amount of waste heat equivalent to 1.5 to 2 kw are mounted on the rear surface of the propulsion module using a total radiating area of 1.8 x 2.3 m. Mounting on the side walls would be ineffectual because of the required solar array rotation that would obstruct free radiation to space from this location. This constraint largely dictates the size of the propulsion module. As seen in the design drawing there are 4 main (beam and accelerator) power processors, with mounting space left open for a 5th unit as required in some missions, plus 6 multiple output power processors that dissipate only about 20 percent of the total waste heat. The heavy main processors are switchable, while the small multiple-output processors are permanently wired to the respective electric thrusters.

An array of six electron bombardment mercury ion thrusters is mounted on an articulated platform at the bottom of the propulsion module. Only three of the thrusters will be used nominally at the start of the prototype Ceres rendezvous mission. The other thrusters are held in reserve. Although, this mission does not require the extra redundancy of three additional thrusters. we selected the six-thruster configuration to meet more stringent thrust time and redundancy requirements of other missions (e.g., the extra-ecliptic probe) and to avoid a change of the number of thrusters from mission to mission. The weight penalty of 11.5 kg for carrying an additional thruster on the Ceres mission is acceptable in exchange for greater commonality of the propulsion module. The same reasoning is applied in making the mercury propellant tank capacity large enough to accommodate the largest propellant mass of any of the primary missions, i.e., 1015 kg

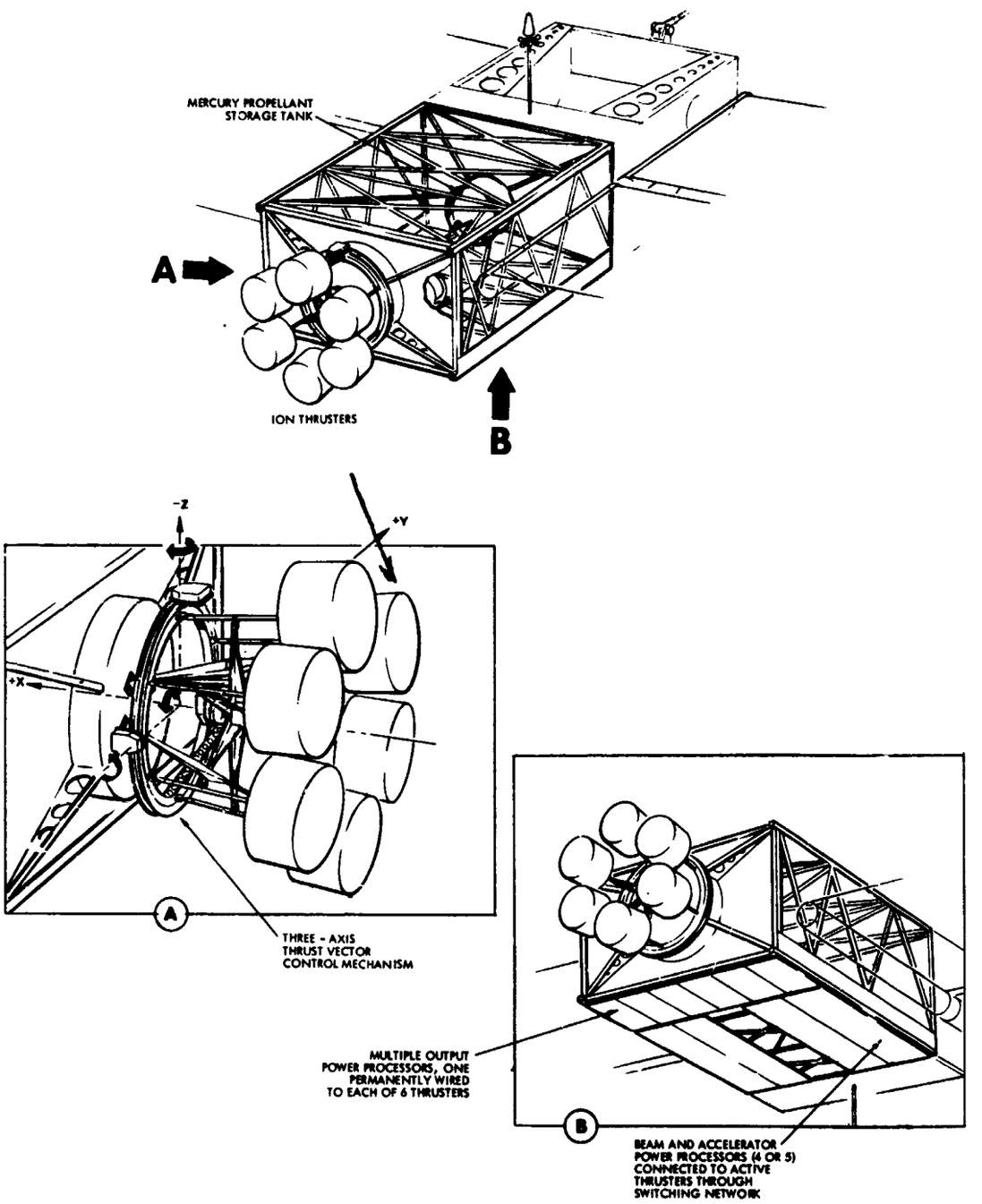

Figure 6-2. Propulsion Module

for the extra-ecliptic mission, whereas the Ceres mission requires only 450 kg which is about 44 percent of full tank capacity.

Small changes in the orientation of the six-thruster assembly can be made by means of a three axis gimbal actuator system, to provide thrust vector control in pitch, yaw and roll* (except when only one thruster is operating and the TVC system can no longer provide pitch control which requires differential gimbal deflections of at least two thrusters). Use of the TVC system for attitude control during the thrust phase is necessary to avoid a large expenditure of attitude control gas through reaction control jets.

The large separation of the thruster array from the stage center of mass (2.6 m) permits adoption of the all-rotational TVC concept with small angle deflections instead of one that uses a translational mechanism as in previous designs by TRW, North American-Rockwell, Hughes and JPL. All thrusters are mounted at a 9-degree symmetrical cant angle, such that thruster switching ideally does not introduce a step change in roll and yaw torques. Solar array deflections due to thermal and dynamic effects change the location of the vehicle's center of mass which will be compensated by changing the orientation of the thruster assembly. Center of mass changes due to antenna repositioning and fuel depletion, and the effect of solar pressure torque unbalance and thruster mounting and operating asymmetries can all be neutralized by TVC gimbal deflections in the range of 4 to 8 degrees. Further details of the design and operation of the novel TVC system will be found in the discussion of the electric propulsion module. (Section 7.2.)

The baseline configuration carries a hydrazine thrust system that augments terminal maneuver capability of the stage at large solar distances. The system uses two thrusters each rated for a nominal thrust of 35 Nt (3 lbs), throttlable over a 4:1 ratio. A single blowdown hydrazine tank with 80 kg capacity is located in the lower half of the propulsion module. The two hydrazine thrusters are mounted in the center of the

*the pitch, yaw and roll axis are identified in the design drawing, Figure 6-1.

hexagonal ion thruster array and can thus be articulated for thrust vector control by the same gimbal system that serves the ion thrusters. The two sets of thrusters will not be operated simultaneously to avoid thermal interaction. The hydrazine system can be readily removed for missions that do not have a chemical propulsion requirement.

Two nitrogen propellant storage tanks with a capacity of 10 kg each are shown located at the bottom of the propulsion module. They provide nitrogen through redundant feed and valve systems to the three sets of four resistojet nozzles that make up the ACS reaction control systems, as previously mentioned.

The stowed configuration of the electric stage and the interstage adapter are shown at the right of the design drawing. The adapter extends the standard conical Centaur adapter structure upward to the four attachment points at the bottom of the stage structure. The load is distributed through (a) vertical members that connect to four points on the Centaur adapter ring and (b) additional support struts that connect to eight mounting points at the base of the adapter cone, where it is joined to the hull of the Centaur stage. This arrangement provides ample fly-out clearance for the lower portion of the propulsion module nesting in the interstage adapter.

Structurally the principal load of the stage body is carried by four longerous to the interstage attachment point. The concentrated load of the heavy mercury storage tank is directly transferred to the stage attachment points through the four tubular struts of a pedestal. The tank itself rests on a cradle on top of the pedestal. In addition it is secured against lateral dynamic loads by a belt structure that is strapped to tie points at the upper end of the propulsion module.

The upper structure of the baseline stage configuration is removable during ground handling and for payload assembly separate from the stage proper. A smaller support structure than that shown in the baseline design may be used if preferred for convenience of payload arrangement. However the support of the upper solar array storage drums during launch must still be provided by structural members that substitute for those shown in the design drawing, Figure 6-1.

6.3 ALTERNATE CONFIGURATION OF THE BASIC STAGE

By the simple rearrangement shown in Figure 6-3 the baseline design can be converted into a configuration more appropriate to missions where the stage is to carry a large separable payload spacecraft. To provide more payload mounting space and improve accessibility of the payload bay in such applications the high-gain antenna is relocated from the top of the payload module to a position near the bottom of the center structure, as shown in the drawing, using a deployment hinge that is located near the thruster assembly. The deployment arm is designed to place the antenna in one of two positions that cover all antenna pointing requirements in the front or rear hemisphere as shown in the side view drawing. Transfer from position 1 to 2 around the thruster assembly is feasible during coast and thrust phases but requires a short thrust interruption in the latter case. The antenna positions 1 and 2 have been selected such that neither the antenna dish nor its feed structure can protrude across the boundary of possible impingement of thrust beam exhaust products which is indicated in the drawing. In this configuration the antenna is made half as large (1.22 m diameter) as the antenna nominally shown in the baseline design. This is considered adequate for missions where the payload is a separable (autonomous) spacecraft that requires little or no communication support from the stage. This would reduce the total data rates by at least a factor of 4. The small antenna size excludes obstruction of solar array or antenna articulation. Figure 6-4 is an exploratory design drawing that illustrates the articulation of a bottom-mounted full size 2.45 m antenna. This concept is applicable in missions where the larger antenna gain is desired and where the solar array remains stationary relative to the center body so that no obstruction of array or antenna articulation can occur.

Actually, the smaller antenna is preferred in the bottom-mounted application (a) to avoid field of view problems if the solar array must be rotated, (b) to minimize star sensor field-of-view conflicts (if the antenna is in the rear location), (c) to minimize interference with free radiation of waste heat from the power processors (if antenna is in the rear location) and (d) to avoid ion beam exhaust impingement that could

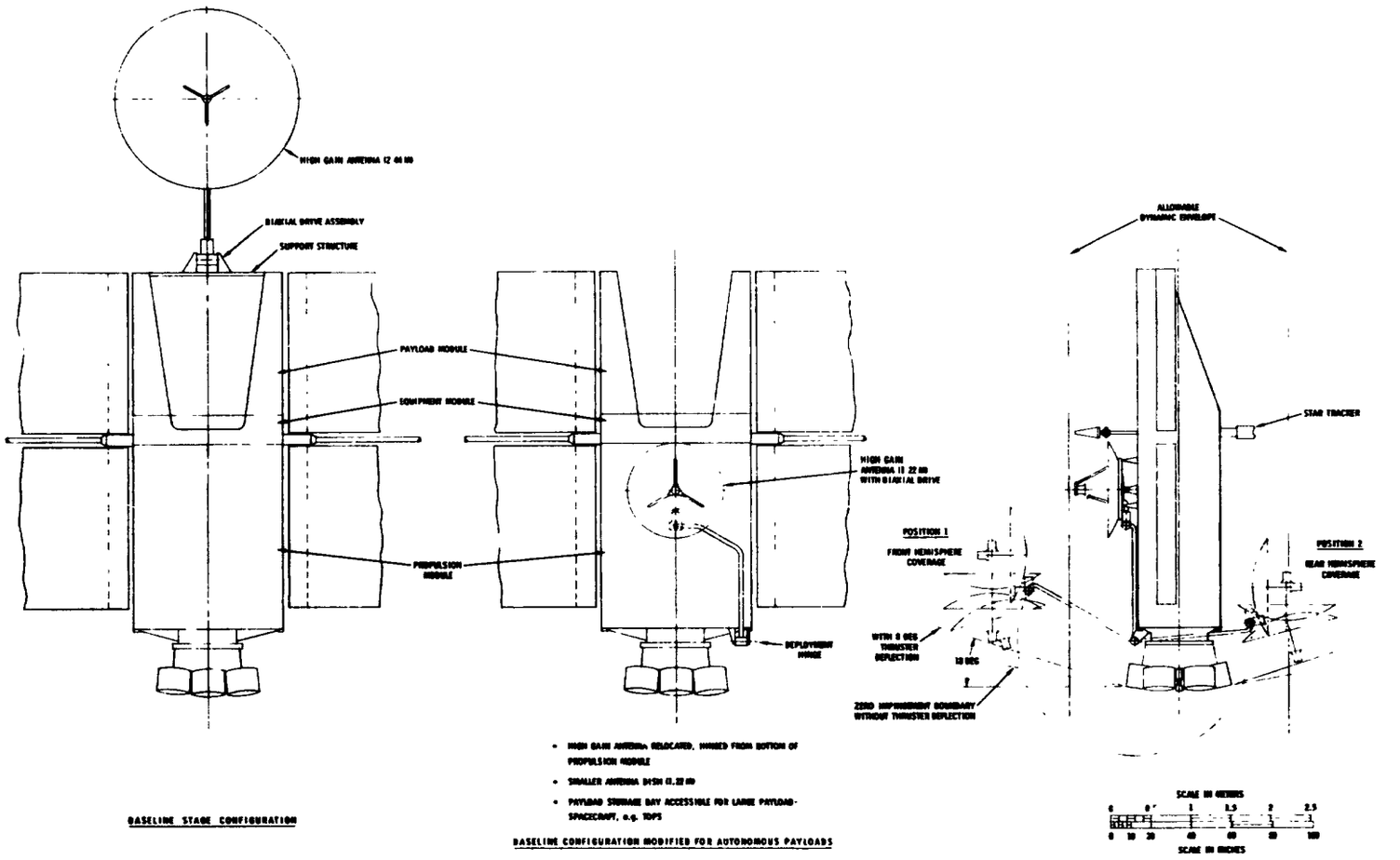

Figure 6-3. Alternative Configuration of Basic Stage with Bottom-Mounted High-Gain Antenna

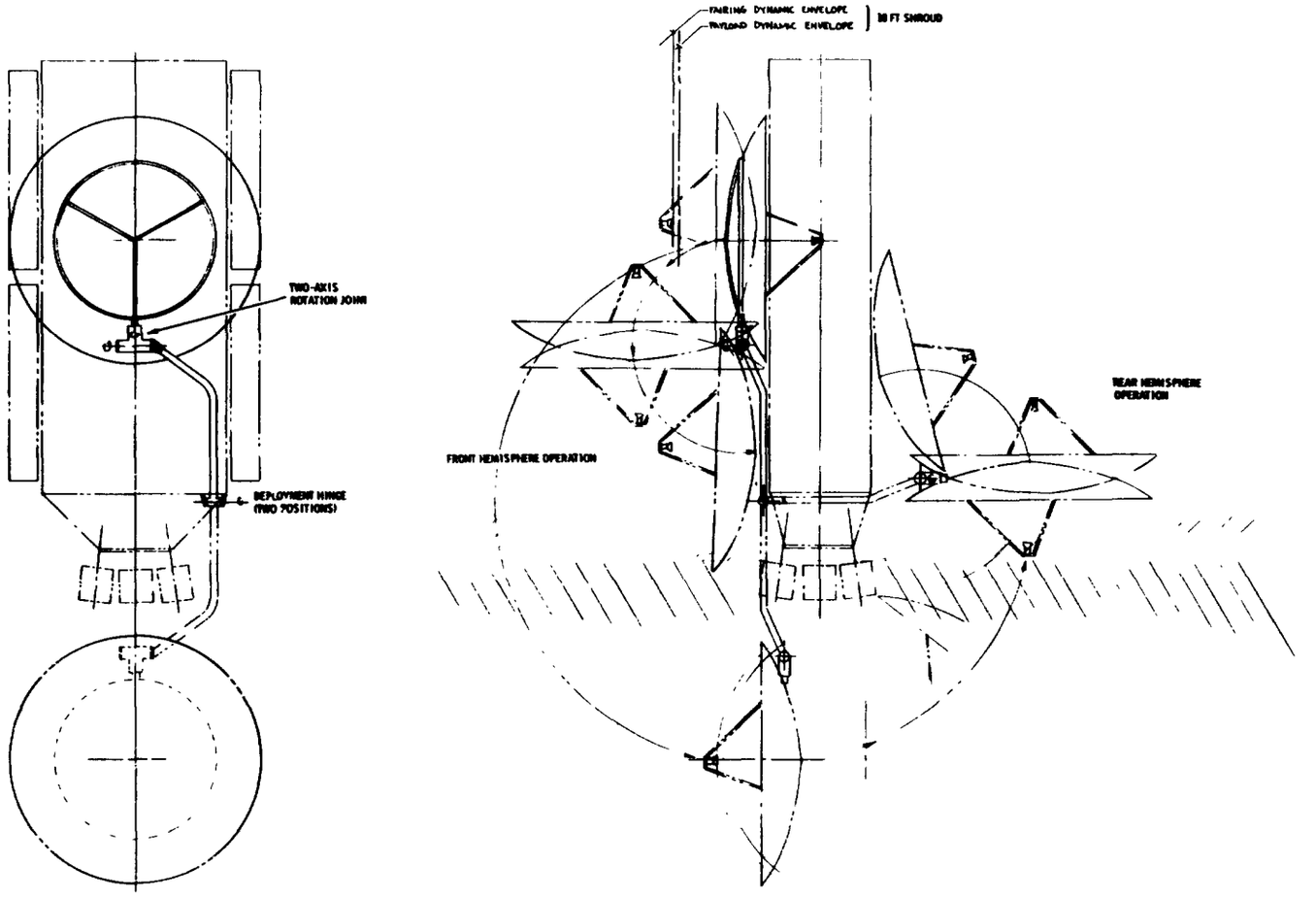

Figure 6-4. Bottom-Mounted High-Gain Antenna

occur in the case of the larger antenna dish. Mission applications to be discussed in the following sections show various other bottom-mounted antenna configurations that could actually be handled by the design shown in Figure 6-3.

Removal of the high-gain antenna and the supporting cross-beam from the top of the payload module eliminates the structural element that connects the two solar array support towers in the baseline configuration. Since these towers are designed with sufficient structural strength to support the upper part of the solar array storage drums during launch without external bracing the conversion of the baseline configuration to an open payload bay does not require any additional structural modification.

In conclusion we note that the two stage configurations shown in Figure 1-1 provide the principal design options required for any of the projected missions to be flown by the stage.

1. The nominal configuration (with top-mounted antenna) is preferred in missions where the payload package is permanently attached and where a sharing of the stage communication subsystem is desired, hence the need for a larger antenna. In this case the stage functions as a "bus vehicle".

2. The alternate configuration (with bottom-mounted antenna) is preferred in missions where the payload is an autonomous separable spacecraft. In this case the stage functions as a "pure stage". Little or no sharing of the stage communication system is required during the transportation phase. However, we note that even in the absence of any active interface between stage and payload in this case the required telemetry of engineering data from the dormant payload spacecraft can be readily handled by the stage. (We do not propose to let the payload spacecraft carry still another communication system in addition to the one that it will be using after stage separation, as long as a simple interconnection to the stage permits the use of the available telemetry link.)

We thus have provided a versatile transportation system that can function either as bus vehicle or pure stage requiring only a minor configuration change between the two options. This versatility does not reflect in greater system complexity, weight or appreciable extra development cost.

6.4 SAMPLES OF PAYLOAD TYPES CARRIED BY THE STAGE

The attachment of several payload types to the stage is illustrated schematically in Figure 6-5. The envelope of the modular payload packages (shaded areas) changes from case to case, but each is compatible with the payload stowage volume provided in the baseline configuration. (A preliminary version of the center body design, considered during the first study phase is used in this illustration but suffices to show the compatibility of the stage design concept with the various payload types.) The examples include:

1) A payload permanently attached to the stage.

2) One or several daughterprobes of the size of Pioneer A through E (about 1 m diameter) that are ejected normal to the plane of the solar array.

3) A lander capsule for a mission to Ceres or other large asteroids.

4) A large, separable spacecraft such as an outer planet flyby or orbiter vehicle.

5) Addition of touchdown and surface operation equipment and earth reentry capsule for the Eros sample return mission.

6) A large unfurlable antenna (10 meter diameter) that would be required if the stage were to be used as a deep space communications relay.

Some examples of payload accommodation on board the stage are shown below in greater detail.

6.5 PAYLOAD EXAMPLE FOR CERES ORBITER AND LANDER MISSION

Figure 6-6 shows the placement on the stage of representative payload instruments for a Ceres orbiter mission, including a lander capsule. This drawing shows a stage configuration very similar to that of Figure 6-1 without including a number of final design revisions. A perspective drawing is shown in Figure 6-7. The drawing shows several boom mounted fields and particles sensors, e.g., a He-magnetometer and two cosmic ray telescopes placed at the solar array tips, an AC magnetometer, plasma wave detector and space particle extractor (used

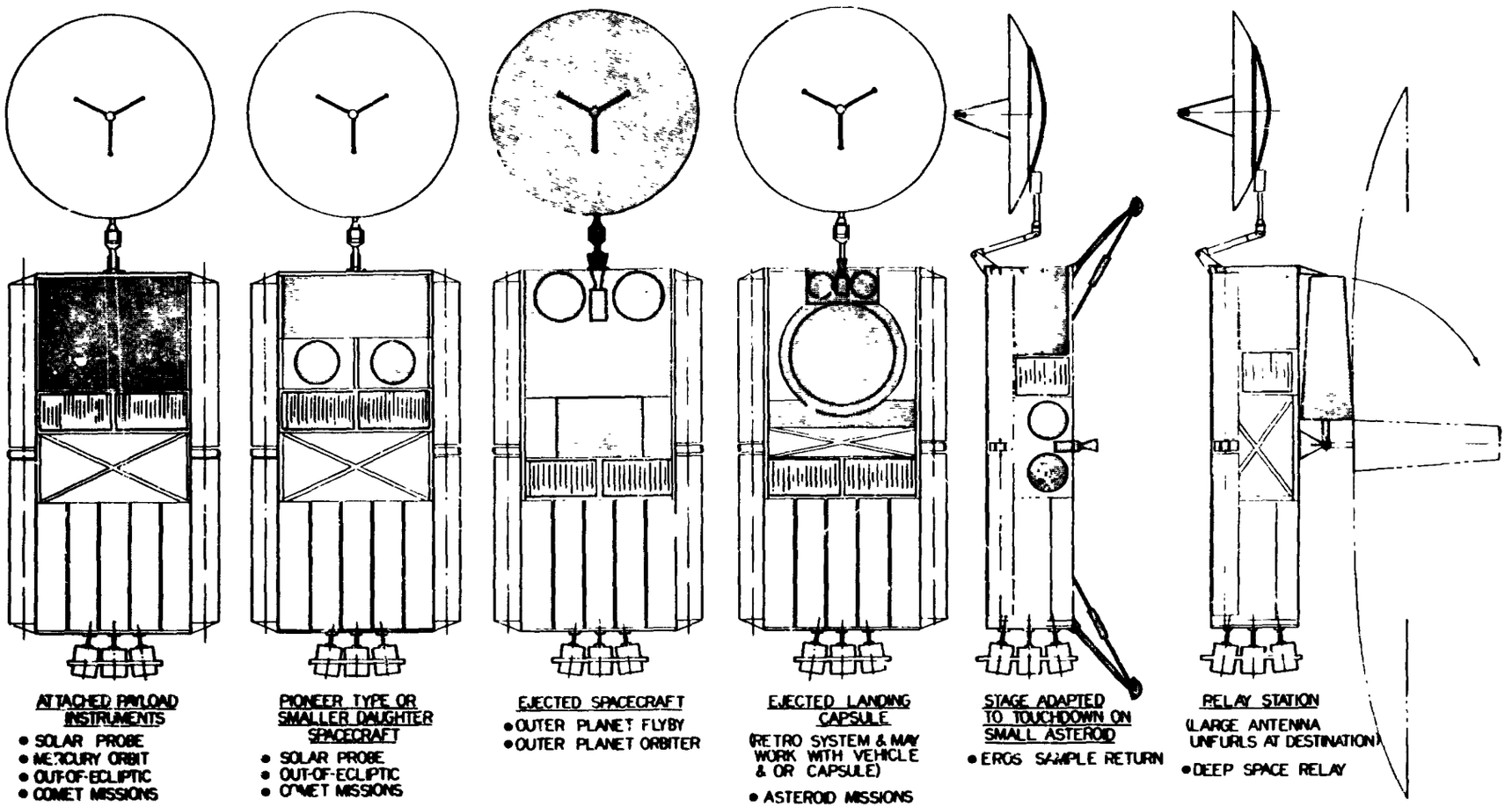

Figure 6-5. Adaptation of Baseline Configuration to Several Missions

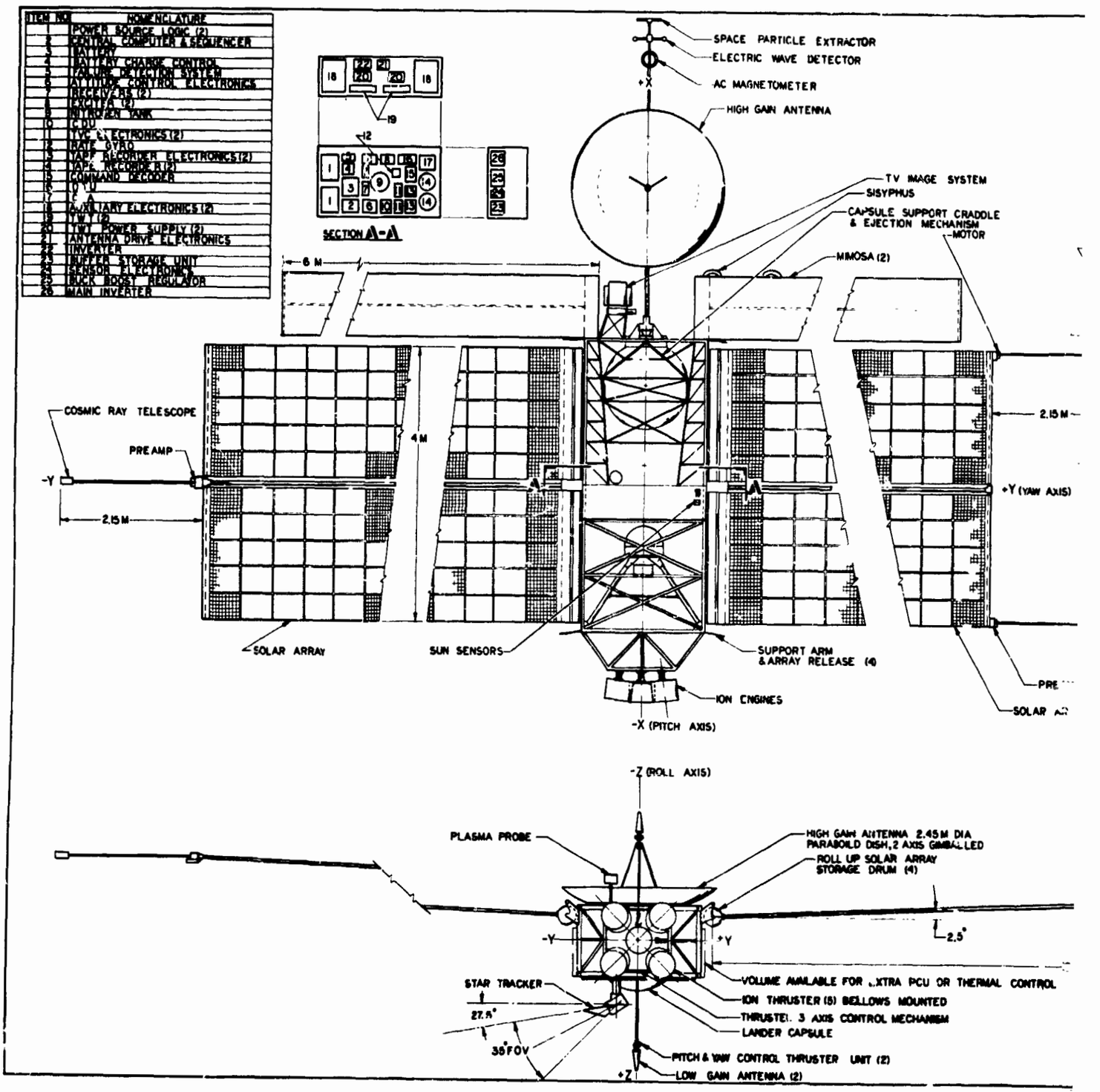

FOLDOUT FRAME 1

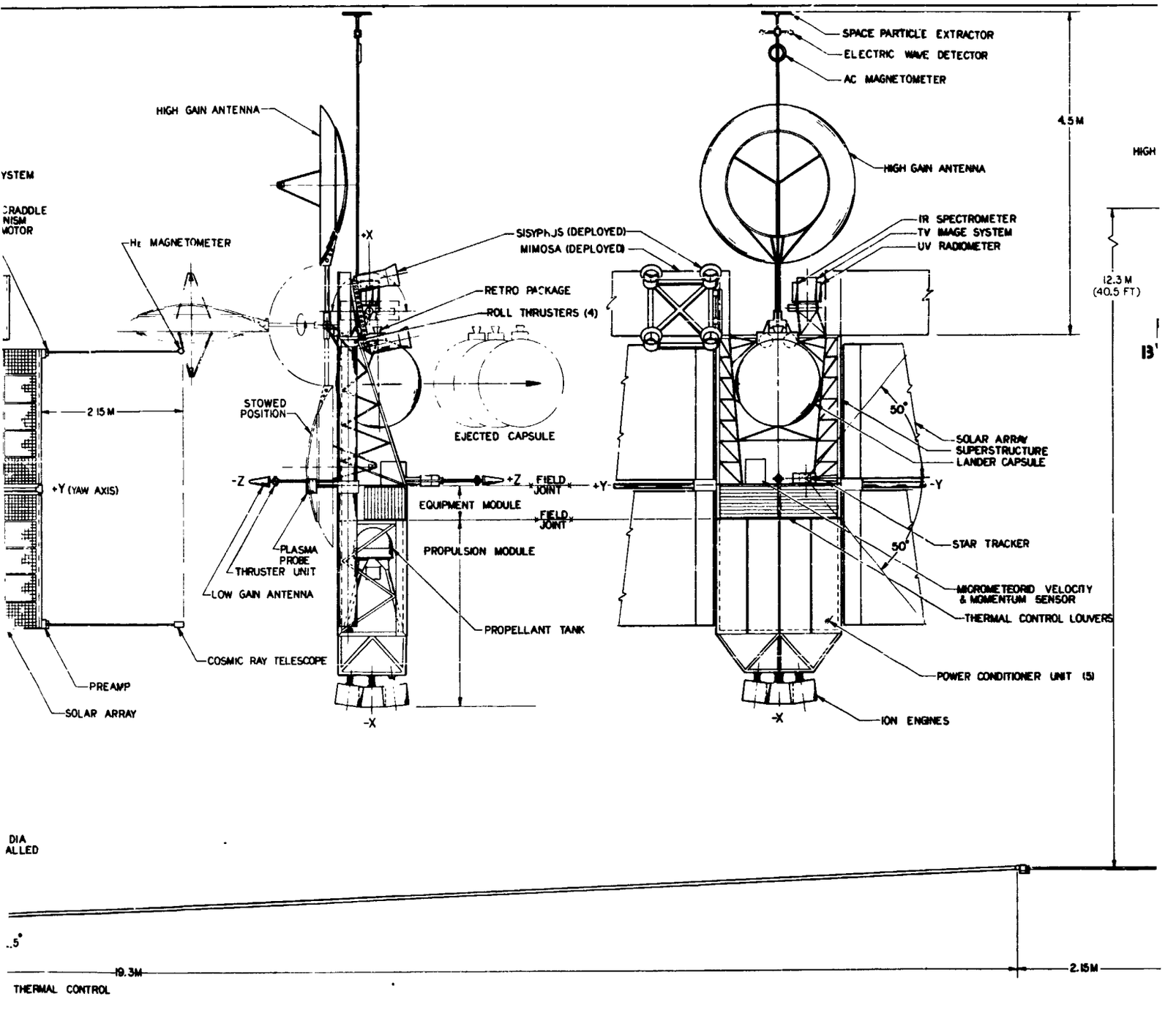

FOLDOUT FRAME 2

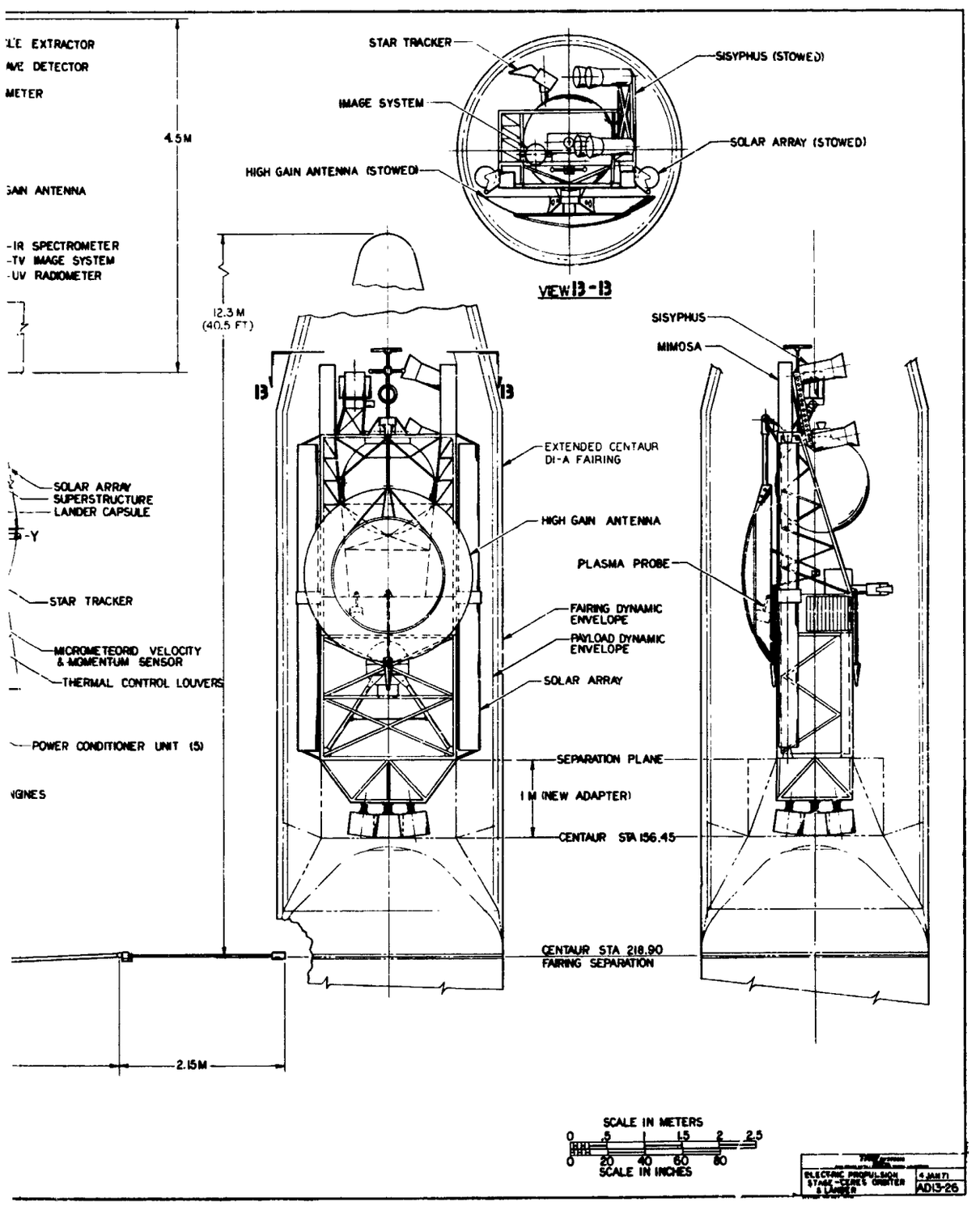

Figure 6-6. Electric Propulsion Stage - Ceres Orbiter and Lander

FOLDOUT FRAME 2

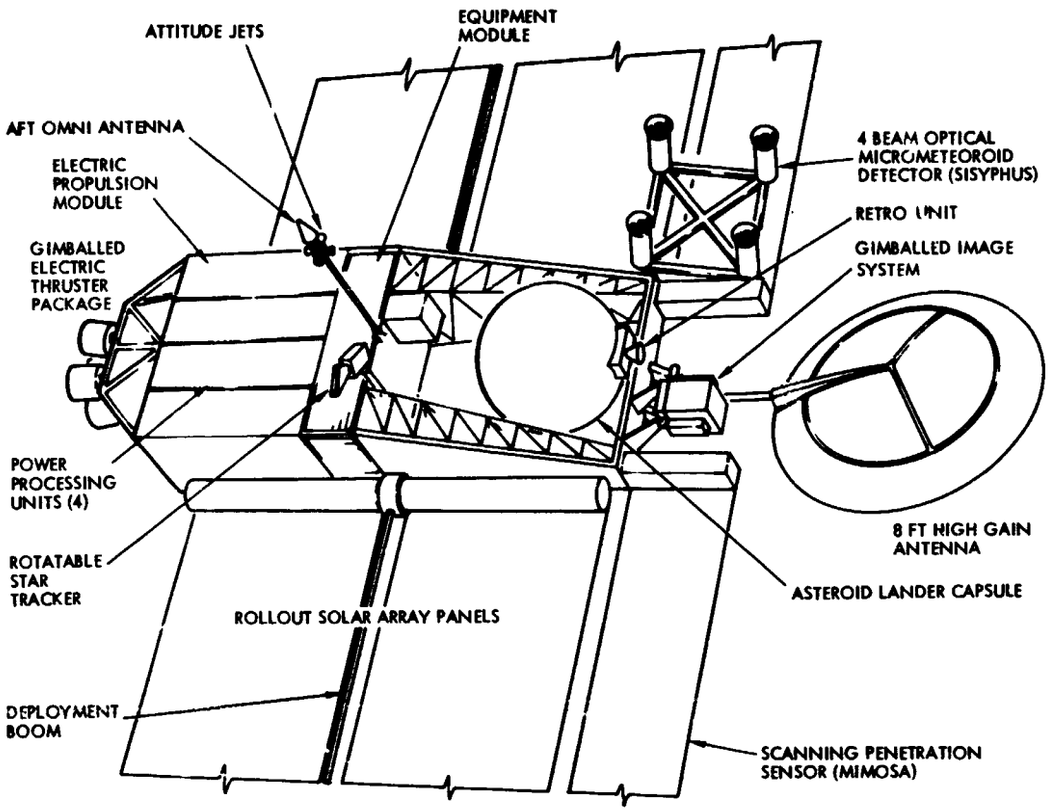

Figure 6-7. Baseline Electric Stage Design Adapted to Ceres Orbiter Mission

for establishing the stage at a desired potential relative to the surrounding plasma) on a separate boom, a gimballed TV image system, and several micrometeorid sensors, e.g., the Sisyphus four-beam optical micrometeroid detector mounted on the payload support superstructure, a pair of deployable micrometeroid puncture detector panels (TRW's Mimosa concept) and a momentum and velocity sensor. A spherical Ceres soft-lander capsule to be ejected by the stage after achieving an orbit around the asteroid is stowed in the upper part of the payload bay. The capsule ejection procedure is illustrated in the sideview shown in the center of the drawing, Figure 6-6.

6.6 ACCOMMODATION OF PAYLOAD SPACECRAFT FOR OUTER PLANET MISSIONS

The compatibility of the baseline configuration with outer planet mission requirements has been investigated. Separation of the stage

proper from the outer planet spacecraft is desirable after completion of the thrust phase because neither the propulsion system nor the solar array are of any further use and only impede the accomplishment of mission science objectives, midcourse maneuvers and, most of all, the orbit insertion maneuver. Also, this separation permits a design lifetime for the stage of only two years as compared to 8 years to destination for an integrated spacecraft such as SEMMS.

Of the spacecraft types that the stage can carry on outbound missions we considered a spin stabilized configuration such as Pioneer F and G (Ref. 5-2) and a three-axis stabilized configuration such as TOPS (Ref. 6-1). The spin stabilized Pioneer would have the advantage of simpler attitude control, greater overall reliability and convenient spin scan of physical phenomena, but it would be less suitable for planetary imaging. Figure 6-8 shows the Pioneer F stowed in the upper part of the payload bay. After launch the RTGs would be deployed to avoid thermal problems and radiation effects.

The TOPS vehicle with a nominal gross mass of about 700 kg and an unfurlable antenna of 4.3 m diameter or an enlarged Pioneer at about 350 kg are in the proper weight and size class for delivery by the electric stage. The advantage of using the stage as delivery system for a TOPS spacecraft is to make it independent from outer planet swingby opportunities which confine the ballistically launched TOPS vehicle to Grand Tour missions of the late '70s and early 80s. The electric stage delivery system provides direct mission modes, shortened flight times and payload capacities not achievable by a Titan 3D/Centaur ballistic launch.

The TOPS vehicle fits into the payload bay as illustrated by the sketch shown in Figure 6-9. This arrangement of the TOPS vehicle relative to the electric stage center body fits the narrow dimension (about 1 meter) of its equipment module into the payload bay opening of the electric stage with stowed appendages in front and rear. The design drawing (Figure 6-10) shows this arrangement in detail. The large high-gain antenna of the TOPS vehicle in the stowed configuration protrudes into the upper portion of the shroud volume. It stays folded

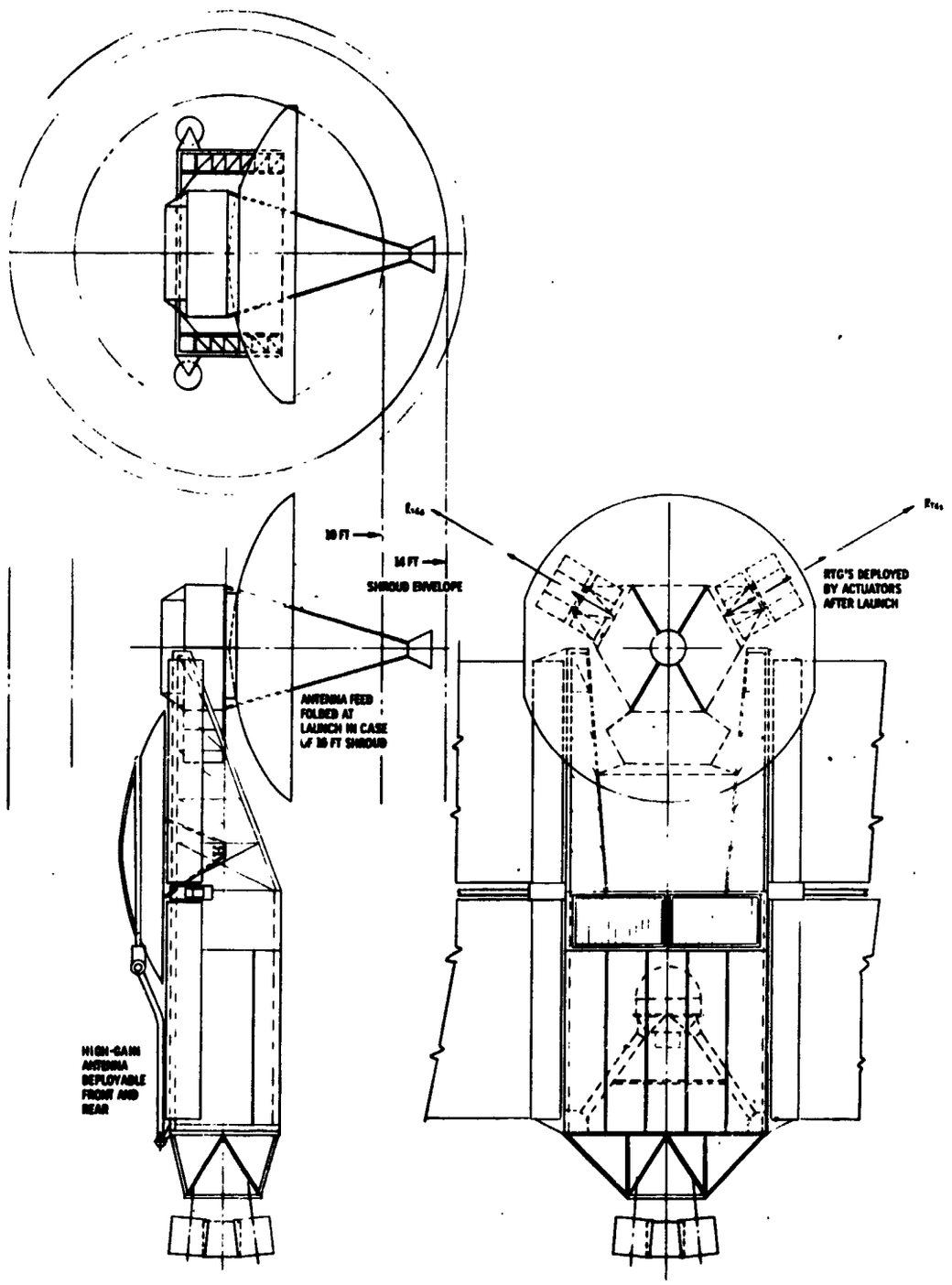

Figure 6-8. Pioneer Outer Planet Spacecraft Mounted on Stage

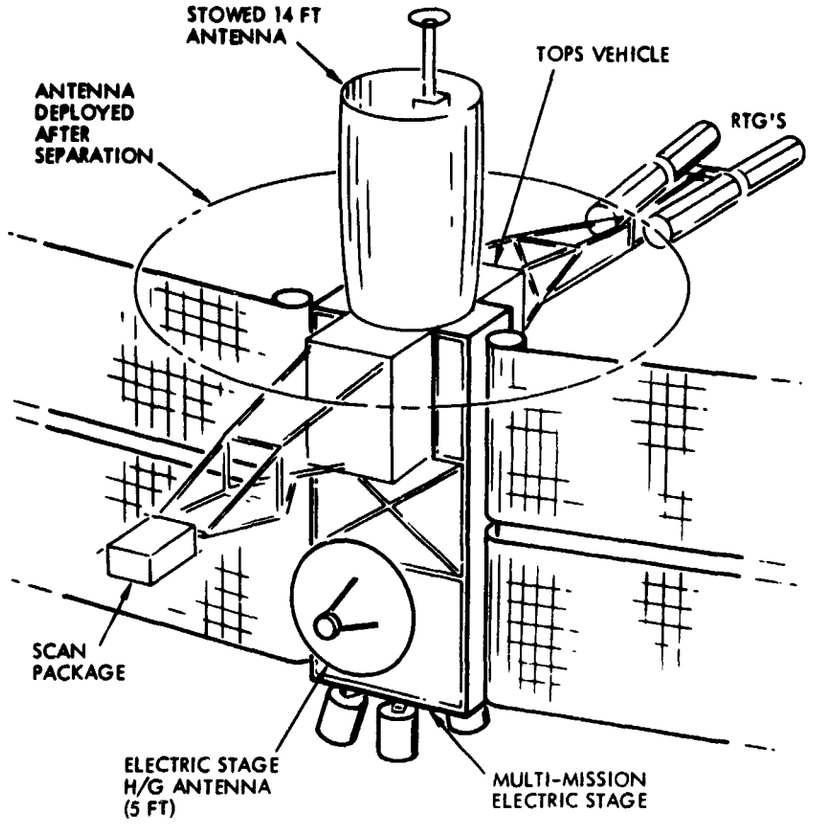

Figure 6-9. TOPS Spacecraft Mounted on Electric Stage

until the spacecraft is separated from the stage. This means that the electric stage must use a separate high-gain antenna articulated for coverage of the forward as well as the rear hemisphere as required by an indirect mission mode where the stage would initially follow an inbound trajectory. The antenna placement is essentially that discussed in Section 6.3. A 1.22 m dish can be substituted for the larger dish shown in Figure 6-10.

The RTG power units are deployed from the stowed configuration after launch to minimize interaction effects due to thermal and isotope radiation from these units. For symmetry of mass distribution the deployment arm carrying the science scan platform on the side opposite the RTG deployment structure should also be deployed after launch. Placement of the TOPS center body well inside the stowage bay of the electric stage achieves a favorable mass distribution which reduces dynamic loading of the electric stage center structure during launch.

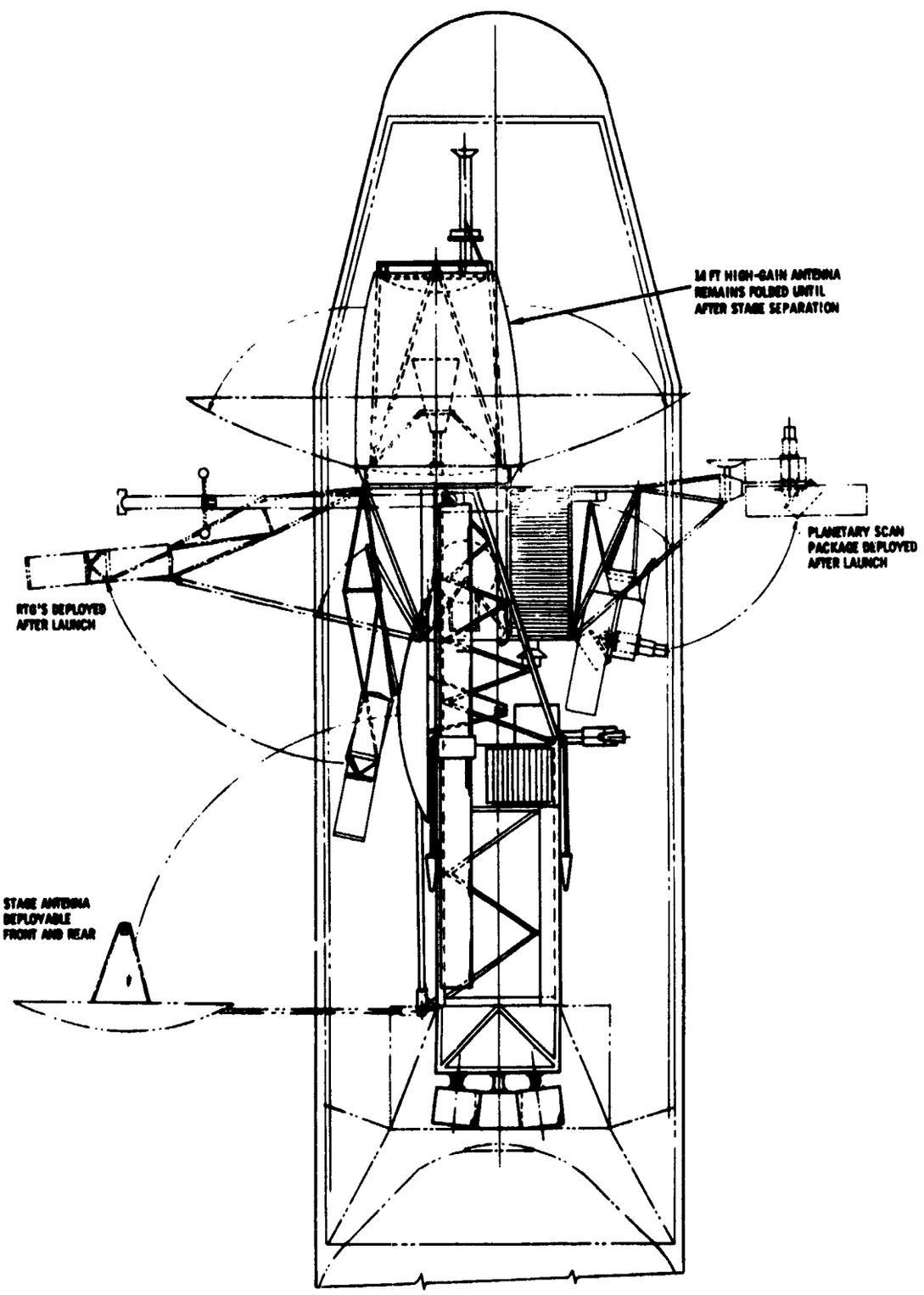

Figure 6-10. TOPS Planetary Flyby Vehicle Mounted on Stage

An orbiter version of TOPS having a large chemical propulsion module attached to the basic vehicle can be accommodated either with the propulsion module placed in the payload bay and the stowed antenna protruding into the upper shroud volume, or in an inverted position as shown in Figure 6-11, in front and side views. This configuration permits a more convenient fit between the TOPS orbiter and the payload bay but causes the combined center of mass to be undesirably high above the stage adapter. Additional design effort is required to show the most effective placement of the TOPS orbiter on top of the stage.

6.7 SOLAR PROBE CONFIGURATION

An adaptation of the stage design to the 0.1 AU solar probe mission was investigated as a worst-case departure from the baseline design concept. Figure 6-12 shows the stage in stowed and deployed configuration with the addition of a shadow shield that must be erected prior to approaching the sun within 0.25 AU. At this time the solar array panels are retracted and the stage must execute a 90-degree yaw maneuver to find protection in the shadow of the heat shield. At closest approach the sun will subtend an angle of about 5 degrees. This angle plus a margin of $\pm$ 5 degrees for attitude control deviations has been taken into account in arriving at the heat shield dimensions, as shown in the upper left of the drawing. The outer portions of the shield are folded back against the mid-portion for stowage under the shroud. The deployment sequence requires an actuator to erect the four folded support struts. Spring loaded hinges are used to facilitate the deployment of the support struts and of the hinged panels of the shield. It appears desirable to postpone deployment of the shield until the thermal protection is required late in the mission, to avoid obstruction of the antenna field of view.

The antenna is mounted on an appropriately shaped deployment arm that can be placed in a fore, aft and side looking position as illustrated in the design drawing. The side looking position below the thruster array is used at the time when thermal protection by the heat shield is required. An elliptical shape of the antenna dish (0.9 by 1.6 meters) is used in this application to obtain the largest antenna area, consistent

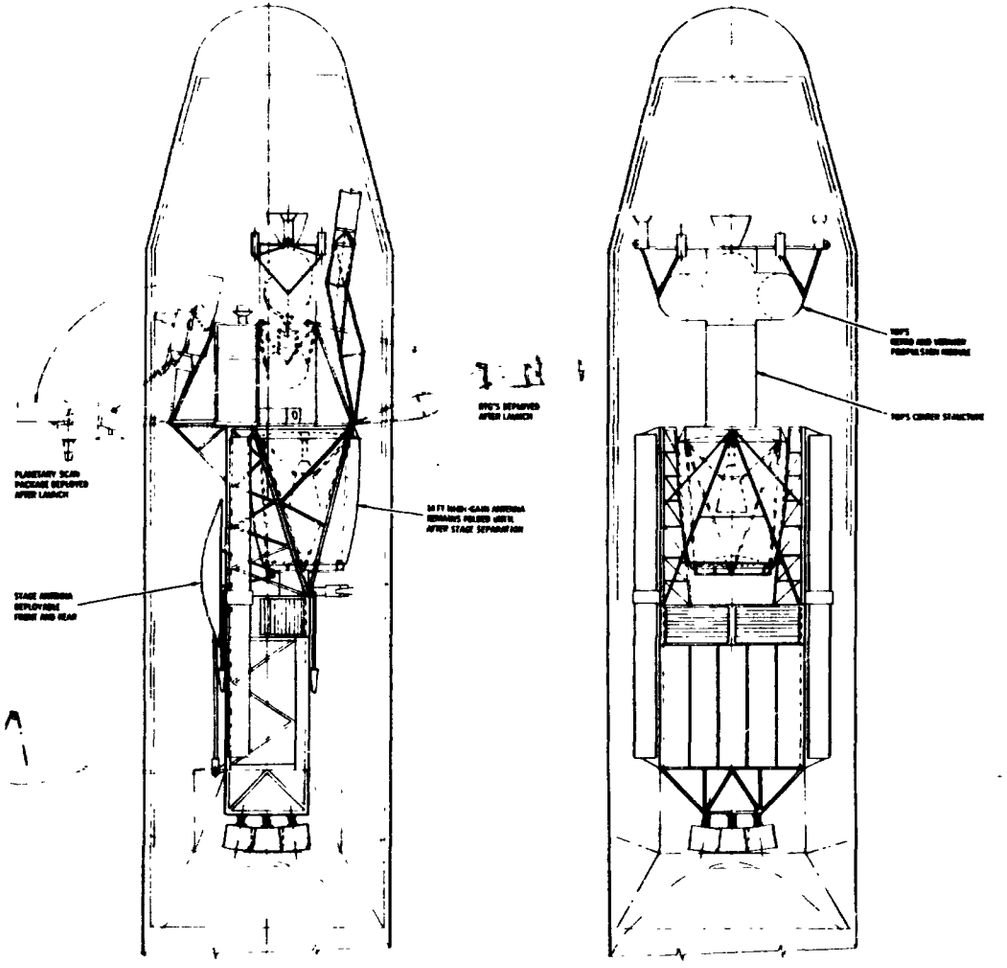

Figure 6-11. TOPS Planetary Orbiter Mounted on Stage

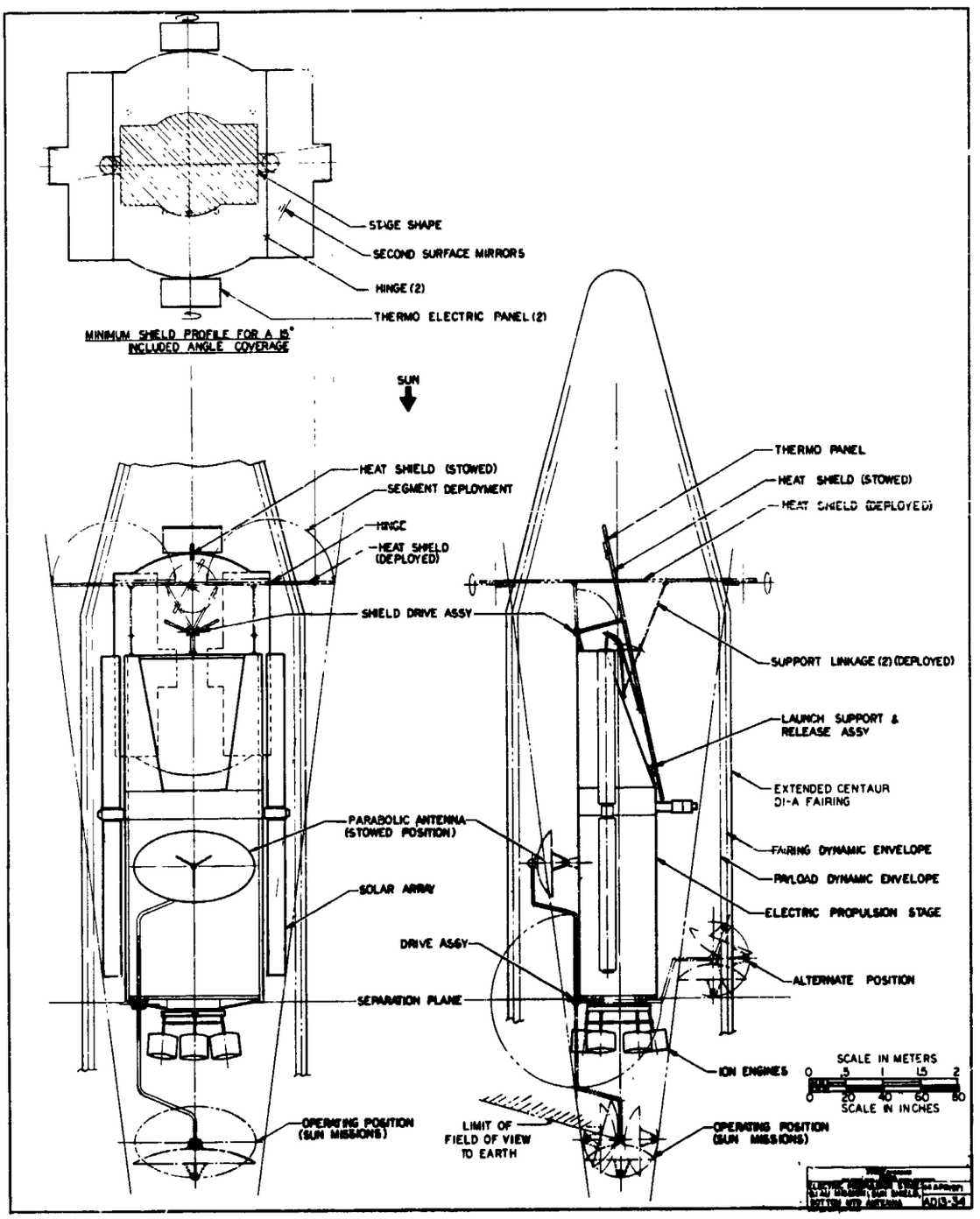

Figure 6-12. Electric Stage Adaptation to Solar Probe Mission

with the oblong shadow cross section cast by the heat shield. Only a single axis rotation joint is required for antenna articulation since the earth is ideally always in the plane normal to the solar array booms.

During periods of close solar proximity the stage will use electrical power generated by two thermo-electric panels, mounted on opposite sides of the heat shield, in lieu of solar array power. The panels are dimensioned to provide 300 watts of housekeeping and telemetry power. With a typical power density of 500 w/m^2 this requires 0.6 m^2 of panel area. The panels are mounted on rotation joints to permit rotation away from full sun orientation as a protective measure for solar distances closer than 0.2 AU. At closest approach the panels are tilted by about 80 degrees to maintain the hot and cold junction at 1050 and 480°C respectively.

Many design problems in addition to the thermal protection of the vehicle (see Section 7.6) require further study, in particular the questions of control sensor operation, payload placement and field of view behind the heat shield.

6.8 ALTERNATE CONFIGURATION FOR MINIMUM STRUCTURAL MASS

During the exploratory design phase we investigated several alternate stage configurations with the objective of minimizing structural mass. The incentive is the large cost saving that may be achieved by using a lower powered version of the baseline vehicle in some mission where 10 to 12 kw of propulsion power can deliver adequate payload. Such missions with generally smaller propulsion energy requirements are the Ceres and D'Arrest rendezvous missions, outer planet flyby, and Mars and Venus orbiters. For such missions the use of a Titan 3C/Burner 2 or Titan 3D/Burner 2 launch vehicle would then be adequate with a cost saving of up to about $7 million for the booster, compared to Titan 3D/Centaur plus $3 to $4 million for reduced stage power and size, i.e., a total savings of about $10 million per mission. Ideally the lower powered version would be identical in all aspects of design except for a reduction of solar array size and the number of electric thrusters and power processor units carried.

A design concept requiring less structural mass is shown in Figure 6-13. In this design one pair of solar array storage drums that form the upper portion of the U-shaped center body is attached to the lower pair of storage drums by a deployment hinge. During launch the upper pair would be folded back along the lower pair for support against dynamic loads. The upper support structure would thus be eliminated and the entire U-shaped upper portion of the stage would become payload stowage volume, however without the benefit of a convenient payload mounting provision. The high-gain antenna would be mounted at the bottom of the propulsion module as previously illustrated in Figure 6-3.

This design option was not pursued in detail because (a) the dual deployment sequence of the solar array appeared too complex and (b) the final structural mass estimate of the selected stage configuration (85 kg) proved to be acceptably small (with only 18 kg allocated to the payload support structure. This low value of structural mass is based on an estimated maximum net payload mass of 350 kg to be carried by the stage in the primary mission. Actually for the stage design option that carries a payload spacecraft of 1000 kg mass or more in alternate missions, strenghtening of the stage structure would be required resulting in an estimated 35 kg increase in structural mass (see Table 6-6).

6.9 SOLAR ARRAY ROTATION ALTERNATIVES

The baseline configuration features a solar array with a $\pm$ 90 degree rotation capability required in Ceres rendezvous and other missions where terminal maneuvers or large thrust steering angle variations are essential. This concept uses a single center boom for deployment and support of the array. The array panel size is scaled up by a factor of more than three from G. E.'s development model, with panel length approximately doubled.

An alternate configuration has been investigated where two smaller panels are mounted side by side each using a center boom for deployment. An auxiliary solar array support structure having a central rotation joint is required which is shown in Figure 6-14 in comparison to the single boom articulation concept.

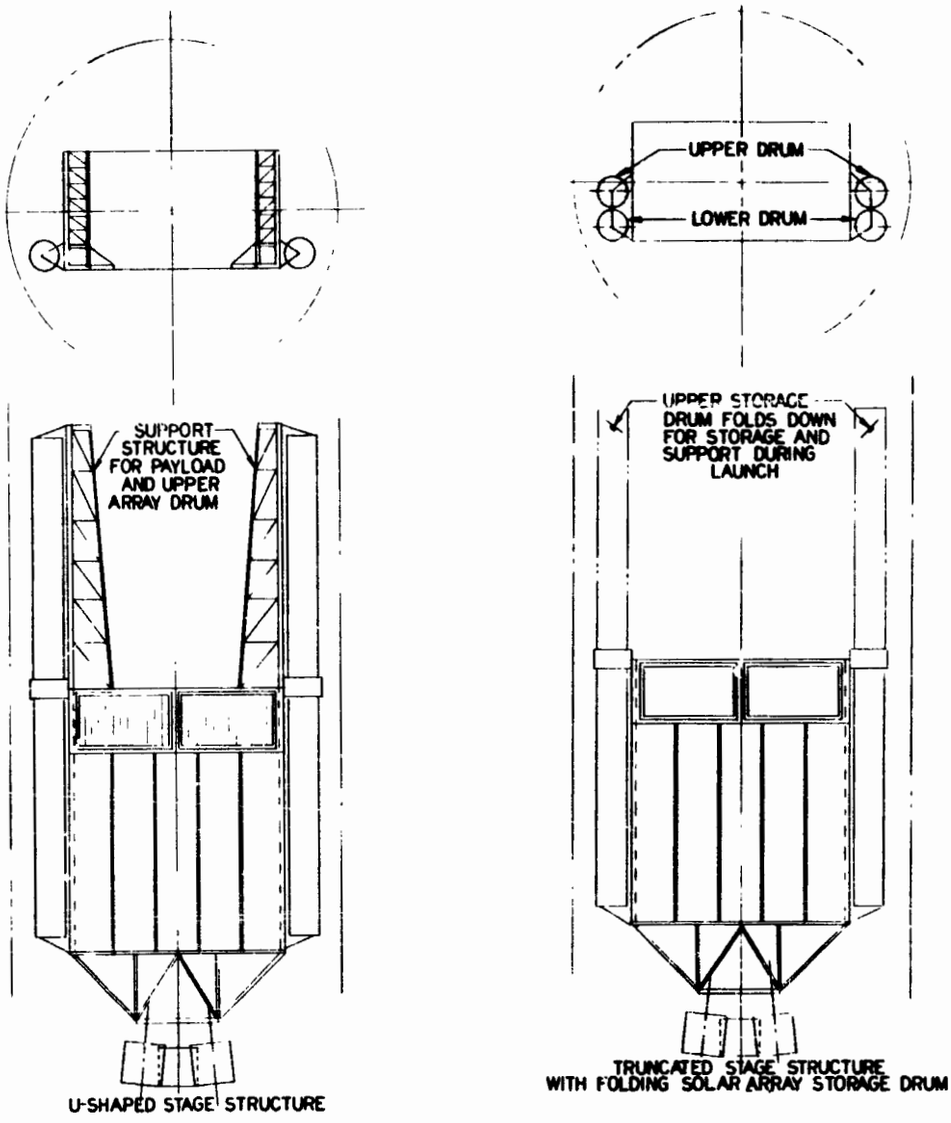

Figure 6-13. Stage Center Structure Configuration Alternatives

The design study also included the use of a rollout solar array using two booms one on each side of the array blanket for increased torsional stiffness. This model has been developed by Hughes Aircraft Co. under USAF contract and will be tested in flight in 1971/72. This model has approximately the same specific mass as the single-boom rollout model developed by G. E. under NASA/JPL contract (15 kw/kg). However the need for array rotation again requires a rotatable auxiliary structure, similar to that shown in Figure 6-14 with either two or four deployment booms attached along the structure.

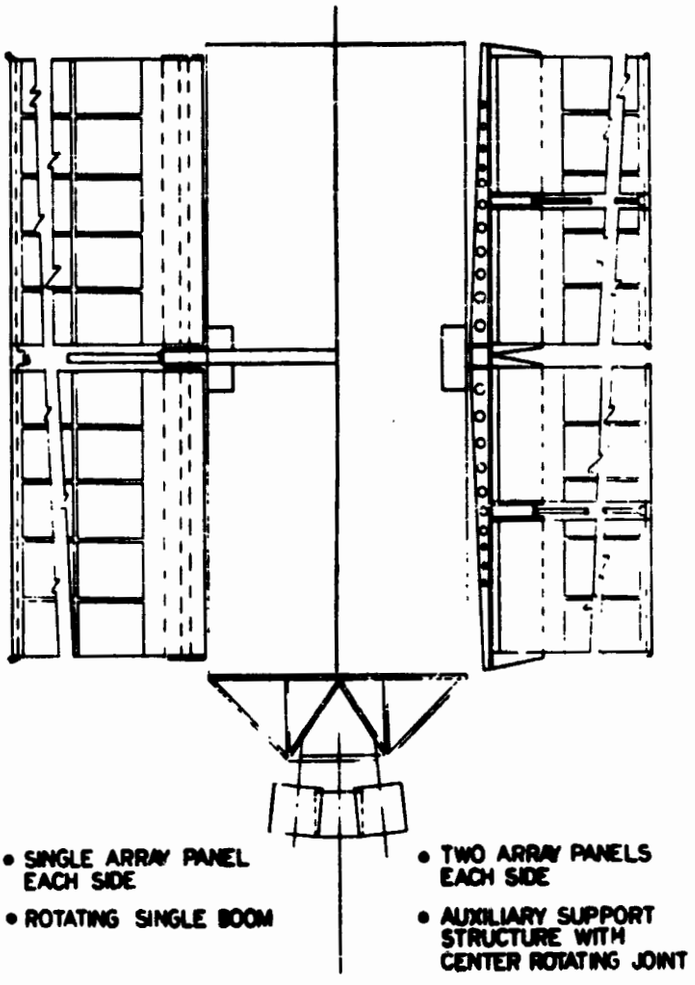

Figure 6-14. Solar Array Rotation Provision for Single and Dual Pair of Array Panels

We selected the simpler central boom deployment concept of the G. E. model, but further study is required to determine how much development is needed to scale it up to the 8.75 kw size required by the stage.

6.10 DUAL LAUNCH CONFIGURATIONS

The flat center body design of the selected configuration facilitates side-by-side mounting of two stages on the launch vehicle in missions where the dual launch concept (see Section 5.9) is selected. As was discussed in that section the large cost savings achievable by this launch mode outweigh the risk of launch vehicle failure.

Figure 6-15 shows two possible arrangements of the stages on a common interstage adapter. If the 10-foot Intelsat shroud is to be used the high-gain antennas must be stowed back-to-back above the vehicles jutting into the conical upper shroud section. The second arrangement uses the new 14-foot Viking shroud currently under development by Lockheed. In this case the two vehicles can be mounted side-by-side with their antennas folded against the side of the center structure, as in the single-launch case. A center support tower could be placed between the vehicles for greater rigidity under the launch environment. The larger shroud is desirable also to accommodate bulky payload complements.

6.11 PAYLOAD FAIRING

The 10-ft diameter Centaur D-1A (Intelsat 4) shroud is assumed as nominal payload fairing in this study (Figures 6-1 and 6-6) rather than the 14-ft Viking shroud being currently developed for the Titan 3D/Centaur which would be unnecessarily large. The cylindrical section of the Intelsat shroud requires an extension by 5 feet (1.5 m) as shown in Figure 6-1, to accommodate the electric stage. This extension is within the 100-in (2.5 m) limit defined as acceptable by Convair.

The Intelsat shroud would give an appreciable performance and recurrent cost advantage compared to the Viking shroud. However its use on the Titan 3D/Centaur has not yet been approved, and the initial cost of integrating it with this booster (estimated to be in the $2 to $4 million range) must be taken into account. On a recurrent basis the savings would be about $0.2 to 0.4 million per flight. The increase in injected payload mass is estimated to be about 120 kg in the velocity range of interest, including the weight penalty for the 1.5 m cylindrical barrel extension, according to data furnished by Convair. This performance increase is not reflected in our mission analysis results. The available margin is conservative and can be used to offset contingencies not included in our study.

The 10-ft Titan fairing, actually not intended for use with Titan 3D/Centaur is shown in some of the preliminary design drawings of this report. It should be replaced by the Intelsat shroud in all cases.

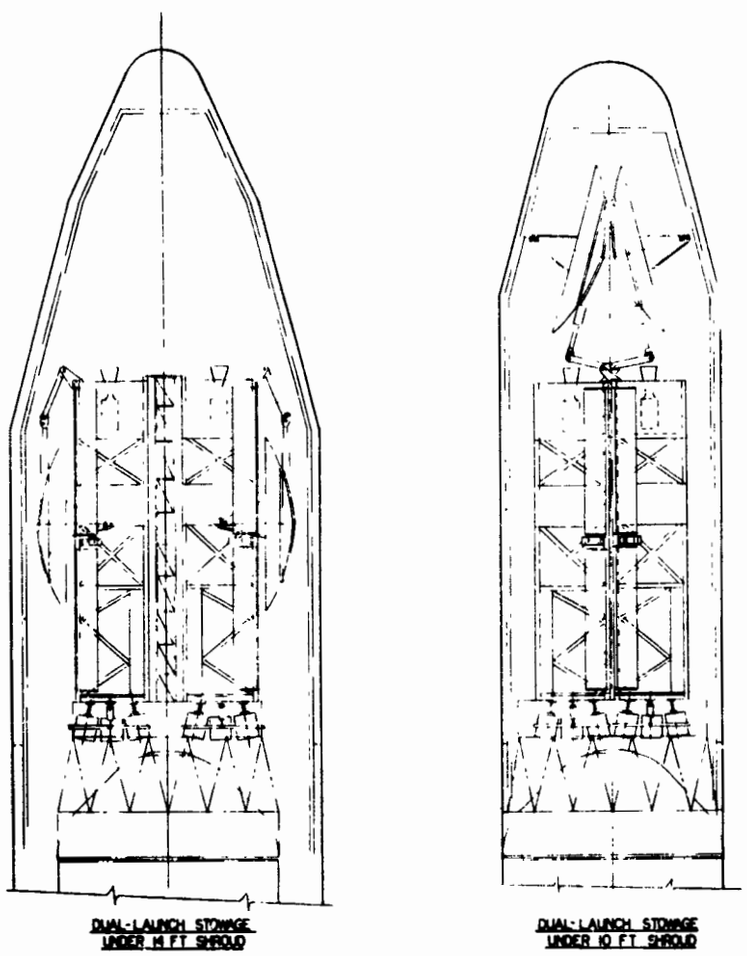

Figure 6-15. Alternate Stowed Configurations for Dual Launch

For purposes of stowing the electric stage as shown in the drawings the shrouds are essentially interchangeable.

6.12 ELECTRICAL SYSTEM DESIGN

The stage electrical design block diagram, Figure 6-16 illustrates the overall electrical design and subsystem interfaces for the stage. The command uplink consists of two command receivers, redundant command demodulators and the electrical integration assembly.

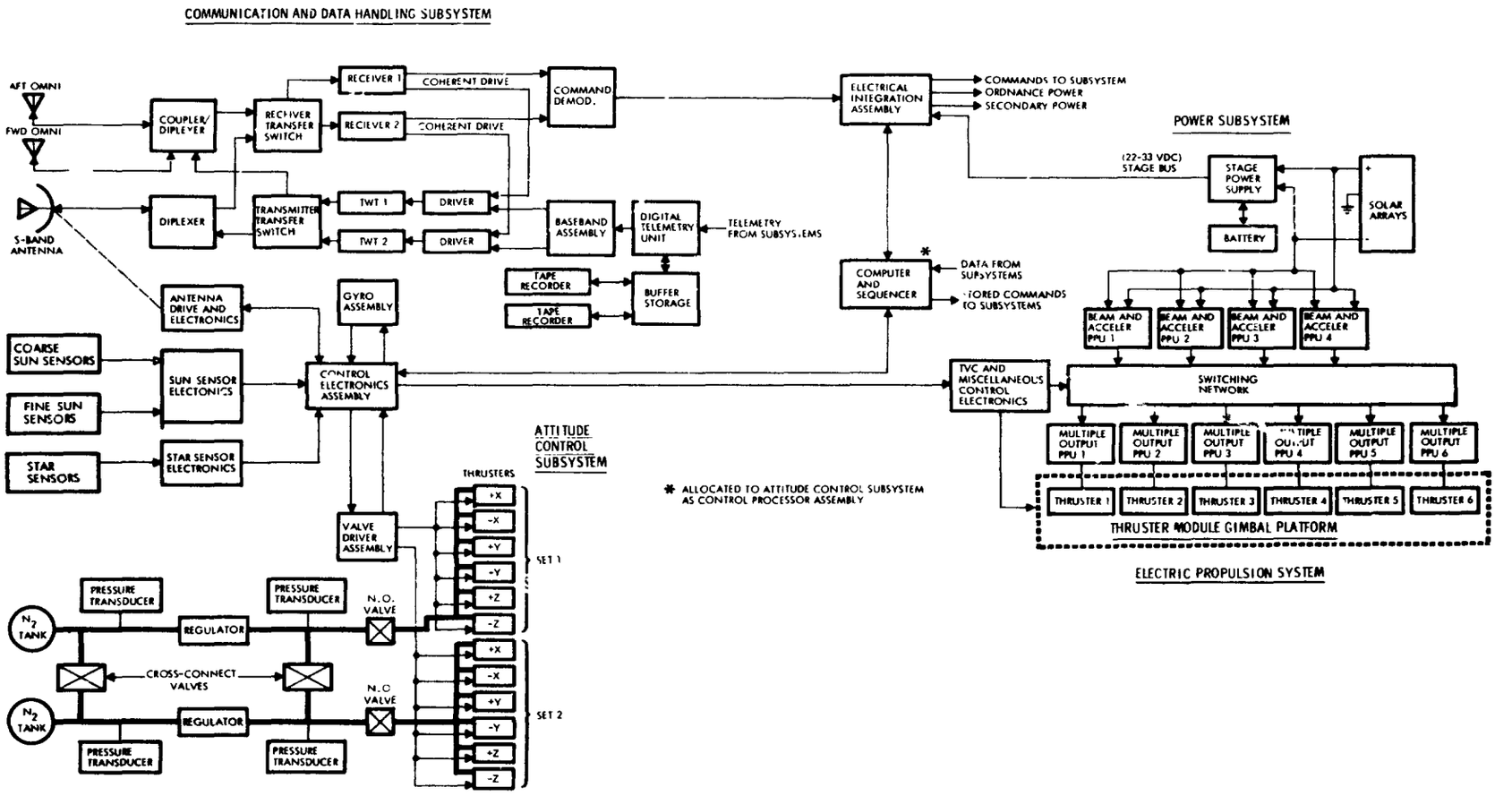

Figure 6-16. Stage Electrical Design Block Diagram

The telemetry downlink elements are two TWTs, two TWT drivers, a baseband assembly, digital telemetry unit, buffer storage, and two tape recorders. The two command receivers and the two TWTs interface with two omni-antennas and the tracking S-band antenna through the receiver and transmitter transfer switches.

Commands are distributed to the appropriate users from the Electrical Integration Assembly (EIA). The computer and sequencer allows the storage of commands and computing for the stage subsystems. Telemetry data is processed by the digital telemetry unit for storage in the two tape recorders or real-time transmission to the ground station.

The power subsystem consists of solar array, battery, and a stage power supply. Array power is delivered directly to the electric propulsion subsystem and to the stage power supply. The stage power supply main bus (22 to 33 VDC) goes to the EIA where it is distributed to the stage users. A secondary power converter is located in the EIA for supplying power at various voltage levels to the stage subsystems.

The electric propulsion subsystem includes power processing units (PPUs), control electronics, thrust vector control and a switching network for flexible interconnection of PPUs and thrusters.

The attitude control subsystem consists of sun sensors, gyro assembly, valve driver assembly, star sensors, antenna drive electronics, and control electronics assembly. The computer and sequencer is allocated to, and used primarily by the attitude control subsystem as control processor assembly for the tasks of operating various control modes, switching functions, pointing sequences, celestial reference acquisitions, etc. It is being shared with other subsystems on a priority-interrupt basis. The N_2 gas system is completely redundant with cross-connect capability. Regulated gas is supplied to two sets of control jets with six jets in each set.

Command Link

The command link equipment includes the two command receivers, two demodulators and the electrical integration assembly. Figure 6-17 shows the stage Command Link Block Diagram. The command receivers accept an r-f signal from either of the two omni-antennas or the S-band antenna.

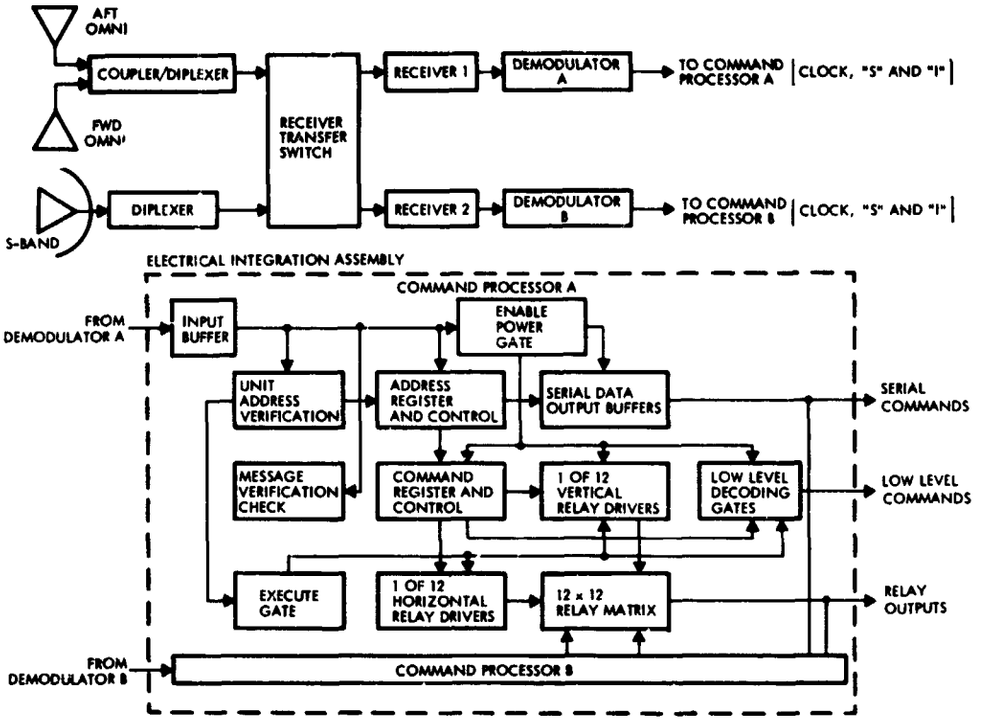

Figure 6-17. Command Link Block Diagram

There are two redundant command paths for the stage. One path consists of receiver 1, Demodulator A, and Command Processor A of the EIA. The output gates of the EIA are power gated, i. e., power is only utilized during command processing, so that if one command path malfunctions, the other path can be used to command the stage. The command processor (EIA) receives the clock "S" pulse, "1" data from its associated demodulator and processes the data for actuation of discrete control functions or distributes the serial data to the appropriate user. The command demodulators accept a command subcarrier from the command receivers and convert this signal to FSK data which drives the command processor.

Subsystem Interfaces

Since the electrical distribution subsystem provides the central control for all command processing and power switching it has an active

interface with all the subsystems of the stage. A simplified diagram of these interfaces is illustrated in Figure 6-18. The major users of serial command data are the attitude control subsystem (CEA), computer and sequencer, and the electric propulsion system. The remaining units require discrete commands. The electrical distribution subsystem can accommodate a serial command interface for the payload if required.

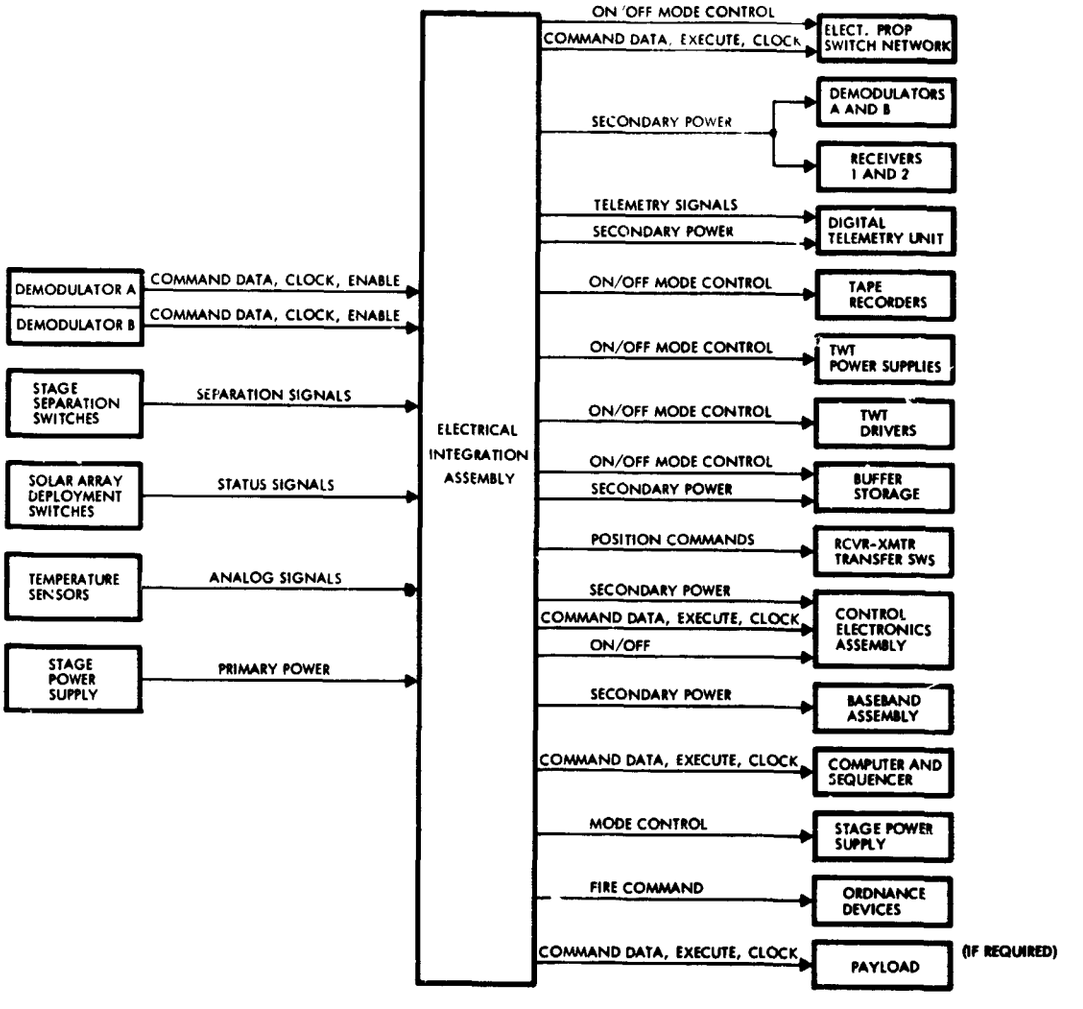

Figure 6-18. Electrical Integration Assembly/Subsystem Interfaces

The command inputs for the EIA come from the two redundant command demodulators. Telemetry signal conditioning interfaces include

separate switches, solar array deployment switches, temperature sensors and other signals not associated with a specific stage unit. This signal conditioning is limited to passive rather than active circuitry. Power interfaces are described as part of power distribution.

Figure 6-18 depicts the input and output functions of the EIA with the various stage equipment.

Power Distribution

The power distribution method for the stage is shown in Figure 6-19. Main bus (22 to 33 VDC) power comes from the stage power supply to the electrical integration assembly (EIA) where it is distributed to all users in the stage. The receivers, command demodulators and the command processors are hard-wired to converters located in the electrical integration assembly. All power, both primary and secondary, is distributed from the electrical integration assembly except for the power delivered to the electric propulsion subsystem. The electric propulsion subsystem receives its power directly from the solar array and conditions it in its own high power processing units (PPUs).

The switchable secondary power users are the control electronics assembly, baseband assembly, digital telemetry unit and the buffer storage. Normally, all secondary stage power will be supplied by EIA converter A, but in case of a converter malfunction the secondary power is supplied by converter B automatically. In the event that a malfunction in one of the switchable loads causes the converter to switch to the other converter, a ground command is available to return to the first converter after the malfunction has been commanded off the line.

The four pressure transducers are the only stage units that are hard-wired to the stage main bus except for the two EIA converters. The switchable main bus loads are the two TWT power supplies, the two tape recorders, and the control electronics assembly.

The control electronics assembly (CEA) distributes power to the valve driver assembly, antenna drive electronics, and the star sensor electronics.

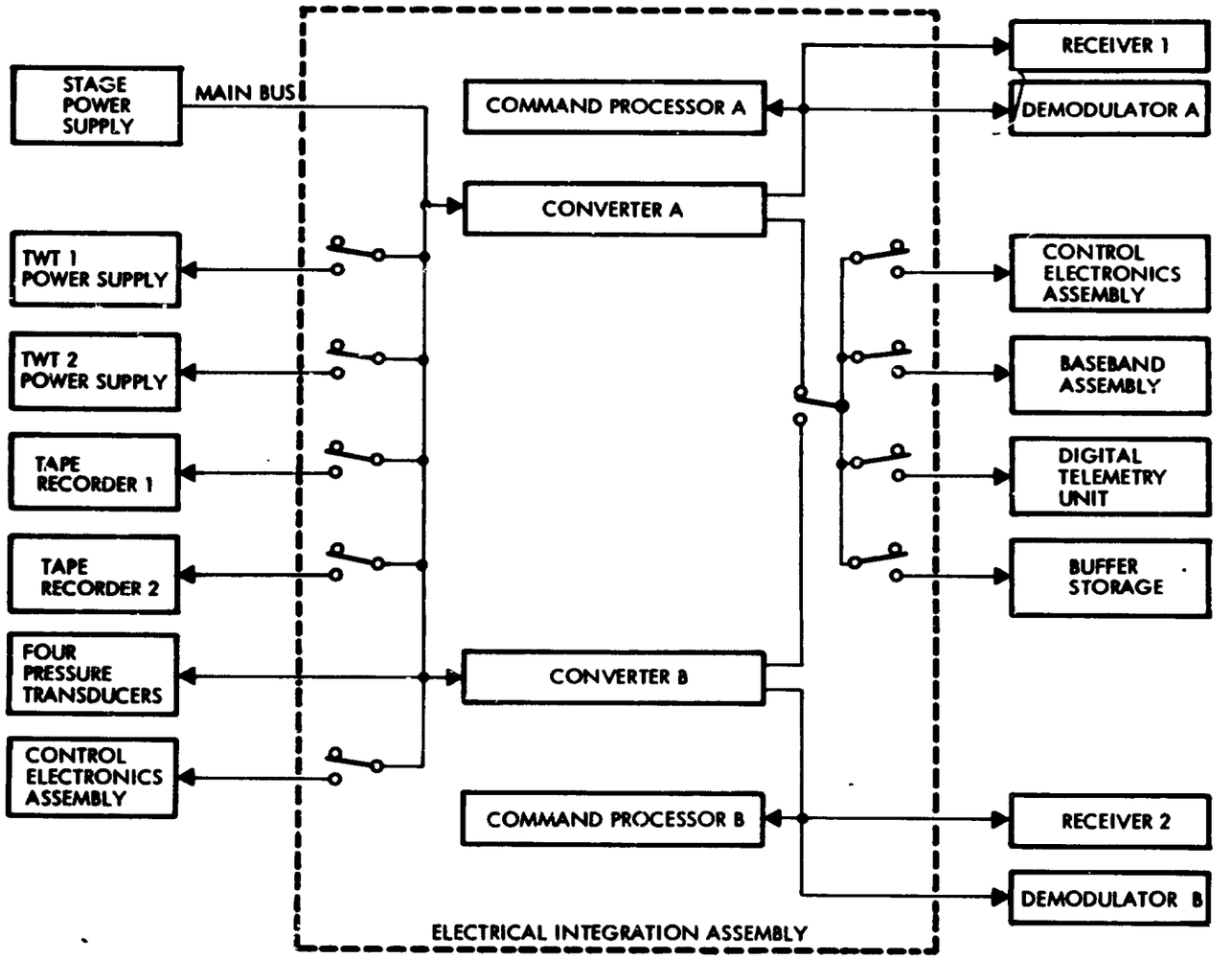

Figure 6-19. Stage Power Distribution Diagram

Power Budget

Table 6-2 tabulates the power requirements for the various units of the stage. The power budget covers various phases of the mission from launch until 700 days after launch at which time the thrust phase is terminated. The cruise mode includes a record and playback mode corresponding to telemetry recording and telemetry transmitting phases respectively. The receivers, command demodulators, baseband assembly, digital telemetry unit, star sensor electronics, control electronics assembly, and the electrical integration assembly all use secondary power from the EIA converter. The power listed for the electrical integration assembly includes the conversion losses associated with supplying these units with secondary power. The converter efficiency is assumed to be 65 percent.

Harness losses for propulsion and stage power are less than 80 watts total owing to the high voltage array design (200 v nominally at 1 AU). This power loss also varies with mission phase.

A net propulsion power budget at mission initiation, referenced to 1 AU, is presented in Table 6-3, to account for various degradation losses and stage housekeeping power in addition to the propulsion power requirement. Solar array degradation (9 percent) consists of 2 percent performance uncertainty and 7 percent solar flare degradation allowance margin although the degradation will occur gradually during the mission (see Section 7.1 for detail discussion). In missions closer to the sun, i.e., the solar probe, Mercury orbiter and extra-ecliptic missions, the degradation will be about twice the amount estimated for the Ceres mission, or 15 percent. Encke and D'Arrest rendezvous have similar degradation as the Ceres mission. Micrometeoroid damage is about 1 percent based on data derived in Reference 1-2, but lower for missions that do not enter the asteroid belt.

Sufficient housekeeping power is provided throughout the mission by allowing a margin of 1.15 kw at mission initiation, which reduces to 195 watts at 2.93 AU. The large total initial margin of about 2 kw for array degradation and housekeeping can initially be allocated to the propulsion system but would not be available toward the end of the

Table 6-2. Stage Power Budget (in Watts) Ceres Rendezvous Mission

Unit	Launch Phase	Sun Acquis.	Initial Coast 0-35	Thrust Phase (Days) 35	100	200	500	700	Post-Rendezvous Phase Record	Playback
Receivers	2.0	2.0	2.0	2.0	2.0	2.0	2.0	2.0	2.0	2.0
Command demod.	0.6	0.6	0.6	0.6	0.6	0.6	0.6	0.6	0.6	0.6
Baseband assembly	1.0	1.0	1.0	1.0	1.0	1.0	1.0	1.0	1.0	1.0
Buffer storage	1.5	1.5	1.5	1.5	1.5	1.5	1.5	1.5	1.5	1.5
Digital telemetry unit	1.5	1.5	1.5	1.5	1.5	1.5	1.5	1.5	1.5	1.5
Star sensor electronics	--	5.0	5.0	5.0	5.0	5.0	5.0	5.0	5.0	5.0
Control electronics assy	--	5.1	10.1	10.1	10.1	10.1	10.1	10.1	10.1	10.1
Control processor assy	17.0	17.0	17.0	17.0	17.0	17.0	17.0	17.0	17.0	17.0
Electrical integ. assy	11.5	16.7	18.9	18.9	18.9	18.9	18.9	18.9	18.9	18.9
Tape recorder	--	--	--	--	--	--	--	--	8.0	20.0
TWT & driver, pwr sup	70.0	70.0	70.0	70.0	70.0	70.0	70.0	70.0	70.0	70.0
Gyro assembly	10.0	10.0	10.0	10.0	10.0	10.0	10.0	10.0	10.0	10.0
Gimbal drives (4)	--	--	10.0	10.0	10.0	10.0	10.0	10.0	10.0	10.0
Heaters	80.0	80.0	80.0	20.0	20.0	20.0	20.0	20.0	80.0	80.0
TVC actuators	--	--	--	30.0	30.0	30.0	30.0	30.0	--	--
Sub-Total	195.1	210.4	227.6	177.6	177.6	177.6	177.6	177.6	235.6	247.6
Stage pwr cond loss	19.5	21.0	22.8	17.8	17.8	17.8	17.8	17.8	23.4	24.8
Stage main bus load (Housekeeping)	214.6	231.4	250.4	195.4	195.4	195.4	195.4	195.4	259.0	272.4
El. Prop. Module Input (PPU's)	--	--	--	15,950	11,620	6,040	2,760	2,480	--	--
Stage harness losses	2.7	3.4	2.7	85.0	62.0	32.0	15.0	13.0	13.0	13.0
Total stage load	217.3	234.8	253.1	16,230	11,877	6,267	2,970	2,688	272.0	285.4
Power margin during thrust phase*	--	--	--	1,095	723	348	45	12	--	--
Nom. pwr less 10% degradation	15,750	15,750	15,750	17,325	12,600	6,615	3,015	2,700	2,682	2,682
Nominal pwr (undegrad)	17,500	17,500	17,500	19,250	14,000	7,350	3,350	3,000	2,980	2,980

*This margin represents initial allowance of 1.15 kw for min. housekeeping power at destination

**Solar array power increases by 10 percent during initial inbound portion of trajectory

mission when power is at a premium. This would permit an increase in net payload capacity by more effective use of solar array power. This approach to power allocation by a revised time dependent net power profile in the trajectory analysis program should be further investigated.

Table 6-3. Net Propulsion Power Budget at 1.0 AU (in kw)

Installed gross power	17.50
Deduction for solar array degradation (9%)	1.58
Deduction for micrometeroid damage (1%)	0.17
Initial allowance for minimum housekeeping power	1.15*
195 W at 2.93 AU (195 x 5.9 = 1150 W)	
Input to Electric Propulsion Module (PPUs)	14.52
Deduction for cant angle losses and steering (2.2%)	0.32
Net power for propulsion	14.20
Required for nominal initial acceleration (M_o = 1500 kg)	14.10

6.13 ILLUSTRATIVE FLIGHT SEQUENCE

Major flight sequence events of the Ceres rendezvous and orbiter mission are listed in Table 6-4 including arrival at the target, orbit insertion and landing capsule ejection. This example illustrates the versatility of the stage in performing various functions required by the science payload, thus saving duplication of separate system and subsystem capabilities. Once rendezvous has been achieved a small additional maneuver suffices to insert the stage into a low altitude

*Conservative margin, assuming housekeeping allowance not to be used to augment thrust power

Table 6-4. Preliminary Flight Sequence Summary for Ceres Orbiter Mission

No.	EVENT	TIME
1	LIFTOFF	L
2	ENTER PARKING ORBIT	L + 15 MIN
3	INTERPLANETARY INJECTION BURN	~L + 30 MIN
4	SEPARATION FROM CENTAUR STAGE	L + 45 MIN
5	INITIATE ATTITUDE STABILIZATION	L + 45 MIN
6	ACQUISITION OF SUN REFERENCE	L + 1 HR
7	DEPLOY SOLAR ARRAY PANELS	L + 1.1 HR
8	DEPLOY HIGH-GAIN ANTENNA AND OTHER APPENDAGES	L + 1.2 HR
9	ESTABLISH UP AND DOWNLINK COMMUNICATION AND TRANSMIT ENGINEERING TELEMETRY DATA	L + 1.3 HR
10	ACQUISITION OF STAR REFERENCE	L + 1.5 HR
11	TURN ON ELECTRIC THRUSTERS	L + 2 HRS
12	DETERMINE INJECTION ERROR BY DSIF TRACKING AND INITIATE LOW THRUST GUIDANCE CORRECTIONS	L + 3 HRS to 2 DAYS
13	THRUSTER SWITCHING AS REQUIRED BY POWER PROFILE	TYPICALLY AT L + 70, L + 140 and L + 380 DAYS
14	INTERMITTENT COAST PHASES OF SEVERAL DAYS FOR UPGRADED DSIF ORBIT DETERMINATION	STARTING AT L + 280, L + 400, L + 500, L + 600 DAYS
15	PERFORM ADDITIONAL GUIDANCE CORRECTIONS DURING THRUST PHASES	AFTER L + 105 DAYS
16	TRANSMIT SCIENCE AND ENGINEERING DATA	STARTING AT L + 1 HR
17	PERFORM TARGET APPROACH NAVIGATION AND TERMINAL GUIDANCE TASKS (OPTICAL ACQUISITION OF CERES)	STARTING AT ABOUT R - 50 DAYS

Table 6-4 . Preliminary Flight Sequence Summary for Ceres Orbiter Mission (Continued)

No.	EVENT	TIME
18	ARRIVE IN VICINITY OF CERES AT NEAR-ZERO RELATIVE APPROACH VELOCITY	R - 12 HRS (L + 700 DAYS)
19	RETRACT SOLAR ARRAY PRIOR TO CLOSEST APPROACH (NEARLY COMPLETE RETRACTION)	R - 2 HRS
20	ORIENT VEHICLE FOR ORBIT INSERTION MANEUVER	R - 1 HR
21	INSERT VEHICLE INTO CLOSE CIRCULAR ORBIT	R
22	REORIENT VEHICLE TO NOMINAL SUN POINTING ATTITUDE	R + 15 MIN
23	RE-ERECT SOLAR ARRAY	R + 1 HR
24	DETERMINE PREFERRED CAPSULE LANDING SITE BY RECONNAISSANCE VIA TV-LINK TO EARTH	STARTING AT ABOUT R + 2 HRS
25	PERFORM IN-ORBIT HOUSEKEEPING SEQUENCES (ECLIPSE VS ILLUMINATED CONDITIONS)	START AT R
26	SEPARATE AND SPIN UP LANDER CAPSULE	R + 48 HRS
27	DEORBIT CAPSULE	R + 48 HRS
28	PERFORM CAPSULE RETRO MANEUVER	R + 49 HRS
29	CAPSULE TOUCHDOWN	~ R + 49 HRS
30	INITIATE LANDED OPERATIONS AND RELAY LINK DATA TRANSMISSION VIA ORBITER	R + 49 HRS
31	PERFORM SURFACE OBSERVATIONS FROM ORBITING STAGE	STARTING AT R
32	MAKE LOW-THRUST ORBIT CHANGES AS REQUIRED FOR SCIENTIFIC OBSERVATIONS AND IMPROVED RELAY CAPABILITY	AFTER R + 2 to 6 DAYS
33	(OPTIONAL: DEPART FROM CERES FOR CONTINUED ASTEROID BELT CRUISE) USE LOW-THRUST DEPARTURE	(AFTER R + 20 DAYS)

circular orbit using either low thrust or high thrust propulsion as discussed in Section 5.0.

Continuation of the mission beyond Ceres after completion of the orbital reconnaissance tasks and/or expiration of the functional life of the landing capsule is feasible by using low thrust orbit departure and subsequent low thrust transfer to other targets. The reduction of stage mass by dropping the capsule helps to raise the available thrust acceleration level.

6.14 MASS PROPERTIES

6.14.1 Detailed Weight Estimates

Assumptions used in developing detailed weight estimates for the electric stage are summarized as follows:

Item	Characteristics	Basis of Assumptions
Solar array specific mass for G.E. type roll up array.	15 kg/kw	Specified by customer for 3 mil cover glass
Additional weight for 6 mil cover glass	1.53 kg/kw	See Section 7.1
Solar array degradation	9 percent	Includes 7% degradation* due to solar flares plus 2% S/A performance uncertainty.
Micrometeoroid damage	1 percent	Results of previous study (Ref. 1-2)
Bus and cabling losses	<80 watts	High solar array voltage (see Section 7.1)
Thruster specific mass for 4.5 kw thruster at I_{sp} = 3000 sec	2.2 kg/kw	Data received from NASA/LeRC (see Section 7.2)
Power processor specific mass	5 kg/kw	Specified by customer (actual breakdown into main and multiple output PPU's discussed in Section 7.2)

*7 percent solar flare degradation is a conservative estimate for an array with 6 mil (0.015 cm) cover glass.

A breakdown of detailed stage weight estimates for the Ceres rendezvous mission launched by Titan 3D/Centaur is given in Table 6-5 The gross performance characteristics of the nominal Ceres mission profile stated in Section 5.0 were adjusted to take into account launch weight penalties (adapter weight and shroud weight penalty), solar array degradation due to solar flare radiation and micrometeroid impact and vehicle design constraints (thrust pointing losses due to thruster cant angle) and thrust offset for guidance maneuvers that were previously ignored.

These weight estimates were compared with those of the previous solar electric spacecraft studies by TRW and NAR (Ref. 1-1, 1-2) and reasonably close agreement was established in equivalent subsystem elements. The larger solar array and vehicle size of the present design reflects in accordingly larger weights of the power and propulsion systems and stage structure.

The results show a total net payload mass of 188 kg which is allocated to on board mounted instrumentation (88 kg) and a small lander capsule (100 kg). Several conservative weight assumptions have been included namely a 3 percent propellant margin (13 kg) and a large estimated hydrazine propellant load (40 kg) for contingencies in terminal maneuvers. Further study is required to show whether these weight margins may be relaxed in order to increase the net payload capacity.

Compared to earlier gross weight estimates used in mission analysis some differences are noted in the following areas.

The solar array weight based on a specific mass of 15 kg/kw was increased by 26.8 kg to reflect a thicker cover glass (6 mil instead of 3 mil) which we consider essential to reduce solar flare radiation damage to an estimated 7 percent in the Ceres mission and proportionately larger in the more critical missions, Mercury orbiter and solar probe. The thicker cover glass also reduces manufacturing cost by 5 to 10 percent, due to less breakage and repair, reflecting in $300,000 of

Table 6-5. Estimated Weight Breakdown for Ceres Orbiter Mission

Item		Weight (Kilograms)	
Structure		85.0	
Equipment module			18.2
Panel assemblies			
Frames and longerons			
Support tubes (solar array)			
Propulsion module			29.1
Panel assemblies			
Frames and longerons			
Separation fittings	(4)		
Propellant tank supports			
Compartment interface			
Payload Superstructure			19.5
Secondary structure and attaching parts			18.2
Thermal Control		28.6	
Louvers			14.5
Insulation			9.1
Paint			3.2
Heater (thermostat)			1.8
Electrical Power		328.2	
Solar array panel	(2)		289.0
Ni Cd Battery	(1)		17.0
Battery charger-discharge control	(2)		2.0
Stage power processor	(2)		4.0
Solar array drive assembly	(1)		15.0
Solar array drive electronics	(2)		1.2

Table 6-5. Estimated Weight Breakdown for Ceres Orbiter Mission (Continued)

Item		Weight (Kilograms)	
Electrical Integration		18.0	
Electrical integration assembly			8.0
Cabling and connecters			3.0
Fault clearing switch gear	(10)		7.0
Attitude Control		57.9	
Star tracker	(1)		4.55
Star tracker gimbal drive	(2)		3.00
Star tracker gimbal drive electronics	(2)		0.90
Sun sensor assembly	(1)		0.90
Rate gyro assembly	(2)		5.00
Control processor assembly	(2)		8.00
Control electronics assembly	(1)		4.53
Biaxial antenna drive	(1)		5.45
Antenna drive electronics	(1)		0.90
Television and gimbal system*	(1)		6.50
Nitrogen tanks	(2)		4.25
Nitrogen gas			6.50
Regulator and relief valves	(2)		1.38
Solenoid valves	(12)		2.72
Lines and fittings			1.27
High pressure transducer	(2)		0.18
Fill valves	(2)		0.09
Nozzles	(12)		0.55
Pressure switches	(12)		0.45
Temperature transducers	(2)		0.27
Thruster booms	(2)		0.50

*Use for terminal navigation

Table 6-5. Estimated Weight Breakdown for Ceres Orbiter Mission (Continued)

Item			Weight (Kilograms)
Communications and Data Handling		59.0	
TWT tube	(2)		1.20
TWT power supply	(2)		9.06
Receivers	(2)		4.50
Ranging - unit	(2)		0.32
Receiver switch unit	(1)		0.25
Exciter	(2)		1.80
Buffer storage unit	(2)		3.00
Tape recorders	(2)		17.80
Digital telemetry unit	(1)		5.40
RF switch	(1)		2.10
High-gain antenna installation	(1)		12.20
Low-gain antenna	(2)		1.40
Propulsion System		735.7	
Ion thrusters	(6)		66.0
Beam and accelerator PPU	(4)		57.2
Multiple output PPU	(6)		48.0
Switching network ans associated electronics	(1)		1.0
Cabling and connectors	(1)		4.0
Thruster gimbal and support mechanism	(1)		11.0
Thrust vector control actuators	(3)		6.0
Thrust vector control electronics	(1)		3.0
Propellant storage and distribution	(1)		25.0
Propellant (Hg), including 3% for contingency			462.0
Hydrazine tank and feed system			6.0
Hydrazine propellant			40.0
Hydrazine thruster assembly			2.0
Hydrazine control electronics			1.5
		Total*	1312.4

*Injected mass is 1500 kg. This leaves 187.6 for net payload.

estimated cost savings per mission flown or $9 million projected for a total program of 30 flights (see Sections 10.0 and 11.0). In addition the gross installed power of 17.5 kw which takes into account all losses and housekeeping power requirements is 17 percent larger than the propulsion power assumed in the nominal mission profile, and 23 percent larger than the net propulsion power of 14.2 kw (at 1 AU) actually used initially in the Ceres mission.

The injected mass of 1500 kg represents a reduction by 90 kg from the nominal injection performance of Titan 3D/Centaur at the hyperbolic departure velocity of 8.5 km/sec assumed for this mission. This difference includes the relatively heavy interstage adapter, 67.4 kg, and a shroud penalty, 22.6 kg, for the 22-ft cylindrical length of the 10-ft Intelsat shroud. A major savings of shroud weight penalty compared to the nominal 14-ft Viking shroud now under development which is not needed in any of the primary missions of the electric stage is realized by the use of the Intelsat shroud, plus a recurrent cost saving of at least $200,000. However, the question of whether the nominal Titan shroud is acceptable as a more economical and weight effective substitute for the 14-ft Viking shroud still requires clarification. (See also Section 6-11.)

In accounting for propellant mass we have taken into consideration the reduction by 5.5 percent of the injected mass by launch penalties which permits a proportional propellant reduction from the nominal 566 kg obtained in trajectory analysis. However, an allowance of 2.2 percent must be added to take cant angle and steering angle losses into account. In addition we have allowed a conservative three percent propellant margin for contingencies.

The propellant tank has been sized for the largest propellant loading, 1015 kg, expected in any of the primary missions. A nominal allowance of 3 percent, used in the mission analysis was found to be over conservative since our design approach using a pressure regulated feed system eliminates the sizeable extra volume for pressurant that would be required in a blowdown system (see Section 7.2). The tankage and feed system estimate includes 1 percent of total propellant weight for ullage. As will be discussed in Section 7.1 it is desirable in the

interest of system commonality to have the same tank size in all missions to avoid new development. The total mass of 25 kg for the nominal tank size and feed system includes a relatively larger weight penalty for missions with offloaded propellant.

The hydrazine propulsion system carried in asteroid and comet rendezvous provides a backup for delayed guidance maneuvers in the event of late target acquisition by the onboard optical sensor. In the Ceres mission it also provides a back up to augment the orbital insertion maneuver for which solar electric propulsion capability would be only marginally effective. Additional study is required to show whether elimination of this additional chemical propulsion capability is possible without degrading success probability appreciably. If so the weight gained for payload purposes would be more than 25 percent.

The engineering subsystem weight estimates are in close agreement with those of the SEMM-1 multi-mission spacecraft study. Attitude control is charged with the weight of the computer and sequencer (control processor assembly) as previously explained, and the television camera used for terminal navigation. The communication system includes 12.8 kg for the large (8-foot) high-gain antenna. By changing the antenna size to 4 feet in the alternate design version that requires lower data rates a net saving of only about 5 kg is achieved, taking into account the extra weight for a new deployment hinge and a longer deployment arm.

In summary, the total weight for structure (85 kg) and engineering subsystems (203 kg) adds up to 288 kg, appreciably less than we had used initially during overall mission analysis. The conservative assumptions for structure and engineering subsystems approximately balance the various weight penalties that were omitted in the initial mission analysis. These factors should be taken into account in interpreting net payload mass data shown in the summary graphs of Section 5.0. We also note that a lower powered version of the stage which can perform some of the less demanding alternate missions, such as Mars and Venus orbiters, can accept the baseline structure and subsystem weights without a requirement for design modification from a weight standpoint.

6.14.2 Summary Weight Characteristics of Primary, and Some Alternate Missions

Table 6-6 gives a summary weight breakdown for five primary and some laternate missions. Differences in weight allocation for thermal protection, propulsion power processors and chemical propulsion capability and antenna size are noted in the weight summaries. The results show the wide applicability of the electric stage, with small adjustments in stage system weight characteristics, and the generally high net payload capacity in all cases considered. The large differences of injected mass from mission to mission directly reflect the large changes in propellant loading, and in payload mass, particularly in the case of the outer planet missions where the payload consists entirely of an autonomous spacecraft such as the TOPS vehicle.

6.14.3 Mass Distribution Characteristics

The variation of mass distribution due to depletion of propellant or ejection of payload mass such as a daughter probe was investigated for five primary missions, and the change in moments of inertia and c.m. position was determined. The results are summarized in Table 6-7. The largest displacement of the center of mass due to propellant depletion occurs in the extra-ecliptic mission (0.34 meters), the smallest in the Ceres mission (0.24 meters). The displacements due to payload mass ejection are smaller by a factor of about 2. During powered flight the effect of c.m. shift on solar pressure unbalance can be readily compensated by the thrust vector control system at a negligible expense of propellant. During coast periods that occur at small solar distance and with a major part of the propellant still on-board the stage an appreciable expenditure of attitude gas could be required to compensate for c.p. unbalance torques. For example 100 days of coasting at an average solar distance of 0.5 AU would require about 6 kg of attitude control gas for a c.m. to c.p. distance of 0.3 meters based on the dimensions of the solar array and the lever arm of the yaw control jets. The unbalance torque increases in inverse proportion with the square of solar distance. However, the reorientation of the solar array around its yaw axis which is necessary on close solar approach for purposes of thermal protection also eliminates most of the solar pressure

Table 6-6 . Weight Breakdown for Primary and Alternate Missions

Power: 17.5 KW I_{SP} = 3000 sec α = 30 KG/KW	PRIMARY MISSIONS					SAMPLE ALTERNATE MISSIONS		
	Ceres	D'Arrest	Out-of-Ecliptic	Mercury Orbiter (SEP Capture)	Solar Probe	Saturn Flyby (Mode A)	Saturn Orbiter (Mode B)	Uranus Flyby (Mode B)
Flight Time (Days)	700	750	700	402	400	1500	2000	2600
Thrust Time (Days)	671	704	521	311	252	610	1200	1600
Departure Velocity (km/sec)	3.5	8.0	7.5	8.0	8.0	7.2	4.8	6.0
Launch Vehicle Capability kg	1590	1860	2143	1860	1860	2250	3600	3200
Injected Mass	1500	1770	1970(5)	1770	1770	2160	3510	3110
HG - Propellant (nominal)	449	565	1015	789	549	383	1390	1490
3% Propellant Margin	13	17	--	24	--	12	42	45
Tankage and Feed System	25	25	25	25	25	25	30	30
Solar Array	289	289	289	289	289	289	289	289
Electric Propulsion Module	199	199	214(1)	214(1)	214(1)	199	214(1)	214(1)
Structure	85	85	85	85	123(2)	120(6)	120(6)	120(6)
Engineering Subsystems	203	203	203	216(3)	243(3)	193(4)	193(4)	193(4)
Chemical Propulsion	50	35	--	35	--	--	--	--
Net Payload Total	188	343	147	170	327	939	1309	729
Attached	88	143	147	170	177	--	--	--
Separable	100	200	--	--	150	939	1309	729

NOTE:

(1) Includes 1 additional main power processor
(2) Includes 28 kg for heat shield and structure
(3) Reflects additional thermal control components and power source
(4) Reflects weight savings in stage communication and data system
(5) Reflects azimuth penalty of this mission
(6) Includes 35 kg for strengthened structure

unbalance effect. We conclude therefore that the c. m. shifts shown in Table 6-7 are of no significant concern to attitude control.

Table 6-7. Summary of Estimated Mass Distribution Characteristics

Mission/Condition	Weight (kg)	Center of Mass[1] (m)			Moments of Inertia[2] (10^3 kg-m^2)			Products of Inertia (10^3 kg-m^2)		
		$\bar{x}$	$\bar{y}$	$\bar{z}$	I_{xx}	I_{yy}	I_{zz}	I_{xy}	I_{xz}	I_{yz}
Ceres Mission										
• Start (Fully Deployed)	1500	1.84	0	-0.06	25.96	1.96	27.54	0	-0.16	0
• Less Propellant	1040	2.08	0	-0.10	25.96	1.74	27.32	0	-0.13	0
• Less Propellant and Separable P/L	940	1.97	0	-0.11	25.94	1.65	27.19	0	-0.14	0
D'Arrest Mission										
• Start	1770	1.92	0	-0.05	25.99	2.38	27.95	0	-0.16	0
• Less Propellant	1190	2.21	0	-0.08	25.99	2.02	27.60	0	-0.11	0
• Less Propellant and Separable Payload	990	2.11	0	-0.10	25.96	1.93	27.50	0	-0.13	0
Out-of-Ecliptic Mission										
• Start	1970	1.60	0	-0.03	25.95	1.86	27.43	0	-0.20	0
• Less Propellant	955	1.94	0	-0.10	25.94	1.61	27.19	0	-0.15	0
Mercury Orbiter Mission										
• Start	1770	1.70	0	-0.05	25.94	1.99	27.55	0	-0.19	0
• Less Propellant	958	2.03	0	-0.11	25.92	1.72	27.28	0	-0.13	0
Solar Probe Mission										
• Start	1770	1.95	0	-0.04	26.00	2.62	28.20	0	-0.16	0
• Less Propellant	1195	2.25	0	-0.08	26.00	2.24	27.82	0	-0.11	0
• Less Propellant and Separable payload	1045	2.05	0	-0.09	25.98	1.73	27.32	0	-0.13	0

NOTES:

(1) Longitudinal c. g. referenced from stage separation plane.

(2) Coordinate reference axis and notations as per Figure 6-6.

7. SUBSYSTEM DESIGN

7.1 POWER SUBSYSTEM

The power subsystem provides unregulated solar array power to the propulsion module during propulsive phases of the flight, and regulated power to the stage engineering subsystems during both propulsive and cruise phases of the flight. Once the stage reaches its destination, the stage power subsystem can be used for providing power for the scientific measurements if desired.

7.1.1 Power Subsystem Requirements

The typical solar array characteristics as a function of solar distance are presented in Figure 7-1 along with the required range over which it must supply power for the primary and secondary missions of interest. These characteristics are based on power source analysis presented in detail in Section 7.1.2. Examination of the solar array characteristics indicates that the solar array is capable of supplying power for all missions with the exception of the 0.1 AU solar probe. Fortunately in this mission, only 300 watts is required at solar distances of 0.62 AU or less since the propulsion system is off and only housekeeping and communications power is required. At distances less than 0.25 AU this power requirement can be met by using a solar heated thermoelectric power source. The solar array is utilized to provide housekeeping and communications power between the point at which the propulsion system is turned off (0.62 AU) and 0.25 AU. During this period, however, it is necessary to rotate the solar array to reduce the angle of incidence of solar radiation and thus maintain the solar array at a safe operating temperature of 140°C. As pointed out in the thermal design section, rotation angles of about 75 degrees are required at 0.25 AU.

The solar array is required to supply maximum power output over a range of 0.37 to 3.5 AU for the primary and secondary missions of interest. This corresponds to an output voltage variation of 2.7:1. However the system must be designed so that the power processors can operate with the open circuit voltage in case the thrusters are shut down and a restart is necessary. Considering the fact that the open

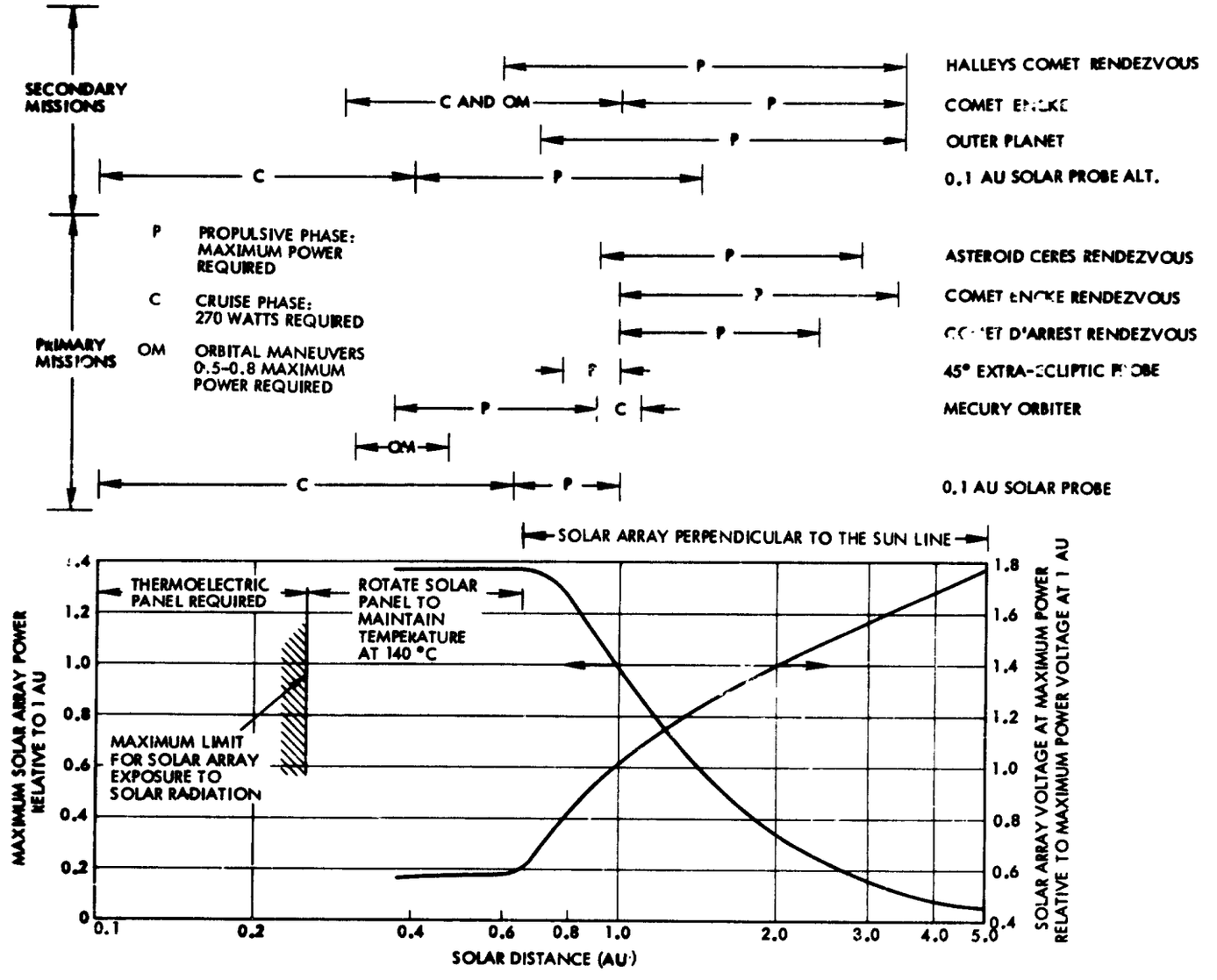

Figure 7-1. Electric Thruster and Power Subsystem Requirements

circuit voltage is about 20% greater than the solar array voltage at maximum power, the power processing equipment must be designed to operate over a 3.3:1 input voltage variation. At the present time, power processors have demonstrated performance over a 2.3:1 range of input voltage variation. Although it is projected that this range can be increased to the desired value with an appropriate new technology program, input voltage variation of greater than 2.3:1 must be considered beyond the state of the art at present. As a result, it will be necessary to consider techniques for limiting this solar array voltage variation as discussed in Section 7.1.2.

The primary missions of interest fall into two general categories, each with a limited solar distance range. The out-of-ecliptic, Mercury orbiter and 0.1 AU solar probe have power requirements in a range from 1.1 AU maximum to 0.1 AU minimum. For purposes of the discussion in the following sections, such missions will be called inbound. For the typical mission profiles examined, these inbound missions require maximum power over a range from 1.1 AU to 0.37 AU. Over the range from 1.1 to 0.37 AU, the input voltage to the power processor decreases by about 2.2:1 including open circuit conditions at 1.1 AU.

The Mercury orbiter mission sets the requirement for the lower solar distance limit of 0.37 AU for maximum power. For the mission profiles examined, this is the point where rendezvous and low-thrust orbit insertion will occur. The stage can then be used, if desired, to perform corrective orbit maneuvers as it follows Mercury to a perihelion of 0.31 AU and back to an aphelion of 0.47 AU. During these maneuvers it is not necessary to utilize maximum power from the array. It should be noted however that the point of rendezvous is in a range anywhere from 0.31 to 0.47 AU. From the standpoint of the power subsystem design and operation, the choice of a rendezvous point in the upper range of solar distances simplifies the task.

The comet D'Arrest, comet Encke and asteroid Ceres rendezvous missions require maximum power between 0.9 and 3.4 AU. Over this range, the input voltage to the power processor increases by about

2.2:1 including open circuit conditions at 3.4 AU. This voltage variation is the same as that for the inbound missions, except the voltage increases rather than decreases. This fact suggests the possibility of utilizing a higher array voltage at 1 AU for inbound missions and a lower value for outbound missions to limit variation of the power processor input voltage during these missions.

The secondary missions present more difficult requirements for the power subsystem with regard to input voltage variation to the power processors. These missions have large variations in solar distance during propulsive phases in both the inbound and outbound directions. As a result, it will be necessary to have a power processor capable of operating over a 3.3 variation in input voltage to meet the requirements for these missions.

A battery and associated battery charge and discharge controls will be required to supply power to the stage before solar array deployment and sun acquisition during solar eclipse on orbital missions such as Ceres or Mercury, and to supply power to the stage during temporary power subsystem malfunctions.

7.1.2 Selection of Power Subsystem Operating Parameters

To establish whether or not it is possible to utilize a common power subsystem for all primary missions of interest, it was necessary to examine the performance limitations of a variety of key power subsystem elements. An outline of the key options examined is presented in Figure 7-2 and the rationale for making each of the indicated selections is discussed below. The primary criteria for selecting an approach was based upon its ability in meeting the multi-mission stage requirements. For a number of key parameters there are only limited experimantal or analytical data available on which to base an evaluation. Final selection of component type and operating mode can only be made after the detailed stage requirements are established along with more precise information on critical component performance.

Maximum Solar Array Temperature. At solar approach distances closer than about 0.7 AU, the temperature of a flexibile solar array whose surface is oriented in a direction normal to the incident solar

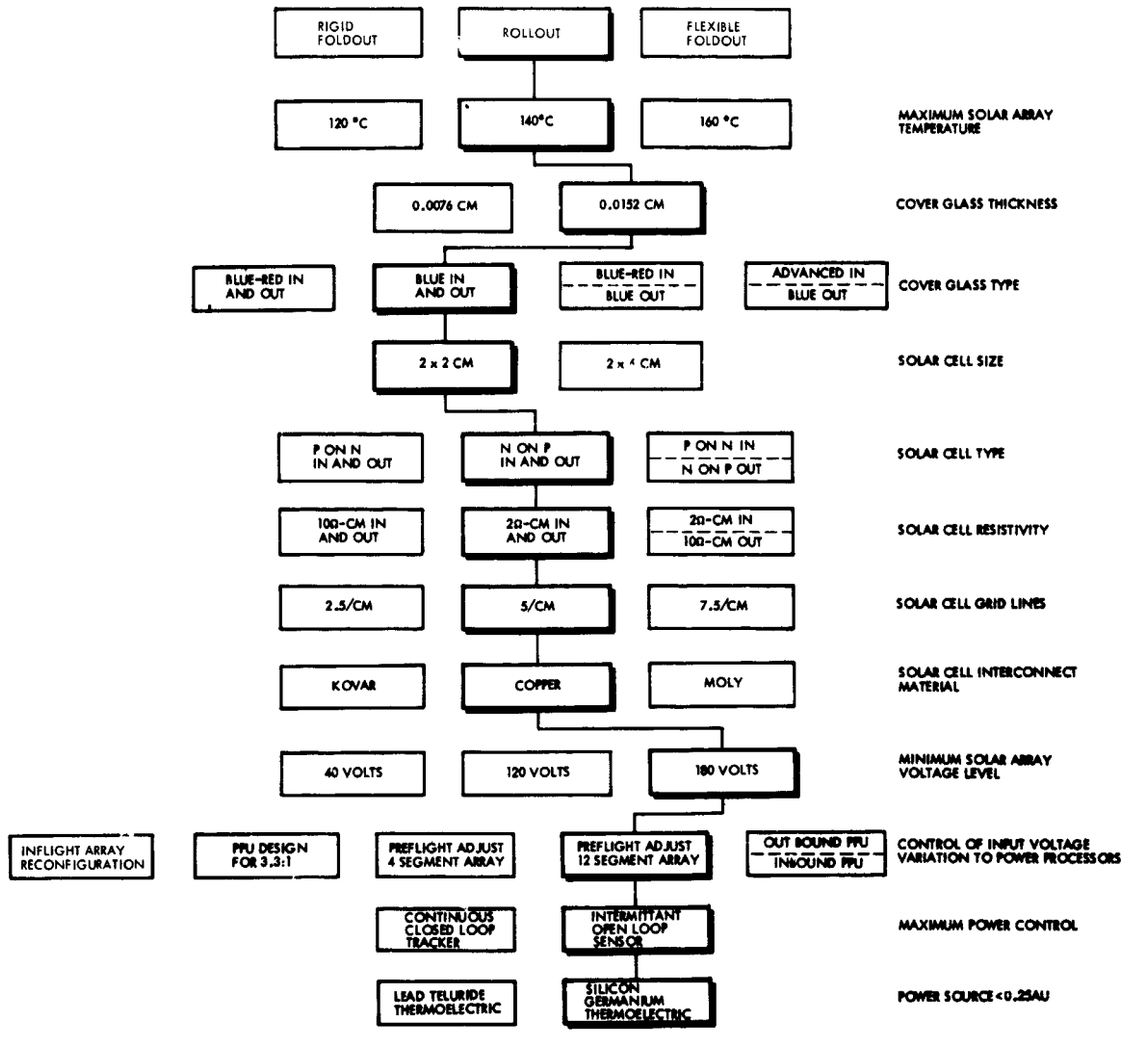

Figure 7-2. Key Power Subsystem Options

radiation can get high enough to result in a reduction of the mechanical strength of the solar cell connections. For the large rollout solar arrays of the type proposed for the stage, thermal expansion or other disturbing forces can cause stresses beyond the mechanical strength of the solar cell connections at elevated temperatures. This can result in a significant number of cells becoming open circuited with a resultant loss of solar array power. Therefore it is necessary to limit the solar array temperature to prevent mechanical and resultant electrical failure. This can be accomplished by rotating the solar array panel relative to the direction of the solar radiation to reduce the angle of incidence.

At the present time the maximum allowable solar array temperature for long term operation at close solar approach is about 140°C. This upper limit on temperature is based upon the safe operating temperatures for conventional solder-dipped solar cell connection techniques. Solder melts at about 177°C and becomes plastic at 160°C. In addition, due to the high activity of tin in the tin-lead-silver alloys used, the solder can break down and lose mechanical strength upon long term exposure to temperatures as high as 150°C (Ref. 7-1). No such problems appear to occur at 140°C. Based upon these considerations, an upper limit on solar array temperature of 140°C appears acceptable for conventional soldered solar cell connections. It is interesting to note that this maximum solar array temperature will also be used on the upcoming Mariner-Venus-Mercury probe.

At the upper temperature limit of 140°C held constant at solar distances below 0.65 AU the maximum solar array output power will also be constant, at a level 38 percent higher than the nominal output at 1 AU, according to data from a recent JPL study, Reference 7-2. (The preliminary value of 40 percent assumed in performing trajectory analyses of inbound missions is in good agreement with these results.)

Increasing the maximum allowable solar array temperature to 160°C does not appear to offer any apparent increase in output power. However the 20°C increase in maximum operating temperature will result in more than a 10% increase in solar array output voltage variation as the stage travels between 1.0 and 0.5 AU. As a result, there

appears to be no incentive for increasing the maximum solar array temperature above 140°C.

Decreasing the maximum allowable solar array temperature at close solar approach distances to 120°C can result in about a 5% loss in peak solar array output power when compared to operation at 140°C. With the relatively high energy required for the Mercury orbiter mission, this power penalty is not justifiable just to gain a ten percent reduction of solar array output voltage variation. However, it is recommended that consideration of 120°C operating temperatures should be given in future more detailed studies where the precise weight penalties associated with operating temperature can be established.

The previous discussion of limitations of maximum array operating temperature was based upon soldered solar array construction. It is expected that by the time the solar electric stage is undergoing the hardware development phase, welding techniques will be used for solar cell connections. In fact such techniques are already being applied for high temperature operation on the 0.2 AU Helios spacecraft (Ref. 7-3). The use of welded construction should result in more than a 20°C factor of safety for the selected 140°C operating temperature.

Cover Glass Thickness. The solar array must provide maximum power to the stage propulsion system for extended time periods at relatively close solar approach distances for a number of primary missions of interest such as the out-of-ecliptic and Mercury probes. In addition, these missions can occur over a long time period with varying solar activity due to the projected usage of the stage over the next 10 to 15 years. As a result, some missions can have a high probability of suffering degradation in output power due to solar flare damage. The stage power subsystem must be designed for the worst case conditions projected so as to avoid subsequent design changes. Previous studies of less challenging missions for solar electric propulsion utilized a nine-percent margin of safety in the installed solar array power to allow for the probability of solar flare degradation during the mission (Reference 7-4). This safety margin was based upon the utilization of a 0.0076 cm (3 mil) thick cover glass. For the conditions of interest to this study, it was found prudent to utilize a 0.0152 cm (6 mil) thick cover glass in order to

reduce the required safety margin against solar array degradation for the most critical mission types and launch dates. Use of the 0.0152 cm cover glass results in a 26.2 kg weight penalty for the 17.5 kw of installed solar array power, while reducing potential radiation damage by a factor of about four.

It is interesting to note that use of the 0.0152 cm thick cover glass results in a 10% reduction of recurring solar array costs. This is due to the fact that breakage and handling problems are greatly reduced by using the 0.0152 cm cover glass instead of the presently utilized 0.0076 cm elements.

Cover Glass Filter. Control of solar cell temperature and output characteristics for a given incident solar flux is obtained through the selection of the cover glass surface thermal and optical characteristics. For this study, three types of cover glass filters were considered; blue, blue-red and advanced multilayer coatings. The blue filtered cover glass has the highest transmission of incident energy and the highest ratio of absorptance to emittance ($\alpha/\epsilon = 0.95$). For a given solar flux this cover glass will result in the highest solar cell temperature due to its relatively high α/ϵ ratio and high transmission of infrared. It has been generally used in the past in missions where the solar distance did not drop appreciably below 1 AU.

The blue-red cover glass has a lower ratio of absorptance to emittance, $\alpha/\epsilon \simeq 0.86$, than the blue element and also transmits less of the incident energy in the infrared region. Therefore solar cells with blue-red cover glasses operate at lower temperatures. Although this characteristic results in the requirement for smaller solar array rotation angles (approximately 5° - 10°) to limit array temperature at close solar approach, the use of a blue-red cover glass results in a slightly reduced solar array output power between 0.3 and 1.0 AU. On missions where maximum power is required between 1 and 3.5 AU, the blue and blue-red filtered cover glasses were found to produce approximately the same output power. Use of blue-red cover glasses can result in a factor of two increase in coverglass cost.

When advanced cover glass coatings such as 4026 filter developed for JPL by Optical Coating Laboratory Inc. (Ref. 7-2), are used, the

solar array output power can be increased by about 20% over that obtained for conventional blue cover glass filters at solar approach distances between 0.6 and 0.3 AU. In addition, use of such new cover glass filters precludes the requirement to rotate the solar array to maintain the operating temperature below 140°C up to about 0.4 AU due to its low α/ϵ ratio. Unfortunately, the 4026 filter results in an output power much lower than that of the blue filter at solar approach distances of 0.6 AU or greater. Since on the inbound missions the major portions of the propulsive phase are required between 0.6 and 1 AU, it does not appear that the 4026 filter offers any significant advantages over the blue filter for the stage.

As a result of the above considerations, it was concluded that use of the blue cover glass filter for all missions of interest will not compromise the performance of any given mission.

Solar Cell Size. Based upon the present state of the art, a choice of a 2 x 2 cm cell over the 2 x 4 cm cell appears to be the most conservative approach technically, although higher assembly costs are projected. Larger cells have been found to encounter thermal expansion and contact material problems for large temperature variations.

Solar Cell Type. Based upon available data, it appears that the N/P type solar cells will perform slightly better than P/N type except at very low solar intensity levels. (Reference 7-5.) When it is noted that the P/N solar cell is subject to more radiation damage than the N/P cell, the selection of the N/P cell for all missions of interest to the stage is clear. In addition, at the present time production of the P/N cell is limited only to small quantities for research efforts. As a result, the solar array costs would probably be much higher if such a cell were desired.

Solar Cell Resistivity. Between solar distance extremes of 0.3 and 1 AU the 2 Ω-cm base resistivity solar cell produces considerably more output power than the 10 Ω-cm cell. For example, at 1 AU the 2 Ω-cm cell produces about 6% more power than the 10 Ω-cm cell while at 0.7 AU it produces about 13% more power. The difference in power output between these two cells decreases until at about 2 AU there is a crossover point whereby the 10 Ω-cm cell begins to produce

more output power than the 2 Ω-cm cell (Ref. 7-6). This increased output power for the 10 Ω-cm cell can be as much as 10% greater than that for the 2 Ω-cm cell as range increases to 3.5 AU. However, when one considers that the incident solar energy drops as the inverse square of distance, the integrated increase in output energy provided by the 10 Ω-cm cell between 2 and 3.5 AU is not sufficiently larger than the loss in output energy between 0.9 and 2 AU to warrant using this cell instead of the 2 Ω-cm cell for most outbound missions of interest. In addition, over the operating range of interest, the 10 Ω-cm cell has a larger variation in output voltage than the 2 Ω-cm cell. Therefore for the purposes of simplifying stage design, a 2 Ω-cm cell will be selected for all missions.

Solar Cell Grid Lines. In selecting a cell design with the highest efficiency for multi-mission applications the question of collector grid spacing is important. Close grid line spacing generally yields a high collection efficiency by shortening the path length to be traversed by the charge carriers without causing much reduction in exposed cell area. At close solar approach distances, it has been shown that cells utilizing 6.5 grids/cm produced a much higher peak output power than those with the conventionally utilized 2.5 grid/cm (Ref. 7-7). This increase in peak power was as high as 25% between 0.6 and 0.3 AU. However extrapolating this data for solar distance extremes of 1 - 3.5 AU, the cells with an increased number of grid lines could produce about 5% less power. The Mercury orbiter is the only mission of interest where the maximum solar array power is required between 0.3 and 0.6 AU. To avoid using different solar cell construction for this mission, the trajectory analysis was based upon a power profile corresponding to 2.5 grids/cm. Since it was found from this analysis that acceptable payload could be delivered to Mercury orbit, it was concluded that the 2.5 grid/cm design was compatible with all missions of interest.

Solar Cell Interconnect Material. Since a common solar array is proposed for all stage missions, this array must be designed for a large temperature variation (i.e., +140°C — -150°C). As a result, there can be relatively large thermal stresses that can arise due to a mismatch in thermal expansion coefficient between the solar cell

and interconnecting tab material. Such stresses can lead to interconnect breakage with a subsequent loss in power due to open circuiting of the solar cells.

Since it results in the lightest weight solar array compatible with the magnetic cleanliness requirements for the stage, copper was selected for the interconnect material. Although the thermal expansion coefficient between the silicon cells and copper is appreciable, it has been estimated that there should be no problems for the operating conditions of interest. This arises from the fact that there will be almost no thermal cycling of the array. An additional factor of safety on interconnect stress level can be achieved by using molybdenum instead of copper. Molybdenum more closely matches the thermal expansion coefficient of the silicon solar cells, however, it has a resistance roughly 3 times that of copper. Assuming a minimum solar array potential of 200 volts, this would result in about a 10 kg mass penalty to prevent serious power losses in interconnects. The penalty will increase for lower minimum solar array potential. Based upon a preliminary analysis, it is felt that it will not be necessary to resort to the use of molybdenum interconnects, however this option should not be ignored in future more detailed studies.

There was one additional interconnect material considered, kovar. This material has a thermal expansion that is closest to that of the silicon solar cell. In addition it has an electrical resistivity lower than that of molybdenum. Unfortunately, kovar is magnetic and can lead to magnetic field contamination of the stage. Since such contamination can lead to faulty readings of some of the key particle and fields scientific payloads carried by the stage, it was dropped from consideration.

Minimum Solar Array Voltage Level. The stage has an installed power level of 17.5 kw. This power level is more than an order of magnitude larger than the solar array power flown previously. In the past when the solar array power levels were less than 1 kw, solar array voltages of 28 to 50 volts were found acceptable. However with the increased power level, the weight of electrical cabling on the stage can become excessive unless there is a corresponding increase in the

voltage level. The electrical cabling weight and power loss must be designed for the highest current condition that the power subsystem will experience. This occurs at the peak power and minimum voltage condition.

For the subject stage the peak required output power from the solar array is 21 kw, when the stage is at solar approach distances of 0.65 AU or closer. This occurs for most inbound missions. On the outbound missions the peak required solar array output power is about 15 kw. It would create an unnecessary expense and design problem to build a different power distribution system for each class of missions. Therefore the mass penalty associated with 21 kw will be charged against the outbound missions. This mass penalty can be reduced to acceptable levels by increasing the minimum operating voltage level of the solar array from the present utilized value of 50 volts to voltage levels of about 200 volts. The recent advances in power processing technology (Ref. 7-8) permit input voltages as high as 400 volts.

The solar-array-to-power-processor cable weight was optimized using a power cable optimization computer program. The program computes the total array current by dividing the array power by the bus voltage and then varies the number of fixed diameter wires in the cable while calculating cable power loss, cable weight, and increased array mass required to compensate for cable dissipation. For each different number of wires, the total cable mass and increased array mass is compared with the value obtained previously, until a minimum value is found. Figure 7-3 presents the computed optimum mass of the 21 kw solar array and cabling for a cable comprised of number 20 copper wires for various separation distances between the array and the power processing units. A mass penalty of 15 kg/kw was used for the excess solar array required for the power dissipation in the electrical cabling. The array-to-power-processor cabling length for the stage is estimated at 3.5 meters from preliminary equipment layout drawings. For this selected design, it can be seen that by increasing the minimum array voltage by a factor of 4 results in a reduction in mass penalty of about 31 kg and a reduction in the power level by about 300 watts. For the Ceres mission, 31 kg corresponds to about a 20% improvement in payload. Since operation at such voltage levels of 200 - 400 volts is within

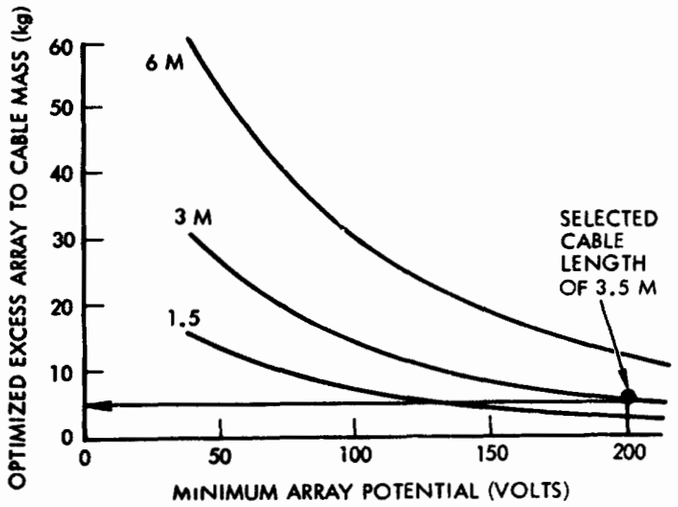

(A) POWER DISTRIBUTION MASS PENALTY VS MINIMUM ARRAY POTENTIAL

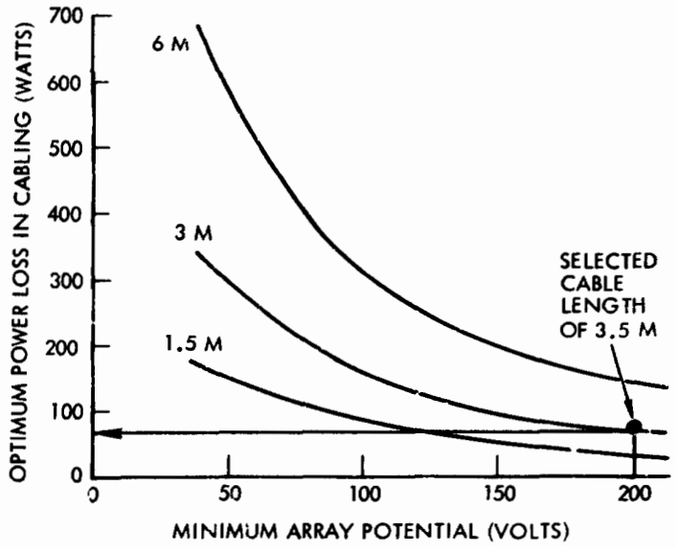

(B) OPTIMIZED POWER LOSS IN CABLING VS MINIMUM ARRAY POTENTIAL

Figure 7-3. Power Distribution Weight and Power Loss

state of the art power processing techniques, the baseline design will utilize a minimum array potential of about 200 volts.

Control of Input Voltage Variation to Thruster Power Processors.

As discussed previously, unless controlled in some fashion, the solar array output voltage will vary by a factor of 3.3:1 for the solar distance extremes of 0.3 to 3.5 AU for all the primary missions of interest. Summarized in Table 7-1 are five of the techniques examined to meet such an operational requirement. In the first, the solar array potential at maximum power is set at 300 volts at 1 AU for all missions. As a result, the power processor must be designed to operate over a range of from 180 to 580 volts. At the present time not only is the 3.3:1 voltage variation beyond the state of the art, but the upper voltage level of 580 volts is approaching SCR and capacitor component limitations. It is projected that with improved components and an advanced technology program a power processor can be developed to meet these requirements. The projected mass penalty associated with such an approach is between 5 and 10 kg for the 15 kw propulsion system of interest. Although this approach offers the most flexible system for the solar electric upper stage, it will not be considered for early application since it is beyond the present state of the art. It is recommended however, that a technology program be undertaken to establish the feasibility and actual weight penalties associated with such an approach. Should component technology be limited to 500 instead of 580 volts, it will be necessary to consider using a 260 volt array at 1 AU with a 150 volt minimum voltage.

The second approach considered an array voltage of 260 volts at 1 AU for all missions, however different power processors were used for inbound and outbound missions. In this approach it was possible to limit the input voltage variation to the power processors to 2.2:1 or less. This is within the state of the art, however the additional development and recurring costs associated with this approach do not appear warranted.

Rather than building different power processors for inbound and outbound missions to limit the total input voltage variation an alternate design approached is desirable whereby the output voltage of the

Table 7-1. Techniques for Control of Power Processor Input Voltage Variation

Approach	Solar Array Potential for Maximum Power at 1 AU (volts)	Maximum Array Potential		Minimum Array Potential at Maximum Power (volts)	Input Voltage Variation to PPU	Comments
		Maximum Power Voltage (volts)	Open Circuit (volts)			
Fixed array potential at 1 AU	300	480 (3.4 AU)	580 (3.4 AU)	180	3.25:1	Most flexible and adaptable to stage Weight penalty associated with 3.25:1 voltage variation 10 kg
Fixed array potential at 1 AU with different power processors in and out	260 (inbound power processor)	290	345	155	2.2:1	Extra development and recurrent costs
	260 (outbound power processor)	420	500	235	2.2:1	
Preflight adjustment of array potential (2 segment panels)	200 (inbound missions)	320	385	180	2.94:1	
	400 (outbound missions)	440	530	240		
Preflight adjustment of array potential (6 segment panels)	200 (outbound missions)	320	385	180	2.2:1	Minimal voltage variation to PPU input No simple way to reconfigure array
	300 (inbound missions)	330	400	180		
Inflight adjustment of array potential	250 (1 AU)	300	350	200	1.7:1	No reliable device available at present Minimizes voltage variation to power processors for all missions

solar array is preset at a different level for inbound or outbound missions. This can be accomplished by breaking up the solar panels into segments and appropriately rearranging the wiring harness on the array before the flight. Such an approach is commonly utilized on present spacecraft to obtain a closer control of the solar array voltage level before flight. No significant additions to the development or recurring costs are expected from such an approach. Two different configurations were evaluated as outlined in Table 7-1. One Approach where a 200 volt solar array potential was set at 1 AU for outbound and a 400 volt potential set at 1 AU for inbound missions resulted in a 2.9:1 variation in the voltage level. This does not give enough improvemcnt over the

3.3:1 worst case voltage variation. The second approach where a 200 volt level was used for outbound and a 300 volt level used for inbound missions resulted in a very acceptable 2.2:1 variation in input voltage to the power processors. It should be noted that the SCR multikilowatt power processor presented in Ref. 7-8 is designed to operate over an input voltage range of 180 to 400 volts. As a result, the baseline approach selected for the solar array design calls for preflight adjustment of 6 segment solar array panels to control input voltage variation. The schematic diagrams for one approach of obtaining such voltage variation control is presented in Figures 7-4 and 7-5.

The previous discussion of solar array output variation control was based upon the requirements for the primary missions. When one consideres the secondary and growth mission requirements as outlined in Figure 7-1, it is clear that the selected voltage variation control technique is not adequate. This problem arises from the fact that these growth missions penetrate to very close and travel out to very distant solar distances on the same mission. Therefore, such missions must be put off until the performance of the power processing units is clearly established over a 3.3:1 variation in input voltage level or as indicated in the final approach in Table 7-1.

Maximum Power Control. Two techniques for maximum power control were considered. In the first, continuous monitoring of the maximum power of the array is performed throughout the powered flight portion of the mission. Based upon this maximum power measurement, a signal is fed back into the propulsion control system to assure operation at the maximum power point. Since it would not be possible to continuously track the stage and adequately update the trajectory this approach was rejected.

An alternate approach where the maximum power is sensed periodically, perhaps once a week, was selected instead. In this approach the power profile and the trajectory are updated at the same time on a periodic basis based upon the tracking and maximum power data. This approach allows adequate flexibility for obtaining peak propulsion system performance, while meeting the mission navigation and guidance requirements.

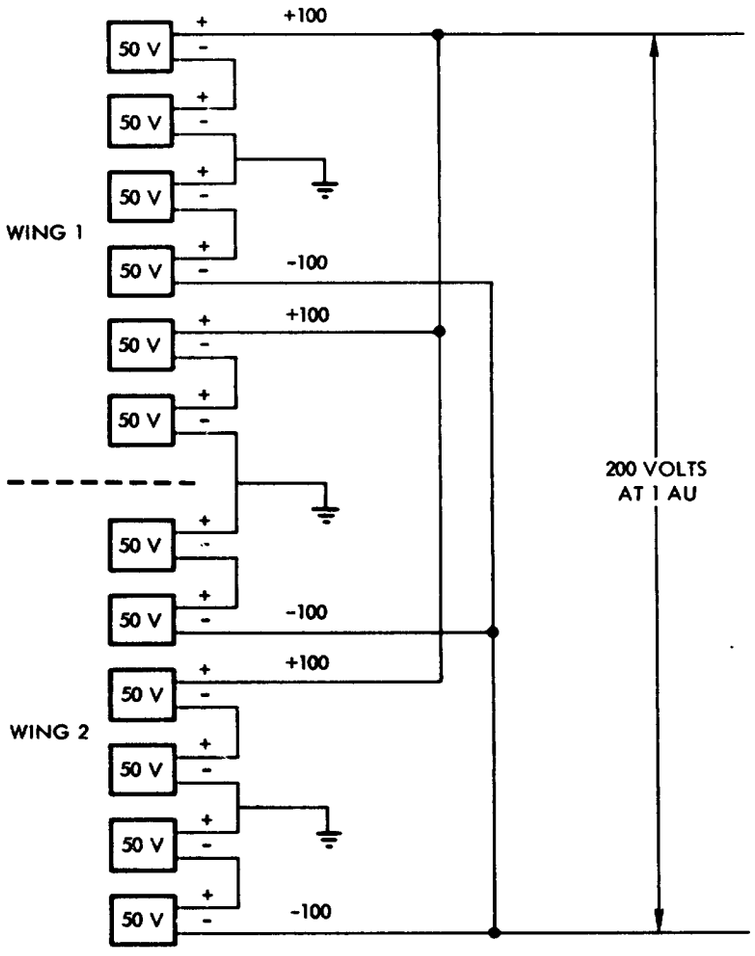

Figure 7-4. Solar Array Configuration for Outbound Missions

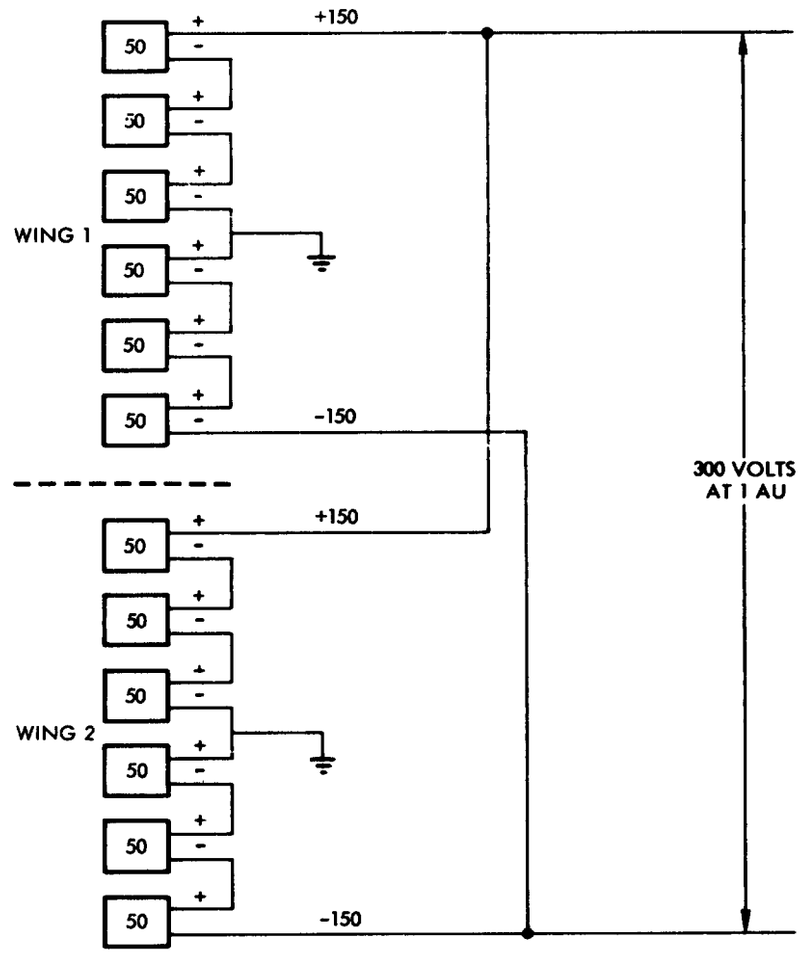

Figure 7-5. Solar Array Configuration for Inbound Missions

Power Source at Close Solar Approach. The solar array is adequate in providing power for all the missions with the exception of the 0.1 AU solar probe. On this mission it will be necessary to retract the solar array at about 0.25 AU to prevent serious damage. Since the solar energy flux is high enough, it is possible to utilize it in a direct conversion to electrical energy with a flat-plate thermoelectric device. Two different techniques were considered, the lead-telluride and the silicon-germanium thermoelectrics. The silicon-germanium device was selected since it produced the desired 300 watts of power with the most compact and lightest weight system for the operating environment of interest.

7.1.3 Power Subsystem Description

A block diagram of the power subsystem is presented in Figure 7-6. The major portion of the array output is fed directly to the thruster power processing system. The remainder of the power is distributed to the subsystem loads through the stage power supply which processes the unregulated solar array input to a 22 to 33 vdc bus. The battery is connected to the subsystem bus through a charge/discharge control unit.

The flat-plate silicon-germanium thermoelectric power source required in the solar probe mission is operated at near maximum power by a shunt regulator. Two power converters located in the EIA provide multiple regulated outputs to the essential and non-essential load buses. The non-essential loads are connected to the stage power supply via a power relay which is activated by a bus undervoltage sensor in the stage power supply. If the 22-33 volt bus falls below 22 vdc for more than 100 milliseconds, all loads not essential to stage survival are disconnected by fault clearing switches. The mass, dimensions and output power of the major power subsystem components are presented in Table 7-2. A summary of their characteristics is presented below.

Solar Array

The solar array selected for the baseline design is the General Electric rollup configuration. The array consists of two deployable panels which are stowed on beryllium drums during launch. Each panel panel consists of two kapton blankets on which the silicon solar cells are

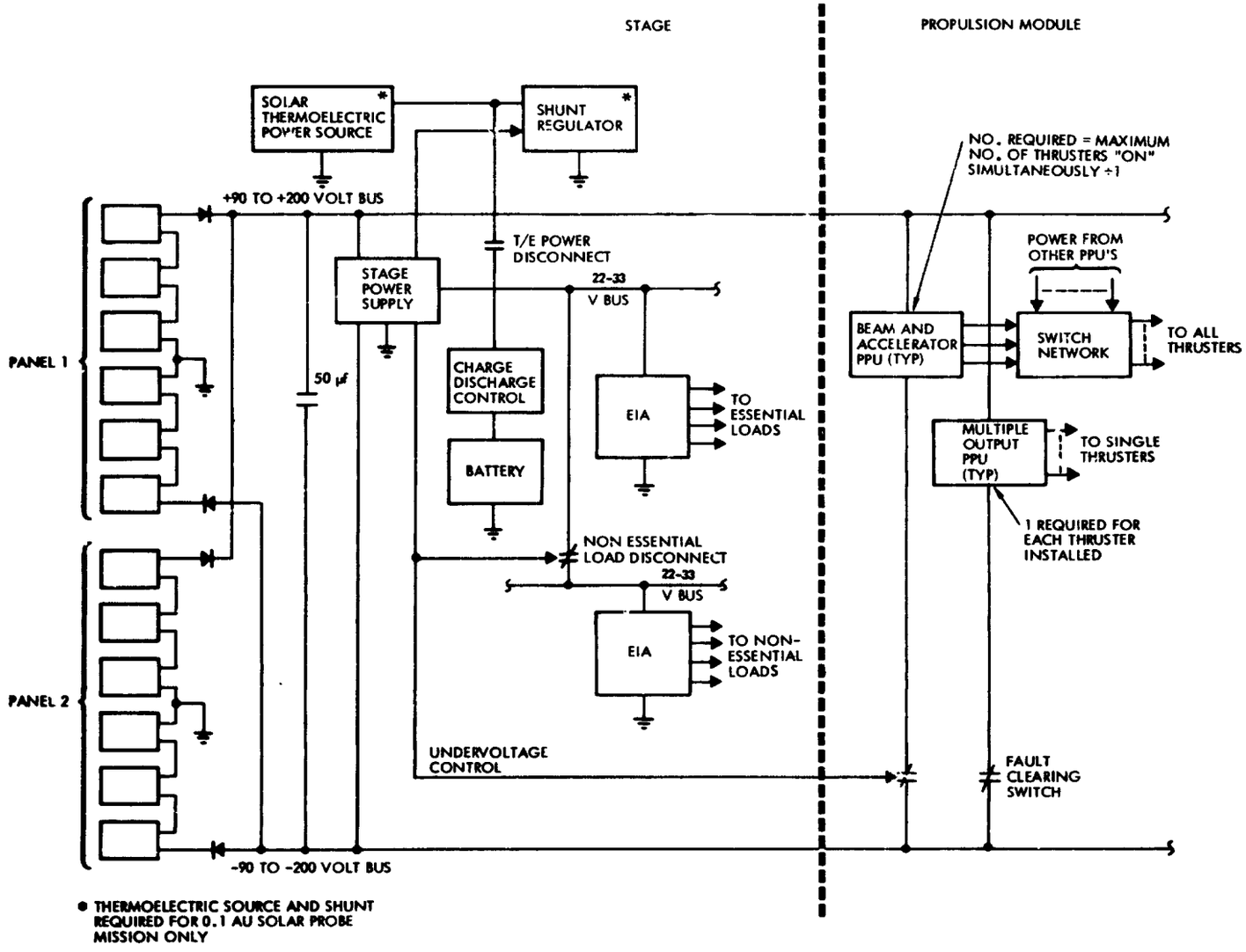

Figure 7-6. Electric Power Subsystem Block Diagram (Inbound Configuration)

Table 7-2. Summary of Power Subsystem Characteristics

Component	Number	Mass		Dimensions (meters)	Power Output	Comments
		Unit (kg)	Total (kg)			
Solar array panel	2	144.5	289	4.2 x 20.4	17.5 kw installed power	GE rollout with 6 mil coverglass
Nickel-cadmium battery	1	17.0	17	0.45 x 0.3 x 0.1	18 amp-hr	Second unit required for Mercury or Ceres orbit
Battery charge-discharge control	2	1	2	0.15 x 0.15 x 0.15	Trickle charge	One unit standby redundancy
Flat plate silicon germanium thermo-electric source	1	9.0	9.0	1.3 x 1.3	0.300 kw	0.1 AU solar probe only
Shunt regulator	1	4.5	4.5	0.9 x 0.25 x 0.05	0.140 kw	0.1 AU solar probe only
Stage power processor	2	2	4	0.2 x 0.2 x 0.1	300 w peak output power	One unit standby redundancy
Solar array drive assembly	1	15	15	0.15 diameter by 0.4 length	--	Includes redundant harmonic drive motors
Solar array drive electronics	2	0.6	1.2	0.15 diameter by 0.4 length	--	One unit for redundancy

mounted. Each pair of wings are attached to a single bi-stem deployment boom. The boom maintains tension on the array when in the deployed state. The tension force is selected such that the array natural frequency is well above the bandwidth of the attitude control subsystem. Summarized below are the typical array characteristics:

Cell type	N/P silicon, 2 x 2 x 0.020 cm, 2 cm base resistivity
Coverglass	0.015 cm thick microsheet
Installed power at 1 AU	17.5 kw
Required output power at 1 AU	14.7 kw*
Maximum total output	400 volts (200 volts relative to stage ground)
Minimum total output	180 volts (90 volts relative to stage ground)
Peak output current	110 amps (at 0.4 AU)
Substrate material	kapton sheet
Deployable boom	Stainless steel bi-stem
Power transfer method	Slip rings

*As discussed in Section 6 the additional 2.8 kw of installed power is required to allow for array degradation and housekeeping power at 3 AU.

Battery

The stage operates from the battery during launch prior to sun acquisition and during eclipse periods. In addition, it is also used to supply power to essential stage loads when undervoltage conditions occur on the stage bus. The battery energy required during launch and sun acquisition can be calculated from the stage power budget in Section 6-12, Table 6-2 and the preliminary flight sequence for the Ceres orbiter mission shown in Section 6-13, Table 6-4. Thus:

$$\text{Battery energy} = (214.6 \text{ watts})(1 \text{ hour}) + (231.4 \text{ watts})(0.2 \text{ hours})$$

$$= 261 \text{ watt-hours}$$

An 18 amp-hour battery with 22 cells in series is capable of meeting this requirement with a reasonable power margin. To provide the charge/recharge capability required during various mission phases and emergency conditions a nickel-cadmium battery was selected. The depth of discharge for such a battery during launch and solar acquisition will be less than 50 percent. For missions such as Mercury and Ceres orbiters the battery is used to supply power to the stage subsystems during eclipse periods which can be as long as one hour. To supply the 250 watts required during such periods will require less than a 50 percent depth of discharge. Under such conditions, the nickel-cadmium battery selected is capable of sustaining the stage subsystems during hundreds of eclipse cycles if required.

Battery Charger/Discharger Control Unit

Since the battery may be dormant for the major part of missions of interest or be periodically recycled, e.g., during eclipse conditions, the charge/discharge unit is designed to operate at several charge rates. The battery may be connected directly to the 22-33 volt bus and charged at the maximum rate when maximum power is available. A trickle-charge method is used when available power is limited. During the extended inactive periods, the battery remains open circuited; however, reconditioning about every two months is recommended to maintain battery capacity and to minimize crystalline buildup on the cell plates.

The charge/discharge control is automatically activated whenever a battery discharge occurs. Command override of this automatic function is also provided.

Silicon-Germanium Thermoelectric Power Source and Shunt Regulators

The thermoelectric power source provides power for payload and subsystems between 0.25 and 0.1 AU in the solar probe mission. In the selected approach, solar power is used to heat a metallic absorber to a nominal temperature of 1100°C. The thermal energy is transferred to the silicon-germanium thermoelectric elements by means of a heat pipe. At the present time there are no known thermal coatings that can be applied to the thermoelectric units to obtain direct energy absorption.

A shunt regulator maintains the output power from this source relatively constant under load changes by dissipating source power which exceeds the load demand.

The thermoelectric power source is connected to the stage bus by power relays which are controlled by ground command.

Stage Power Supply

The stage power supply processes the unregulated solar array output to a 22-33 vdc bus. The power supply consists of parallel-redundant SCR series inverters whose basic design concept is similar to that of the thruster power processors.* Also included in this unit are the telemetry, conditioning, command and undervoltage circuits for control of power subsystem operation.

Solar Array Drive

The solar array drive assembly is mounted at the center of a common shaft that connects both solar array paddles. Two drive motors are used to provide adequate redundancy. The drive mechanism is designed to rotate the solar array by ±90 degrees from the nominal orientation parallel to the stage center body. A simple cable wrap-up technique was selected to transfer the solar array power to the stage

*See Section 7.2.3 for a more detailed discussion.

center body. This is possible because of the small ±90 degree rotation angle of the paddles and preferable to slip rings because of the extremely slow rotation rate required. In some mission phases the solar array drive will remain inactive over prolonged periods which would make the use of slip rings problematic. The mechanical design of the drive assembly was shown previously in Figure 6-1.

7.1.4 Power Subsystem Interfaces

7.1.4.1 Solar Array

Capacitive Impedance Control. Figure 7-7 illustrates the solar array and power distribution cabling impledance as a function of frequency. At low frequencies, the solar array impedance is resistive. At about 2 kHz the array becomes more capacitive. Unless corrected, the power distribution cabling is inductive and as a result its impedance is directly proportional to frequency. At frequencies of 10-50 kHz, corresponding to switching frequencies in the power processing equipment, this impedance can get so high as to produce an appreciable ripple in the power distribution bus. One approach to controlling this increase in impedance is to place a 50 μfarad capacitor across the output terminals of the power distribution bus as indicated in Figure 7-6. The resultant drop in impedance is presented as a dashed line in Figure 7-7.

Maximum Power Sensor. Accurate prediction of the time-varying solar array output characteristics before launch is not possible owing to the random nature of degradation effects. It will therefore be necessary to measure the actual characteristics periodically during flight and to determine the operating point at which maximum solar array power is available for thrust purposes. The measured solar array characteristics can be telemetered to the ground where they are referenced to the actual distance of the vehicle from the sun. This permits periodic updating of the projected power profile and adaptation of the trajectory and thrust profile if necessary.

A promising implementation of such a measurement was recently conceived at TRW. This approach is based on an adaptative control technique where the thrusters are utilized as a variable load for exercising the current-voltage characteristics of the solar array. This is illustrated in Figure 7-8.

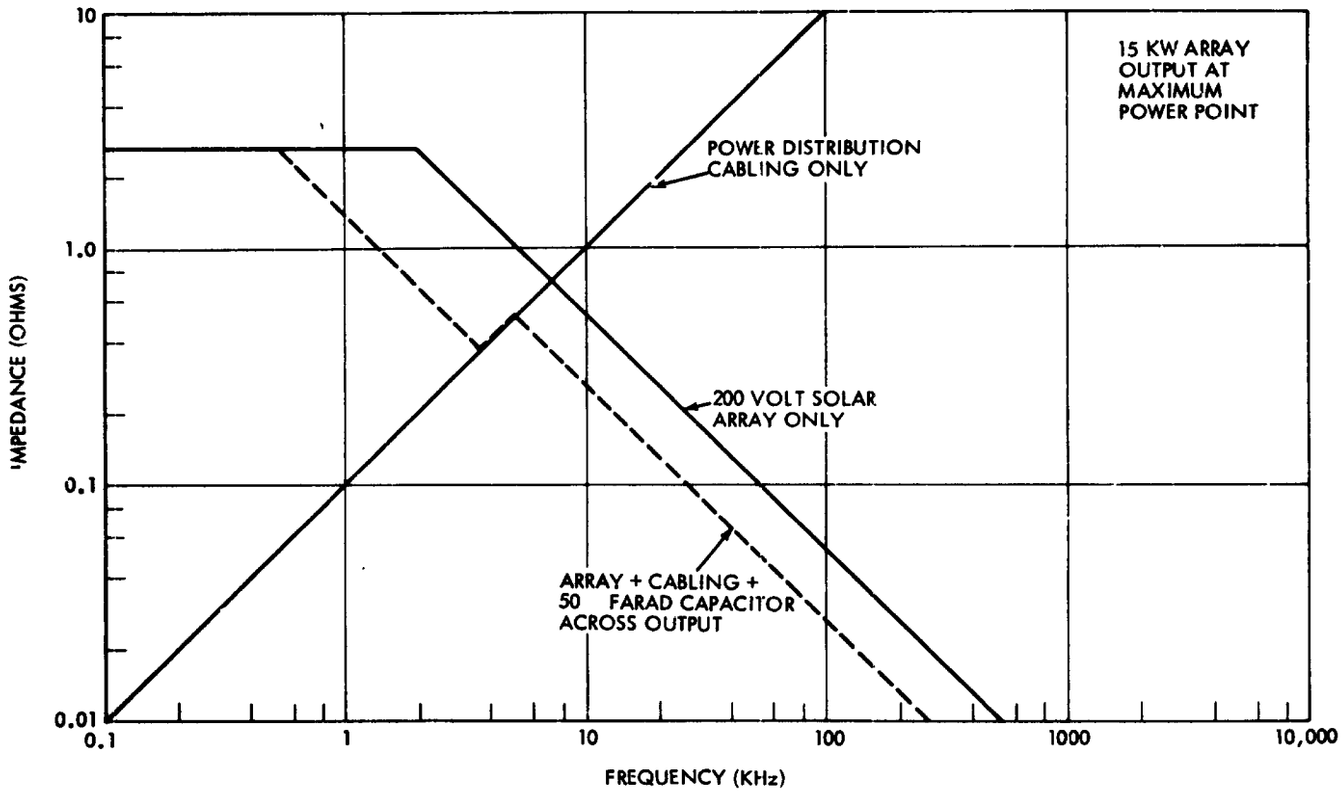

Figure 7-7. Solar Array Impedance as a Function of Frequency

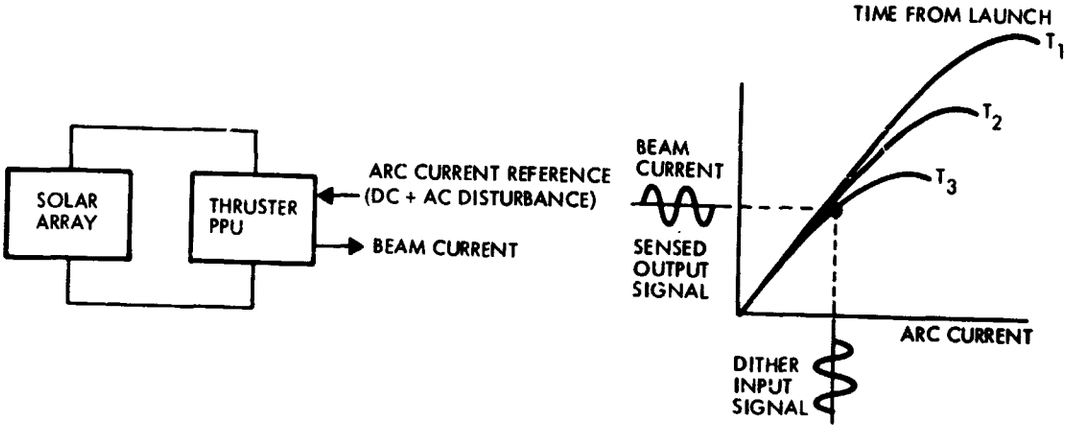

Figure 7-8. Maximum Power Point Sensing System

A low amplitude, low frequency "dither" input is applied to the arc current reference. This variation in arc current causes a change in the ion current density in the discharge chamber and hence the output beam current. For purposes of discussion we assume that the thruster operates initially at a point where it uses less than the available maximum power. As the dc level of the arc current is increased, the thruster beam current and the power drawn from the solar array increases (assuming a constant net accelerating voltage). When the maximum solar array power point is reached, the charge in beam current with arc current will approach zero. Further increases in arc current would cause a reduction of beam current.

To determine the point of maximum solar array power, the amplitude of the beam current dither component is monitored in relation to the amplitude of the input dither signal. The maximum power point can thus be determined as the point where the beam current dither amplitude goes to zero.

Space Plasma Drainage. The proposed solar array potential of $\pm$200 volts relative to the space plasma is higher by about a factor of four than voltage levels used on lower power spacecraft flown previously. Based upon the preliminary data of Reference 7-9 this voltage level is well below the values at which performance and lifetime degradation may be expected due to electron and ion drainage currents from the ambient space plasma.

7.1.4.2 Power Processor

Input Current Transients. The input current transients drawn by the ion thruster power processor at instances of power processor turn-on and thruster shorting must be controlled so that the solar array does not become overloaded. At these instances a serious undervoltage condition may occur. Protection against such undervoltage conditions is an inherent functional characteristic in the SCR series inverter that is used in the selected pow processing system.

Suppression of Noise Generated in Power Processor. Because of the switching action of the power processing equipment, significant levels of ripple current can be generated in the stage power bus. This ripple must be suppressed to acceptable levels so that it will be possible to operate as close to the maximum power point as possible without causing the solar array voltage to collapse. In addition, unless suppressed, ripple currents can cause interference with operation of stage subsystems.

To achieve the desired attenuation it is necessary to utilize a properly sized filter on the input terminals of the power processing equipment.

Unfortunately, at the present time an EMI control specification for a 20-kw stage is not available. If present EMC specifications for existing low-power spacecraft such as TOR-1001-4 are used to establish attenuation levels for the stage, filter mass penalties as high as 15 kg will result. Instead, as discussed in Appendix H, a preliminary estimate of an EMI control specification that should be more compatible with the stage requirements was used to compute the input filter mass. The results of this analysis indicate that for a two-stage filter, the mass penalty should be less than 3 kg.

7.1.4.3 Electrical Distribution

As pointed out previously, it will be necessary to isolate the power subsystem from shorts that might occur in key elements such as thruster power processors. The design of such a device is complicated by the requirement that it operate over a relatively large power range at high power levels. At the present time there are no existing passive fuse

devices or active switches available. As a result, it will be necessary to develop such a fault clearing switch before the stage can be flown.

7.2 ELECTRIC PROPULSION SUBSYSTEM

The electric propulsion subsystem imparts the necessary energy and momentum increment to the stage after launch by a chemical booster so that it will achieve the desired transfer trajectory to destination, and in the case of rendezvous mission, match the velocity of the target. Typically, the total thrust impulse required in the specified missions is of the order of 10 to 30 $\times$ 10^6 Newton seconds. The propulsion subsystem must also provide the corrective torques for stage attitude control during the propulsive phases of the mission, thus saving a large amount of attitude control propellant. Guidance corrections can be made during the main thrust phases or by separate maneuvers at a very low propellant cost.

At the present time the thruster with performance characteristics, demonstrated lifetime and flight history most suited to the stage, is the discharge cathode mercury bombardment thruster. This type of thruster was invented by Harold Kaufman at the NASA/Lewis Research Center and has been flight tested twice. A short-term thruster test was performed on the SERT I spacecraft in 1966 and two long-term tests performed with durations of about 90 and 160 days on SERT II (Reference 7-10).

A discussion of the subsystem requirements, design philosophy, operating parameter selection and characteristics follows.

7.2.1 Propulsion Subsystem Requirements and Design Philosophy

A summary of the propulsion subsystem performance requirements, based upon the selected mission profiles (Section 5.7), is presented in Table 7-3. When these requirements are compared with those of previous SEP studies, it becomes apparent that the present requirements are much more difficult to meet. Key factors that have a strong impact on the design include:

- Long thrust firing: this requires increased component redundancy
- High power levels: this requires higher-power thruster modules and increased propulsion module size

Table 7-3. Summary of Propulsion Subsystem Requirements*

Mission	Propellant Mass (kg)	Total Impulse (10^6 Nt-sec)	Input Power (kw)		Total Thrust Level (Millipounds)		Power Profile Type	Nominal Subsystem Burn Time (Days)
			Maximum	Minimum	Maximum	Minimum		
Asteroid Ceres Rendezvous	450	13.5	16	2.0	155	20	Gradually decreases for 700 days	671
Comet D'Arrest Rendezvous	565	16.9	14.5	4.0	140	40	Gradually decreases for 400 days then increases	704
0.1 AU Solar Probe	550	16.5	20	14.5	190	140	Varies between maximum and minimum with 200 duty cycle	330
45-Degree Out-Of-Ecliptic Mapper	1015	30.4	19	14.5	180	140	Varies between maximum and minimum with 300 duty cycle	521
Mercury Orbiter	790	23.6	20	16.0	190	155	Rapidly increases to maximum value in 40 days	311
Comet Encke Rendezvous	470	14.0	14.5	2.0	140	20	Gradually decreases to 500 days then increases	914

*(3000-second thruster I_{sp}, 69 percent overall thruster efficiency, 91 percent power processing efficiency)

- Operation in inbound and outbound missions: this leads to increased component mass, complexity and number of units

The principal design approach that we selected to meet these stringent requirements is to provide adequate component modularity, redundancy, burn time characteristics and thruster power level. As a result, the system can accept multiple thruster failures without jeopardizing mission success; redundancy is provided without an unduly large weight penalty; and excessive development cost can be avoided, as will be shown in the following sections.

7.2.2 Selection of Propulsion Subsystem Operating Parameters

An outline of the options examined in developing a common propulsion module design for the missions of interest is presented in Figure 7-9. The factors considered in the selection of the most desirable design options (boxes in heavy outline) are discussed below.

Specific Impulse

A range of specific impulse, I_{sp}, between 2000 and 3500 seconds was evaluated. (Thruster efficiency as function of specific impulse was assumed in accordance with NASA furnished data, as shown in Figure 5-1.)

A typical example of the effect of specific impulse on net spacecraft mass and payload is presented in Figure 7-10 for the D'Arrest, Mercury, and Ceres and extra-ecliptic missions. With the specific mass of the propulsion subsystem plus solar array assumed as 25 kg/kw in this graph (and similarly with larger more realistic values of specific mass) a specific impulse of about 2000 seconds would be highly desirable. However, the only thrusters presently capable of operation at I_{sp} values below 3000 seconds are of a developmental type, requiring dielectrically coated electrodes for operation (Reference 7-11). Since the lifetime limitation of such thrusters are not as yet well understood we did not consider this thruster model as a candidate for our electric propulsion subsystem, but selected a thruster design with more conventional two-electrode ion extraction having a lower I_{sp} limit of 3000 seconds, and accepted the weight penalty resulting from operating at this I_{sp} value.

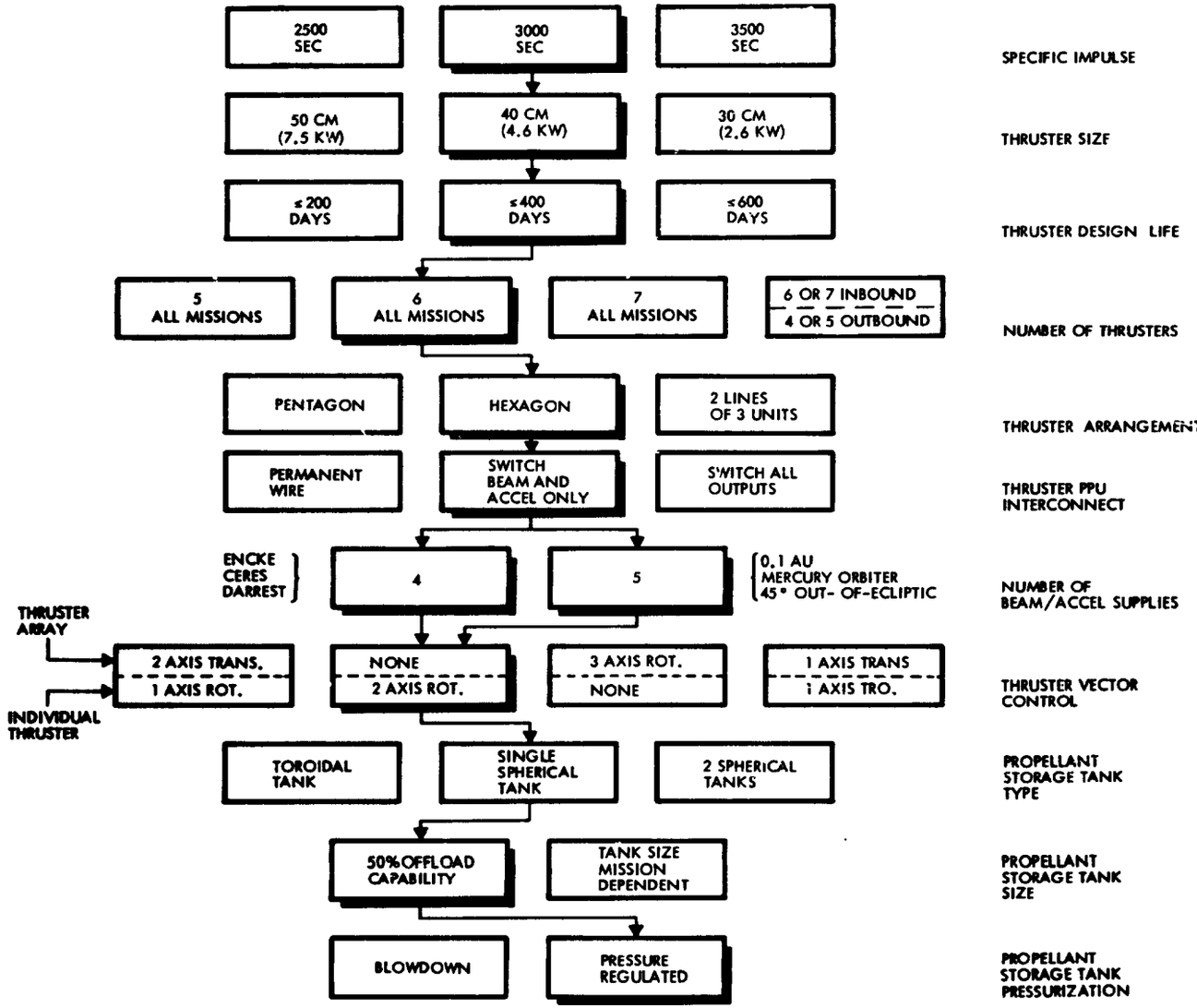

Figure 7-9. Key Electric Thruster Subsystem Options

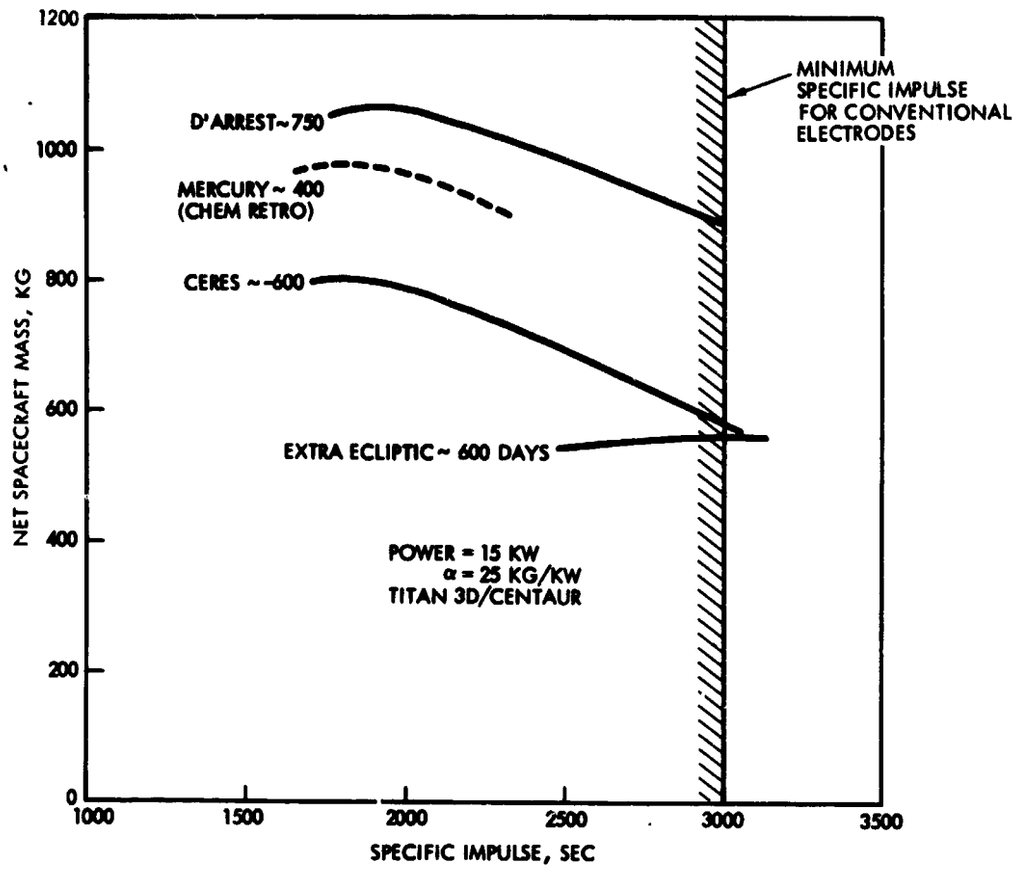

Figure 7-10. Net Spacecraft Mass Variation with Specific Impulse

Thruster Power Level, Size, Number and Design Life

Based on the results of mission and system analysis, the solar array must supply a minimum power at 14.5 kw to the propulsion module at 1 AU. Allowing a nine percent power loss in the power processing equipment, as specified by study guidelines, the input power to the thruster array is 13.7 kw at 1 AU, but reaches a maximum level of 18.2 kw at solar distances below 0.65 AU and a minimum level of 1.7 kw at 3.5 AU.

A variety of different thruster modules were examined to establish the size and power level most suited to the stage application. A summary of the characteristics for these devices is presented in Table 7-4. The first column lists the thruster input peak power levels that correspond to integral numbers of active thrusters for the power ranges of interest.

Table 7-4. Summary of Assumed Characteristics of Thruster Module Options*

Peak Input Power (kw)	Nominal Diameter (cm)	Active Units at 0.6 AU (18.2 kw)	Active Units at 1 AU (13.2 kw)	Active Units at 3.5 AU (1.7 kw)	Ion Beam Current (amps)	Ion Beam Current Switch (ma/cm)
6.6	50	3	2	1	4.65	2.36
4.5	40	4	3	1	3.15	2.52
4.5	30	4	3	1	3.15	4.4
2.6	30	7	5	1	1.83	2.6

*(I_{sp} = 3000 sec and net accelerating potential = 1100 volts)

The large variation of thruster input power that occurs in most of the specified missions requires a combination of thruster throttling and switching operations. For example, in a period of diminishing thrust power the thruster beam power of each thruster is reduced until a smaller number of thrusters, operating at peak power capacity, can handle the remaining input power. At this time one thruster is shut off and the remaining thrusters continue in operation, at peak beam power. Further reduction in available power requires another throttling cycle until the next thrusters is turned off, a.s.f. Figure 7-11 shows the minimum throttling requirements of the specified missions for the different thruster power levels obtained previously.

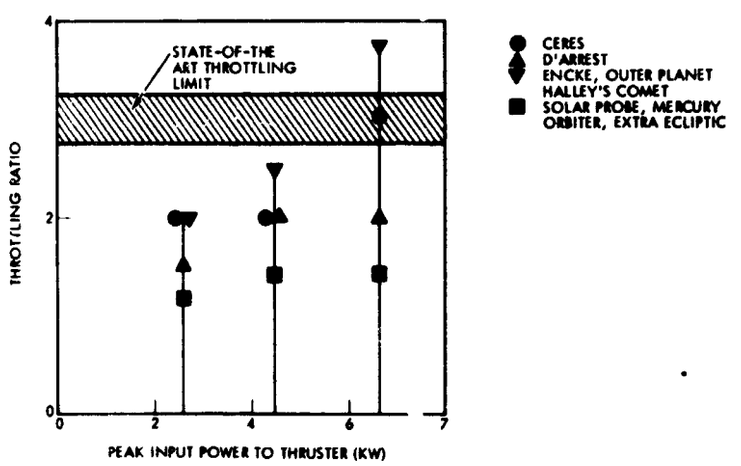

Figure 7-11. Minimum Throttling Level Requirements for Candidate Thruster Modules

We note that for a 6.6 kw thruster module a throttling range well above the present state of the art limits would be required. This thruster size is therefore eliminated from further consideration.

The minimum number of thrusters required to meet a propulsion module reliability of ≥0.95 with a maximum unit burn time not exceeding 400 days is presented in Figure 7-12. We note that in the most demanding missions six 4.5 kw thrusters or eleven 2.6 kw thrusters would be required.

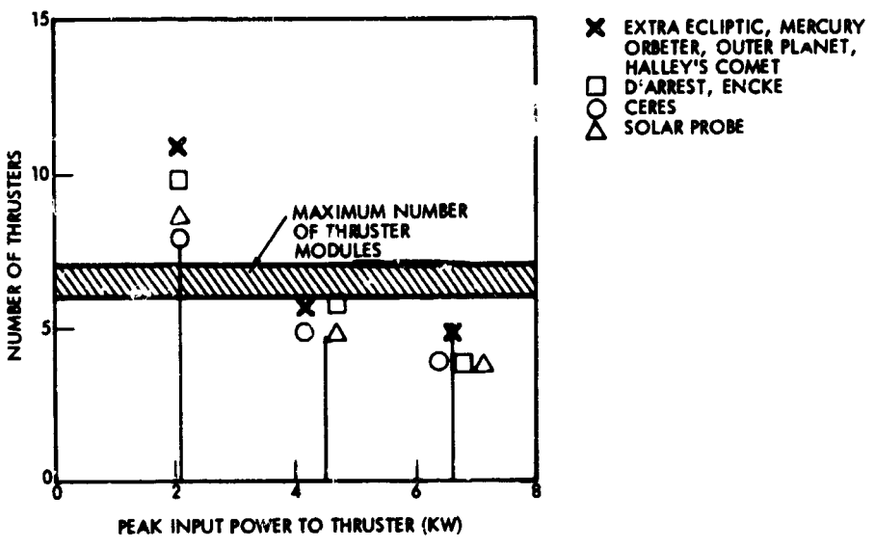

Figure 7-12. Thrusters Required for 0.95 Propulsion Module Reliability and Maximal Thruster Unit Burn of 400 Days

The 4.5 kw thruster module was selected instead of the 2.6 kw module for the following reasons.

- Cost. The recurring cost for eleven 2.6-kw thrusters would be about twice as much as for six 4.5-kw thrusters.
- Mass. The 4.5-kw thruster significantly reduces propulsion module mass since the specific mass of the thrusters and power processors is smaller at the higher power levels. In addition, the thruster array size becomes smaller and requires fewer mounting brackets and caging mechanisms.
- Thrust Vector Control. With increased thruster array dimension the gimballed thrust vector

control technique adopted for the stage is subject to much larger mass and performance penalties.

For the selected thruster module power level of 4.5 kw there are two size options, i.e., 30 or 40 cm, as indicated by Table 7-4. In each case it will be necessary to scale up the current level of an existing 30 cm thruster prototype from 2.0 to 3.2 amps. This can be done either by increasing the diameter to 40 cm while holding the current density at or below the present value of 2.8 ma/cm^2, or by increasing the current density in the existing design to about 4.5 ma/cm^2. While both approaches appear feasible it is not clear at the present time which one should be persued. The 40 cm module was selected for preliminary design purposes.

Propulsion module reliability in the primary missions as a function of thruster design life and number of thrusters is presented in Figures 7-13 (a) through 7-13 (f) for the selected 4.5 kw thruster peak power rating. Underlying the derivation of these curves is the model for thruster failure rate as a function of burn time which is illustrated in Figure 7-13 (g) for a 13,500 hour design life. The design life is defined as that burn time at which the probability of thruster failure due to burnout is 50 percent. The principal conclusion to be drawn from these figures is that for a design life of 400 days six thrusters are needed to meet the desired reliability goal of 0.95 in the most demanding missions considered, viz, the extra-ecliptic and Mercury orbiter missions. Four of these thrusters are initially active and two are spares.

It should be noted in Figure 7-13 (f) if more than two thrusters fail, the mission time can be extended beyond the nominal 700-day value at reduced thrust level and still achieve its objective.

Other missions such as Ceres rendezvous or the solar probe require only five thrusters for acceptable reliability. To eliminate modifications of the thruster arrangement from mission to mission, we preferred to use the same configuration of six thrusters for all missions thus carrying more than the minimum number of thrusters than required in some cases.

If the thruster design life were increased to 600 days, it would be possible to meet the reliability requirements for all missions with only five thrusters. However, the mass saved by eliminating one thruster (about 15 kg) does not warrant the additional testing and development costs

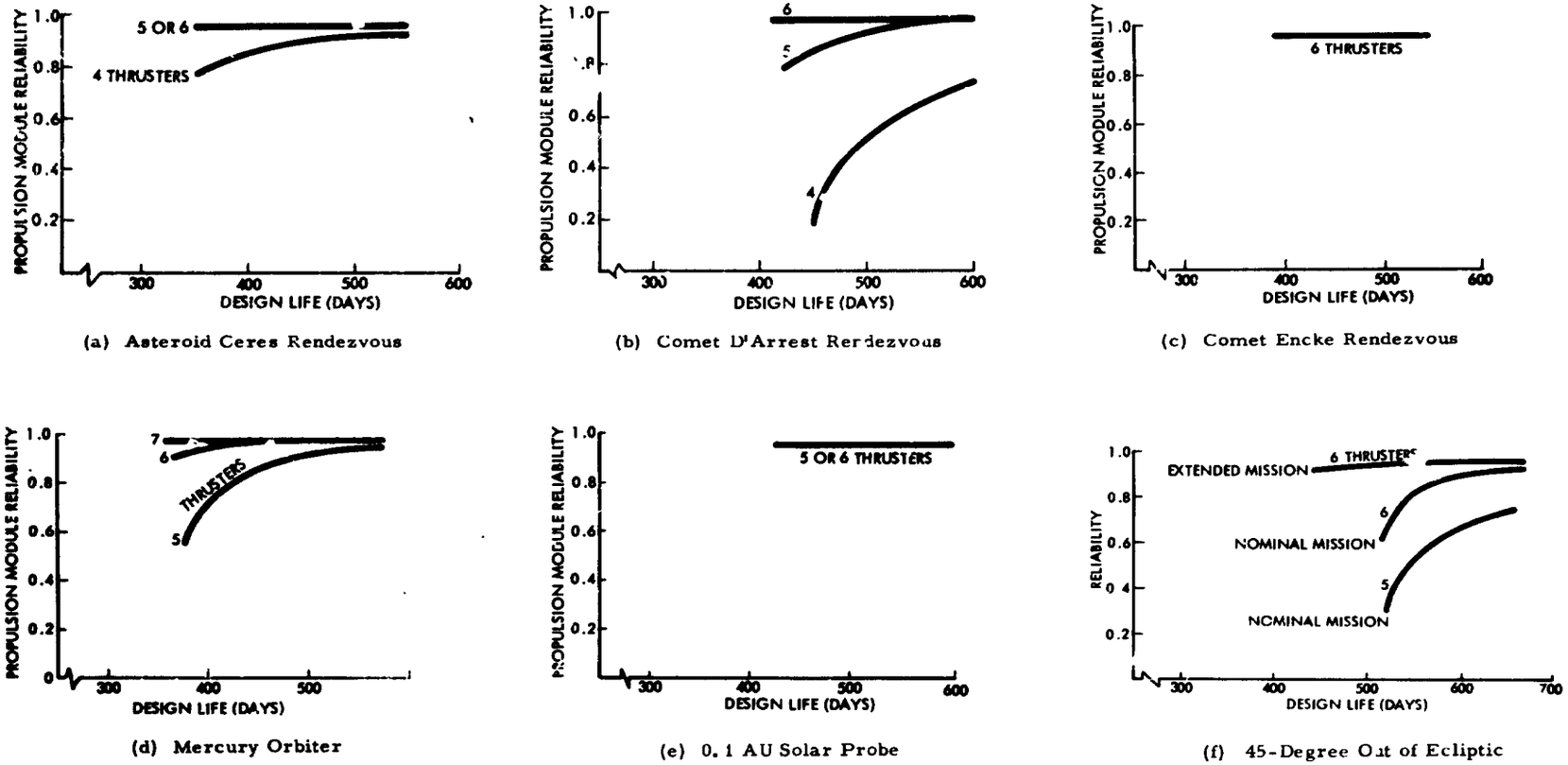

(a) Asteroid Ceres Rendezvous

(b) Comet D'Arrest Rendezvous

(c) Comet Encke Rendezvous

(d) Mercury Orbiter

(e) 0.1 AU Solar Probe

(f) 45-Degree Out of Ecliptic

Figure 7-13. Propulsion Module Reliability as a Function of Thruster Design Life (Thruster Peak Power 4.5 kw)

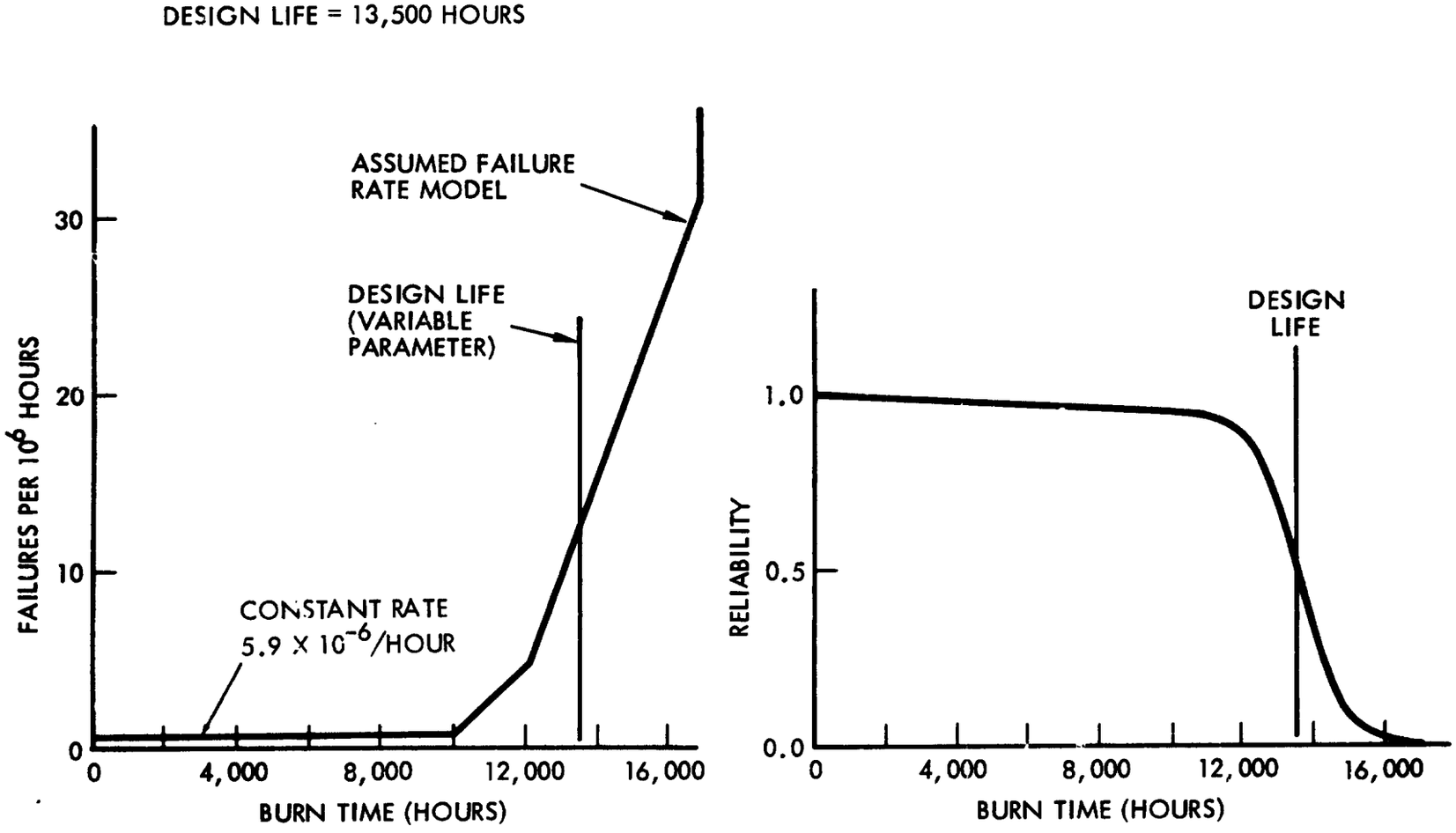

Figure 7-13 (g). Propulsion Module Reliability as a Function of Thruster Design Life (Thruster Peak Power 4.5 kw) (Continued)

associated with achieving and demonstrating the 600-day thruster lifetime, particularly since present thruster component design experience is limited to 400 days in most cases.

Thruster Arrangement

Three different thruster array configurations were initially considered:

- Five thrusters arranged in a pentagon with a sixth thruster in the center, and
- Two parallel arrays of three thrusters
- Hexagonal array

We rejected the first configuration since the centrally located thruster might reach inadmissibly high operating temperatures due to radiation blockage by the thrusters grouped around it and since it was felt desirable to mount hydrazine thrusters in the center of the array. We also rejected the second configuration because of asymmetry in pitch axis control that complicates the TVC electronics.

By selecting the hexagonal configuration we minimize thermal control problems due to radiation blockage, obtain greater symmetry in pitch axis control under various combinations of active thrusters, and provide the desired central mounting area for hydrazine thrusters. The gimballed TVC arrangement of the ion thrusters thus also provides convenient thrust vectoring for the hydrazine propulsion system.

Power Processing

Three different approaches for interconnecting the power processors and thrusters were evaluated. These approaches are illustrated in Figure 7-14. In Options A and B each power processing unit (PPU) is an integral system that provides all thruster power processing and control functions. In Option C the power processing units are subdivided into two separate modules with a distribution of output functions as shown in Figure 7-15.

This block diagram is representative of a power processor concept utilizing an SCR series inverter circuit approach. Such an approach conventionally meets the high modular power levels, 5-kw, moderate input voltage range, 180-400 volts, and power subsystem interface requirements

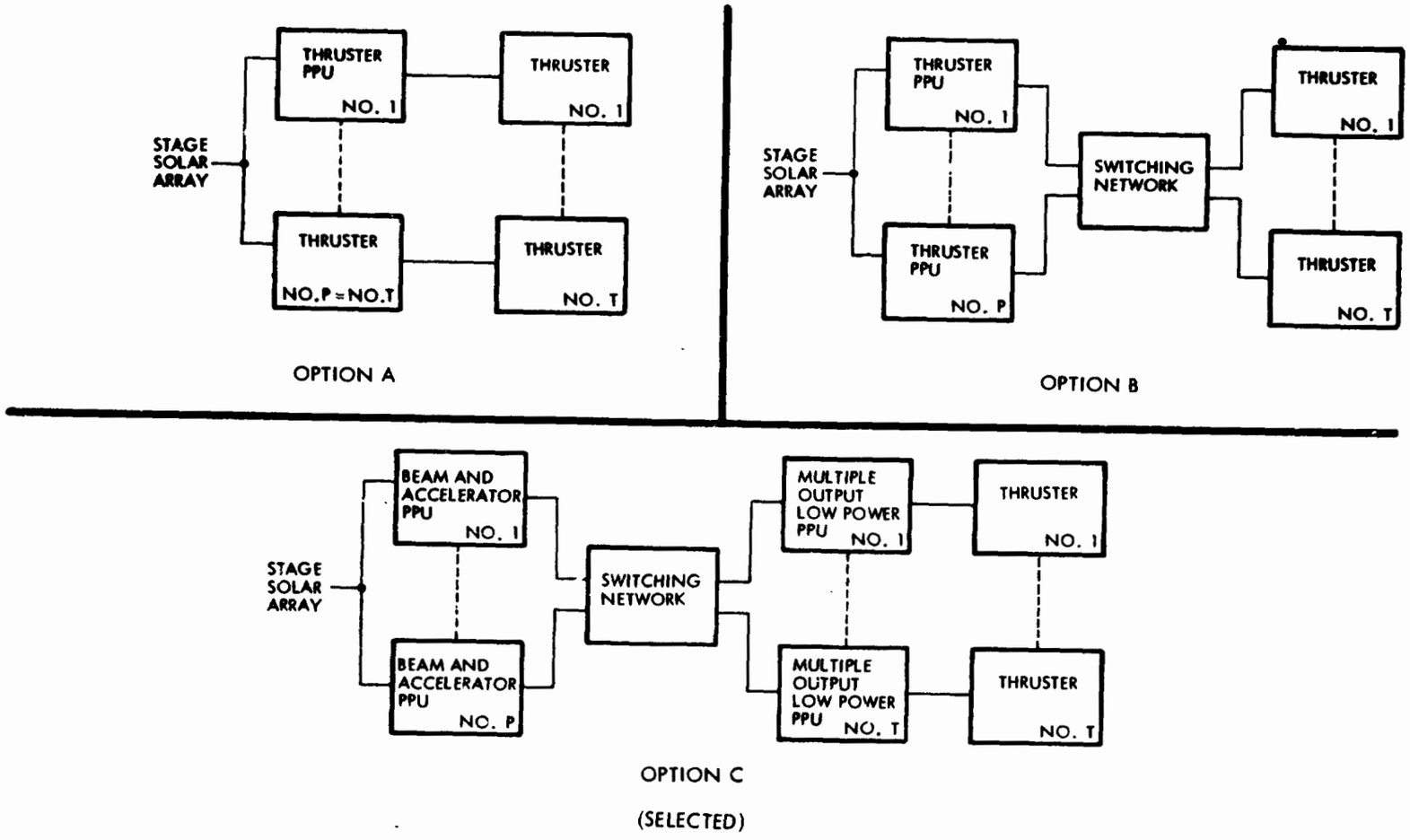

Figure 7-14. Power Processing Unit Design and Switching Options

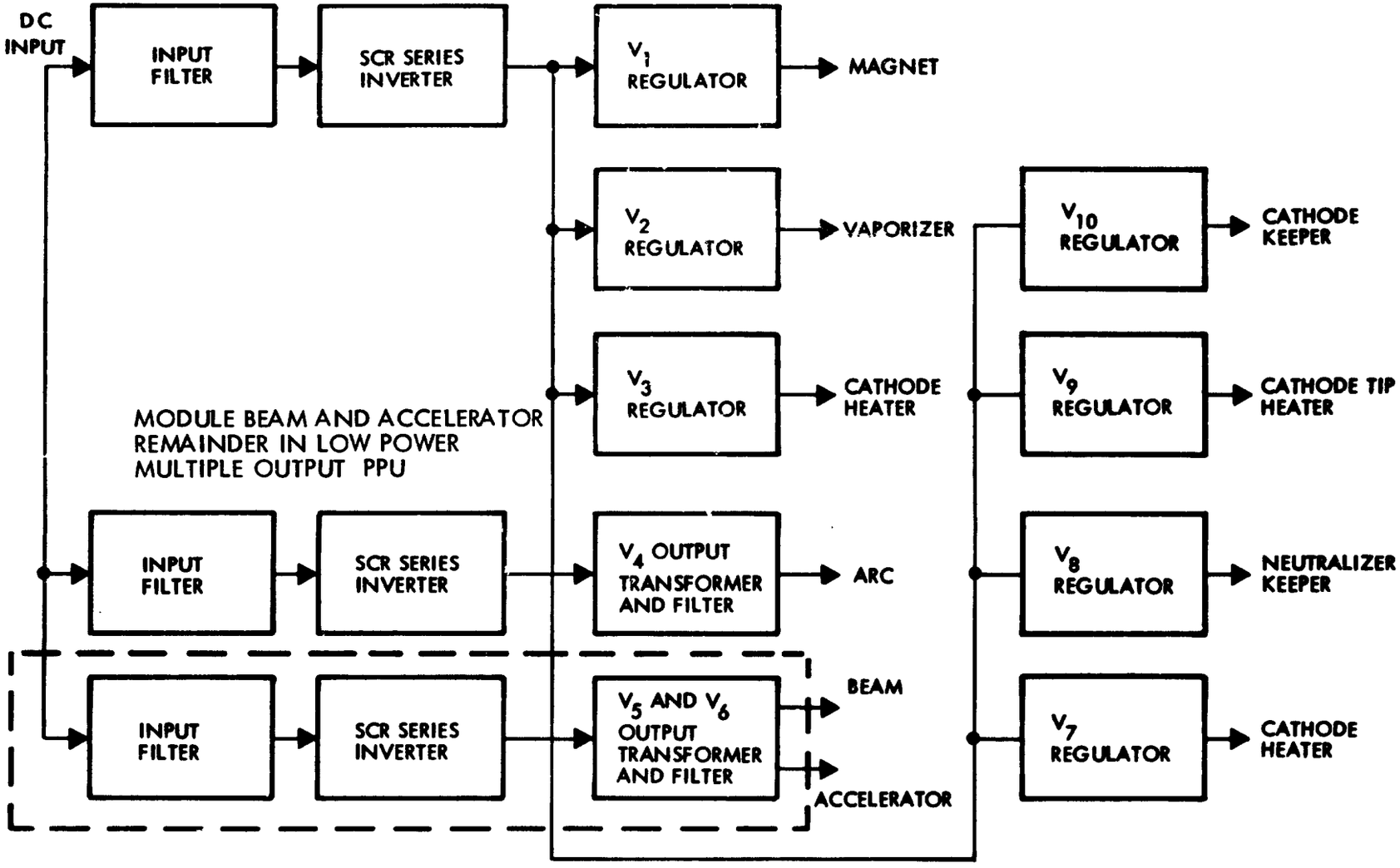

Figure 7-15. Power Processing Unit Block Diagram

outlined previously (Section 7.1.4). An alternate approach which is at a higher state of development incorporates a transistorized modular parallel inverter (Reference 7-12). For the purposes of developing a preliminary stage design in this study, the SCR approach was selected.

In the SCR circuit approach a power stage SCR series inverter converts the dc solar array voltage to an ac signal for the various regulated circuits. This unit inverts 42 watts of power. An SCR power stage and regulator is used to regulate and invert the input power to the arc supply. It is also used to provide protection for the spacecraft bus from engine faults. This circuit processes about 1000 watts of power. The second SCR power stage ac regulator regulates and inverts the 3.5 kw of power required for the thruster beam and accelerator. It also provides isolation for the solar array bus from thruster fault conditions.

The series inverter consists of an LC tank circuit placed in series with an SCR power switch and load transformer. The power capacity of this power stage can be as high as 10 kw. As a result it is not necessary to utilize modular units. The function of the LC elements is to make the circuit a current source and to self commutate the SCR's off. A current source circuit is highly desirable for ion engine applications where load impedance can go from normal to almost zero in less than a microsecond. Such a circuit is virtually immune to such transients because as the output impedance drops, the LC elements automatically limit the current in this condition and thus assure that semiconductor elements are not overstressed. In addition, these LC elements act to isolate the spacecraft bus from current surges during a thruster short.

Another feature of interest for this circuit relates to the fact that it has a current shaping network that produces sine wave currents. As a result, during switching when the peak voltage is across the SCR, there is no current. Therefore, there are no-power surges in the SCR during switching. If present, such power surges can lead to long-term switch reliability problems. Finally, the SCR device is capable of operation at power levels as high as 5 to 10 kw with single elements. As a result this design has the desired growth potential for future missions.

In Option A the integral power processing units are directly wired to each thruster, thus a separate power processing unit is required for

each thruster. However, for the specified primary missions, it was found that fewer redundant power processors are needed than thrusters to achieve an acceptable system reliability, e.g., four or five PPU's could be used with six thrusters if a switching network is used to interconnect active PPU's and thrusters. Since the PPU mass is 23 kg there is the potential of a significant mass reduction through PPU switching, except in Option A where the PPU's are permanently wired to the thrusters.

In Option B the switching required to connect operating PPU's and thrusters would be carried out by a complex 14 pole - 7 throw switching network rated for 1100 volt and 30 amp operation. Such devices are not within the present state of the art.

The selected approach, Option C, avoids the disadvantages of Options A and B while providing a practical and weight saving interconnect capability. In this approach only the multiple output PPU modules which contain the bulk of the complex thruster control circuitry are directly wired to each thruster. This PPU module has a lower mass (about 8 kg) and higher projected failure rate (2.9×10^{-6}/hour) than the other module. To carry six of these units, although no more than four are required on any mission, does not entail a large weight penalty but simplifies the design. The beam and accelerator PPU modules which have about twice the mass (15 kg) and a lower failure rate (7×10^{-7}/hour) are connected to active thrusters through a simplified switching network (two pole/seven throw switches rated at 1100 volts and 3 amps). All switching operations are performed with the thrusters off.

Owing to the relatively low-failure rate of the beam and accelerator modules, four units are sufficient for the inbound, and five units for the outbound missions to meet the propulsion subsystem reliability goal of ≥ 0.95. Allowing a mass of 4 kg for the switching network, Option C offers a mass saving of 26 kg for outbound missions and 11 kg for inbound missions over Option A.

Thrust Vector Control

Three different mechanical techniques for thrust vector control were evaluated. They are shown in a schematic diagram, Figure 7-16, along with a summary of projected characteristics. Electrostatic

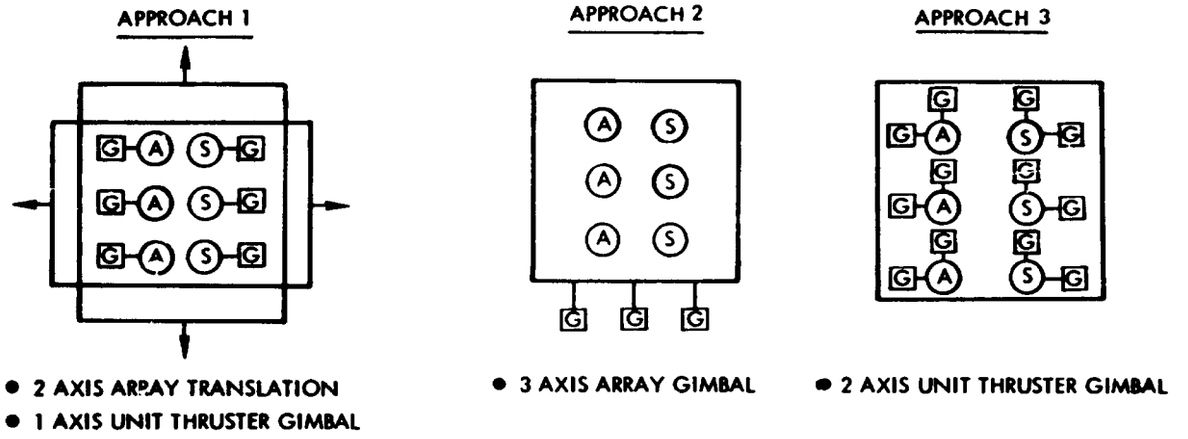

APPROACH	STATE OF DEVELOPMENT	TYPICAL MECH. MOTION	CANT ANGLE	REL. FOR CERES MISSION	NUMBER OF ACTUATORS	SWITCHABLE CHANNELS	ESTIMATED MASS INCLUDING CANT LOSSES
1	PROTOTYPE	1 M	NONE	0.975	8	3	56 KG
2	DESIGN	0.10 M	9°	0.970	3	0	36 KG
3	PROTOTYPE	0.05 M	9°	0.999	12	6	45 KG

Figure 7-16. TVC Alternatives

vectoring or the ion beam was not considered since it is in the research stage.

In Approach 1 corrective torques about the yaw and roll axes are provided by translating the entire thruster array parallel to the roll and yaw axes. Pitch control is obtained by differential gimballing of thruster pairs. Since the thrusters do not point through the stage nominal center of mass, translation of the array over distances as large as ± 0.5 meters is necessary to eliminate major perturbation torques when engines are switched on or off in asymmetrical combination.

Approach 2 uses gimbal control of the thruster array about the roll and yaw axes of the vehicle. Pitch control is obtained by twisting the thruster array about the pitch axis. All thrusters are canted outward by a small dihedral angle (nominally nine degrees) so as to point through the nominal center of mass the stage. This eliminates unbalance torques due to switching thrusters on or off in asymmetrical configuration.

In Approach 3 each thruster is separately gimballed about two axes. Yaw and roll control is obtained by vectoring thrusters separately. Pitch control is obtained by differential gimballing. As in Approach 2 the thruster axes are canted to pass through the nominal stage center of mass.

The use of a small cant angle in Approach 2 and 3 is made feasible by the large separation between the thruster array and the vehicle center of mass. A cant angle of nine degrees causes a penalty of 1.2 percent in the effective utilization of installed power, propulsion hardware and propellant. Additional gimbal deflections for TVC do not cause an appreciable increment in the mass penalty. However, the thrust offset due to TVC gimballing and/or engine switching must be compensated by an equal and opposite body angle offset to avoid an undesirable effect on guidance. This compensation is achieved by inserting a corrective decoupling signal obtained from the TVC actuator pickoffs into the attitude control circuit. The mass penalty and control circuit complication introduced by the gimballed TVC approaches is outweighed by the design simplification and mass savings of the system itself. The estimated weight penalty of Approach 1 is 20 kg compared to Approach 2 and 11 kg compared to Approach 3.

Approach 3 is much more reliable than Approaches 1 and 2 because it has no in-line elements whose failure can result in the failure of the entire TVC system and hence the mission. In Approach 1 or 2, if either thruster array actuator fails, the stage will cease to function, while in Approach 3 if a gimbal actuator fails, it will only result in the loss of one thruster.

At the present time it is not clear which TVC approach is optimal. A final selection can only be made after more detailed analyses have been performed. Perhaps at that time more data will be available on electrostatic TVC techniques currently under study. For the purposes of developing a preliminary stage design concept in this study the attractively simple design Approach 2 was selected.

Propellant Storage Tank

Solar array rotation is available to the stage on all missions, as discussed in Section 6.2, to reduce the solar pressure torques that can occur during intermittent coast periods when the center of mass and center of pressure do not coincide. Thus a single spherical propellant tank located near the stage center of mass is acceptable eventhough depletion of propellant can lead to a shift in the center of mass by as much as 0.5 m during flight.

To eliminate the use of different propellant tank sizes for each mission the propellant tank was sized for the maximum load of any of the primary missions (1015 kg for extra-ecliptic) and off-loaded in other missions. For the range of missions of interest, off-loading of roughly 50 percent is required. Under off-loaded conditions the propellant bladder must be protected from tearing during launch. One promising technique requiring further development is to use moldable material such as styrofoam to fill the unused tank volume.

A pressure regulated rather than a blowdown system was selected for two reasons: in a blowdown system the pressure drop towards the end of the mission may be so large as to cause oscillations in the liquid mercury feed line. These oscillations can arise due to back pressure created by mercury vapor. By use of a constant pressure system a fixed pressure margin is always available to prevent feed line oscillations.

Another advantage of the pressure regulated system is better use of available propellant tank volume since the propellant can fill almost the entire tank. In the blowdown system the required tank volume may be three to four times larger than the propellant volume. Thus for the large quantity of mercury that must be stored (up to 1015 kg) a blowdown system would require relatively large tank sizes and introduce an appreciable mass penalty.

7.2.3 Propulsion Subsystem Description

The electric propulsion module shown in perspective view in Figure 7-17 and as a block diagram in Figure 7-18 houses the ion engines, power processors, tankage and feed system in a standardized configuration that requires little or no modification from mission to mission. The self-contained propulsion module can be readily removed from the remaining stage structure for simple assembly and to permit independent test of the electric thrusters and power processors in the vacuum tank. This reduces program costs and simplifies facilities scheduling.

The total propulsive power, nominally 15 kw (14.5 kw in the Ceres rendezvous mission) at earth departure, is used for thrust periods of varying duration in different missions ranging from 400 days (solar probe) to 900 days (Encke rendezvous) in the specified primary missions. Some of the alternate and growth missions demand even longer thrust periods (e.g., 1400 days for Uranus flyby).

Unregulated electric power supplied by the solar array is conditioned by the power processing units to operate and control the ion thrusters. The propellant tank is dimensioned for the largest propellant load required in any of the primary missions, vis. 1050 kg, for the extra-ecliptic probe.

The dimensions of the propulsion module, (3.12 meters long by 1.85 meters wide by 1.04 meters deep as shown in Figure 7-17) are dictated primarily by the panel area of the power processor units that must radiate a total of 1.8 kw of dissipated heat based on a 91 percent PPU efficiency factor specified by NASA. This maximum is reached during inbound missions when solar distance decreases below 0.65 AU

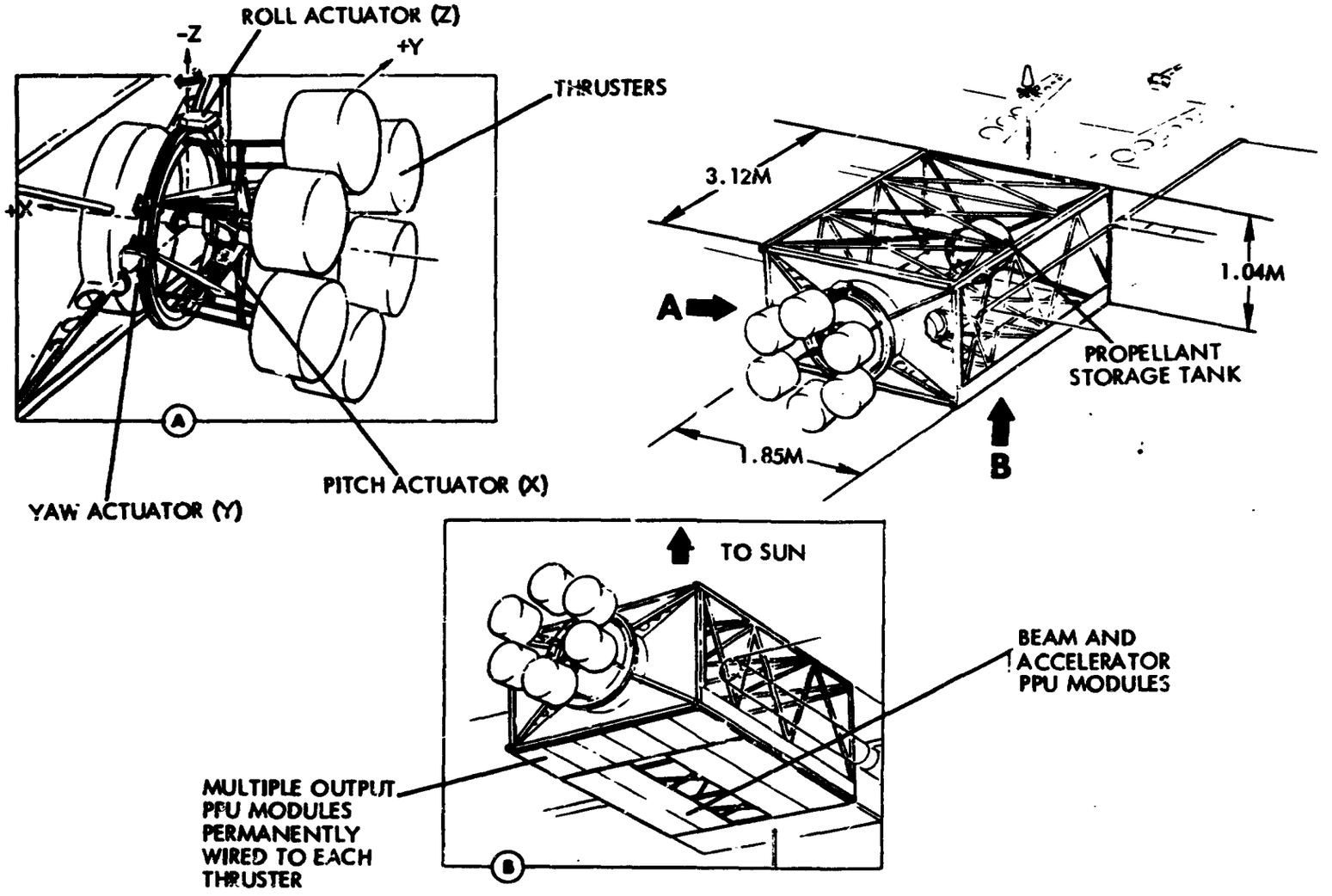

Figure 7-17. Electric Propulsion Module

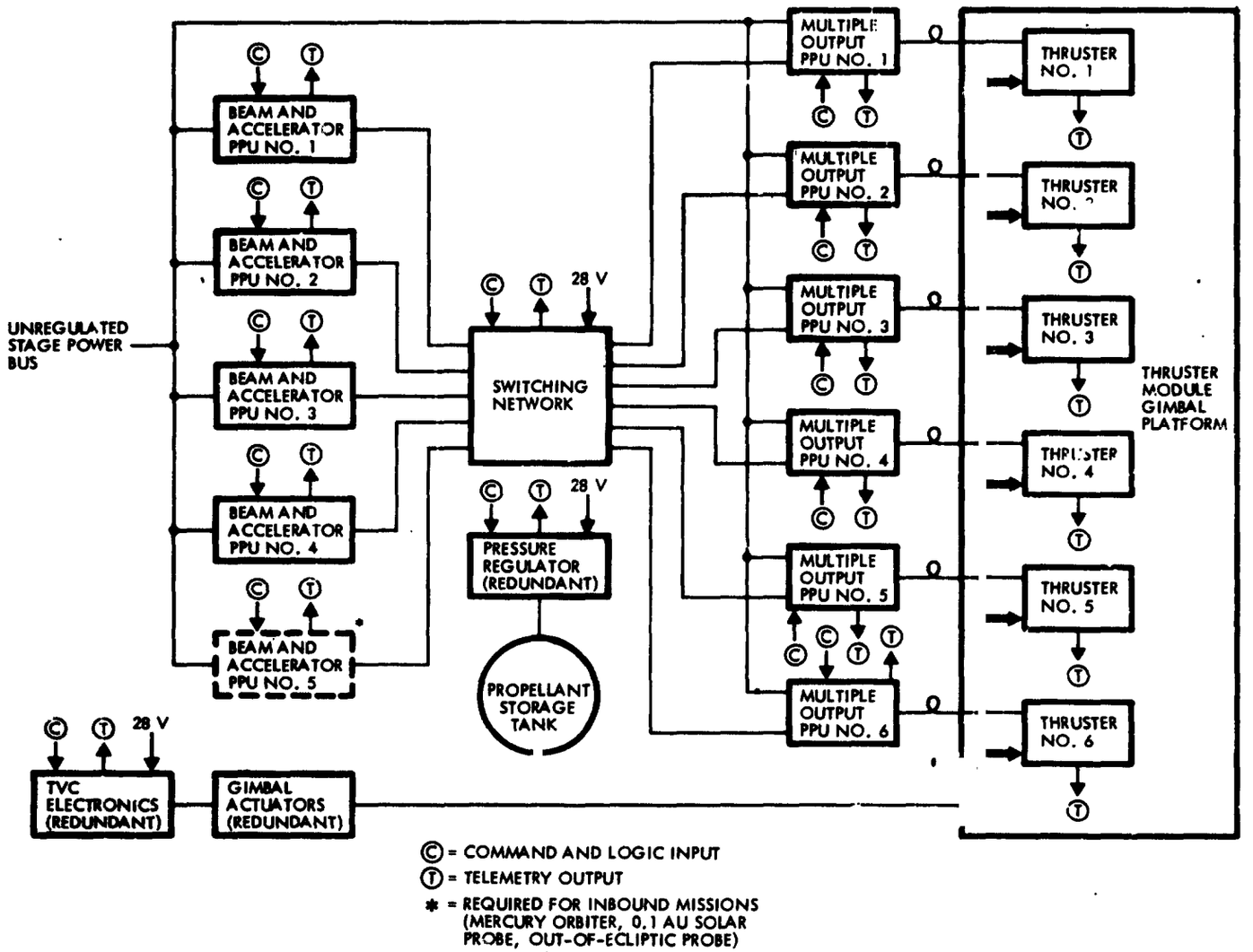

Figure 7-18. Block Diagram – Electric Propulsion Module

All of this heat must be radiated from the rear area of the propulsion module where the power processor panels are mounted. Side-mounted panels would be subject to radiation blockage by the rotatable solar array.

The thrusters are mounted in a hexagonal array on a three-axis gimbal structure which provides the desired thrust vector control functions. The gimbals use flexure pivots to eliminate friction and wear and are driven by three actuators with anti-backlash gearing based on a design developed by JPL for electric propulsion TVC of a different type. The advantage of the all-gimballed TVC concept adopted in this configuration is the relative simplicity, lightweight and absence of conventional bearings. The use of the simple flexure joints is predicated on the small gimbal excursions required in this application. A caging mechanism, not shown in the detail stage design drawings, is required to support the 15-kg thrusters during launch. Our preferred design concept consists of a scissors linkage and holding brackets that grip and support a pair of thrusters during launch and are subsequently released by spring action. Three of these simple and lightweight retention mechanisms are used to support the six thrusters.

The small amount of TVC deflection of the gimballed thruster package simplifies the connection of flexible power cables and propellant feed lines to the thrusters. A coiled arrangement supported in the center of the assembly permits deflection of the cables and feed line by ± 10 degree without an appreciable reaction torque.

Gimbal actuator Z shown in the drawing provides roll control by a ± 10 degree gimbal deflection around the Z-axis; actuator Y provides yaw control by a similar deflection around the Y-axis; and actuator X deflects the thruster through a twisting action around the X-axis for pitch control. These deflections are required to correct for variation of the center of mass, due for example to solar array deformation, thrust vector errors in individual thrusters and to counteract solar pressure unbalance torques.

Each thruster is rated for a nominal input power level of 4.5 kw, a specific impulse of 3000 seconds, and a thrust level of 48 millipounds.

For the selected thruster power level six thrusters are needed to meet desired reliability goals (i.e., a propulsion module reliability of at least 95 percent and burn time on each thruster not exceeding 400 days) in the most demanding missions considered, viz. the 45-degree extra-ecliptic and Mercury orbiter missions. Other missions such as the Ceres rendezvous or the 0.1 AU solar probe require only five engines for acceptable reliability. In order to eliminate modifications of the thruster arrangement from mission to mission we preferred to use the same configuration of six thrusters in all missions thus carrying more than the minimum number of spare thrusters required in some cases.

The electric propulsion power processors supply 12 different regulated outputs required for thruster operation. In addition these units control thruster operation, implement commands from the CC&S, correct for thruster failures and adapt the operating point of the thrusters for maximum solar array power utilization at any time in the mission.

To maximize reliability and minimize mass and volume, the power processing units were separated into two modular segments as indicated in the schematic diagram in Figure 7-18, for the purpose of achieving a higher system reliability at lower weight than would be possible for integral power processor modules. The multiple output PPU's which contain all of the control circuitry and low power heater, keeper, and arc supplies are directly wired to each thruster. Owing to the relatively low-failure rate of the beam and accelerator PPU modules, four units are sufficient for inbound and five units for outbound missions to meet the propulsion system reliability goals.

The spherical pressure-regulated propellant storage tank of 0.6 meters diameter is placed near the stage center of mass. This tank is sized to carry a maximum load of 1015 kg of mercury propellant. In missions which require less propellant the tank will be off-loaded. Thus a small weight penalty is accepted in exchange for cost savings by avoiding redesign.

Four support struts transfer the tank launch loads directly to the stage adapter mounting points thereby reducing stress in the main propulsion module structure and saving weight.

A summary of the electric propulsion subsystem characteristics is presented in Table 7-5.

7.2.4 Propulsion Subsystem Operation

The nominal thruster switching profiles for the six primary missions are presented in Figure 7-19 (a) through (f). A description of the sequence of events for the Ceres rendezvous mission, Figure 7-19 (a) is presented below to indicate the typical propulsion subsystem operation.

Component	Number	Mass		Unit Envelope	Peak Input Power (kw)	Comment
		Unit (kg)	Total (kg)			
Thrusters	6	11.0	66.0	45 cm diameter by 30 cm long cylinder	4.55	I_{sp} = 3000 sec
Beam and accelerator PPU	4*	14.8	57.2	35 x 170 x 10 cm	3.85	Four required for Ceres, D'Arrest, and Encke. Five required for 0.1 AU probe, Mercury orbiter and 45-degree extra-ecliptic
Multiple output PPU	6	8.0	48.0	30 x 70 x10 cm	1.15	Six required for all missions
Propellant storage and distribution	1	25.0	25.0	55 cm diameter sphere	0.005	Includes valves, ullage, feedlines, and pressure regulator
Switching network and associated electronics	4*	1.0	4.0	10 cm x 10 cm	0.010 (during switching only)	One required for each beam and accelerator supply. Switch with power off.
Cabling and connectors	1	4.0	4.0	Multiple output PPU's directly wired to thrusters. Beam and accelerator PPU's connected through switching network	--	Losses included in 91 percent PCU efficiency
Thrust vector control and thruster launch support mechanism	1	11.0	11.0	85 cm diameter by 25 cm deep	--	Holds six thrusters all movable joints are flexure pivots
TVC actuators	3	2.0	6.0	20 cm x 20 cm x 10 cm	--	JPL gimbal actuator with redundant drive motor
TVC electronics	1	3.0	3.0	20 cm x 20 cm x 10 cm	--	--
			224.2 kg			

*Four required for Ceres, D'Arrest, Encke. Five required for 45-degree extra-ecliptic, 0.1 AU Solar Probe and Mercury orbiter.

Table 7-5. Summary of Electric Propulsion System Characteristics

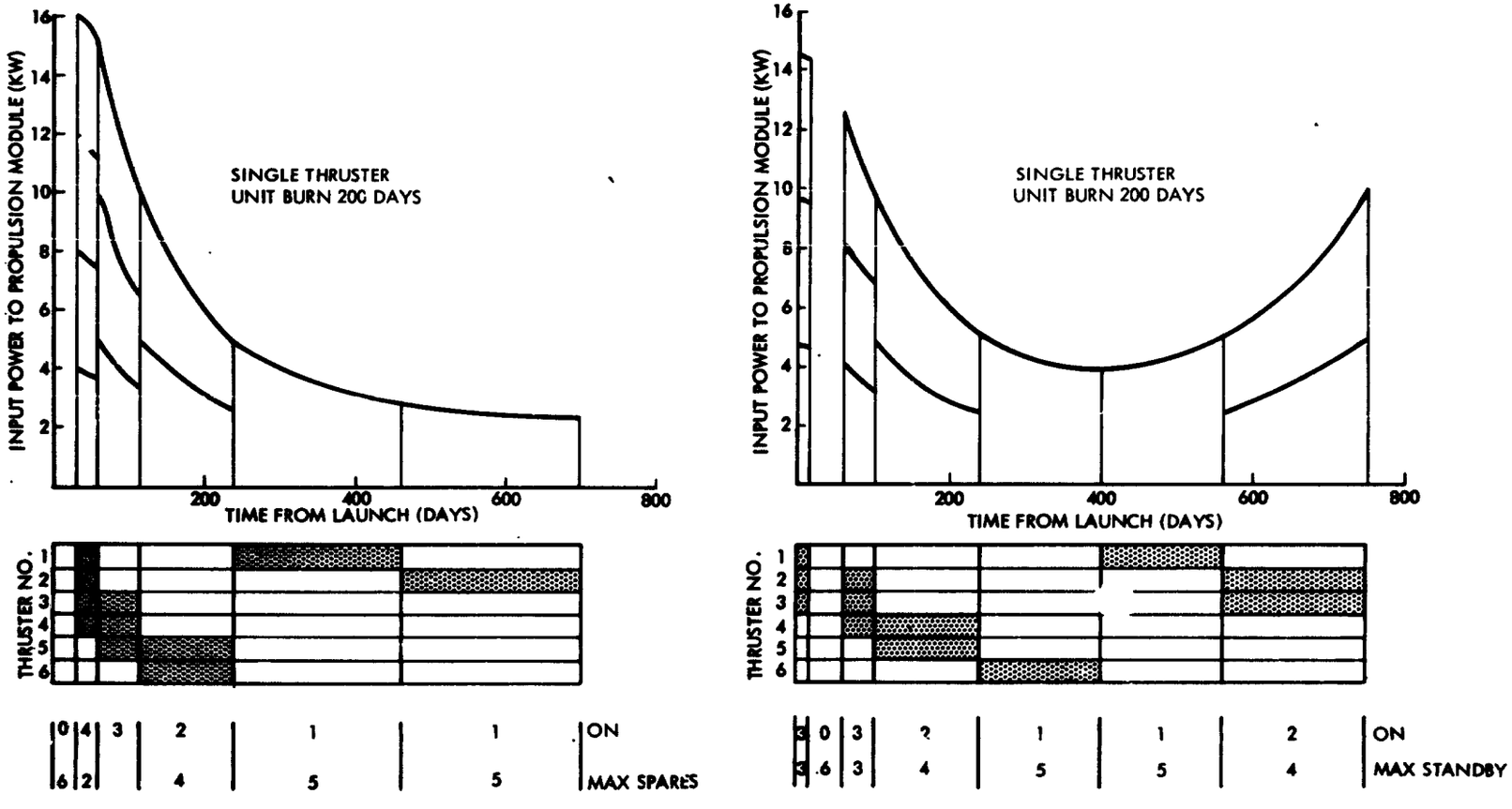

(a) Asteroid Ceres Rendezvous

(b) Comet D'Arrest Rendezvous

Figure 7-19. Thruster Switching Profiles

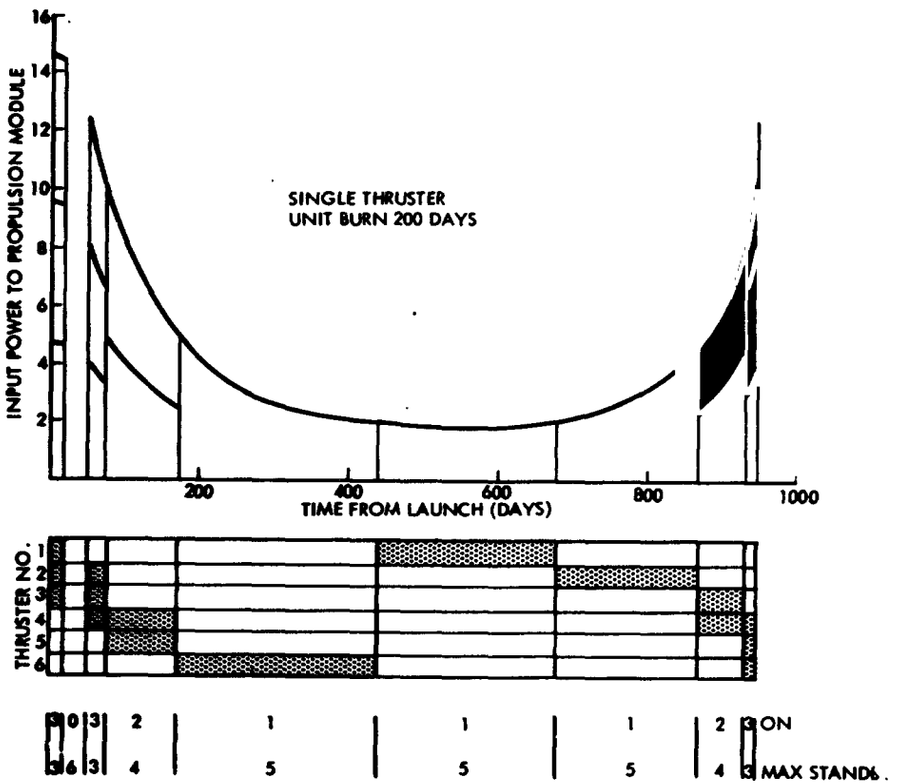

(c) Comet Encke Rendezvous

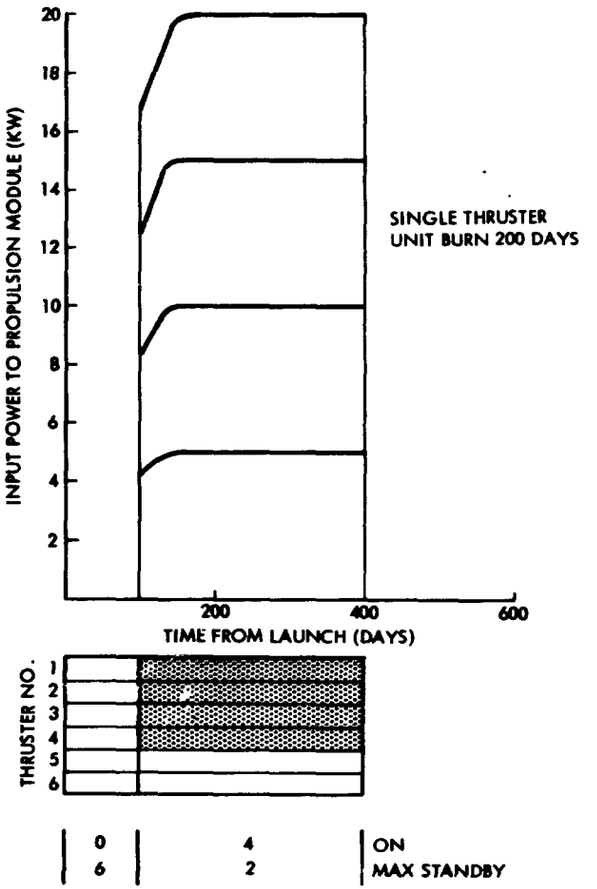

(d) Mercury Orbiter

Figure 7-19. Thruster Switching Profiles (Continued)

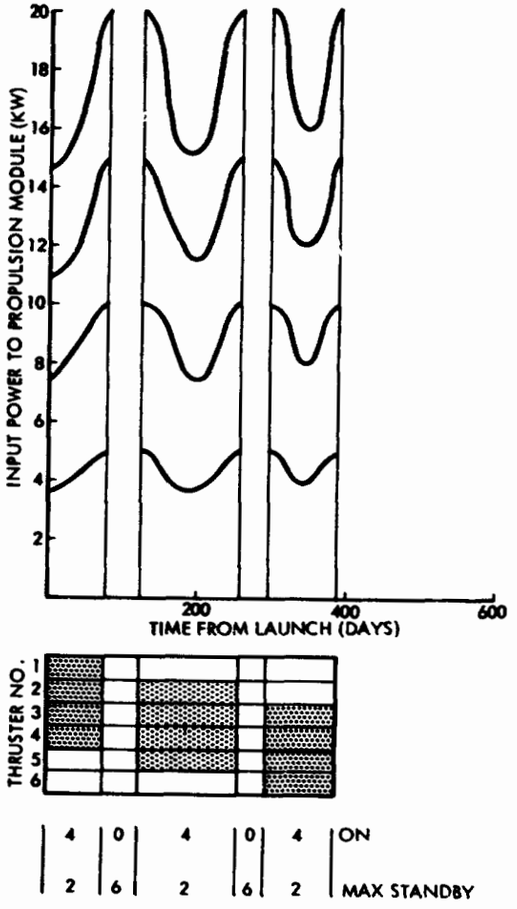

(e) 0.1 AU Solar Probe

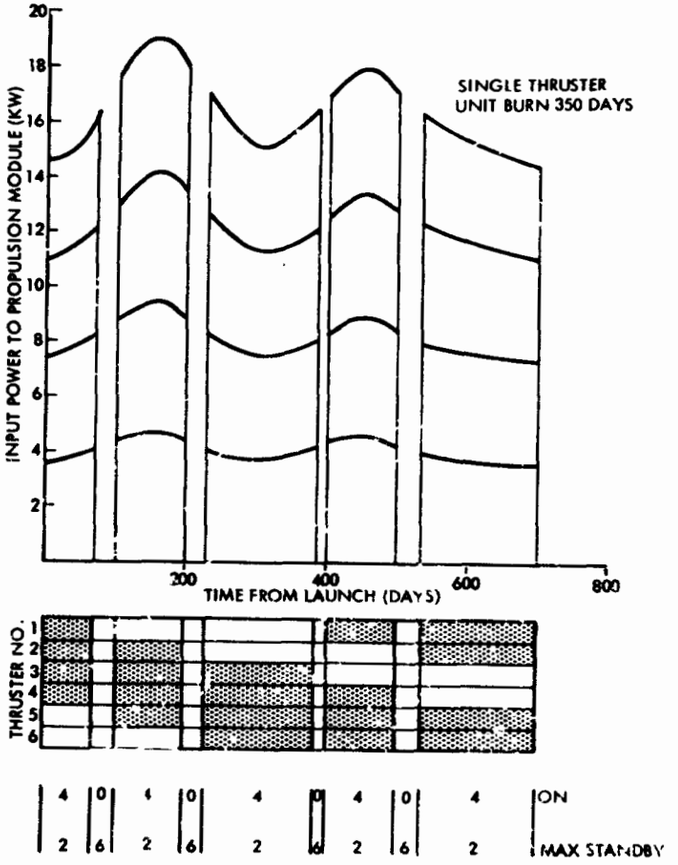

(f) 45-Degree Extra-Ecliptic Probe

Figure 7-19. Thruster Switching Profiles (Continued)

The propulsion subsystem is dormant during the first 30 days after launch while the stage coasts inbound to a perihelion distance of 0.92 AU. At this point 16 kw of power is available. Since each active thruster and power processor combination have a peak input power rating of 5 kw, four modules are initially required; each unit operating at an input power level of 4 kw.

As the mission further progresses the available power decreases and all thrusters are uniformly throttled down. Physically this means a reduction of propellant mass flow into each thruster and a corresponding reduction of the beam current. Seventy days after launch only 1.51 kw of input power is available per thruster. At this point one thruster can be shut off and the three remaining active thrusters return to their peak input power of 5 kw. The same process is repeated twice more until only enough power is left to operate a single thruster, 230 days from launch which is then used to complete the thrust phase.

At the start of each new propulsive phase the thrusters are rotated, as one might rotate the tires on a car, to minimize the probability of an early thruster failure.

For the mission profile illustrated in Figure 7-19 (a), the single thruster unit burn time is limited to 200 days even though the total thrust time of the mission is 619 days. This is accomplished by carrying two spare thrusters initially and proper rotation of active units.

The thruster switching sequence is similar for the five other mission profiles presented in Figure 7-19, the major difference between missions being the shape of the power-time history time. For example, on the comet missions the power first decreases as the stage travels out and then increases again as the stage returns toward rendezvous.

7.3 ATTITUDE CONTROL SUBSYSTEM

The attitude control subsystem (ACS) selected for the baseline stage configuration performs the following functions:

- Celestial reference acquisition after separation from the booster and reacquisition at any time during the operating life of the system.

- Three-axis stabilization of the vehicle attitude within ± 1 degree (about each axis) and thrust vector orientation by rotation of the spacecraft through maximum ranges of ± 90 degrees about the yaw and ±180 degrees about the roll axis.
- Attitude stabilization of the stage with ± 1.5 degree accuracy about each axis during the coasting phase.
- Antenna pointing at the earth with an accuracy of 0.5 degree.
- Experiment pointing with 0.5 degree accuracy by rotation of the spacecraft about the yaw axis with a maximum range of ± 90 degrees.
- Solar array rotation through a ± 90 degree range.
- Longitudinal ΔV propulsion for boost/deboost and orbital corrections.
- Computational support to the propulsion and power subsystems on a non-cyclic basis.

This section contains detailed descriptions of the conceptual baseline design providing the above listed capabilities, its modes of operation, interfaces with other subsystems, performance characteristics, and problem areas requiring further investigation.

7.3.1 Attitude Control Subsystem Description

The coordinate systems used in the following discussions for defining attitudes, equipment locations, and pointing directions are as shown in Figure 7-20.

The ground rules and assumptions made to arrive at the conceptual design presented are as follows:

- Essentially no design changes will be made, nor equipment modifications will be required to perform the primary missions.
- The design will be modular, providing growth capability by addition of equipment.
- The control subsystem will have minimum sensitivity to system parameter changes.
- Dynamics interactions between the array and the attitude control system will be minimized.

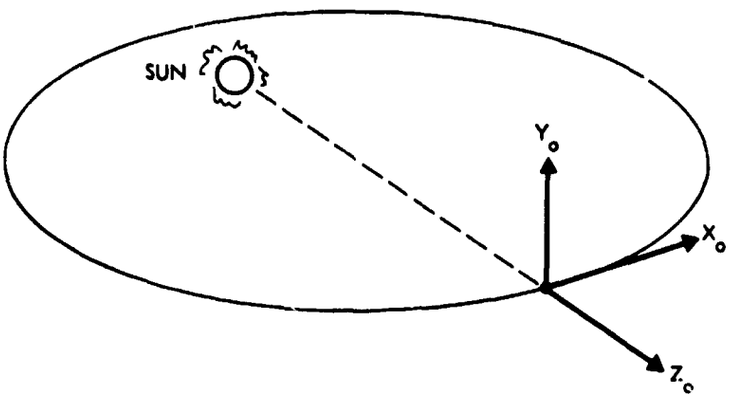

Orbital Reference Coordinates

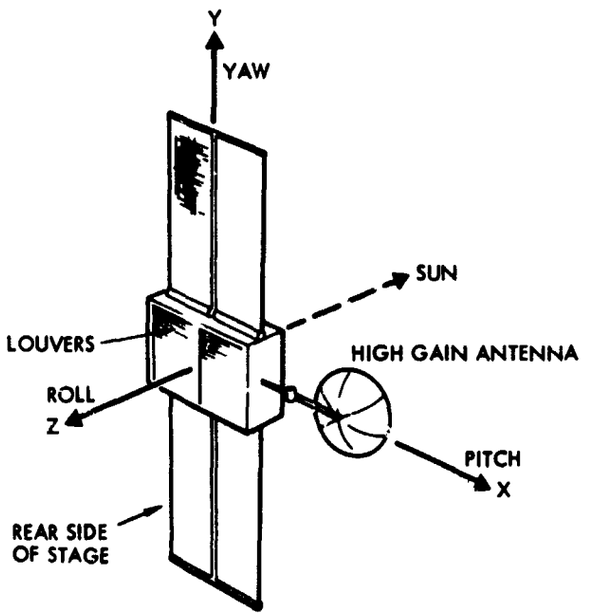

Stage Reference Coordinates

Figure 7-20. Attitude Control System Coordinates

7.3.1.1 Functional Description

The block diagram of Figure 21 (a) shows the main component assemblies of the ACS and their functional organization. The components and individual functions are delineated below. Of particular interest is

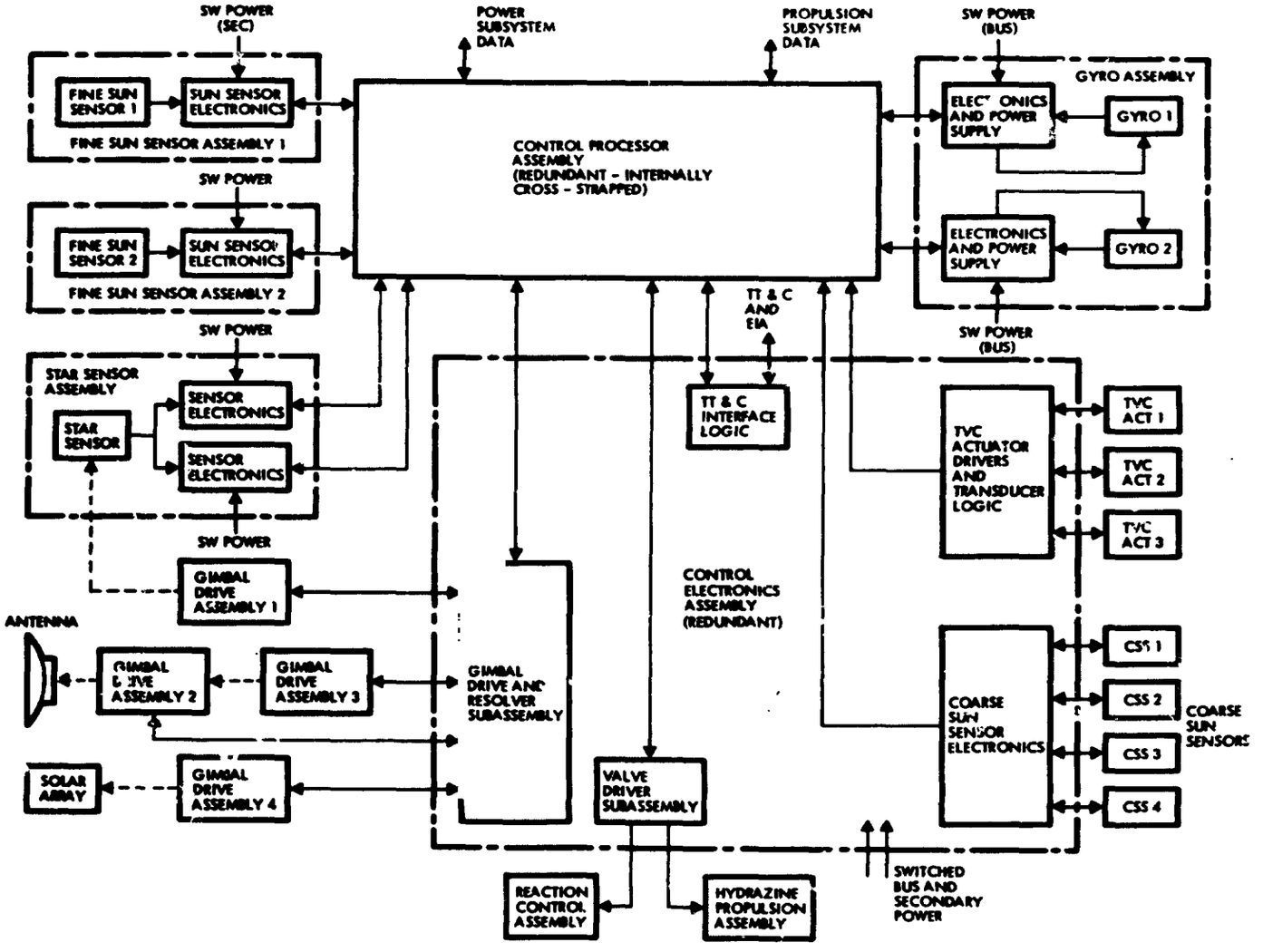

Figure 7-21 (a). Baseline Attitude Control Subsystem Block Diagram

the control electronics assembly (CEA) which integrates all subsystem functions of the ACS. A block diagram of the CEA is shown in Figure 7-21 (b).

Fine Sun Sensor Assemblies (2)

Each assembly consists of a biaxial fine sun sensor and the associated signal processing and AGC electronics. One sensor is mounted on the stage body and the other is located on the solar array support structure. The FOV about each axis is $\pm$ 10 degrees and the accuracy is $\pm$ 0.1 degree.

Coarse Sun Sensor Assemblies (4)

The four coarse sun sensors provide a combined FOV of 4π steradians for acquisition purposes.

Star Sensor Assembly

The star sensor assembly consists of an instrument of the Mariner Mars '69 type mounted on a single-axis mechanical rotational drive. The mechanical rotation range is $\pm$ 120 degrees in clock angle (about roll axis). The tracker field of view is electronically offset in discrete steps over a total range of about 35 degrees for each mission. The star tracker provides a roll attitude reference for gyro calibration by tracking selected stars as commanded by the Control Processor Assembly.

Gyro Assembly

This assembly consists of a redundant set of rate integrating gyros (operating in the caged mode) and the associated electronics. The unit is identical to the 2-pack used in the TRW Precision Pointing Control System. The gyro assembly provides rate information for acquisition and roll search (at a constant rate for star acquisition) and attitude data for normal-mode roll control.

Reaction Control Assembly

The reaction control assembly includes all the pneumatic equipment for attitude control propulsion such as nitrogen gas, tanks, regulators, solenoid valves, nozzles, lines, fittings and miscellaneous valves, and transducers. The main function of this assembly is the provision of control torques by mass expulsion in response to signals originating in the control processor assembly.

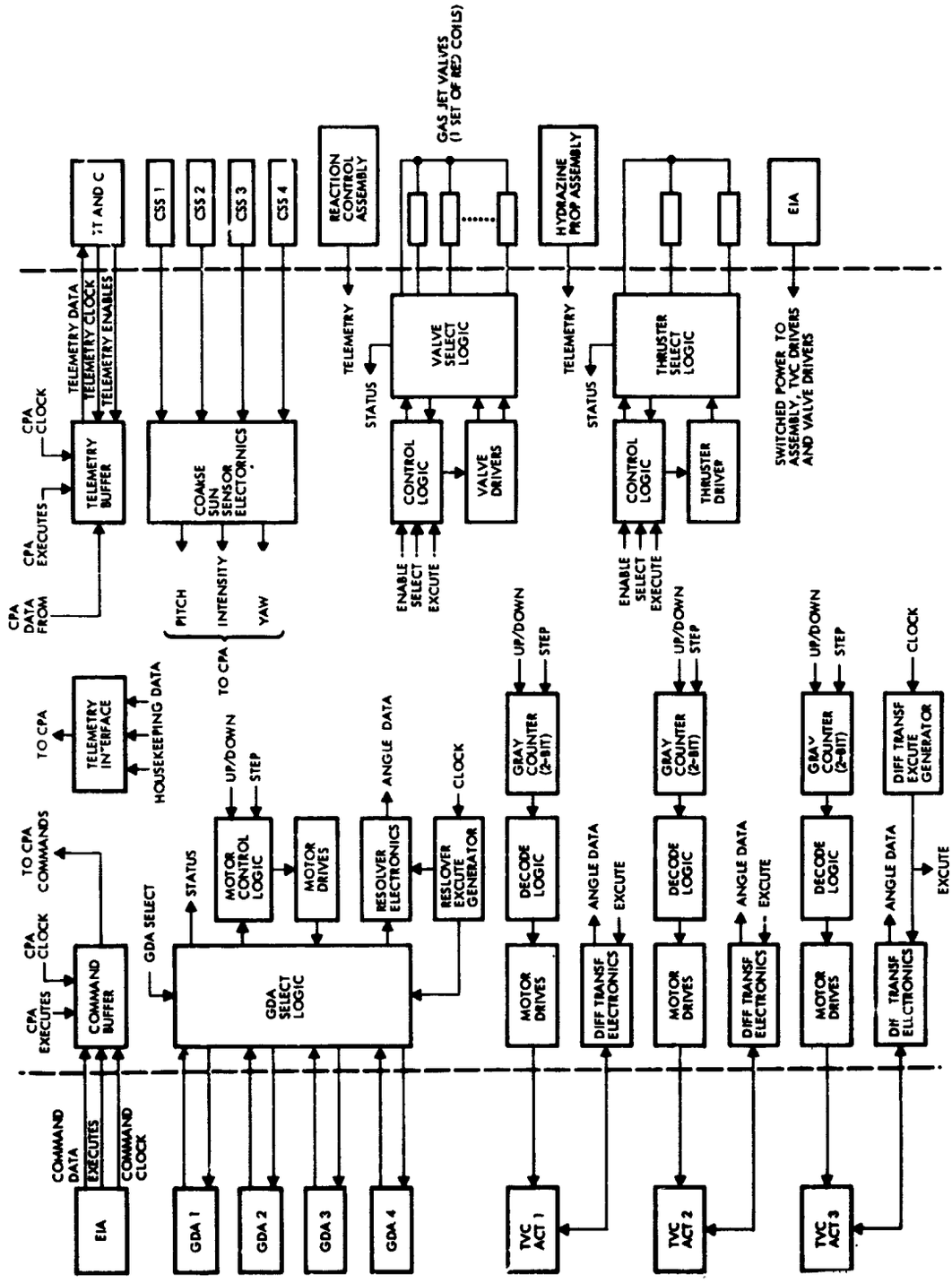

Figure 7-21 (b). Block Diagram of the CEA

Hydrazine Propulsion Assembly

This assembly (a part of the propulsion subsystem) includes the propulsion equipment for boost/deboost and orbit correction maneuvers. It consists of two redundant thrusters, a storage tank, a pressure transducer, a propellant filter, and a fill and drain valve.

Gimbal Drive Assemblies (4)

These assemblies provide single-axis star tracker gimbaling, two-axis antenna drive and single-axis solar array drive. Each assembly consists of a stepper motor (with a gear reduction and harmonic drive) and a two-speed resolver.

TVC Actuator Assemblies (3)

Each actuator consists of a stepper motor, a gear reduction, a leadscrew system and a linear differential transformer. The three assemblies provide driving and holding torques to the electric thruster gimbaling mechanism.

Control Processor Assembly

This assembly consists of a redundant set of internally cross-strapped digital computers. The assembly provides logical, control and computation functions to the subsystem on a priority interrupt basis. Support to other subsystems is provided on a non-cyclic basis.

Control Electronics Assembly

This assembly includes circuits for driving gimbal motors, TVC actuators, gas-jet valves and hydrazine thruster valves. Also, the assembly processes coarse/fine sensor, resolver and differential transformer signals and provides interfaces with the CPA, the EIA, and the TT&C subsystem.

7.3.1.2 Operating Modes

The attitude control subsystem has the following operating modes.

Sun Acquisition

The sun acquisition mode can be established by ground command or can be initiated automatically by the control processor assembly in the event that loss of the sun reference in either the yaw or pitch control axes occurs. Prior to the sun acquisition maneuver, the high gain antenna is slewed automatically out of the coarse sun sensor field of view. The sun is acquired by operating the reaction control system under coarse sun sensor and gyro control. Once the sun is acquired, the roll axis is left in the attitude hold mode, and the other axes operate in their normal

limit-cycle conditions with control torques provided by the attitude control jets.

Attitude Hold

This mode pertains to the roll axis only and can be initiated by ground command or by the Control Processor Assembly as part of the acquisition or reacquisition sequence. The roll attitude rate is reduced to zero by any of the control torque sources in operation using rate error signals provided by the gyro assembly.

Roll Search

The roll search can be started and stopped by ground command or by the control processor assembly. The stage is rotated at a constant speed by biasing the rate gyro loop with a preselected input. During the search, the gyro rate is integrated and the star tracker output is analyzed by the control processor assembly to obtain a star pattern identification. Once the desired star location has been determined, the stage is rotated to the desired position on the basis of integrated gyro rate references and rotation is stopped. The star tracker gimbal drive is then operated until the star is inside the field of view of the instrument. A roll fix is computed from star tracking data and then the stage is returned to its final orientation by another constant rate maneuver.

Cruise Mode

The cruise mode is established automatically after sun acquisition. In the cruise mode control is exercised by the gas jets with error information originating in the fine sun sensors and the gyro assembly. The sun sensors can be biased by quantitative commands to obtain attitude offsets within $\pm$ 10 degrees about the pitch and yaw axes. Attitude offsets up to $\pm$ 90 degrees about the yaw axis can be obtained by operating with the fine sun sensor mounted on the solar array and rotating the solar array by the required angle relative to the stage body. Roll attitude angles up to $\pm$ 180 degrees can be attained by biasing the gyro error counter.

Thrust Vector Control Mode

This mode can be initiated by ground command or automatically by the control processor assembly. The gimbal control circuits are energized and the reaction control deadzones are increased from their nominal $\pm$ 1 degree limits to $\pm$ 2 degrees. Proportional-plus-rate compensation is implemented by the control processor which provides three-axis control on the basis of fine sun sensor and gyro error signals. Non-interacting gimbal control is

performed on the basis of gimbal transducer signals and solar array deflection angles. The reaction control system operates automatically on a priority-interrupt mode when attitude deviations exceed any of the ± two degrees deadbands.

Detailed Equipment Descriptions

Appendix G contains descriptions, block diagrams, and summaries of physical and performance characteristics of the assemblies forming part of the attitude control subsystem.

7.3.2 Attitude Control Subsystem Operation

Acquisition

Initial acquisition begins with a booster vehicle maneuver that places its roll axis (parallel to the pitch axis of the spacecraft) perpendicular to the sun line. This maneuver is executed under control by the booster guidance system. Immediately following its completion, the stage gyro heaters are turned on and the gyro rotor is spun-up. Separation of the stage is initiated by timer or ground command. One minute later, the solar arrays and the attitude control booms are deployed and the ACS is turned on. Tipoff rates developed during the separation process (prior to solar array deployment) are estimated to be in the 0.5 to 1.0 deg/sec (3σ) range. The ACS begins its operation in the acquisition mode by nulling the roll rate under rate gyro control. Once the roll rate has been nulled, the pitch and yaw channels are enabled, and sun acquisition begins with signals provided by the coarse and fine sun sensors. After acquiring the sun with the fine sun sensors, the -Z axis is pointed at it and the roll angle has any arbitrary value. The preceding maneuvers are performed with battery power. Subsequently, the solar arrays and other appendages are deployed. The star acquisition sequence begins with a slewing maneuver of the tracker mechanical gimbal. If the desired star is not in the field of view, the roll search is initiated by command and, while it is executed, star tracker data are telemetered to the ground for identification purposes. The search is terminated by command when the star pattern is identified. The tracker gimbal is backed off until the selected star is acquired. After completing the fix the ACS is switched to the cruise mode and the desired roll attitude is established by biasing the gyro loop in the opposite

direction until the accumulated roll angle is equal to the angle between the fix and the desired orientation.

Thrust Vector Control Mode

Before the thrusters are started, the gimbal drives are pre-positioned at their nominal operating points. The thrusters are started while the system is still in the cruise mode (with reaction control). When the initial disturbances diminish in magnitude, the ACS is switched to the TVC mode and the gimbal drives are activated. The reaction control system remains active, but the deadbands are increased from ± 0.5 to ± 2.0 degrees. The stage orientation required for guidance purposes is established by biasing the fine yaw sun sensor (if within $\pm$ 10 degrees) mounted on the stage body or by operating with the sun sensor mounted on the solar array and offsetting the stage-center-body orientation. Roll angle offsets are obtained by biasing the gyro counter by the required angle. Gyro calibration is required only every two or three days. Calibration data is generated by the control processor assembly on the basis of star tracker observations. There are a number of stars, brighter than magnitude 2, that can provide reliable roll references. The choice depends on the stage orientation in inertial space. References 7-13 and 7-14 discuss the tradeoffs involved in the star reference and gimbal angle selections for each particular mission.

Cruise Mode

Before thrust turn-off, the system is switched to the cruise mode. Then the thrust is cut off and the coast phase begins with minimum disturbances. The attitude biases are adjusted to satisfy the needs of the science experiments. Star references during the cruise mode are more numerous than in the TVC mode because roll attitude constraints are less restrictive.

Antenna Pointing

The control processor assembly generates the gimbal control programs for the high-gain antenna and compensates for attitude deviations of the stage on the basis of sun sensor and gyro data.

7.3.3 ACS Conceptual Design Description

TVC Loop

The basic principles on which the control loop design is based are:

- The pointing accuracy per axis should be of the order of ± 0.7 degree to yield an overall pointing accuracy of about ± 1 degree.
- The closed-loop bandwidth should be at least one decade below the lowest natural frequency of the structure (estimated to be of the order of 0.01 Hz) to minimize dynamic interactions.
- The system should not exhibit conditional stability conditions in the rigid-body dynamics and should allow a 12-db total variation in the torque coefficients without severe stability degradation.
- The gimbal drives should require no power to hold their positions constant.
- The system should withstand temporary thrust cut-off transients caused by arcing in the thrusters without having to reacquire.
- The system should provide capability for slewing the gimbals upon command from the ground or automatically under control by logic signals provided by the propulsion subsystem.

The concept selected for thrust vector control is shown in Figure 7-22 for the yaw-axis loop. Attitude error information is supplied by a fine sun sensor in analog form. After conversion to digital form the data is processed by an estimating algorithm which provides noise filtering and corrects for long-term steady state errors. A position bias is added to orient the stage away from the sun pointing direction as required for thrust guidance purposes. The biased digital error signal is processed to provide proportional plus rate compensation and the resulting sample sequence is input to a non-interacting control matrix where commanded gimbal angles are generated for all three TVC actuator channels on the basis of thruster status and gimbal angle information. The gimbal angle command from the matrix is input to a closed-loop actuator system consisting of a stepper motor drive and a differential transformer. At each sampling instant the control law generates a

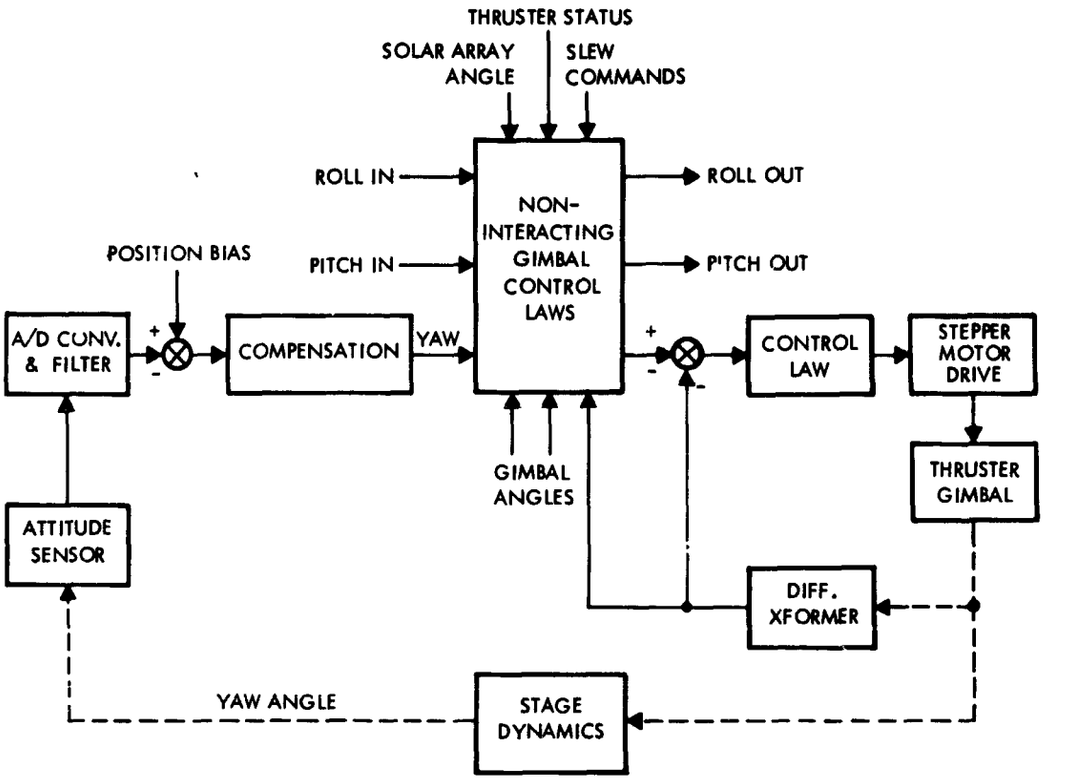

Figure 7-22. Thrust Vector Control System Conceptual Block Diagram Showing Yaw Axis Closed-Loop Dynamics

number of pulses proportional to the difference between the present commanded angle and the past gimbal angle. A deadzone with semi-amplitude equal to twice the gimbal step size is provided to minimize actuator operation due to noise and backlash.

The control loop designs for the three TVC axes are identical in concept, except for parameter values such as sensor scale factors, loop gains, time constants, deadzones and transducer scale factors.

The gimbal actuator dynamics at the sampling instants can be represented approximately by the linearized block diagram of Figure 7-23.

A simplified linear model of the control system is given in Figure 7-24. The spacecraft is assumed to be rigid and actuator delays are neglected for preliminary design purposes. A typical root-locus diagram for this simplified model is shown in Figure 7-25. For low values

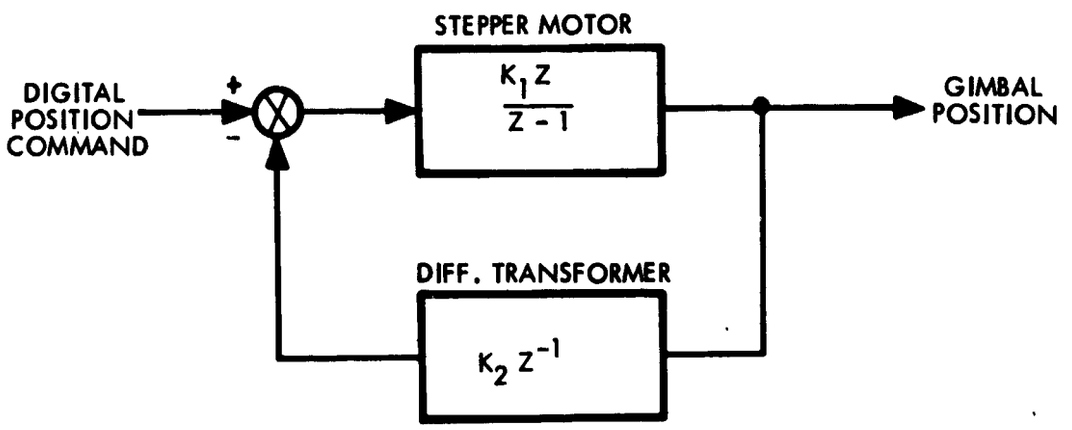

Figure 7-23. Linearized Block Diagram of Gimbal Actuator Dynamics at the Sampling Instants

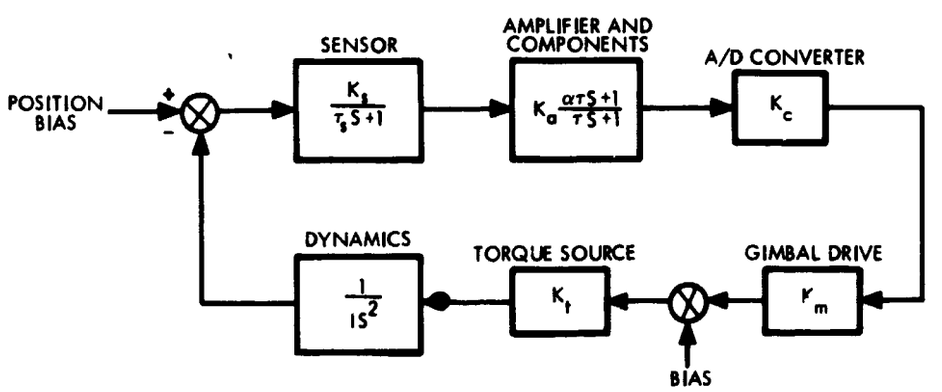

Figure 7-24. Simplified Linear Model of Thrust Vector Control System Assuming Rigid Body Dynamics

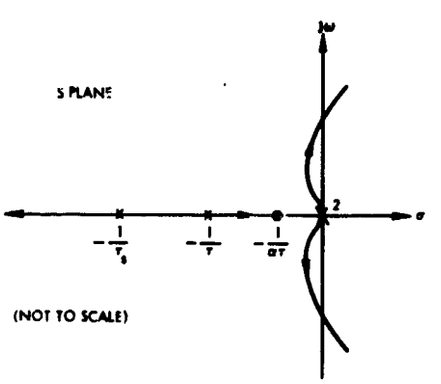

Figure 7-25. Typical Root-Locus Diagram for the Simplified System of Figure 7-24

of gain the system is underdamped but stable. Figure 7-26 shows typical root loci for the same system but with additional proportional-plus-integral compensation. The addition of a pole at the origin (going into the left half-plane) makes the system conditionally stable. This type

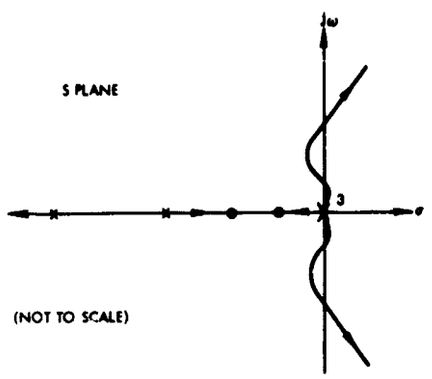

Figure 7-26. Typical Root-Loci for a System with Proportional-Plus-Integral and Lead Compensation

of constraint on the system gain is not desirable because reduction of the lower bound to acceptable levels requires excessive amounts of lead compensation (which involves long time constants) that can make the system too sensitive to noise. Proportional-plus-integral compensation has the advantage of making the system type 1, which responds with zero steady-state error to step inputs. The selected concept is type zero and the steady-state error produced by a step disturbance torque T_d is

$$\xi = \frac{T_d}{IK_B}$$

where I is the moment of inertia about the control axis (assumed to be a principal axis) and K_B is the corresponding Bode gain, given by

$$K_B = \frac{K_s K_a K_c K_m K_t}{I}$$

The steady state error is independent of the moment of inertia and can be bounded for a given disturbance torque fluctuation range by choosing adequate values for the system parameters.

Details of the root loci of interest are given in Figures 7-27 and 7-28, in which the gain values shown correspond to the root-locus gain defined by

$$K_{RL} = \frac{\alpha}{\tau_s} K_B$$

The linear model presented above represents approximately the large-signal dynamics of the system. The small-signal behavior is nonlinear because of deadzones and quantizations in the over-all and actuator loops, which cause limit cycles.

Thrust Vector System Interaction

The gimballed TVC system described above is similar in mechanical and electrical design than other TVC concepts previously considered but it can, under some thrust operating conditions, introduce pitch-yaw and pitch-roll coupling effects. In addition it can also introduce thrust steering errors which must be compensated to avoid guidance perturbations. These effects and the required compensations have been analyzed and are briefly discussed below.

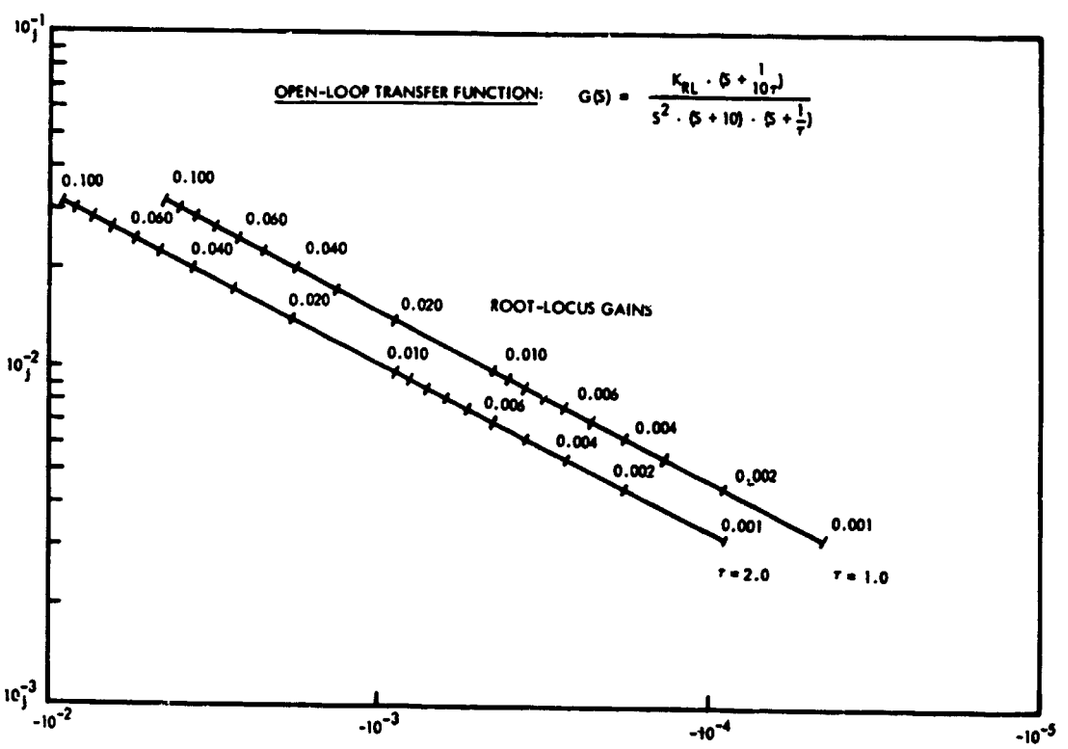

Figure 7-27. Detailed Root-Loci for the Simplified Model of Figure 7-24 with α = 10 and Two Values of τ

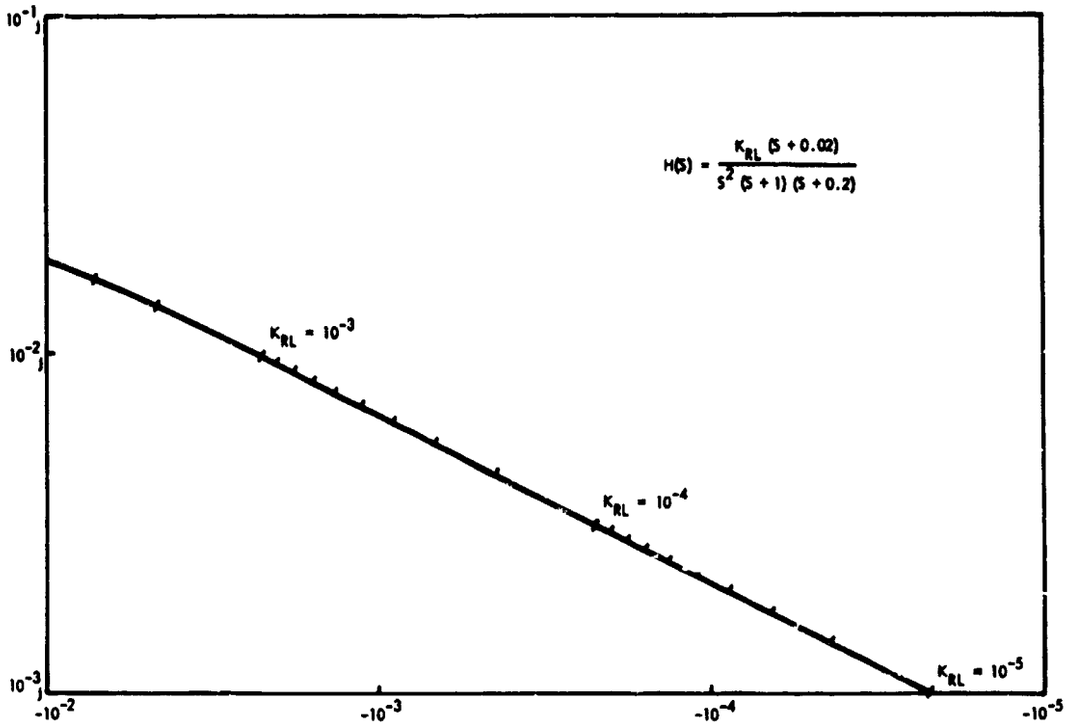

Figure 7-28. Detailed Root-Locus for the Simplified Model of Figure 7-24 with α = 10 and τ = 5 sec

We consider the case of four symmetrically arranged thrusters as shown in Figure 7-29. If all thrusters are operating and a pitch deflection is applied by a twisting action of the actuator ring no coupling torques around the yaw and roll axes are introduced by virtue of the symmetry of the four components contributing to the pitch torque. However, if as a result of thruster cutoff an asymmetrical set of thrusters (two or three) are left in operation, as shown in Figure 7-29, a pitch deflection also produces yaw and/or roll torques. By insertion of compensation signals into the yaw and roll control channels the undesirable coupling effect can be eliminated. A switching logic is required to control the amount of compensation in each channel in accordance with the configuration of operating and non-operating thrusters. A flow diagram at the bottom of Figure 7-29 shows the required mixing of input signals into the yaw and roll control loops. We note that the compensation signal illustrated by arrow symbols in the thrust deflection geometry has the effect of reducing the effective pitch control deflection. However the coupling and compensation signals do not decrease the stability of the respective

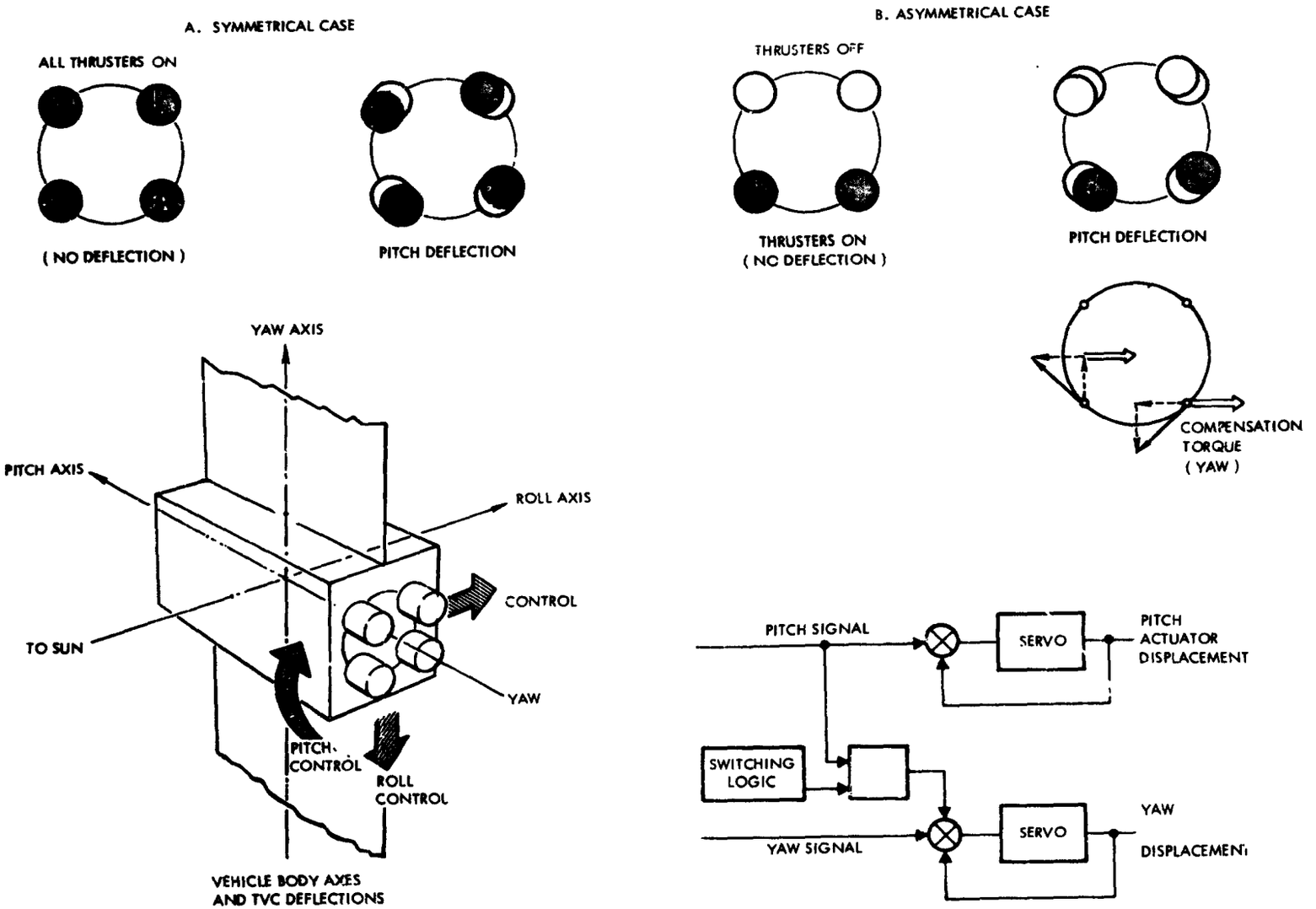

Figure 7-29. TVC Cross-Coupling and Compensation Method

control loops since no dynamic interactions are involved. In fact, more detailed analysis shows that the dynamic effect due to the momentum exchange that results from the thruster displacement relative to the center body has a stabilizing effect in each attitude control loop.

The interaction of TVC displacements with guidance results from the effective change of thrust vector orientation in inertial coordinates if the vehicle center body remains fixed. Figure 7-30 illustrates how a yaw displacement of the TVC system can be compensated by rotating the center body by an equivalent angle in opposite directions. This requires adding an offset signal to the sun sensor output which has the effect of changing the sensor's null position. Similarly, an offset signal corresponding to a roll deflection of the thruster package must be added to the star sensor output. The instantaneous orientation of the thruster package relative to the center body is measured accurately by a potentiometer pickoff or shaft angle encoder mounted on the TVC actuators.

Reaction Control Loop

The reaction control system provides pitch-axis control capability during periods of thrusting with a single engine and full three-axis stabilization and control during coast or cruise phases. In addition, this system executes initial sun and star acquisition (and subsequent reacquisitions) and provides backup stabilization to the stage during powered flight in case of anomalies in the operation of the thrust vector control system (for stopping attitude deviations that could exceed the normal operating limits of the sensors.)

The basic ground rules on which the reaction control system design is based are:

- The limit cycle amplitudes shall be of the order of 1 degree to limit their contribution to the error budget to about $\pm$ 1.4 degree.
- The reference sensors are the same ones used for TVC control.
- Control torques shall be applied to the stage with minimum excitation of vibration modes.
- The propulsion concept selected shall provide maximum reliability (as the primary requirement) and minimum weight.

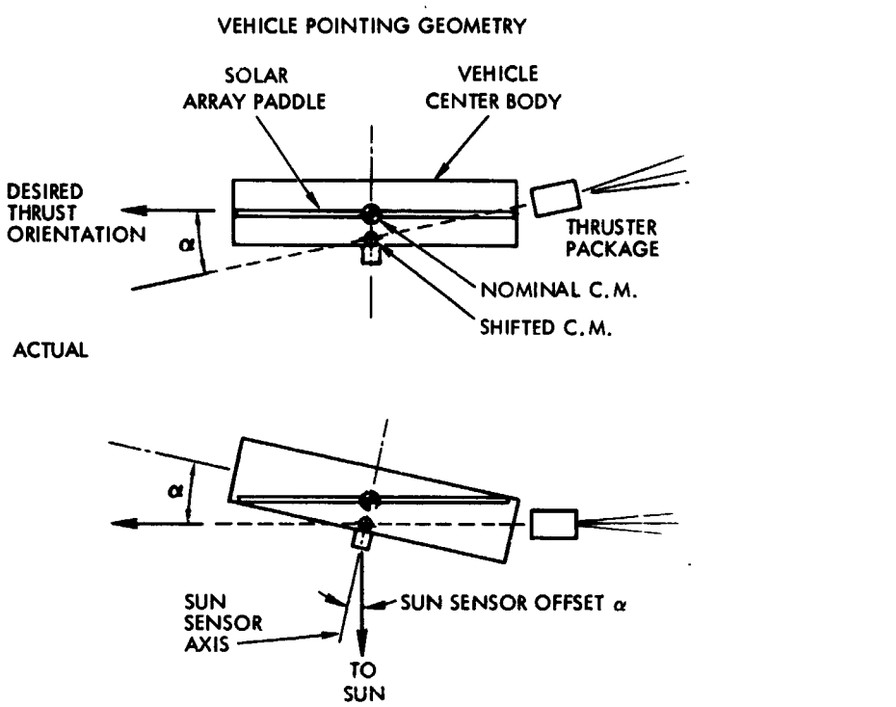

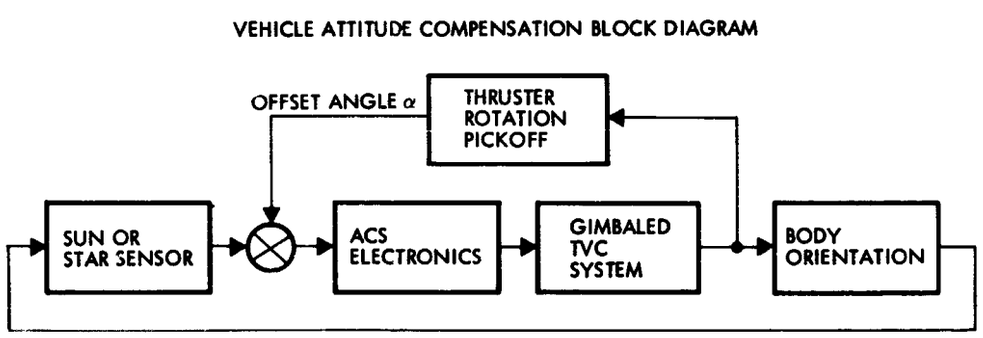

Figure 7-30. TVC Interaction with Guidance and Compensation Method

- Thruster locations shall be selected to provide moment arms of 1.52 m (5 ft) or longer (for the pitch and yaw control axes) and minimize the excitation of symmetric modes during thrust vector control with a single engine.

- The system shall operate automatically on any axis during TVC if the attitude errors exceed $\pm$ 2 degrees.

Control impulse is required for acquisition, undisturbed limit cycling, roll search, and unbalanced solar pressure torque compensation. Also, additional gas is required because of leakage. A preliminary estimate of impulse requirements for the baseline stage configuration is of the order of 2000 lb-sec (8900 Nt-sec).

The gas jets are located on the stage as shown in Figure 7-31. The yaw and pitch jets are installed on two booms providing moment arms of at least 1.52 m (5 feet). The booms are made intentionally flexible for minimizing dynamic interactions caused by the fast rise times of the gas-jet thrust. Essentially, the flexible booms behave as mechanical filters reducing the spectrum of the thrust pulses to a discrete set of frequencies chosen so that excitations of vibration modes are minimized. The roll jets are mounted in pairs on the stage body as shown in Figure 7-31 with offset angles such that the moment arms of the individual jets providing positive and negative roll torques are equalized. This also avoids impingement of the hot gas exhaust on the solar array. Placement of these jets at the bottom of the propulsion module has the advantage of very short gas lines from the N_2 tanks.

To satisfy the pointing accuracy requirements, limit cycle amplitudes of $\pm$ 1 degree were chosen. The limit-cycle rates are determined by the minimum impulse bit obtainable from the pneumatic propulsion system. Minimum pulse durations of 0.10 second were selected because these are values providing acceptable impulse-bit reproducibilities. Thrust levels of 0.22 N were selected in order to limit the gas consumption due to symmetrical limit cycling.

The concept selected for reaction control is based on the use of derived-rate impulse modulators, as shown in Figure 7-32. In the roll loop, the gyro provides true roll rate information for acquisition pur-

poses. The pitch and yaw control systems operate with derived-rate information only.

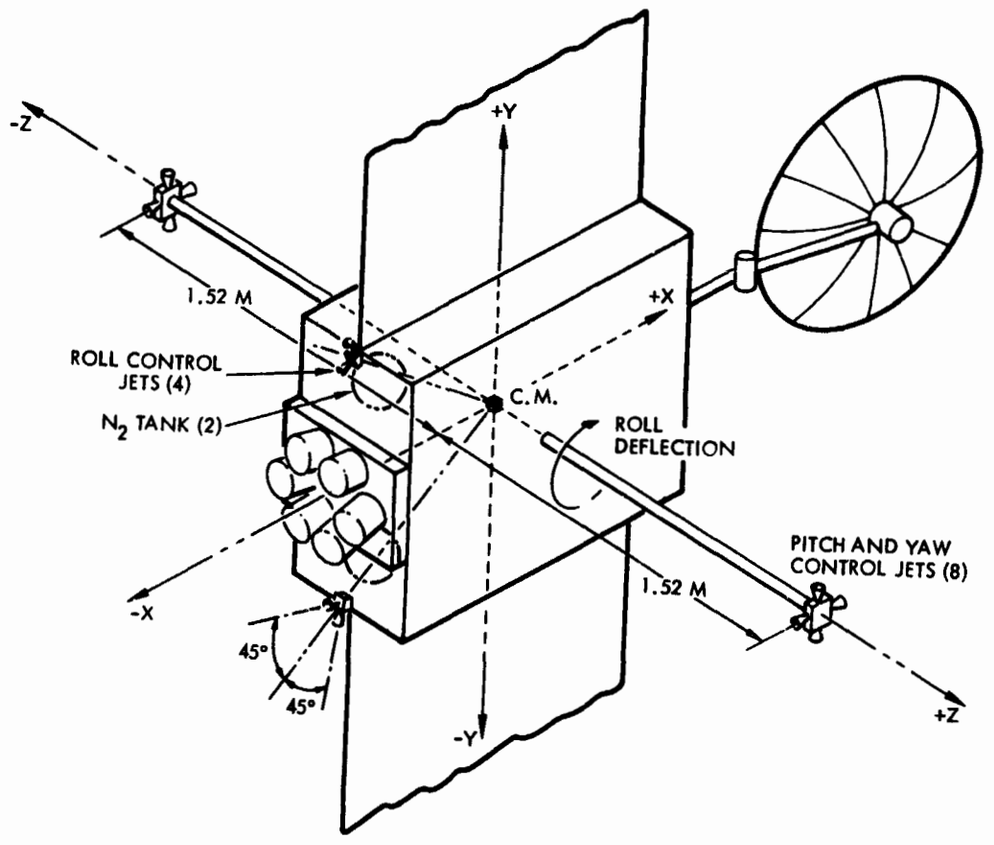

Figure 7-31. Location of Gas Jets on Stage

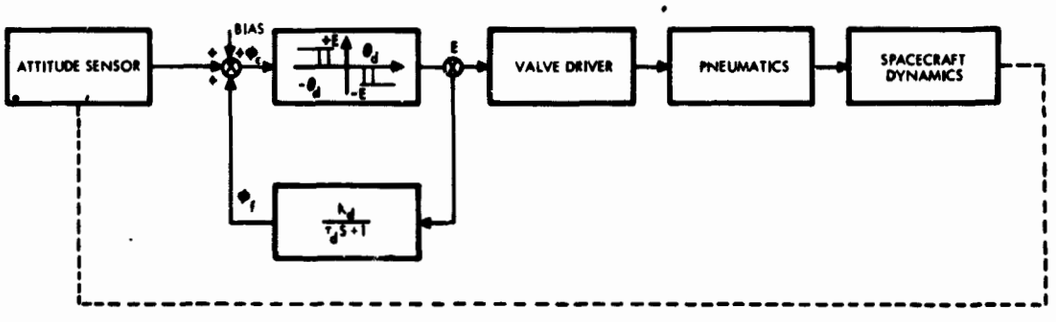

Figure 7-32. Reaction Control System Conceptual Block Diagram

7.3.4 Attitude Control Propulsion

The baseline attitude control system is a conventional nitrogen pneumatic system with electrothermal thrusters of the vortex type. A similar approach was successfully demonstrated on the advanced Vela spacecraft built by TRW Systems. All components of the attitude control propulsion system are flight qualified with the exception of the electrothermal thrusters. The thrusters are considered in a state of advanced development and have been informally flight qualified for another program.

The thrusters are of the fast heat-up type. Heating power is applied only when the propellant valve is actuated. The integrated power usage of these thrusters is much lower than that of the thermal storage type. Heated systems show less mass advantage compared to cold gas configurations when a power penalty is included as part of the system mass. In the present application the average power is negligibly small because of the low duty cycles of the normal mode operation. In addition, because the gas jet system operates only when the system is in the coast phase and during single electric thruster propulsion, the heating power demand can be supplied without requiring an increase in the capability of the power subsystem.

The system selected for the baseline configuration uses nitrogen heating to 816°C (1500°F) because this approach has been flight proven and involves minimum development risks. If the heaters fail, the system is still operational with a reduced specific impulse. In normal operation the hot gas I_{sp} is 145 seconds, in the emergency mode the cold gas jets operate at an I_{sp} of about 72 seconds. The required amount of gas is stored in two pressure vessels which can be interconnected by means of a normally-closed squib valve. Each tank feeds a set of six solenoid valves through a redundant-seat pressure regulator and a normally-open squib valve. When the two circuits are operative, the system develops pure couples about any of the three axes. In case of open failure of one of the valves, the entire circuit affected can be bypassed by means of the corresponding squib valve. This type of failure is highly improbable because all solenoid valves have redundant seat arrangements.

A schematic of the pneumatic system is shown in Figure 7-33. As indicated by the figure, two completely redundant half-systems are employed; each contains one-half of the mission total impulse. Each half system is comprised of a storage vessel (or propellant tank) filled with nitrogen under high pressure, a pressure regulator and relief valve, six internally-redundant solenoid valves, six thrusters, a fill valve, high and low pressure transducers, and the necessary plumbing, valves, and manifolds to interconnect the components.

Figure 7-31 indicates the installation of the system on the spacecraft. The roll and yaw thrusters are boom mounted; the pitch thrusters are body mounted. The thrusters are operated in pairs to exert couples about each control axis. The valves are located within the spacecraft envelope and are connected to the thrusters with penumatic tubing. This approach degrades the pneumatic response characteristics of the thrusters somewhat, but greatly simplifies thermal control. Table 7-6 lists the capabilities of the baseline attitude control propulsion system. A weight summary is given in Table 7-7 for the 2000 lb-sec, baseline system. Several of the key components are described in the following paragraphs.

Pressure Vessel

The propellant tanks are welded titanium spheres each having an internal volume of 676 cubic inches, at 4000 psia, the total propellant weight is 14 pounds. Each of the tanks is strap mounted to the equipment platform as shown in Figure 6-1. Several other flight-qualified propellant tanks of various capacities are available which will allow a total-impulse growth capability.

Pressure Regulator and Relief Valve

The regulator reduces the pressure of the nitrogen to a constant level of 50 psia for delivery to the solenoid valve/thruster assemblies. The regulator assembly also includes a relief valve and manifolding for the transducers. The relief valve protects the regulated pressure side of the penumatics system in the event of thermally-induced gas expansion in the lines between the regulator and solenoid valves or internal leakage of the regulator. The pressure transducers provide telemetry signals for monitoring the system status.

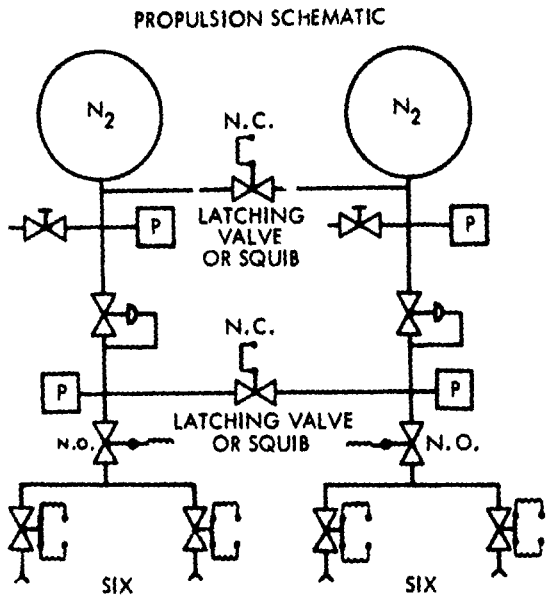

Figure 7-33. Reaction Control Assembly

Preliminary Characteristics	
Total impulse	8900 Nt-sec (2000 lb-sec)
Propellant	Heated N_2-820°C (1500°F)
Specific impulse	143 sec (at 1500°F)
Thrust level	0.22 N (0.05 lbf)
Heating energy	9.5 Joules (for 100-msec pulses)
Tank pressure	2760 N/cm^2 (4000 psi)
Tank volume (each)	11.1 litere (676 cu-in.)
Propellant mass	6.50 kg
Total mass	22.73 kg (50 lb)

Table 7-6. Characteristics of Reaction Control Assembly

Table 7-7. Reaction Control Assembly Mass Summary

	kg
Propellant tanks (2)	6.50
Tank brackets (2)	0.45
Fill valves (2)	0.09
Regulators (2)	1.02
Latching squib valves (4)	2.00
Pressure transducers (4)	0.63
Solenoid valves (12)	2.72
Nozzles (12)	0.55
Lines and fittings	2.27
Total dry mass	16.18
Propellant	6.50
Total mass	22.53

Solenoid Valves

The solenoid valves control the flow of propellant to the thruster upon receiving a signal from the attitude control electronics. The valves are coaxial with dual elastomeric seal poppets and dual solenoid coils. The coils are connected in parallel and either coil is capable of actuating the valve.

Electrothermal Thruster Assembly

Each thruster consists of a cylindrical cavity with a coaxial spirally-wound heater element (75 percent tungsten - 25 percent rhenium) as shown in Figure 7-34. The propellant gas is injected tangentially at high velocity. The gas spirals radially inward with high tangential, but low radial velocity. In passing around and through the heater element many times, the gas is heated. It is then expelled through a conventional convergent divergent nozzle.

The thrusters weigh less than 0.1 pound each. The low-mass helical configuration of the heater element provides rapid thermal response and minimizes the effects of the thermal transients on delivered specific impulse. Moreover, a heater failure will not impair the stability of the thruster to perform in an unheated mode. In the event of a heater failure, the delivered specific impulse will be degraded by about 50 percent but the thrust will remain constant.

A promising alternative to the baseline attitude control propulsion system is the use of hydrazine resistojets coupled to the same propellant supply as the hydrazine velocity correction system. The hydrazine resistojet offers significant weight advantages because of the higher specific impulse and more favorable tankage weight factor. Since the hydrazine tank is "off-loaded" for most of the missions, no tankage weight penalty will be incurred by the hydrazine resistojet attitude control system for these missions.

7.3.5 Problem Areas and Recommendations for Further Study

Two of the most sensitive areas requiring extensive analytical work are the dynamics and stability of the attitude control subsystem with highly compliant flexible structures and booms subject to thermal deformations.

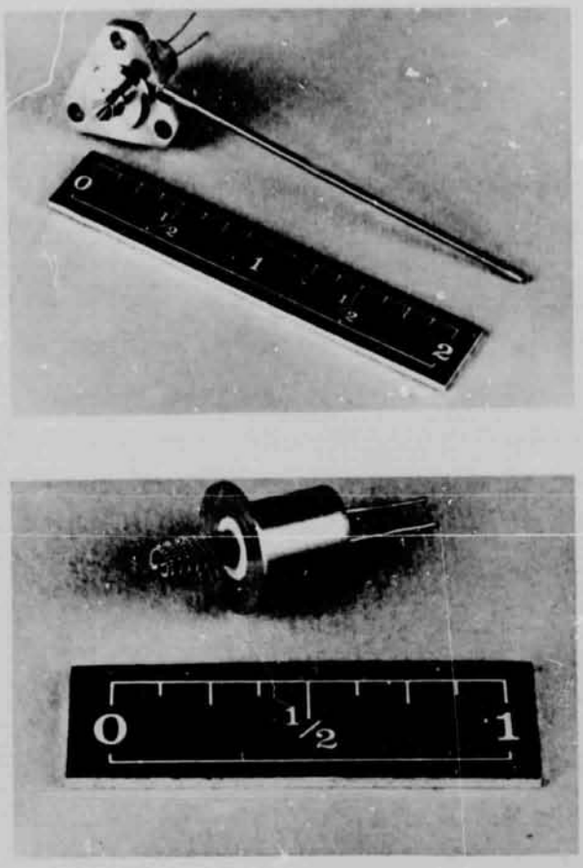

Figure 7-34. TRW Electrothermal Vortex Thruster

The basic problem of the solar electric stage is the extreme difficulty of testing it realistically under 1-g conditions. Dynamic behavior of the system has to be predicted mainly by analysis and, consequently, modeling becomes one of the most delicate tasks. Various mathematical models with different degrees of complexity and specialization must be developed for computer analyses and simulations.

The use of a general purpose digital computer provides capabilities for adjusting control system parameters and control laws after launch. Further study should be devoted to the problem of defining control configurations (to be employed during the initial launch, deployment and testing-in-space phases) and test programs.

The definition of detailed computer requirements is also one of the areas that should be given particular attention in order to arrive at an integrated and cost effective configuration (from the system standpoint). The object is to satisfy most logical and computational requirements (of both the ACS and other subsystems) by efficient use of priority interrupt capabilities.

7.4 COMMUNICATIONS AND DATA PROCESSING

7.4.1 General

A Communications and Data Processing subsystem for a Solar Electric propulsion stage should be extremely flexible to provide support to the wide variety of missions in which it may participate and also because the number of modes in which it may be called upon to operate. Moreover since many of the missions may be of great duration a communications subsystem placing least demand on the DSN is also of extreme importance.

7.4.2 Categories of Operation

The communications capability required for typical mission should be considered in three broad categories.

a) The stage carries the communications subsystem for itself and the payload.

b) The stage and the payload each carry their own autonomous subsystems.

c) The subsystem which supplies this capability is mounted in the payload.

It is apparent that (c) is beyond the scope of this study but as discussed elsewhere, categories (b) and (a) should be considered. Since it appears quite likely that some missions (outer planet missions) clearly fall into category (b) and others are more compatible with category (a), a subsystem concept has been explored which is suitable for either of these categories with virtually no change except for the size of the High Gain Antenna. The chosen concept imposes virtually no penalty for the gains obtained through equipment commonality and at the same time places least demand on the DSN network. Table 7-8 summarizes the anticipated capabilities for the two operation categories and shows that they differ only in telemetry data rates and maximum communication distances.

7.4.2.1 Category A - Combined Payload and Stage Communications and Subsystem

An investigation of possible missions in this category shows maximum communication distances to about 4 AU and with a broad range of telemetry data rates. There are three or four modes of operation in this category.

Table 7-8. Anticipated Requirements for Two Categories of Interest

REQUIREMENTS	CATEGORY A (Combined Payload and Stage Communications Subsystem)	CATEGORY B (Autonomous Payload and Stage Subsystems)
Command Rate	1 bps to maximum range	1 bps to maximum range
Tracking	Angles, range rate, possibly ranging to improve accuracy	Angles, range rate and possibly ranging to improve accuracy
Communications Distances (Max.)	Approximately 4 AU	Approximately 2 AU
Telemetry Data Rates	Stage Housekeeping 32 bps max. 8 bps average Stage transients 2048 bps Science Payload and Housekeeping Data: Max. 32 bps; Thrust Average 24 bps; Coast Average 16 bps Payload Vidicon: Vidicon readout onto tape 16, 200 bps; Vidicon transmission data rates max 16, 200 (DSN limitation)	Stage Housekeeping 32 bps max. 8 bps average Stage transients 2048 bps Low definition vidicon for navigation To be determined

a) Thrusting mode. In this mode, stage and payload housekeeping and science data must be telemetered and in addition, it may still be necessary to monitor transients during propulsion turn on and turn off, if only to permit correlation of possible effects on other telemetered data. Similarly a high average rate of science and payload data may be necessary to check the effects of the thrust (if any) on other measurements, resulting in a combined data rate of 32 bps.

b) Coast Mode. Payload housekeeping and low data rate science data must be elemetered during this mode with an average rate expected to be about 16 bps.

c) Terminal Mode. During the terminal mode of operation (e.g., Ceres rendezvous or Mercury orbiter) the vidicon camera telemetry will require the greatest data rates and place the greatest demands on the communications subsystem. However, at this point in the mission the maximum DSN support may be anticipated and the use of a 210-ft antenna is assumed.

d) Relay Mode. Required either for the mother/daughter concept in comet rendezvous or to support an asteroid lander. The data rates for this mode vary considerably from the low science data rates to the highest possible readout rates of vidicon camera data. This rather special mode is discussed briefly in a later subsection.

In summary it can be seen that Category A requires a high capability communications subsystem because of the high data rates and the maximum communication distances. However, since the payload and stage subsystems are combined, only one high gain antenna is required and this can be of the largest possible size compatible with shroud dimensions and pointing accuracy problems. A two and one half meter diameter antenna appears appropriate for this category of operation.

7.4.2.2 Category B - Separate Payload and Stage Communications

In this mode of operation the demands on the stage communications system are very considerably reduced since not only is the data rate of the stage alone much smaller (8 bps) but generally, it will have completed its mission at a distance of 2 AU. Thus assuming everything else the same, the antenna could be reduced in size by a factor of more than two thus permitting more freedom in locating payload and its antenna. A 1.25 meter diameter antenna is recommended, however, for a bigger communications system margin, to permit more flexibility in mission planning, for example to permit ranging out to at least 1 AU using the 85 foot antenna (as can be seen from Figure 7-35). Ranging out to 2 AU would require a 40 Kw transmitter at the 85-foot antenna ground station. The vidicon camera may be used in this mission category as a navigation aid for the terminal phase. In this case, however, a much lower data rate would be required for readout since the amount of detail required (star pattern backgrounds for example) would be much less. Thus the smaller antenna would not cause difficulties for vidicon readout in this mode of operation. It is assumed for reasons of economy that identical communications and data handling systems would be maintained for the two categories of mission except for the different antenna size.

7.4.3 Overall System Concept

7.4.3.1 General Considerations

It is apparent that a very flexible communications and data handling system is required to meet all of the possible mission variables, to impose the least demands on the DSN and to provide adequate reliability. The latter is provided by means of numerical and functional reliability. Many functions can be implemented by stored commands from spare capacity in

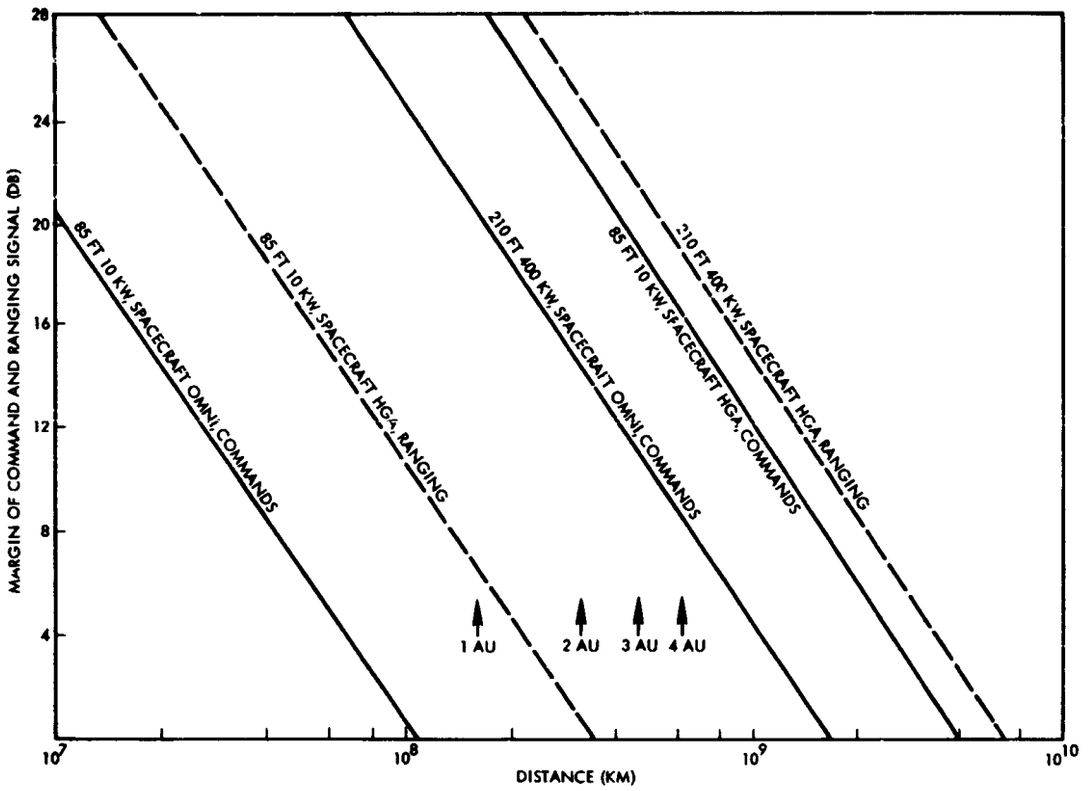

Figure 7-35. Command and Ranging Performance (High-Gain Antenna Diameter 2.45 m)

the small CC&S but an override command capability at greater rates than the one bit per second for emergency use may be required for some missions. Detailed discussion of mission peculiar commands is beyond the scope of this study.

The subsystem will store low data rate science and housekeeping data on tape and dump this every 13 days during a transmissior of 10 hours or less to an 85 foot antenna system. During encounter it is assumed that a 210 foot antenna may be available for direct vidicon readout but provision is also made to store a limited number of frames on tape. Data compression techniques (delta modulation) will be used to reduce the number of bits per vidicon frame readout by a factor of about two for a conventional television type picture. When used as for navigation by star background recognition, however, the compression factor should be improved

by several orders and it should be possible to store several frames in the buffer storage for fast retrieval or many frames on tape. A multi-speed tape recorder does not have adequate reliability for the contemplated missions and in order to simplify the design the use of a single speed reversible motor for the tape machine was envisaged in conjunction with output and input buffers of adequate capacity. The buffer storage permits the use of a much simpler tape drive thus enhancing reliability and reduces the running time of the recorder which also lengthens its life. The optimum tape speed for readout from the buffer storage ultimately chosen was, however, rather slow for direct tape recording and readout from the vidicon camera, and so a dual speed reversible motor (with a 4 to 1 speed rate) may be advisable for the tape transport if it does not reduce reliability. If a reliable dual speed transport does not seem attainable, some sacrifice in speed (4 times) of vidicon output recording will have to be accepted. However, it is expected that most high definition vidicon data will be transmitted directly and thus a single speed motor may be acceptable.

7.4.3.2 Command and Ranging Performance

Figure 7-35 shows the command and ranging performance from the proposed command system using a three stage transistor preamplifier with a 3 db noise factor ahead of the original Pioneer type receiver. The command performance is more than adequate with the stage high gain antenna (HGA) of 2.5 meters diameter and the 85-foot ground antenna with a 10 KW transmitter or using the 210-foot antenna installation with the stage omni-antenna for emergency conditions. The conservative ranging data threshhold (providing 15 meter accuracy and an acquisition time of less than 10 minutes) can be obtained by a standard 85 foot antenna installation at distances up to 2 AU using the stage HGA. If ranging data is required by an 85 foot antenna ground installation at 4 AU with the 2.5 meter stage antenna (or to 2 AU with the 1.25 meter antenna in a Category B mission) an increase of ground transmitter power to 40 Kw is necessary.

7.4.3.3 Downlink Capability

7.4.3.3.1 Choice of Frequency

The uplink frequency for the stage is at 2110 MHz since the DSN ground capability is restricted to this frequency band. However, there

is a choice of frequency band between S- and X-band to be made for the downlink since the DSN has a capability of receiving in either band. Since the stage must receive commands at S-band, its antenna system must operate in this band. S-band has a very definite advantage of providing better omni-directional coverage for emergency telemetry and thus there are strong reasons for providing a downlink transmitter at 2200 MHz. There are however, a number of reasons for providing an X-band downlink in addition to an S-band link. The greatest advantage is the considerable increase in data rate which can be obtained for a given space vehicle antenna size and transmitter. This enables faster vidicon readout time and needs less ground station usage time for the same transmitter power, or less power can be used for the same capability which may be a strong motivation for inclusion in a severely power limited space vehicle.

In addition, the X-band downlink is less susceptible to possible refraction effects by the ion beam and provides additional redundancy.

There are, however, a number of disadvantages. The improvement to be gained from the system actually is less than the theoretical increase in antenna gain based on the ratio of the square of the frequencies. The ground antenna capability is diminished at the higher frequencies by deformations produced by wind and other effects and propagation losses are much more dependent on weather conditions. The dual frequency system would require additional transmitters, power converters and exciters and an X-band feed. The spacecraft antenna design would be more complex and require tighter tolerances in a severe thermal environment. Pointing accuracy problems would be greater and a weight penalty of 40 to 60 pounds may be incurred.

It is apparent that a compelling reason is required to justify the use of X-band, which might be the considerable improvement of data rate capability which theoretically could be as high as 11 db (from the square of the ratio of 8149/2790).

Deterioration of X-Band Performance Due to Weather

Assuming adequate performance may be obtained from the space vehicle antenna the losses in an X-band system will result from the following effects:

1) Deformation of ground antenna structure

2) Attenuation due to bad weather

3) Increase of ground system noise temperature

At X-band much smaller deformations may cause boresight shift or loss of efficiency and large antenna structures in high winds may be subject to deterioration of performance. The greatest loss of performance, however, is due to atmospheric absorption which causes signal attenuation and increase of antenna noise temperature. The magnitude of these effects is shown as a function of frequency and precipitation rate in Figure 7-36 based on a Spring or Fall weather model (these data are slightly conservative because the height of the rainstorm is lower in winter). Figure 7-37 shows the effect of bad weather on the performance of the DSIF antennas on downlink performance. The fine weather performance is based on data published in JPL-810-S Rev. A, October 1970. It is understood that no operational X-band 85-foot antennas are presently planned for the DSN but the estimated performance is included in the event that this modification may become available at some future time. The "bad weather" performance for the 210-foot antenna at X-band includes degradation due to winds up to 30 miles per hour (which occur about two percent of the year at Goldstone) for elevation angles between 10 and 70 degrees and atmospheric absorption.

The weather effects at 30 degrees elevation are considered extreme (6 mm/hr rain) occurring only about five hours per year in the Goldstone area. However, this precipitation rate could occur more often at overseas sites (possibly as much as 40 hours per year) and the attenuation could be slightly higher for the same precipitation rate. Thus the baseline attenuation value and its corresponding increase in noise temperature are conservative values for Goldstone and still reasonable values for the overseas sites.

It can be seen from Figure 7-37 that a considerable increase in capability is achieved by the use of an X-band downlink even under bad weather conditions.

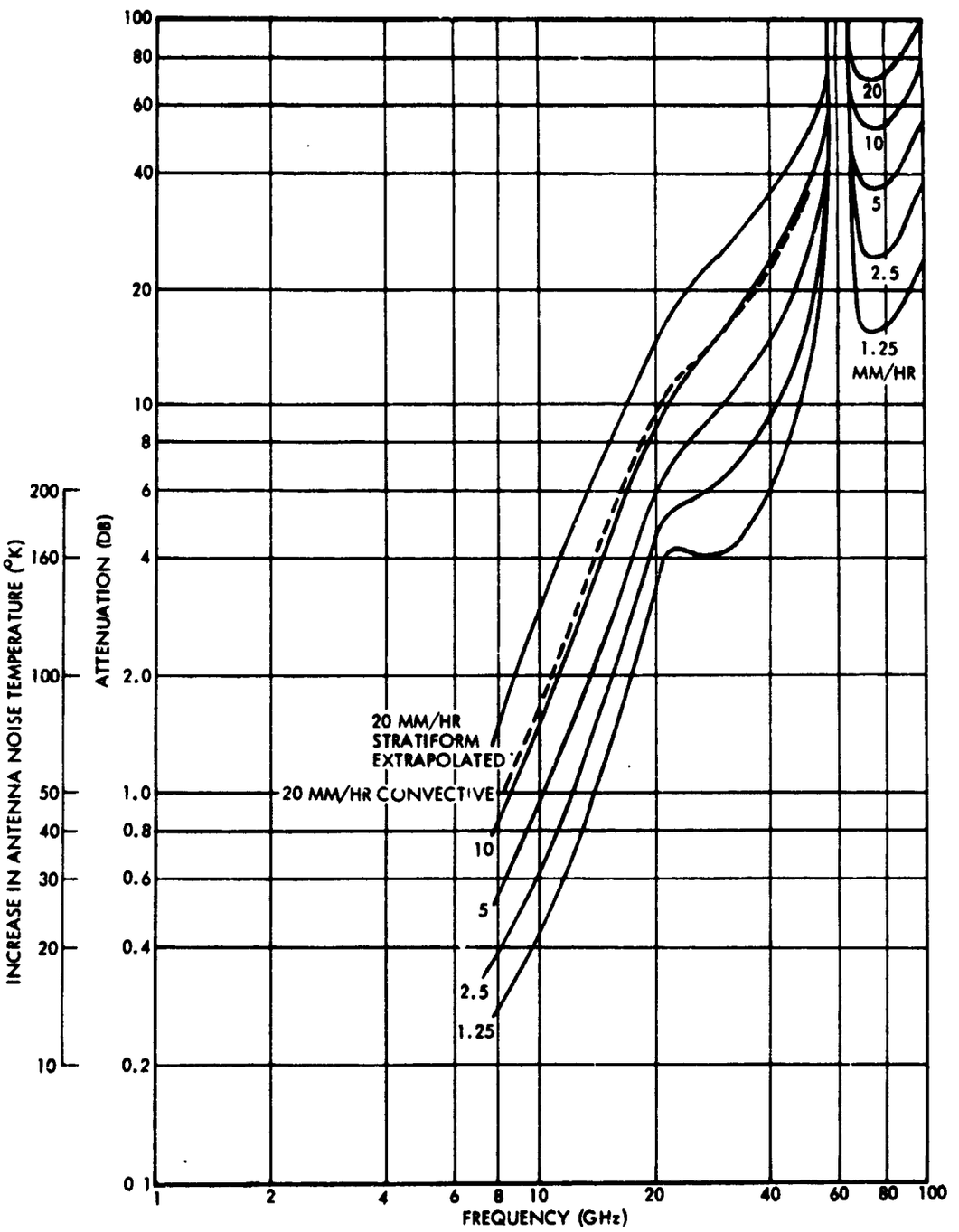

Figure 7-36. Total Attenuation and Increase of DSIF Antenna Noise Temperature at 30 Deg. Elevation vs Frequency (Spring/Fall Model, 2.4 km Freezing Level)

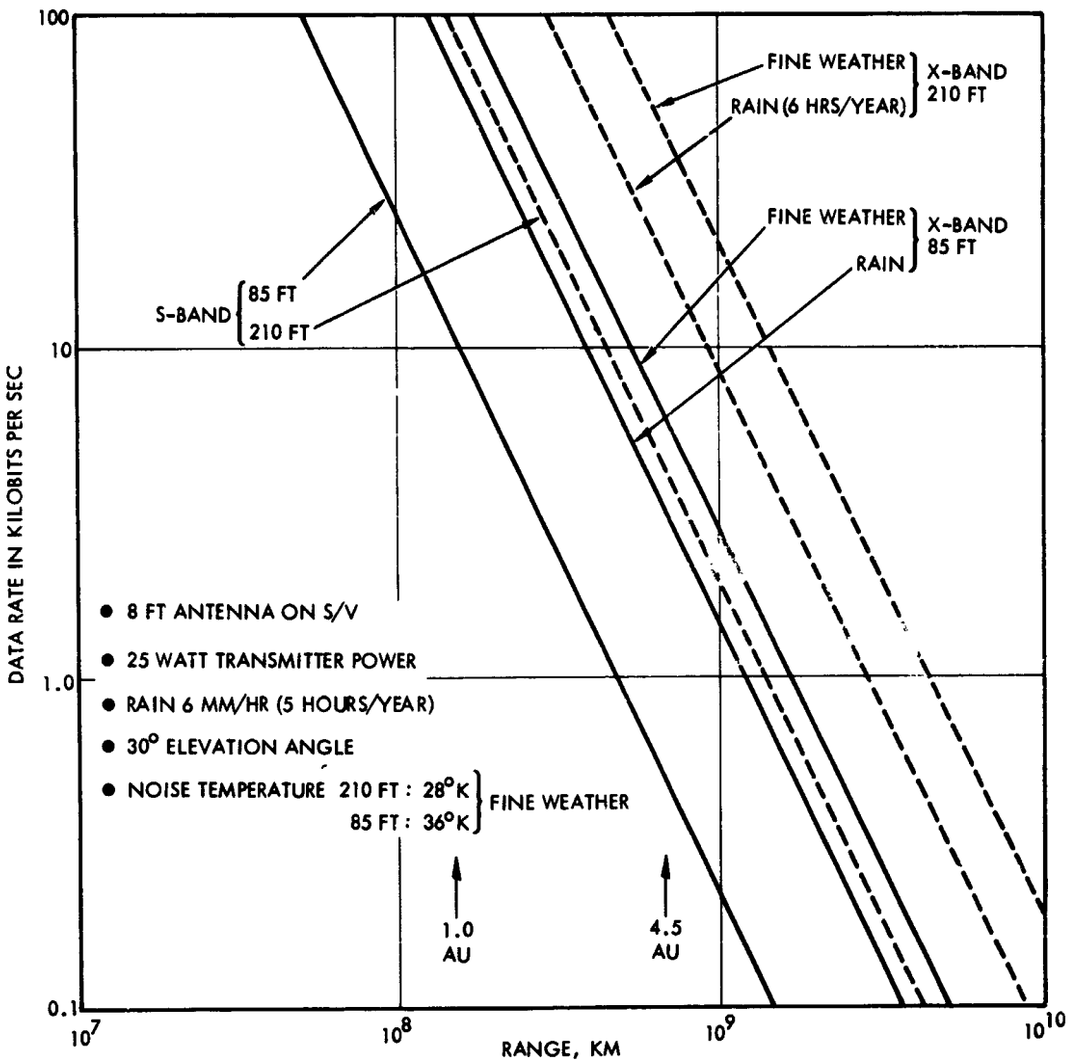

Figure 7-37. Communications Capability of Electric Stage

7.4.3.4 Downlink Support for Ceres Rendezvous Mission

In order to evaluate the chosen concept capability it is necessary to compare the capability with the requirements of a typical mission. Figure 7-38 shows that the communications distance increases from launch to a maximum of 3.6 AU and then decreases to rendezvous at 2.4 AU.* Table 7-9 shows some communications parameters which illustrate the maximum demands on the system.

*The data rate points on the curve show where zero margin (above negative tolerances) is reached. It is assumed that the data rate will be reduced before zero margin is reached, possibly at about the +2.0 db margin point.

Table 7-9. Ceres Rendezvous Mission Communications Parameters (Assuming 25-watt S/V Transmitter, 8-Ft High-Gain Antenna Diameter)

Time from Launch in Days	Max Comm Distance AU	Average Data Rate (Bps)	Maximum Transmission Time in Hours Every 13 Days, and Data Rates (Bps)				Comment
			85 ft (S)	210 ft (S)	85 ft (X)	210 ft (X)	
350 - 500	3.6	32	20** (512)*	2.5 (4096)	2.5 (4096)	0.3 (32,768)	Using one tape recorder (36 million bits capacity)
500 - 600	2.4	32	10 (1024)	1.25 (8192)	1.25 (8192)	0.16 (65,536)	Using one tape recorder
Ceres Orbit (Nominal)	2.4	16	5 (1024)	0.6 (8192)	0.6 (8192)	0.08 (65,536)	Using half of one tape recorder capacity per 13 days
Ceres Orbit S.E.C. Vidicon Readout			Maximum Time Per Frame (Seconds) (2 to 1 Data Compression Ratio)				Direct Vidicon readout
			2448	306	306	38	

*Actual data rates in bps shown in parenthesis (Multiply by 4 for 100-watt transmitter)

**In practice during this period the storage would be read out every 6-1/2 days for a period of 10 hours

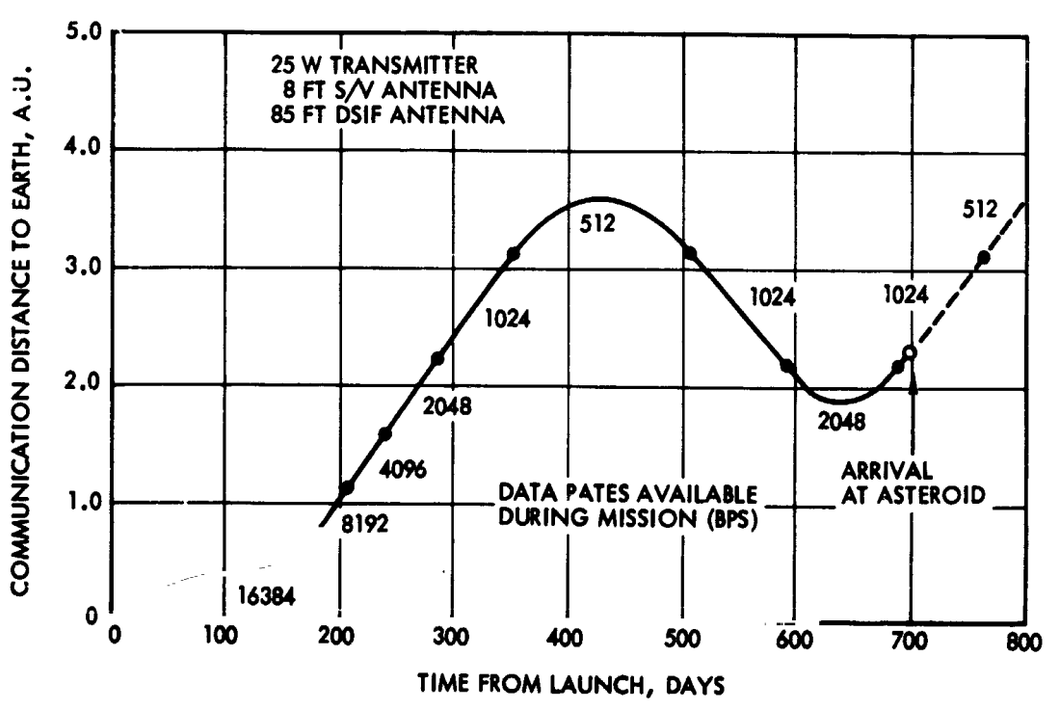

Figure 7-38. Ceres Rendezvous Mission (700 Days) Communications Distance and Bit Rates as Function of Time from Launch

We assume as first option the case of a system that provides telemetry for stage housekeeping plus science data during cruise and on arrival at Ceres. The average combined data acquisition rate, with a 2:1 data compression is estimated as 32 bps. The most severe demand is for image system telemetry in Ceres orbit at other times we estimate a lower data rate of 16 bps in orbit. We assume a tape recorder with 3.6×10^7 bits storage.

The table shows that at the time of greatest communication range, 3.6 AU, and at a data rate of 32 bps the transmission time to an 85-ft DSIF antenna at S-band is about 20 hours every 13 days, (in practice 10 hours every 6.5 days). If the 210-ft ground antenna is used at S-band (or an 85-ft antenna modified to X-band) only 2.5 hours of telemetry time would be needed every 13 days. The performance of the larger antenna at S-band is much greater than needed.

If the 85-foot ground antenna is used for high definition vidicon data the readout time per frame is excessive but it is assumed that the 210-foot antenna capability would be available at encounter, reducing the time per frame to about 5 minutes or roughly a quarter of the propagation time. When the vidicon is used in the low definition mode for navigation (star mapping) the data rate should be adequate with the 85-foot antenna.

Table 7-10 shows the total hours an 85-foot dish may be operating to support the Ceres mission from launch (when the limiting factor is the maximum data rate handled by the ground equipment) to encounter. If the 210-foot antenna is used after 260 days from launch the total support hours of the DSN could be reduced from 590 hours to 100 hours (30 hrs 85-ft and 70 hrs 210 ft).

The second option would be the case of a telemetry system that covers the stage housekeeping needs only. We assume that science data are not accruing from the payload during the transit phase and payload housekeeping functions are either minimal or handled by a separate system. We assume an 8 bps stage data acquisition rate. If the high-gain antenna is reduced in size from 8 foot (2.5 m) to 4 foot (1.25 m) then the downlink data rate is cut by 4 and the same telemetry intervals as those shown in Table 7-9 for an 8-foot dish are applicable.

Table 7-10. Theoretical Total Usage of the 85-ft Antenna System for Ceres Rendezvous Mission (up to Encounter)

Time from Launch (in days)	Maximum Communication Distance**	Data Rate	Hours per Transmission	Number of Transmissions	Total Hours
0 - 169	0.6 AU (0.48)	16,384	0.625	13	8.1
169 - 195	0.9 AU (1.105)	8,192	1.25	2	2.5
195 - 221	1.2 AU (1.56)	4,096	2.5	2	5.0
221 - 260	1.8 AU (2.2)	2,048	5	3	15
260 - 286	2.4 AU (3.12)	1,024	10	2	20
286 - 572	3.6 AU (4.42)	512	10	44*	440
572 - 700	2.4 AU (3.12)	1,024	10	10	100
				Grand Total	590.6

*at 6-1/2 day intervals

**Numbers in parenthesis show range at which margin becomes zero (taking into account the sum of negative tolerances). In practice it may be advisable to change to the next lower data rate before this point. The more conservative figures suggested allow a margin of just over 2 db.

7.4.3.5 The Use of the Electric Stage as a Communications Relay

In addition to the typical communications requirements some missions may have some special requirements, in particular those which may arise from the use of the electric stage as a communications relay. There are two possible modes of operation of the stage in this role, namely:

(a) Store and forward mode

(b) Direct relay

which are particularly useful for two specific missions. The store and forward mode achieves the greatest maximum capability between the stage and a "daughter" vehicle or probe for better comet exploration or to achieve time and spatial correlation of various events. In this mode the 2.5 meter antenna is pointed continuously at the "daughter" satellite or probe and receives data (from separation distances up to 10^6 km) which are stored in the tape recorder. The relay then intermittently turns its large antenna away from the probe and points it to

earth to transmit the stored data but does incur some loss of data while transmitting to earth. If this should cause problems in some missions the loss of data from the prime source could be minimized by use of the 210-foot ground antenna to permit a higher data rate transmission and hence a shorter period during which the relay is not receiving data from the probe. Figure 7-39 shows the data rates possibly transmitted from probe (assumed similar to Pioneer 6-9) to relay assuming a preamplifier or parametric amplifier mounted directly on the antenna feed horn to avoid cable losses. However to avoid severe thermal problems it may be necessary to place all active elements in the equipment compartment thus reducing performance by roughly 1-1/2 db (preamp) or 3-1/2 db (paramp).

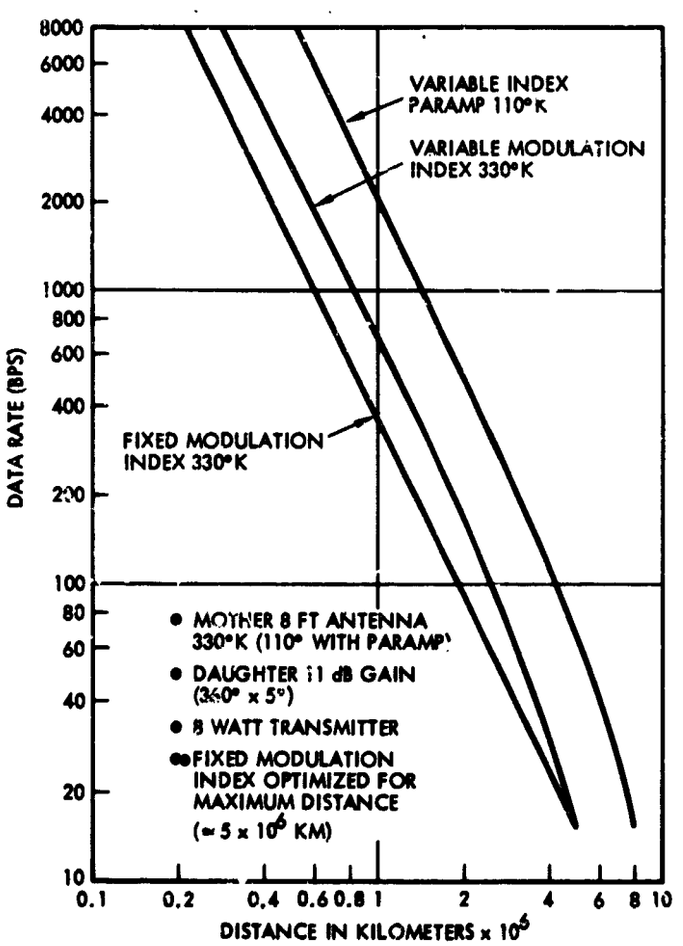

Figure 7-39. **S-Band Communications Capability - Daughter to Mother Spacecraft**

Direct relay without storage of science and vidicon data may be required (particularly from an asteroid lander) requiring a continuous link from the relay to earth and a separate link from relay to lander. In this case a second high gain antenna does not appear feasible and the use of a lower transmission frequency appears attractive, particularly at the shorter distances anticipated for the asteroid landing mission. Figure 7-40 shows the capability of the probe to relay link as a function of frequency for a number of antenna configurations at the probe and relay. Better noise figures and wider antenna beams are available at the lower frequencies but galactic noise is more significant. However data rates may be adequate for some missions at distances of 10^6 km at frequencies as low as 136 MHz. At the shorter distance of 10^3 km as expected for an asteroid landing mission, more than adequate performance can be obtained for direct transmission of vidicon pictures at 136 MHz using a 2 watt transmitter and a dipole on the lander and a 136 MHz dipole and receiver on the electric stage. The 2.5 meter antenna of the stage will be used to maintain contact to earth and in fact this link set the limit on data rate even when using the 210-foot ground antenna. The choice of 136 MHz for the lander to relay link appears most appropriate since it provides roughly optimum performance using single dipoles, and very efficient solid state amplifiers and a considerable amount of space qualified hardware are available at this frequency.

7.4.3.6 Choice of the Baseline Communication System

7.4.3.6.1 General

A review of the previous considerations enables a choice of the baseline communications subsystem to be made as shown in Figure 7-41 This configuration meets all of the mission requirements defined, uses a minimum of new development and consists of the following major items.

7.4.3.6.2 Antenna Subsystem

The antenna subsystem for the Category A missions (Para. 7.4.2.1) consists of two hemispherical coverage antennas ("aft omni" and "forward omni") coupled together to provide an approximation to isotropic

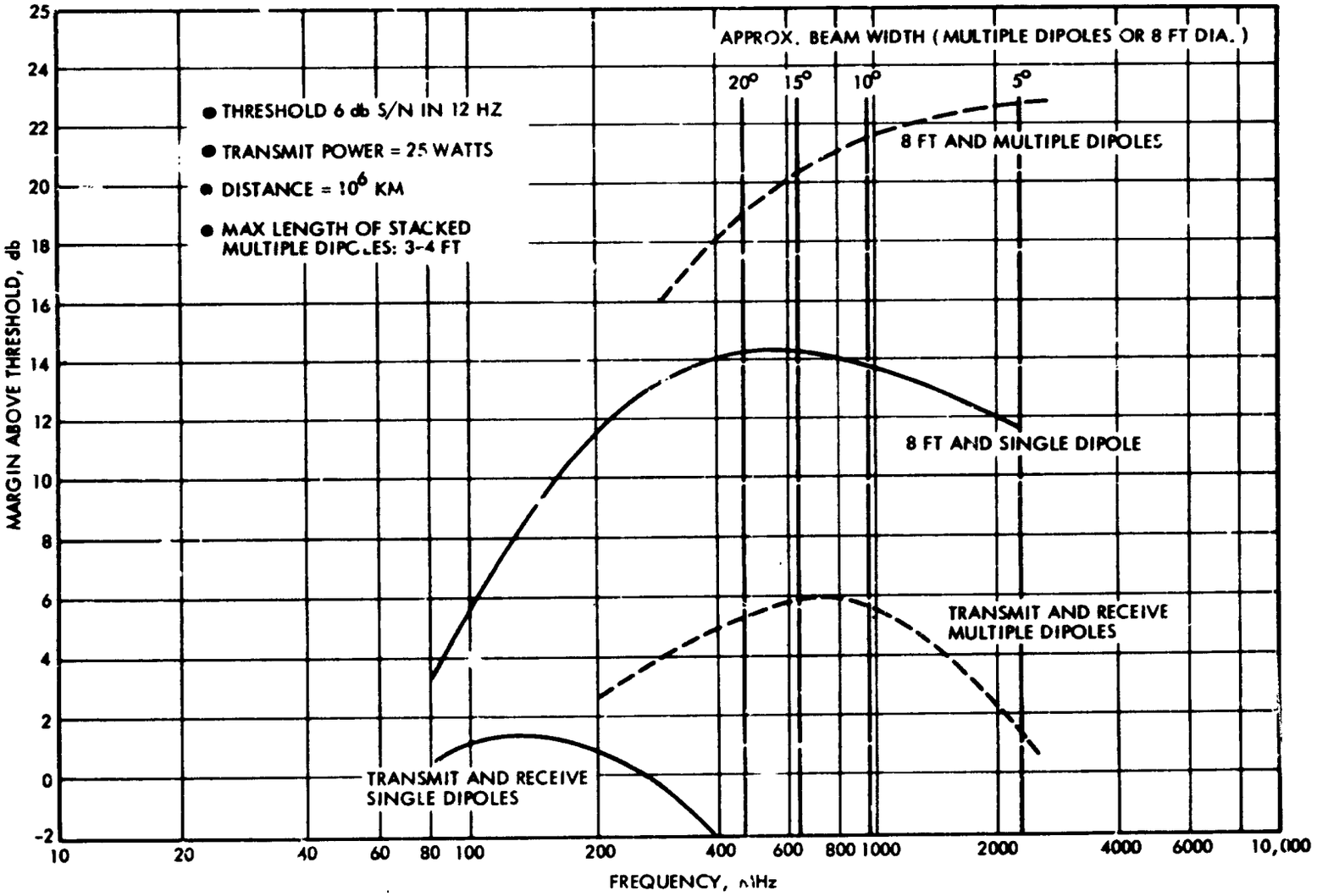

Figure 7-40. Mother-Daughter Relay Margin Above Threshold vs Frequency

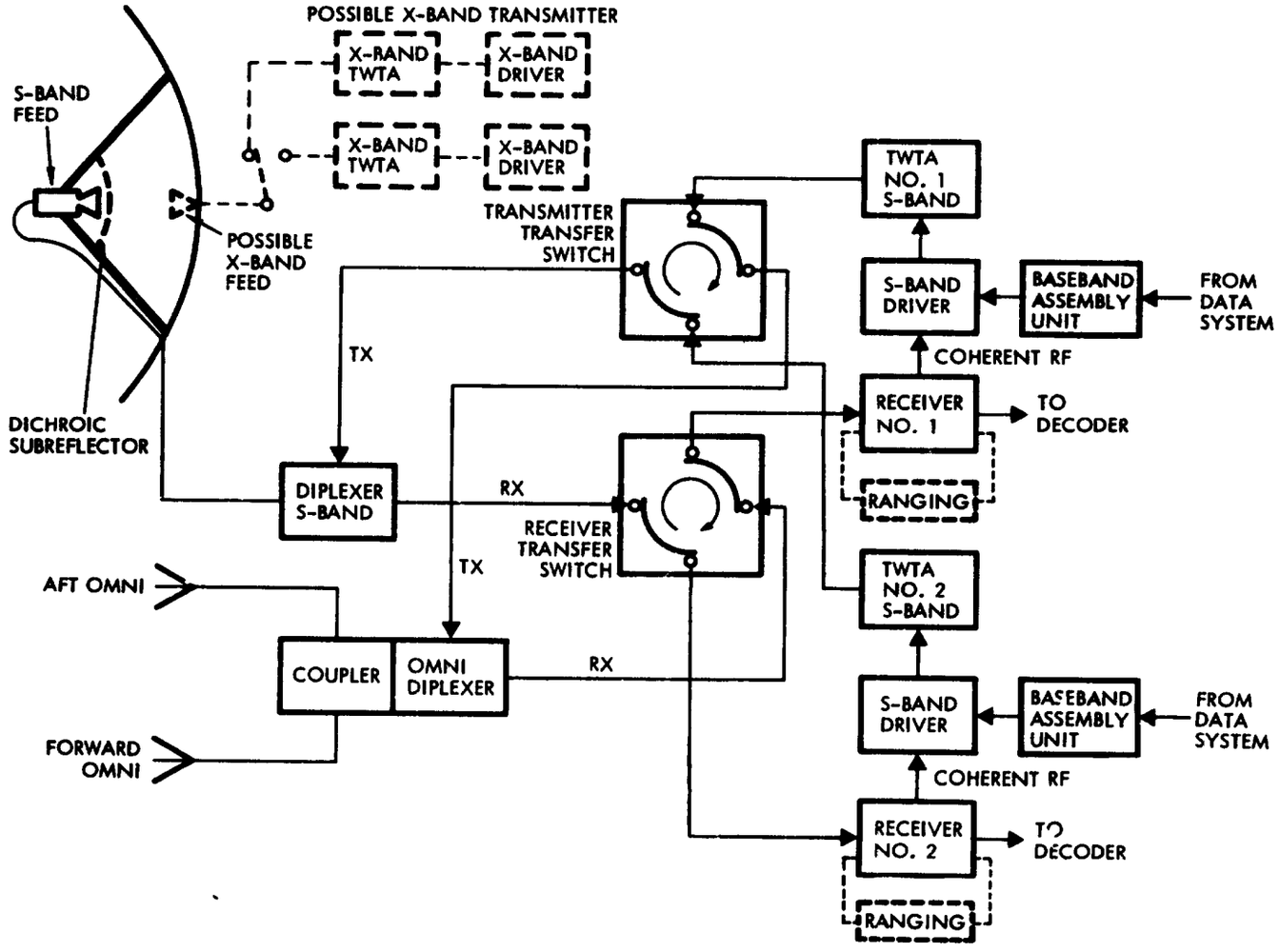

Figure 7-41. Communications Subsystem Block Diagram

coverage. The high gain 2.5 meter antenna uses a conventional paraboloid with an S-band focal plane which could be identical with the Pioneer F & G antenna without the offset feed and possibly with a different dish construction to minimize thermal problems if used for the Mercury orbiter and close-to-sun missions. Although an X-band downlink could increase data rate appreciably, in the missions envisaged its use is not justified particularly since the DSN is not presently contemplating an X-band capability for the 85-foot antenna. It appears that the latter can take most of the DSN workload for the electric stage missions and that the 210-foot antenna capability at S-band is adequate when the use of the larger ground antenna is required.

However it may be worthwhile (in order to increase stage versatility) to make provision for adding an X-band capability by building the 2.5 meter dish with adequate tolerances and so that a dichroic reflector and S-band feed could be added in a Cassegrain configuration. The receiver and transmitter transfer switches and the diplexers would be similar to those used in the Pioneer F & G spacecraft but would be rated for S-band operation at the 25-watt power level.

The 1.25 meter antenna subsystem used in Category B missions (Para. 7.4.2.2) would be the same apart from the high-gain dish which in addition to its smaller size and possibly different feed configuration, would not be capable of the addition of an X-band capability in a Cassegrain configuration since the size of the subreflector would be too great and cause loss of gain and considerable secondary pattern degradation. It is assumed that in either case the antenna will be pointed with $\pm$ 1 degree accuracy by commands from a stored (and updated) program of sun-probe earth angles, appropriately compensated for stage attitude variations.

7.4.3.6.3 Receiver Subsystem

Two redundant S-band receivers are used in a similar configuration to that of the Pioneer F & G communications subsystem. The Pioneer receivers are adequate for commands under emergency conditions using the stage omni-antennas and the 210-foot ground antenna system. If range measurement is required under routine (non-emergency conditions) however some improvement of receiver noise figure is required

even when the high gain antenna of the electric stage is used. Thus, unless the 210-foot antenna can be used for routine range measurements a low noise (3 db) transistor preamplifier may be needed, or 10 kw ground transmitters at the 85-foot antennas may require increased power.

7.4.3.6.4 Transmitter Subsystem

Table 7-11 shows a list of candidate traveling wave tubes some of which are supplied as a traveling wave tube amplifier (i.e., a TWT and high voltage power converter in a single package). The WJ-1171-1 is designed for a 3-year life and high overall efficiency but has inadequate output power. The Hughes 394H TWT approaches the minimum output power requirement but it also suffers from low efficiency. The WT-1171-2 is a higher power model (24 watts) of the TWTA developed for the Pioneer F/G spacecraft and thus also designed for long life and high reliability. Insufficient life test data has yet been accumulated but it is expected to be fully space qualified in the near future.

Table 7-11. Candidate TWTs and TWTAs

Type	Power Output Watts	Overall Efficiency Percent	Advantages	Disadvantages
WJ-1171-1 (TWTA)	9	33.6	Proven reliability	Low power output
Hughes 394H (TWT)	20	33 (tube only)	Space qualified Accumulated 264,153 hours of life testing on 8 tubes Used on Apollo and TACSAT	Uses 1960 design and construction techniques Low efficiency
WJ-1171-2 (TWTA)	24	36.8	6-year design life Some life test data available	Insufficient life test data and actual space experience Moderate output power
WJ-395 (TWT)	100	47 (tube only)	Qualified and flown on Saturn V rocket High power output High efficiency	Limited life test data Not yet space qualified Early tubes unstable under high power conditions

The 100-watt WT 395 TWT offers high power and efficiency but limited life test data as yet, although the early instability problems appear to have been solved and it is believed that adequate life test data will soon be available. The WJ-1171-2 appears to be the optimum choice for the baseline design but there may be some advantage in planning for eventual

use of the 100-watt TWT for later missions since the WJ 395 appears to have considerable potential as a dual level output power tube without a severe drop in efficiency at the lower output level.

The exciters for the Pioneer F&G are designed to drive a 9-watt tube with a gain of 32 db. The WJ-1171-2 however will require an increased drive power of about 7 db to compensate for the higher output power and the slightly lower gain compared with the WJ-1171-1. Thus the exciters will require some modification, which may consist of an additional low power amplifier transistor stage.

7.4.3.7 Data Handling Subsystem

7.4.3.7.1 General

The data handling subsystem must accept and process data from science instruments and propulsion and other engineering subsystems. Selectable modes of operation and formats are required to support all mission phases and a variety of science and housekeeping needs. The subsystem is required to perform the following functions:

- Accept and multiplex all analog, discrete and digital signals from the payload and engineering subsystem.
- Condition and encode data into digital word format.
- Store data in tape recorders and core memory.
- Detect and decode commands (for transmission to the command distribution unit.)

The range of information rate to the data handling subsystem varies from 8 bps to 16,000 (Table 7-8) and the data rate transmitted to the DSN from 8 bps to about 16,000, the maximum which the DSN data processing can manage using the bio-orthogal code (Ref. 7-15). Moreover it is not considered economical to require constant support from the DSN ground station. The data handling system must thus be very flexible.

Figure 7-42 shows a functional block diagram of the recommended data system illustrating the wide variety of inputs it may be called upon to handle. Note that many of the units may be combined in practice for engineering reasons but are shown separately in the block diagram, to emphasize function. Since the amount of bulk storage required makes

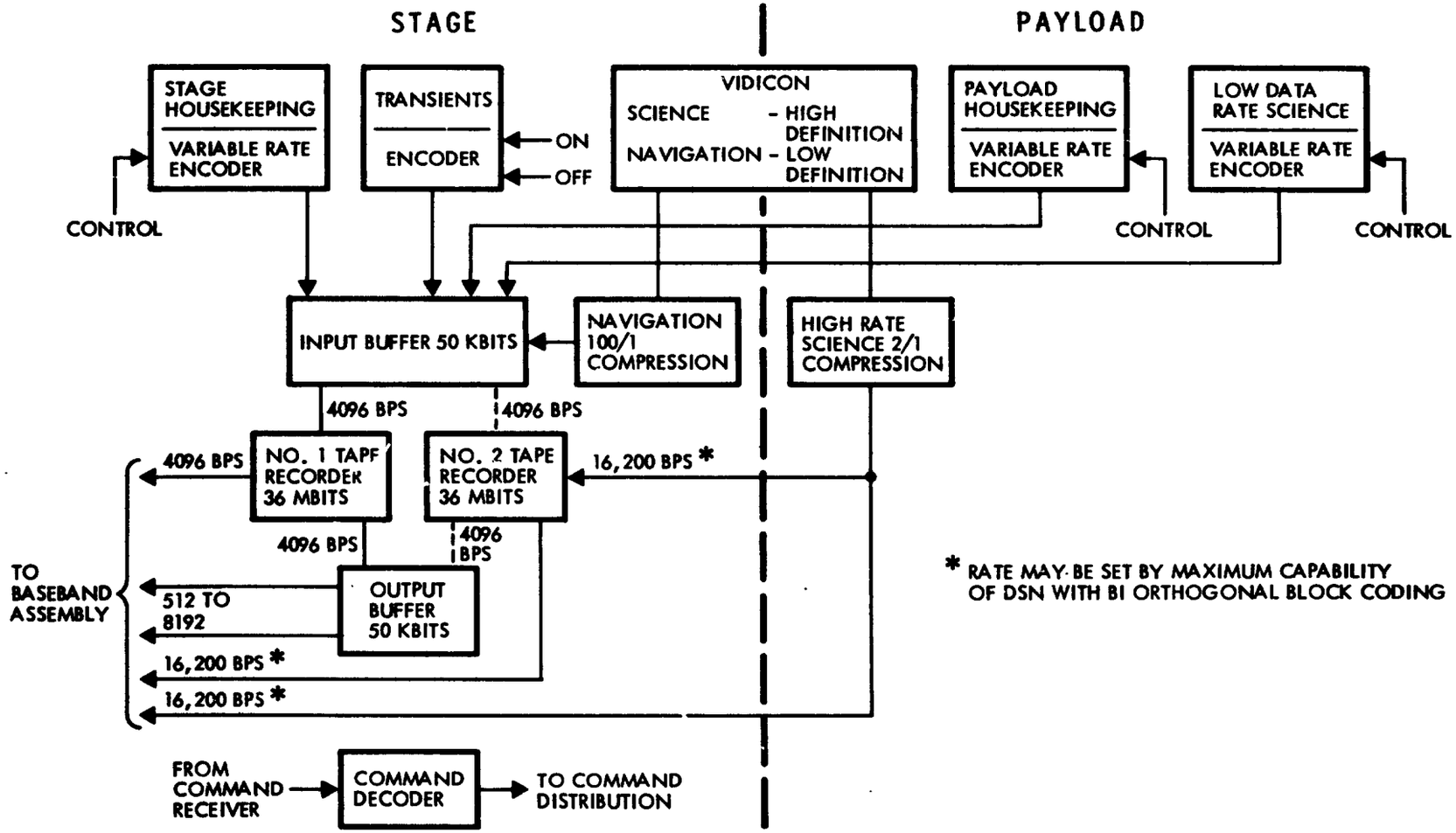

Figure 7-42. Functional Block Diagram of Data Handling Subsystem

tape recorders essential the first concern is in the design of a tape recorder of sufficient reliability to survive a two-year mission. Ideally the tape transport should require only a single speed record and read-out drive in spite of a wide range of information rates. Moreover the machine should not have to run continuously for the whole mission or at a very low or high tape speed. By using input and output buffers the design of the tape recorder is simplified and reliability increased. As can be seen from Figure 7-42, payload and stage housekeeping and transients and low rate science data are encoded and fed into the input buffer. The Pioneer F&G storage unit chosen for its low weight, size, and power consumption may be filled in from 30 minutes to 2 hours in the absence of a start or turn-off of the ion engine. If repeated starts and stops of the ion engine are expected for a particular mission it may be advisable to bypass the input buffer and record the transients directly on tape at a speed of 16-1/4 cm/sec. High data rate vidicon data is compressed 2 to 1 and forwarded to the base band assembly unit directly for transmission to earth or recorded on tape without buffering in the output storage. If the vidicon is used as a star mapper for navigational purposes the data may be compressed as much as 1000 to 1 and transmitted directly or stored directly on tape or through the input buffer.

The input buffer, when full, is read out in about 12 seconds onto tape at a recording speed of 16-1/4 cm/sec (or 4096 bps). When the first tape recorder is full, data is stored in the second tape machine and the data in the first recorder is transmitted to earth at the first opportunity. The second tape machine is also used for redundancy and to record vidicon data while the first is being used to store low rate science data.

The stored data is transmitted at a 4096 bps rate directly from tape to an 85-foot antenna at distances less than 1.2 AU (or beyond if the 210-foot antenna is used) but otherwise the taped data is transferred via the output buffer at the appropriate data rate.

High definition vidicon data is recorded at 16,200 bps directly onto tape and can be played back to a 210-foot ground station at the same tape speed (65 cm/sec) from a distance of 1.4 AU (e.g., Mercury orbiter).

At greater distances the tape is read out at a rate of 4096 bps using the slower tape speed of 16-1/4 cm/sec. The tape recorder thus requires two tape speeds 16-1/4 cm/sec (4096 bps) and 65 cm/sec (16, 200 bps) in each direction. If rapid transfer of high definition vidicon data onto and from tape is not required a single tape speed (16-1/4 cm/sec for 4096 bps) could be used. Alternatively the other tape speed could be 4-1/16 cm/sec to permit direct readout from tape at 1024 bps to an 85-foot ground station at distances up to 2.4 AU.

7.4.4 Required Technology Improvements

7.4.4.1 Communications Subsystem Improvements

The communications subsystem has been configured to avoid the necessity for major technology developments. The majority of the components required are in existence already or require small modifications. For example, an increase of output power of the exciter used for Pioneer F&G to drive the higher power TWTA and a better noise figure in the receiver. However many of the Pioneer F&G components may be used without modifications but will require qualification at the higher power level.

7.4.4.2 High Gain Antenna Design

The high gain antennas, 2-1/2 meter and 1-1/4 meter in diameter for the two mission categories could be of conventional design for the majority of the missions. However in the stages which will approach more closely to the sun (e.g., Mercury orbiter and solar probe thermal problems will be severe and may be intensified by shadowing effects. The use of a mesh construction for the paraboloid would reduce thermal problems to the antenna itself by reducing the amount of solar energy directed towards the feed and also help to minimize solar cell thermal gradients by reduction of shadowing effects. A mesh size of 0.2" using 0.005" diameter wire appears feasible at S-band and could reduce the thermal problems of the antenna feed and the solar cells.

7.4.4.3 All Solid State S-Band Transmitter

Remarkable reliabilities have been achieved by travelling wave tube amplifiers, but it is felt that even better reliability could be obtained

from all solid state transmitter output stages. All solid state transmitters of 15 watts output and 25% efficiency have been demonstrated at about 2.6 GHz with inherently better reliability than can be expected from tubes using high voltage power supplies. A number of devices may be operated in parallel with diode switches permitting the disconnection of a particular chain to avoid loading the others. This feature can be used to provide operation at several power levels if available prime power varies during a mission, or to allow graceful degradation in the event of a failure of one chain. A possible configuration is shown in Figure 7-43 which could conveniently provide 25, 12-1/2 or 6-1/4 watts. The efficiency of existing transistors is not as good as in the best available tubes and the significant drive power required (because of the low gain of 5-7 db) reduces the overall efficiency to about 17-1/2%. Improvements to 40% efficiency per stage and 7-10 db gain have been obtained recently at 2.3 GHz with a corresponding increase of overall efficiency to about 25%. This value is still not fully competitive with the best TWTAs but offers a much lighter and more reliable alternative, particularly in many electric propulsion missions where prime power consumption is not quite as critical as in corresponding conventional propulsion systems.

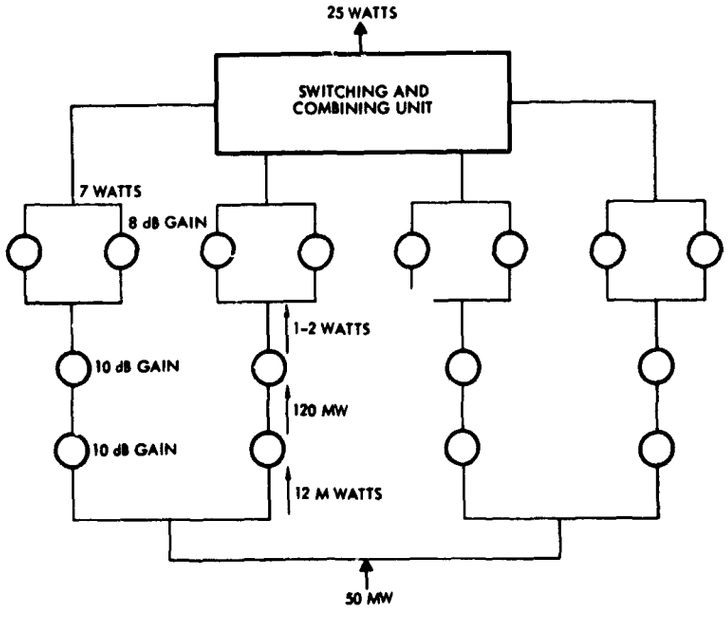

Figure 7-43. Outline Configuration of a 25-watt Transistor Amplifier Using Existing Circuits

7.4.4.4 Data Handling Subsystem Improvements

This subsystem also makes use of previously developed components such as the existing Pioneer F&G buffer storage units, and it is probable that existing telemetry encoders and command decoders can be used with little modification. Data compression techniques for television type images have been extensively developed and magnetic tape recorders of adequate capacity also. However there are no present tape recorders with adequate reliability for the mission durations contemplated and some development in this area is required. It should be noted that the subsystem has been configured with input and output buffers and a dual speed machine (with a 4 to 1 speed ratio) for record and playback in spite of a wide variety of input and output data rates. This system in fact could use a single speed machine if there was no requirement for fast recording of the high definition vidicon data. It is expected that the avoidance of the requirement for multiple speeds will considerably ease the design problems of a very high reliable tape recorder.

7.5 ELECTRICAL DISTRIBUTION SUBSYSTEM

The electrical distribution subsystem accomplishes the electrical integration of the various subsystems into the total stage. This subsystem consists of an Electrical Integration Assembly (EIA) and the Stage System Electrical Wiring Harness Assembly. The functions performed by this subsystem include:

- Decoding and processing of all ground commands
- Conditioning telemetry signals
- Providing undervoltage protection
- Controlling and distributing primary and secondary power
- Providing safe/arm and fire control for all ordnance devices
- Interconnection of all stage signals and power interfaces.

The subsystem hardware required to accomplish these functions is derived from units utilized on previous TRW spacecraft programs to the maximum possible extent to minimize both the engineering design costs and the development risk.

7.5.1 Electrical Integration Assembly (EIA)

The electrical integration assembly provides three types of command outputs to the users:

- Discrete commands in which an individual function is accomplished by each command.
- Serial commands which contain a serial stream of command data bits allowing ground input of data as required by the subsystem.
- State commands in which relay contacts accomplish an individual function.

The electrical integration assembly included as part of the electrical distribution hardware provides the following capability:

1) Perform unit address checks on all received commands
2) Perform a check on command validity

3) Route commands to the appropriate user.

4) Transfer data commands in a serial fashion to specified using units.

5) Condition discrete commands into a form compatible with the using unit.

6) Provide sequencing of certain commands after separation from the launch vehicle.

7) Provide conditioning of telemetry signals originating either within the distribution subsystem or other subsystems.

8) Distribute primary power to all stage users except the electric propulsion subsystem.

9) Provide secondary power to certain units.

10) Undervoltage protection.

11) Clear faults in power processing equipment.

Spacecraft Address Check Because of the possibility of several satellites or spacecraft being within the range of a ground station, it is necessary to prevent undesired commands from entering the system. This is accomplished in the circuitry included to verify the spacecraft address. To permit each unit to be fabricated in an identical manner, the identification for a particular stage is accomplished within a dummy connector attached to the EIA allowing a selection of one of eight possible addresses. Implementation of this circuitry consists of a series of flip-flops, the state of which is set by the first three bits of the command. This forms a pattern established in the dummy connector and checked in an enabling gate. Since the parity of a command may vary as a function of the stage address, it is necessary to include the capability of varying the command parity for each stage. This is also accomplished by a connection routed through the dummy connector allowing standardization of odd parity for all stage commands. Figure 7-44 stage address detection implementation depicts this approach.

Command Verification - Upon receipt of an enable signal from the command demodulators, a clock counter in the EIA is reset. This counter, by counting the individual command pulses, verifies the length of the command message. At the same time, the counter provides outputs utilized in circuitry associated with the stage address check, the routing address

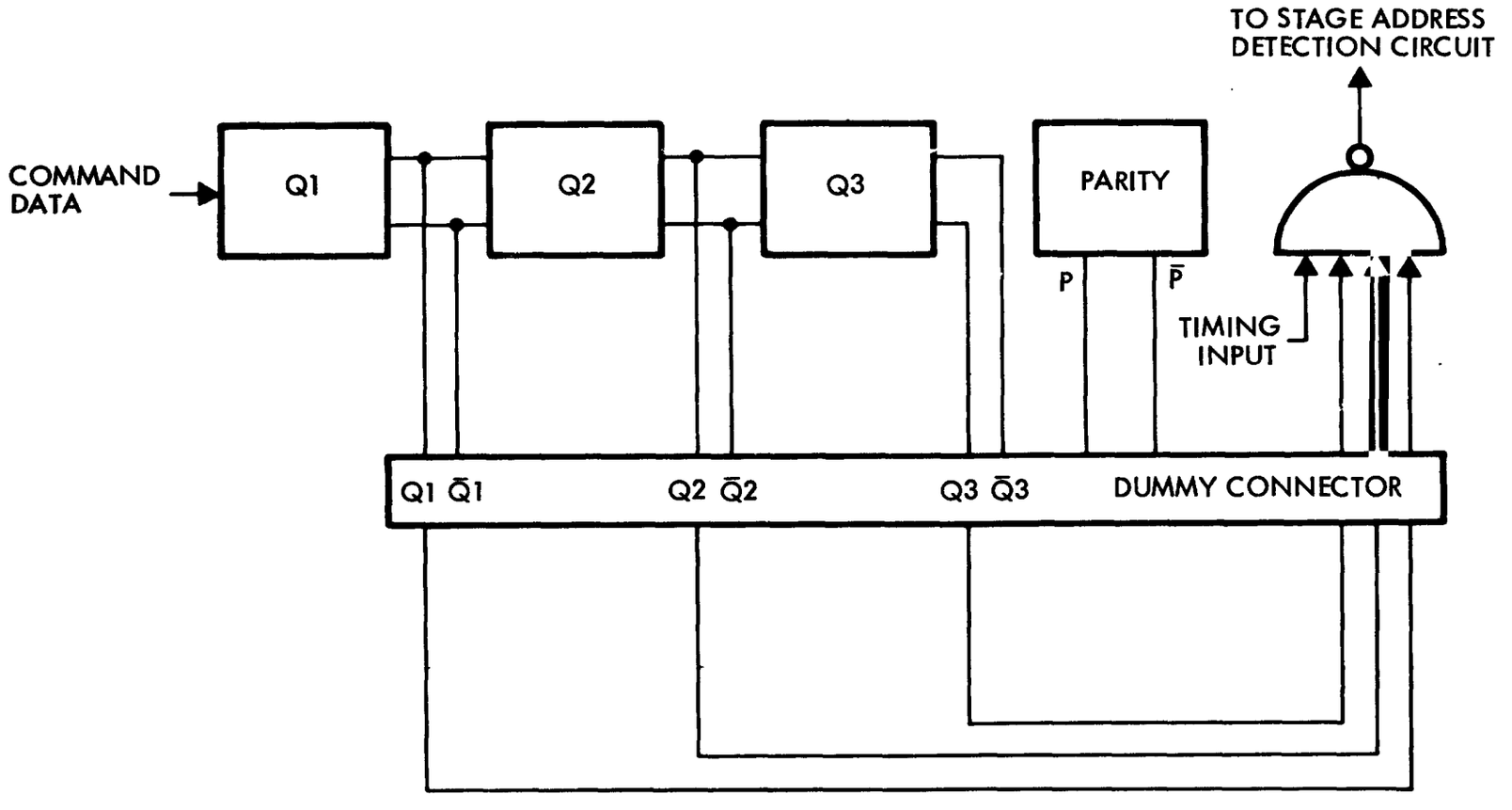

Figure 7-44. Stage Address Detection Implementation

check, the command register control, and the parity check. The parity check is accomplished by a flip-flop which counts the number of logic "ones" contained in the command message. At the end of the command message, the flip-flop must be in a specified state identifying the fact that an odd parity message was received. On successful verification of:

A) The number of command pulses,

B) The parity of the command.

C) The command message length and,

D) The stage address,

an execute signal is generated that enables the further processing of the command within the EIA. Figure 7-45 illustrates the command verification technique.

Routing Address Check - The routing address consists of 5 bits in the command format. The first of the 5 bits determines whether a command is to be routed to the Computer and Sequencer for future execution or whether it is to be routed to the processing circuitry for immediate execution within the EIA. For real time commands the remaining 4 bits are decoded by the routing address circuitry. The output of the flip-flops utilized in the decoding process provides an input to an enable circuit. The enable output is routed to the intended user of the command allowing power gating of the interfacing circuitry. In the case of serial data commands, the data bits are transferred to the user without further processing in the EIA. In addition to the enable and data lines, the electrical integration assembly provides a clock line to the user to permit synchronization of the serial data transfer. The enable signal starts just prior to transfer of data and lasts until completion of the transfer to the user.

Discrete Command Processing - For discrete commands, the enable signal is routed to a buffer register where the command data is stored for decoding into various forms of discrete outputs. Decoding is accomplished by a series of first level gating which in turn drives second level gates, the output of which are low level discrete commands. These low level discretes may be used as outputs to other units directly or may be used internally in the EIA as an input to buffers and amplifiers to provide the necessary power amplification to perform such functions as energizing relay coils, activating ordnance functions, etc.

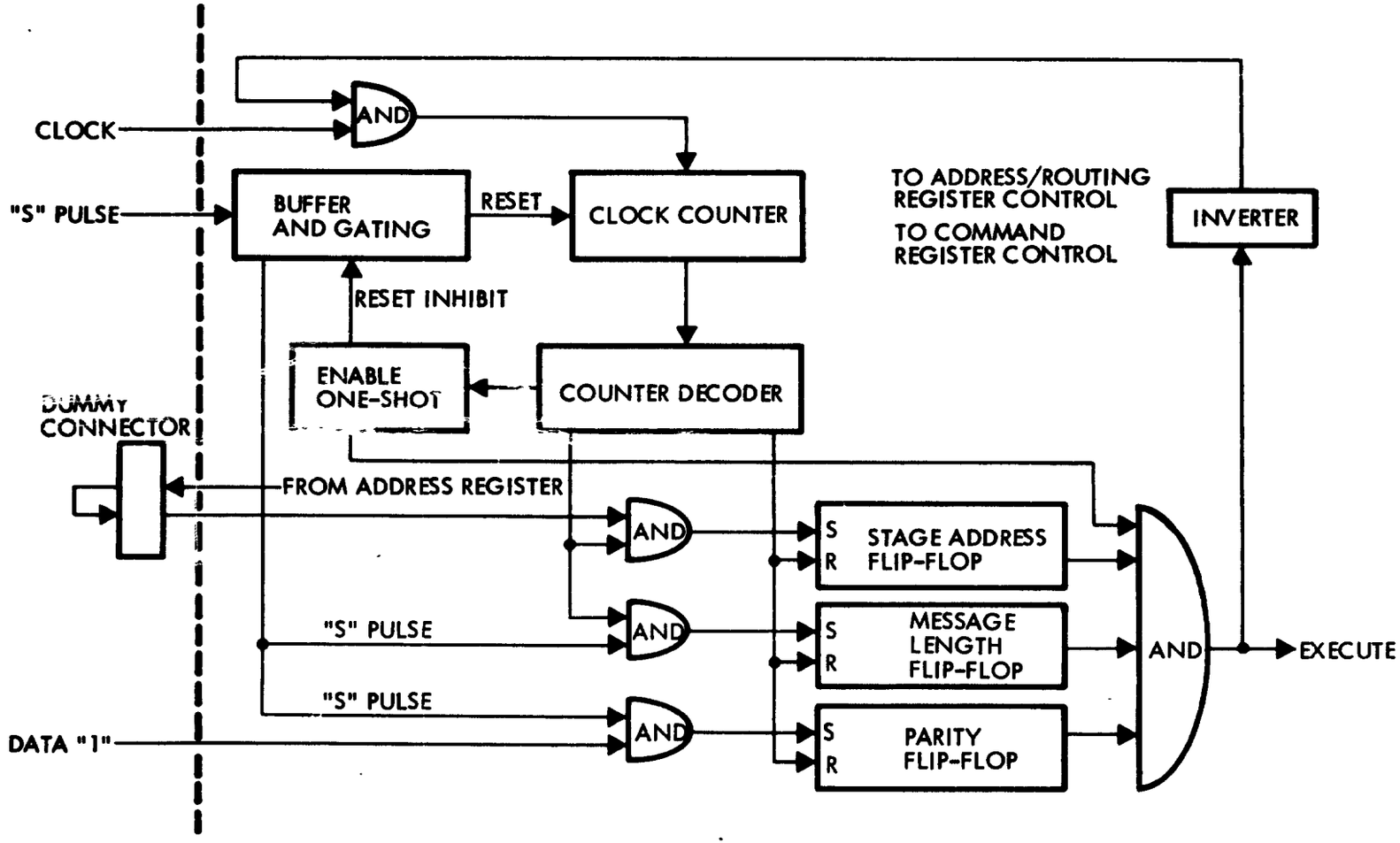

Figure 7-45. Command Verification Block Diagram

State commands generally are relay contact closures and have a set of contacts utilized to provide position status for telemetry. The execution time of other discrete commands is too short to allow real time monitoring of the command on telemetry. For specified critical commands the low level pulse may be routed to a flip-flop for storage until the telemetry indication can be read out.

In addition to the command functions discussed, the electrical integration assembly (EIA) contains ordnance firing circuits, redundant converters, signal conditioning circuits, and command sequences.

Ordnance - The EIA provides the ordnance firing circuits for the stage. This includes safe/arm functions implemented with latching relays and ordnance fire functions with momentary contact relays. The actual firing circuits contain a current limiting resistor to protect the stage power bus. This resistor opens the ordnance device shorts after the application of power through the non-latching firing relays. Redundant arm/safe and firing circuits are utilized. To satisfy Eastern Test Range safety requirements and to provide access for ordnance firing circuit testing, an ordnance inflight jumper connector is incorporated on the stage.

During ordnance testing, a mating connector is used which simulates a short circuit of the ordnance device or simulates an ordnance load for the firing circuits. For flight, a second mating connector is used to connect the EIA to the ordnance devices.

Converter - Redundant power converters are located in the electrical integration assembly that accept unregulated +28 VDC power and converts part of it to $\pm$ 15 VDC and +5 VDC. The command link elements (receivers, demodulators, and electrical integration assembly) are hard wired to the converters.

Signal Conditioning - Signal conditioning for telemetry includes bilevel status indication for power switching, ordnance relay contact position, solar array position, and separation switch positions. Also analog signals are conditioned such as temperature sensors.

Sequencer - The sequencer is initiated by separation switches and provides multiple time sequenced command outputs during early phases of the mission.

Undervoltage Protection - The EIA contains circuitry to protect the stage main bus in the event of a malfunction. The stage power supply has a main bus sensor and if the main bus voltage reaches 22.0 VDC $\pm$ 0.5 volt for 100 milliseconds, a signal is sent to the EIA. Upon receipt of this signal, the EIA turns off all non-essential loads automatically. The only stage equipment remaining on in an undervoltage condition are:

A) Command receivers (2)

B) Command demodulators (2)

C) Electrical integration assembly

This permits the command link to remain operative. As the stage bus increases in voltage, the non-essential loads can be turned on by ground command. In the event of a failure in the undervoltage sensor in the stage power supply, ground commands are available to inhibit and/or override the undervoltage control feature.

Fault Clearing - In the event that a fault occurs in the power processing equipment for the thrusters or stage, it will be necessary to utilize some type of isolation switch to prevent the solar array from overloading. In the past, on lower power spacecraft, it was possible to use fuses to solve this problem. Unfortunately, the peak power levels are in excess of existing hardware limits. In addition as a result of the great variation in power level, it may not always be possible to have enough current available to have enough current available to blow a fuse. As a result, it will be necessary to utilize high voltage, high power conventional relays or gate assisted SCR solid state switches. At the present time neither of these devices are in a flight qualified status.

7.5.2 Stage System Electrical Wiring Harness Assembly

The stage electrical harness is designed to distribute power and signals to the various stage units continuously with no degradation of performance. Cable routing and construction will employ proven TRW techniques to minimize electromagnetic interference. Among these techniques are:

- Termination of exposed shields to the connector shell or standard back shell by using conductive epoxy and/or "Halo rings".

- Termination of exposed shields to a special RFI type connector, using circumferential shielding, for ordnance and other noise-susceptible circuits.

The harness consists of a main trunk with multiple branches of standard insulated wires soldered or crimped to subminiature connectors. The optimum routing of the harness will be developed on a spacecraft mockup.

The components in the cabling hardware are current TRW non-magnetic specification parts, having a proven performance record on previous deep space missions. The cable utilizes solder type and crimp type "D" series subminiature and circular miniature connectors throughout. All harness connectors are potted with semi-flexible compounds to provide wire-to-wire insulation resistance, to protect against entry of contaminants which can cause shorting or arcing, to retain contact float characteristics and to provide increased reliability and stress relief.

A power inflight jumper connector allows opening the lines between the load and the electrical power subsystem to permit application of power to the main bus during ground test operations. During system tests, bus power measurements are made at this connector interface. The inflight jumper connector also provides a means of de-energizing the stage power bus when necessary.

The ordnance harness utilizes twisted shielded wire to maintain electrical balance and to minimize inductive pickup. Continuous circumferential shielding is used, grounding to structure at both ends and containing no electrical discontinuities.

7.6 THERMAL CONTROL SUBSYSTEM

The design objectives of the thermal control subsystem is to satisfy the following stage temperature requirements with a reliable, light, cost-effective system that will meet all missions with as little modification as possible:

- Maintain propulsion module unit temperature between 70 and -55°
- Maintain equipment module unit temperatures between 40 and -20°C
- Maintain solar arrays below 175°C (welded connection) or 120°C (soldered connection)
- Maintain ion engines, antennas, and other external equipment within their respective temperatures

The design must provide adequate temperature control for both outbound and inbound missions. The only problem associated with the outbound missions is the heater power required to maintain equipment above minimum temperature limits during the cruise mode. Inbound missions pose significant thermal control problems, however. Orbits about Mercury at the anticipated low periapsis altitude of 500 km will subject the stage to sizable planetary radiation and albedo heat in addition to the solar heat. Solar probe missions within 0.1 AU will subject the stage to solar radiation heat that will require a stage shadow shield and specific stage orientation with respect to the sun.

7.6.1 Design Approach: Inbound Missions

Since the inbound missions pose the most difficult problems, thermal control for these missions is discussed first in terms of the elements of the stage.

7.6.1.1 Equipment Module and Propulsion Module

As shown in Figure 7-46, the equipment and propulsion modules are insulated with multilayer aluminized Kapton insulation blankets and structural thermal isolators. Individual louvered radiating surfaces are located on the shaded side of each module. The louvered surfaces are sized (using open emittance) to maintain unit temperature below maximum limits under maximum heat dissipation conditions. The

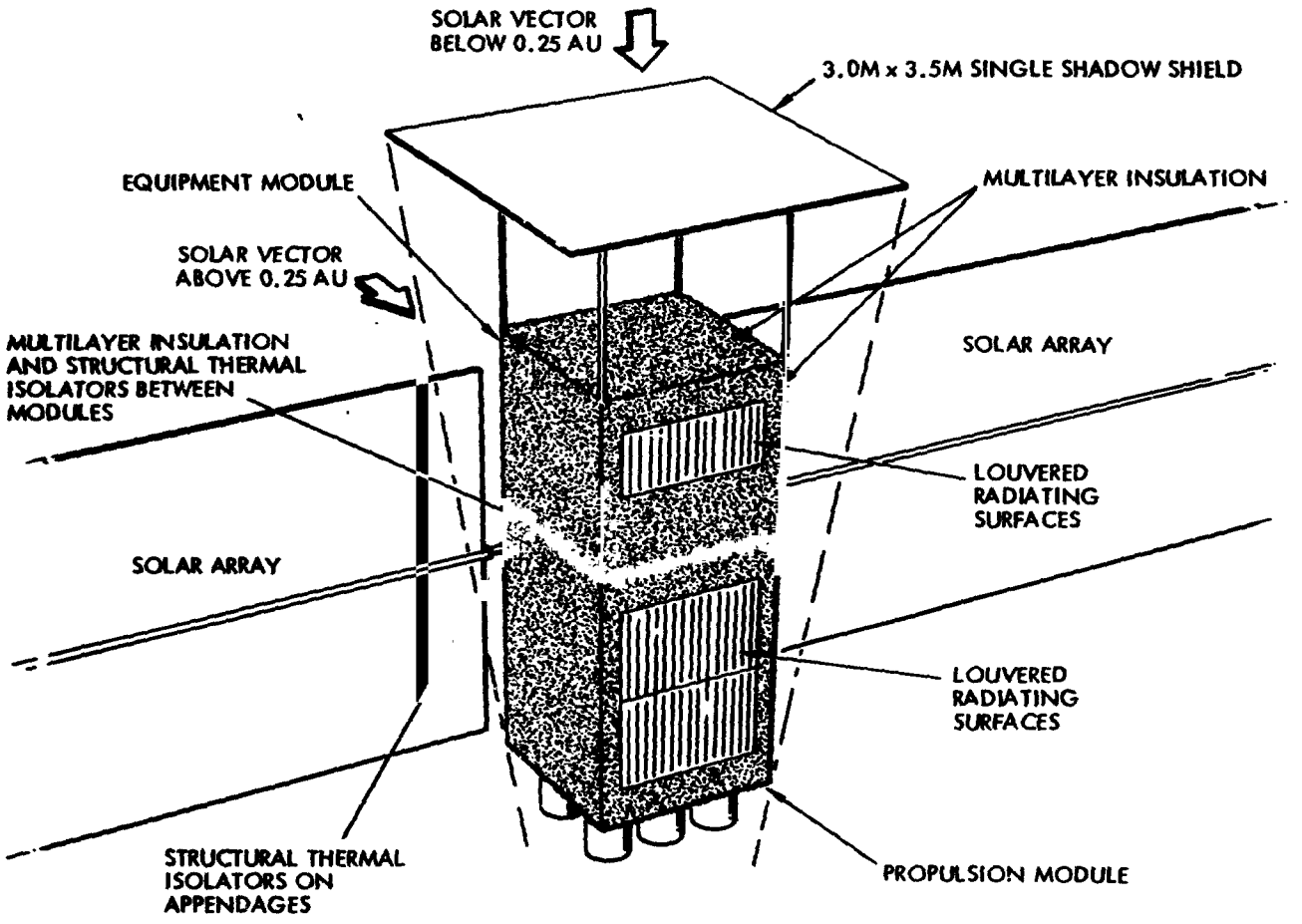

Figure 7-46. Thermal Control Design

propulsion module requires 3.0 m^2 of louvered radiating area, the equipment module 1.15 m^2.

Propulsion module heaters (50 watts) maintain unit temperatures above minimum limits during nonoperating conditions. Heaters are not required on the equipment module under minimum heat dissipation conditions. Louvers are used on all radiating surfaces to reduce heater power requirements. This reduces the thermo-electric power module size, cost, and weight that is required for inbound missions below 0.25 AU when the solar array must be retracted behind a shadow shield.

7.6.1.2 Solar Arrays

Close contact is established between solar cell and substrate to enhance heat transfer to the aft side of the solar array (minimum adhesive thickness, maximum contact area). The solar array requires rotation relative to the solar vector starting at 0.57 AU (maximum rotation 80 degrees) to maintain maximum solar array temperatures below 175°C (welded connections) or starting at 0.72 AU (maximum rotation 83 degrees) to maintain maximum solar array temperatures below 120°C (soldered connections). To maintain the temperature at 140°C (soldered connections) in the actual design, as discussed in Section 7.1, rotation must start at 0.65 AU. Below 0.25 AU the solar arrays are rolled up and stowed behind a stage shadow shield. See Figure 7-47.

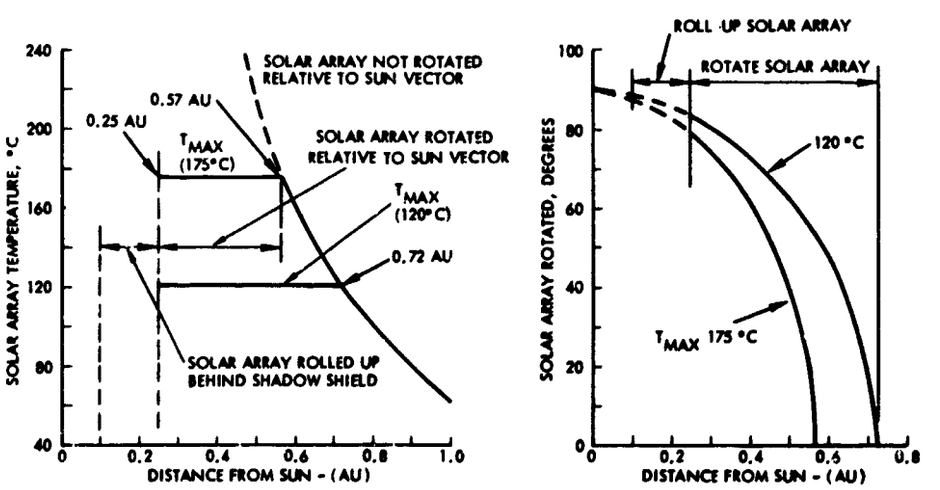

Figure 7-47. Solar Array Temperature vs Solar Distances and Required Array Rotation (Inbound Missions)

7.6.1.3 Ion Engines

The ion engines are arranged in a hexagonal array, with only three engines nominally firing, interspersed with cold engines. However, after an engine failure or with maximum power available during inbound mission two or more adjacent engines may be operating simultaneously. Under these worst-case heating conditions local high temperatures may reach 295 to 320°C. Use of permanent magnets rather than electromagnets makes this condition acceptable. A low solar absorptivity (α) and high emissivity (ϵ) coating is applied to the external surface of the engine to minimize absorbed solar heat and maximize radiant heat to space (α = 0.2, ϵ - 0.85, Z-93 high temperature white paint). The stage is oriented to place engines in the shadow of the stage or shadow shield for inbound missions below 0.25 AU to maintain nonoperating engine temperatures below maximum limits. Without shielding, the nonoperating engine temperature may rise well above 250°C, as shown in Figure 7-48.

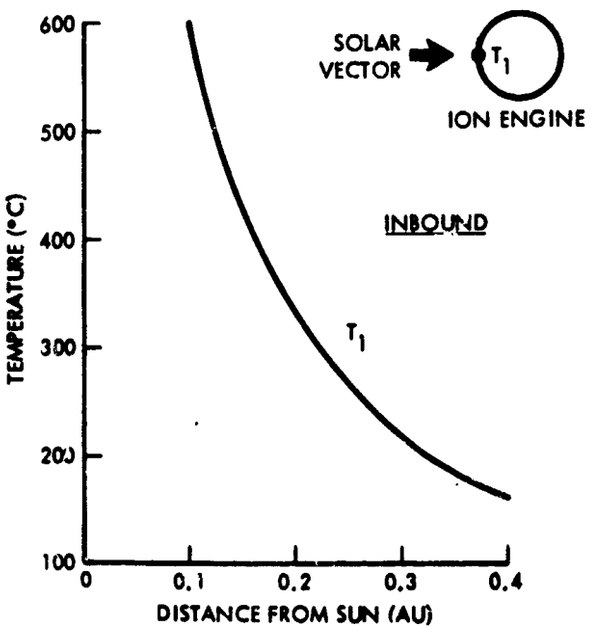

Figure 7-48. Maximum Temperature of Ion Engines, Not Operating, Inbound

7.6.1.4 Antenna

A mesh antenna is essential to reduce:

- Blockage of the propulsion and equipment module louvered radiating surfaces

- Solar array shading in tilted body orientation
- Heat focusing on the antenna feed

The mesh is formed of stainless steel wire coated with silver and covered with an 0.001-inch thick teflon sleeve. This combination produces a low solar absorptivity ($\alpha = 0.15$) and high emissivity ($\epsilon = 0.6$). The stainless steel and teflon combination mesh will withstand temperatures in excess of 260°C without degrading thermally, allowing the antenna mesh to be positioned in the sun continuously for distances as close as 0.15 AU. See Figure 7-49.

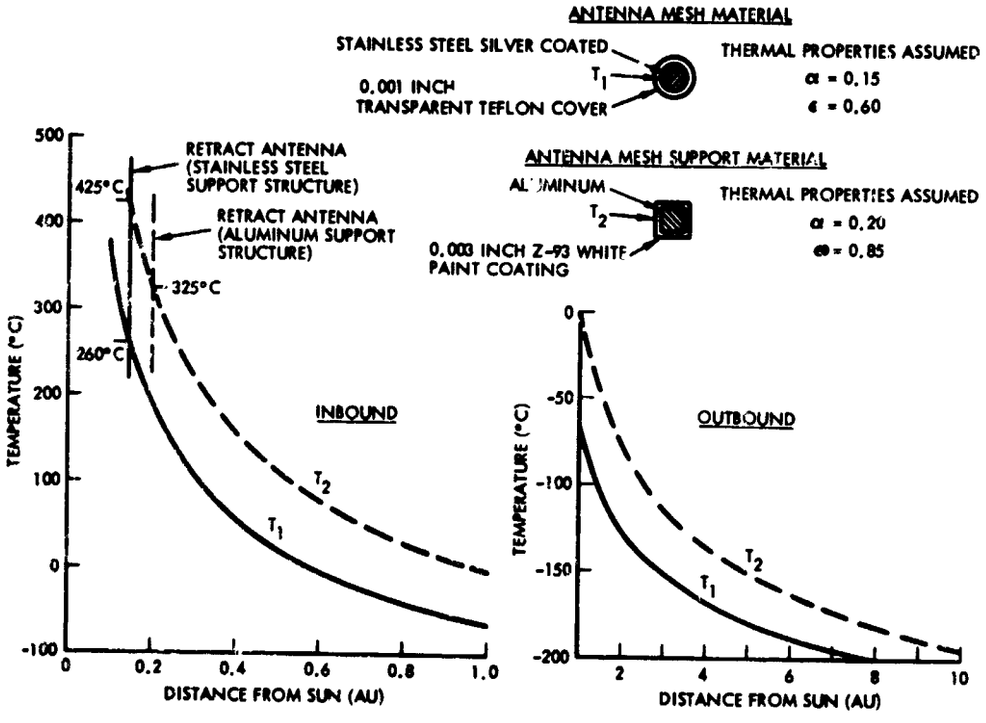

Figure 7-49. Antenna Temperature vs Solar Distance

The antenna mesh support structure will probably be aluminum for minimum weight. The support structure is coated with a low solar absorptivity ($\alpha = 0.2$) and high emissivity ($\epsilon = 0.85$) white paint (Z-93, high temperature). The support structure coating will maintain temperatures below 325°C for distances as low as 0.2 AU. If stainless steel is used as support structure material, the coating will maintain

temperatures below 425°C for distances as low as 0.15 AU. See Figure 7-49. The antenna needs to be positioned behind the shadow shield at solar distances below 0.2 AU (aluminum support structure) or below 0.15 AU (stainless steel support structure).

7.6.1.5 External Equipment

Z-93 high temperature white paint will be used on external equipment surfaces (α = 0.2, ϵ = 0.85) to minimize absorbed solar heat and maximize radiation to space. High temperature multilayer Kapton insulation will be utilized as required to minimize heat leaks into and out of the equipment. It will also be necessary, at close heliocentric distances, to reorient the stage and retract external equipment behind the shadow shield.

7.6.1.6 Shadow Shield

A single 3.0 by 3.5 meter shadow shield is required at a distance of 1 meter from the forward end of the stage below 0.25 AU to shield the propulsion module, equipment module, solar arrays, communication antenna, and other external appendages from excessive solar heating. The shadow shield uses second surface mirrors on the side facing the sun. The mirrors have a low solar absorptivity (α = 0.08) to emissivity (ϵ = 0.80) ratio and are stable at temperatures in excess of 325°C (0.1 AU). They can be attached to the support structure mechanically or with high temperature adhesive. The shadow shield uses Z-93 white paint on the aft surface to maximize heat transfer to space.

The shield is positioned at least 1 meter away from the forward end of the stage to produce a significant view factor to space so that a substantial amount of heat can be radiated off the aft surface. The 1-meter spacing also lowers adjacent stage surface temperatures by minimizing the heat transferred from the shield. See Figure 7-50.

7.6.1.7 Thermoelectric Power Modules

The thermoelectric power modules required for inbound missions below 0.25 AU to substitute for the retracted solar array will be tilted away from the sun at solar distances approaching 0.1 AU to maintain temperatures below maximum limits. See Figure 7-51.

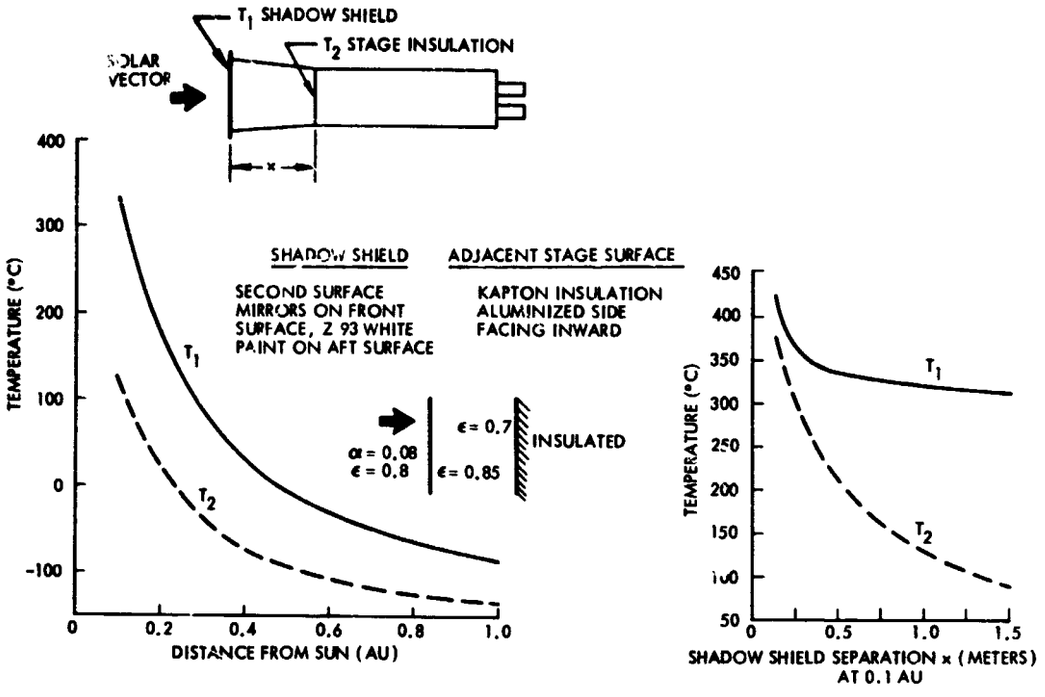

Figure 7-50. Shadow Shield and Adjacent Stage Temperature as Function of Solar Distance and Shield Separation

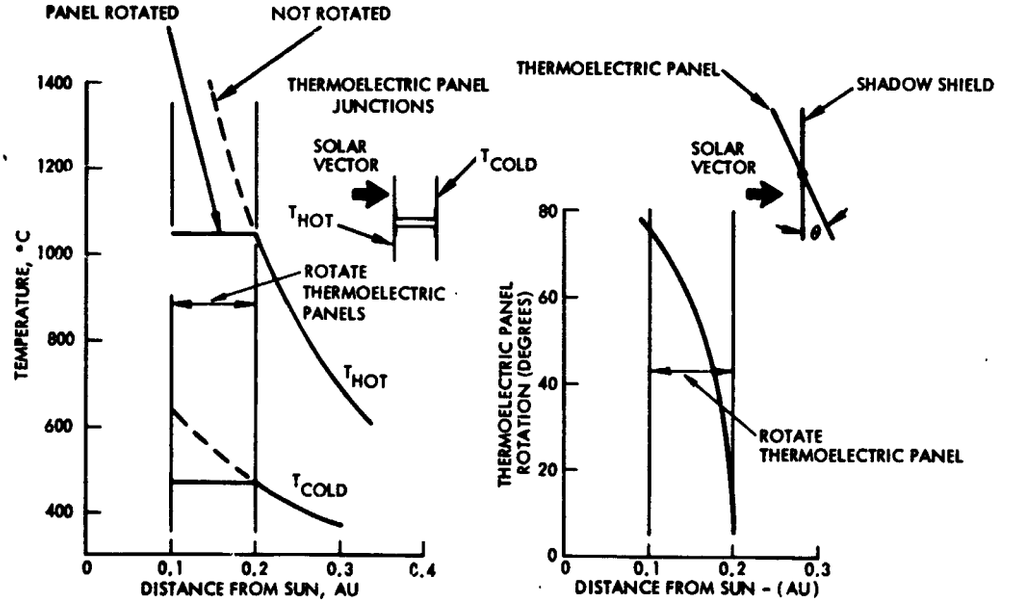

Figure 7-51. Thermoelectric Panel Temperatures vs Solar Distance and Required Panel Rotation

7.6.2 Design Approach: Outbound Missions

The outbound missions do not require all of the thermal control techniques applicable to inbound missions. However, in the interest of design commonality the same thermal control techniques are used in both inbound and outbound missions wherever possible.

The equipment and propulsion modules are insulated with multilayer aluminized Kapton insulation blankets and structural thermal isolators to minimize heat transfer with the surroundings. For outbound missions, multilayer aluminized Mylar insulation can be used in place of the high temperature Kapton insulation if the overall installation cost is less. Both types of insulations will perform adequately from the thermal standpoint. Louvered radiating surfaces are located on the shaded side of each module. The propulsion module will require 2.45 m^2 of radiating area, the equipment module 0.93 m^2. Heaters are needed in the propulsion module (50 watts) only to maintain unit temperatures above minimum limits during low heat dissipation cruise conditions. The use of louvers minimizes the required heater power. Once the propulsion module is inoperative, excess solar array power is available for the heaters.

On the solar array, close contact is established between solar cell and substrate to maximize heat transfer from the aft side of the solar array. The resulting array temperature is shown in Figure 7-52.

Thermal control of the ion engines is the same as for inbound missions. The temperature for a nonoperating engine receiving maximum solar radiation is shown in Figure 7-53.

The same antenna mesh material and antenna support coating as for inbound missions can also be used on outbound missions. If a cost saving can be achieved by a plain stainless steel mesh in place of the stainless steel and teflon composite mesh, it can be done without adversely influencing antenna temperature control.

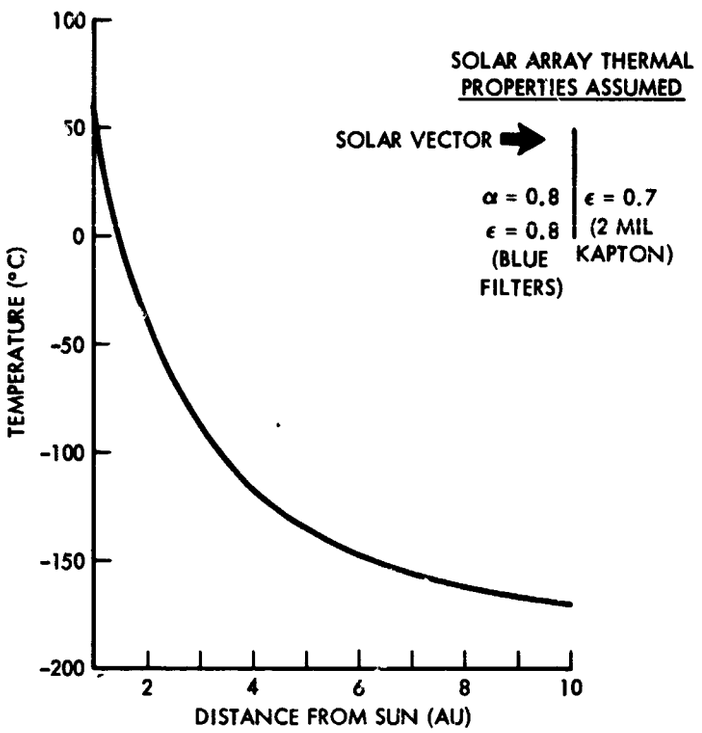

Figure 7-52. Solar Array Temperature vs Solar Distance (Outbound Missions)

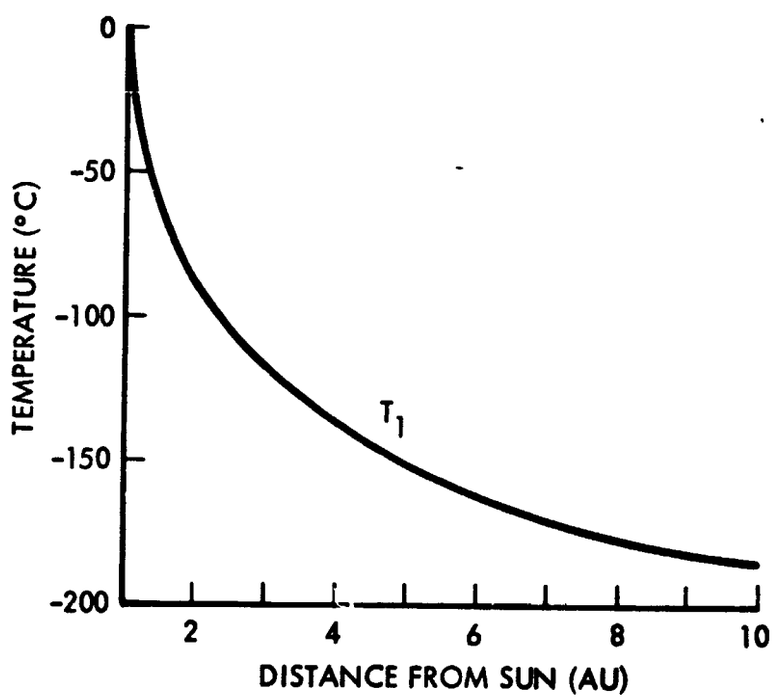

Figure 7-53. Maximum Temperature of Ion Engines, Not Operating, Outbound

Heaters may be required on some of the external equipment. The heater power required will be minimized by extensive use of insulation and stabilization of unit heat dissipations.

7.6.3 Thermal Control Components

In addition to the forward-mounted shade needed for inbound missions and the high-temperature paint ($\alpha = 0.2$, $\epsilon = 0.85$), four component parts make up the thermal control subsystem, multilayer insulation blankets, louver assemblies, radiation plates, and heaters.

The insulation blanket, typified by that illustrated in Figure 7-54 consists of 20 layers of 0.006-mm aluminized Mylar sandwiched between 0.05-mm aluminized Mylar cover sheets, with the aluminized side facing inward. Kapton substitutes for Mylar on the inbound missions. This blanket provides a thermal conductance of less than 3.3 joules/hr-m^2-^oC. A total of 18.56 m^2 of insulation is required for the stage, weighing approximately 9 kg.

Radiator plates of the type shown in Figure 7-55 provide a calibrated area at the surface of the stage to reject component heat dissipation while minimizing absorbed solar radiation. The plates consist of 0.5-mm aluminum covered on the outside surface with 0.2-mm of black Cat-a-lac paint. A 1.15-m^2 plate is required on the shaded side of the equipment module, a 3-m^2 plate on the shaded side of the propulsion module on inbound missions. Total weight of the plates is 4 kg.

Figure 7-54. Typical Spacecraft Application of Multi-Layer Insulation Blanket

Figure 7-55. Typical Spacecraft Radiator Plate

Thermal louver assemblies (Figure 7-56) are placed over the entire surface of the radiator plates to control the surface emittance of the plate as a function of its temperature. Fully closed, the louvers create an emittance of less than 0.15. Fully open, the louvers create an emittance of greater than 0.7. The louvers move from one extreme to the other over a 12°C range. The assemblies are formed of the same bimetallic actuated blades and supports used on the Orbiting Geophysical Obs[illegible]vatories. Total weight is 14.4 kg.

To provide the heat needed to maintain unit temperatures above minimum temperatures, themostatically controlled electrical resistance strip heaters are needed on both inbound and outbound missions. Standard 10-watt heaters are available with on-off themostatic switches, but proportional type controllers may need to be substituted for the switches to avoid unwanted magnetic fields. A total of five 10-watt heaters, weighing 36 grams is needed for outbound as well as inbound missions.

7.6.4 Special Aspects

Fabrication and assembly are extremely critical in achieving a thermal control subsystem with the desired properties. The louver assemblies must be properly integrated with the insulation assemblies to minimize heat leaks at the edges. The bimetallic springs must be thermally coupled to the radiator plate. Louver assemblies must be readily removable for calibration and repair as required. Louvers are fragile and must be handled with care to prevent alteration of surface properties.

The radiator plates must also be properly integrated with the insulation assemblies to minimize heat leaks at the edges. The plates must be capable of being removed for making adjustments in second surface mirror coverage. External surfaces must be kept clean to ensure that the required thermal properties are maintained.

The strip heaters must be securely bonded to the surface. Incomplete bonding or localized debonding could cause the heater to operate improperly or burn out. The surface that the heater is bonded to must be capable of conducting heat away to prevent the heater from overheating, or being switched off prematurely when the thermostat reaches the upper temperature limit.

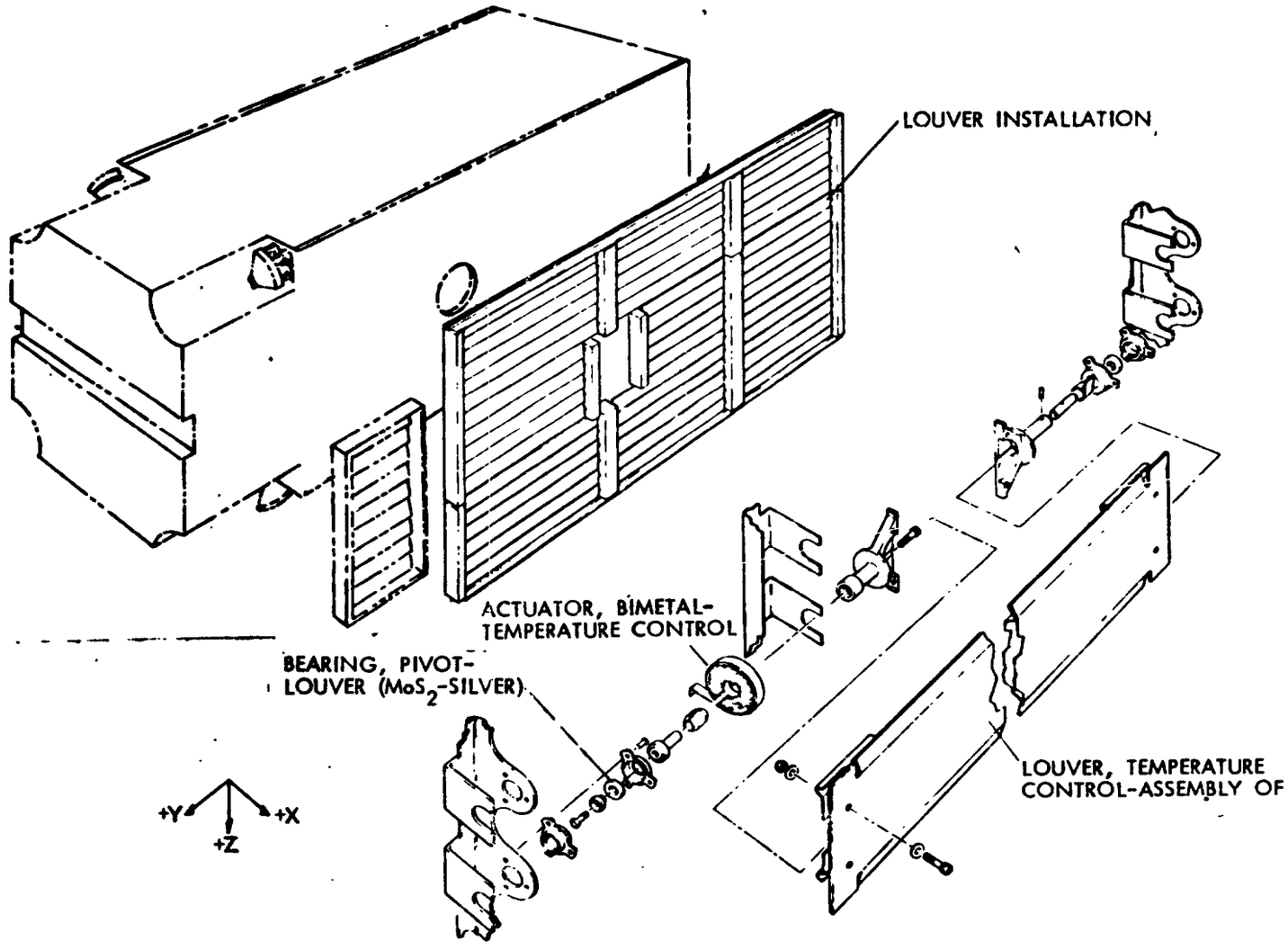

Figure 7-56. Thermal Louver Assembly (OGO Spacecraft)

7.7 STRUCTURE AND MECHANISMS

7.7.1 Structural Design

The structural configuration selected for the baseline is a combination of truss and semi-monocoque construction. It utilizes state of the art processes and materials to minimize costs and give high reliability. Rigid supports are provided for equipment and experiments and provisions have been incorporated for change and growth.

The stage main structure is a rectangular prismatic box which is divided into propulsion, equipment, and payload modules. (Figure 6-1.). Structural members were sized to meet Titan 3D/Centaur stress and dynamic requirements, with margins of safety sufficiently high to allow for various mission configurations, including support of payloads weighing between 300-500 kg.

The propulsion module contains the electric propulsion subsystem and its propellant. The main structural elements are four aluminum corner longerons which support the equipment and payload modules. The longerons attach to the four lower corner fittings at the interstage interface. Diagonal braces are added on all sides of the module to provide stiffness and shear load capability. The mercury propellant tank is supported on four tubular struts to the corner fittings, and braced by additional struts to the upper corners of the propulsion module.

The engine cluster is supported by a ring and web structure that is suspended from the four corner fittings forming the base closure of the propulsion module. The ring base provides mounting space for two attitude jet propellant tanks, for the hydrazine tank and for the ion engine gimbals and three launch phase retainer assemblies.

The equipment module contains the stage electronic equipment and other subsystem elements. The equipment is mounted on aluminum honeycomb panels which form the basic structure of the module. The panels are assembled in a box configuration on an aluminum framework. which transfers the loads into the propulsion module longerons and diagonal braces. The equipment module is completely enclosed by a thermal insulation blanket except for the louvered radiation areas, to control the range of temperatures imposed on the electronic equipment.

The payload, ejected capsule, and some appendages are supported by the payload module. Its structure consists of two rigid main towers, which are essentially tapered box beams, fabricated from aluminum sheet and angles. Mounting points are provided on the towers for the payload and appendages. Each tower provides support during launch for one half of a stowed solar array assembly, by means of a retractable bracket.

Storage drums and deployable booms for the two rollout solar arrays are mounted on the two opposite outer sides of the equipment module. The solar array storage drums are restrained at each end during launch by support arms and braces mounted at the top of the payload module and the base of the propulsion module. Prior to array deployment the end braces are separated from the storage compartment and the array is supported at its center from the equipment compartment. The array panels are deployed by extending a central BI-STEM boom which also serves as support for the array after deployment. The high-gain antenna support structure is mounted on top of the payload module; omni-antennas are mounted centrally on the front and rear sides of the stage. The high-gain and low-gain antennas are deployed from stowed position after launch.

A launch vehicle interstage truss supports the stage on the Titan 3D/Centaur vehicle. This interstage provides the mechanical interface between the launch vehicle and the electric stage structure. The selected combination of an inner and outer truss structure provides a rigid transition from the stage to both the Centaur and the standard payload adapter. The support struts of the outer truss are 3-inch diameter aluminum tubes, the much shorter ones of the inner truss, 2-inch diameter aluminum tubes. The truss is designed to allow the engine platform and its support structure to extend down inside the adapter with ample fly-out clearance.

7.7.2 Deployment and Articulation Mechanisms

The deployment and articulation mechanisms provide release, deployment, and positioning of the two solar arrays, the high-gain parabolic antenna, the booms which support the attitude control jets and low-gain antennas, and certain experiments. All of these items are restrained during launch, and subsequently released by redundant space-qualified pyrotechnic pin pullers or bolt cutters, similar to those used on other spacecraft such as OGO and 777.

The solar array is deployed by a motor-driven BI-STEM boom which extends up the center of the array and supports it after deployment. In the baseline configuration a rotatable shaft connects both array panels to a common drive assembly mounted centrally at the top of the propulsion module. In some mission configurations of the stage, additional experiment booms are deployed from the end of the extended array by springs.

In the baseline configuration, the high-gain antenna is supported by its feed structure and deployment arm during launch. Following its release, the antenna is deployed and positioned by a bi-axial drive motor located at the base of the antenna deployment arm.

In the alternate configuration, the top of the stage must be left unobstructed for payload mounting and therefore a smaller 4-ft high-gain antenna dish serves the needs of the stage, excluding science payload telemetry. This antenna is stowed during launch against the front wall of the stage on a deployment arm that is hinge-supported at the bottom of the propulsion module. This deployment arm can be moved from the nominal position covering the front hemisphere to a second one, on the other side of the thruster assembly, for coverage of the rear hemisphere. Transfer is made past the thrusters during a short interruption of the thrust phase. Articulation is provided as in the baseline configuration by a bi-axial drive assembly located at the end of the deployment boom.

Some booms and appendages will be deployed by torsion springs in the hinges. This method was successfully used on other spacecraft such as OGO. Other appendages will be deployed and positioned by electrical drive-motors.

7.7.3 Dynamic Analysis of Structure and Deployment Mechanisms

A primary design objective is for the stage primary structure to have sufficient rigidity so as to avoid boost vehicle control-stability problems, excessive deflections and high structure responses. A preliminary dynamic analysis of the stage configuration was conducted to assist in the design of the main structure to meet this objective.

Lumped-mass modeling techniques were used with the TRW Structural Modal Analysis Program to determine natural frequencies

and mode shapes. The interstage stiffness coefficients were incorporated in the model to simulate the support interaction. The lowest calculated lateral frequency is 6.8 Hz while the first axial mode occurs at 37.8 Hz. This compares well withthe Martin Co. design goal minimum frequencies of 6 Hz lateral and 25 Hz axial.

Preliminary structural load factors for the Titan 3D/Centaur launch vehicle have been assumed to be 9 g vertical combined with 3.5 g lateral. Component load levels have been assumed as 20 g vertical and 10 g lateral acting separately. These load levels were conservatively selected and are similar to those used for other Titan payloads.

A preliminary analysis of solar array bending frequencies was performed to determine potential dynamic interactions between the highly flexible solar array structure and the attitude control system. Dynamic coupling during attitude correction limit cycling at frequencies in the range of 0.01 to 0.02 cps could excite the two solar arrays and the center body into large-amplitude resonant oscillations. To avoid this the lowest natural bending frequency of the structure must be made larger than the excitation frequency by at least a factor of two or three. Table 7-12 gives the fundamental bending frequency of the cantilevered solar array for three values of deployment boom cross-section diameter. The assumed solar array size and weight characteristics were as follows:

Mass of each solar array panel	131 kg
Length of boom	21.1 m
Boom cross-section diameter	2.0, 3.12, 5 in.
Boom material thickness	0.01, 0.014, 0.025 in.

The boom is a stainless steel BI-STEM type. Two simplified structural models have been used in this calculation: (a) the equivalent of half of the solar array blanket is considered as a lumped mass attached to the free end of the boom; (b) the blanket mass is considered to be distributed uniformly along the boom. The first model is a better representation of the actual design of the rollup array than the second, because the blanket is actually attached only at the tip and root of the boom. In addition, the natural frequency for this case is somewhat lower and therefore more conservative than for the distributed-mass model.

Table 7-12. First Natural Bending Frequencies of Solar Array Boom (in Hz)

Boom Diameter		Natural Bending Frequency (Hz)	
inches	(cm)	Lumped Mass	Distributed Mass
2.0	5.1	0.020	0.033
3.12	7.9	0.052	0.071
5.0	12.7	0.090	0.115

Based on the above data we have selected a boom diameter of 4 inches (10 cm) giving a natural frequency of 0.07 Hz which is more than 3 times higher than the typical limit cycle frequency. Based on calculations performed during the SEMM-1 study it is estimated that for the overall stage consisting of a center mass plus two flexible arrays, the frequency of the first symmetric bending mode will be about 0.2 Hz and the frequency of the first unsymmetric mode about 0.35 Hz. This preliminary analysis shows that the selected boom diameter provides ample structural rigidity against resonances due to attitude control excitation frequencies.

7.7.4 Stage/Booster Separation Mechanism and Pyrotechnics

The stage/booster separation system consists of a pyrotechnic release system and separation springs of the type used by TRW on the Model 35 and 777 spacecraft. The separation impulse is provided by four compression springs at the interface, one at each corner. Explosive nuts at each spring location are fired simultaneously to release the spacecraft tie down bolts.

The separation system must be designed to assure separation of the electric stage from the booster with adequate clearance and at minimum angular rates so as not to exceed control subsystem capabilities.

Stage tipoff rates are minimized by carefully matching of the spring rates for each set of springs. Also, the springs are oriented so as to cancel out any lateral force components.

8. RELIABILITY

This section presents the results of reliability analyses performed during the study. In particular, the following information is included:

- Reliability versus weight tradeoffs to optimize payload data return.
- Unit and subsystem reliability allocation.
- A failure modes and effects analysis.
- A discussion of design details affecting reliability.

The reliability data derived under TRW's earlier solar-electric spacecraft study, SEMM-1, served as reference material and was updated as required to support the present study.

The Ceres rendezvous mission was used as the prototype mission model in performing a quantitative analysis. Changes in system reliability resulting from application of the electric stage to other missions have been considered only in a qualitative sense.

Reliability tradeoffs specifically involving the electric propulsion module and the impact of mission profile changes on propulsion system reliability have been previously discussed (Section 7.1).

8.1 ASSUMPTIONS

The following assumptions have been employed during the course of this analysis:

- All subsystems are in-line for reliability. Payload reliability is not included in the analysis.
- Although the operating time varies from 400 to 700 days for different missions, this analysis is conducted on a nominal 700-day Ceres mission.
- Whenever possible, consistent with the preliminary nature of the current design, failure rates are taken from similar existing equipment on other programs.

8.2 OPTIMIZING PAYLOAD DATA RETURN

Table 8-1 identifies the weight and reliability properties of each unit/subsystem in the baseline design. For each electronic unit, there are normally at least two alternate configurations with and without redundancy. There may be other choices, such as double redundancy. For a given unit with no redundancy, its mission reliability R_{NR} for a given non-redundant weight W_{NR} can be determined. As redundancy is added, reliability is improved (R_R) corresponding to larger weight W_R, at the expense of payload capacity, and increased weight W_R can be determined. From these data, an improvement coefficient I corresponding to each change in configuration can be defined:

$$I = \frac{\ln R_R - \ln R_{NR}}{\ln (W_R - W_{NR})} = \frac{\Delta \ln R}{\Delta W}$$

The various reliability improvement measures are ranked according to the magnitude of the improvement coefficient I (see Table 8-2). Redundancy candidates should be implemented in this order so as to improve reliability most efficiently as a function of weight; i.e., changes with the largest ratio of $\Delta \ln R$ to ΔW should be implemented first, for they achieve the largest reliability improvement per pound of weight expended.

Included in Table 8-2 are columns which show the added weight and improved spacecraft reliability as each step is taken. Figure 8-1 shows the reliability increase as a function of increased redundancy weight, and the corresponding loss in payload capacity.

The booster is capable of injecting 1500 kg into orbit. The wet weight of the nonredundant stage is 1214 kg, leaving a total of 286 kg to be used either for payload instruments or redundant system elements. If the amount of weight allocated to redundancy is W_{SR}, the weight remaining for payload is

$$W_{PL} = 286 - W_{SR}$$

The tradeoff between reliability improvement and payload reduction can be expressed by the product of reliability times payload weight, which

Table 8-1. Candidate Redundancy Configuration, and Their Reliability and Weight Properties

UNIT (Proposed Configuration †)	R_{NR}	R_R	$\ln R_{NR}$	$\ln R_R$	$\frac{\Delta\lambda\tau}{\text{or}}$ $\Delta \ln R$	W_{NR}	W_R	ΔW	$\frac{\Delta \ln R}{\Delta W}$
Structure Subsystem									
Basic Structure (NR)	0.9999*	---	-0.0001	---	---	91.3	---	---	---
Separation Hardware (R)	0.986	0.998*	-0.0141	-0.0020	0.0121	0.86	1.81	0.95	0.0127
Deployment Hardware (R)	0.980	0.990*	-0.0202	-0.0105	0.0097	0.86	1.81	0.95	0.0097
Thermal (NR) Subsystem	0.994*	---	-0.99613	---	---	28.6	---	---	---
Electrical Power Subsystem									
Battery (NR)	0.970*	0.9991	-0.0305	-0.0009	0.0296	35.4	76.4	40.0	0.0374
Power Source Logic (NR) 2 Units	0.963*	0.9986	-0.00379	-0.0014	0.0365	15.0	31.5	16.5	0.00221
Main Inverter (R)	0.951	0.9976*	-0.0503	-0.0024	0.0479	1.9	4.0	2.1	0.0228
Buck Boost Regulator (R)	0.985	0.9998*	-0.0148	-0.0002	0.0146	1.95	4.1	2.15	0.00679
Inverter (1.2 KHz)(R)	0.982	0.9997*	-0.0177	-0.0003	0.0174	2.0	4.2	2.2	0.00791
Battery Charger (NR)	0.994*	0.9_46	-0.00613	-0.0_24	0.00609	2.3	4.8	2.5	0.0243
Solar Array (NR)	0.994*	---	---	---	---	258.0	---	---	
Solar Array Gimbal Drive Assy (NR)	0.9945*	0.9_483	-0.0051	-0.0_417	0.00549	12.0	25.2	13.2	0.000416
Solar Array Drive Electronics (R)	0.9600	0.9991*	-0.0408	-0.0009	0.0399	0.286	0.6	0.314	0.1271
Electrical Integration Subsystem									
Command Distribution (R)	0.966	0.9988*	-0.0348	-0.0012	0.0336	4.6	10.7	5.1	0.00659
Cables	0.99825*	---	-0.00175	---	---	25.0	---	---	---
Attitude Control Subsystem									
Star Sensor Assembly (R)	0.921	0.9965*	-0.0822	-0.0035	0.0787	8.45	17.80	9.35	0.00842
Sun Sensor Assembly (R)	0.975	0.99966*	-0.0250	-0.00034	0.0247	0.9	1.89	0.99	0.0249
Antenna Drive Assembly (NR)	0.977*	0.99971	-0.0231	-0.00029	0.0228	6.35	13.35	7.0	0.00326
Rate Gyro Assembly (R)	0.983	0.99985*	-0.0166	-0.00015	0.01645	2.4	5.0	2.6	0.00632
Control Processor Assy (R)	0.810	0.979*	-0.2107	-0.0212	0.1895	3.8	8.0	4.2	0.0451
Control Electronics Assy (R)	0.965	0.99933*	-0.0354	-0.00067	0.0347	32.4	6.80	3.56	0.00975
Reaction Control Assy (R)	0.940	0.99802*	0.0612	-0.00198	0.0592	14.84	17.66	2.82	0.0210
Communications and Data Handling S/S									
TWT and Power Supply (R)	0.982	0.9_286*	-0.0183	-0.0314	0.0182	4.89	10.26	5.37	0.00339
Receiver (R)	0.865	0.9818*	-0.1447	-0.0184	0.1263	2.2	4.5	2.3	0.0549
Three Receivers	0.9818	0.9990	-0.0183	-0.00100	0.0173	4.5	6.8	2.3	0.00752
Ranging Unit (R)	0.982	0.9_386*	-0.0183	-0.0_314	0.0182	0.32	0.67	0.35	0.0520
Exciter (R)	0.998	0.9_57*	-0.00233	-0.0_530	0.00233	0.86	1.8	0.94	0.00248
Buffer Storage Unit (R)	0.997	0.9_57*	-0.00292	-0.0_530	0.00292	1.43	3.0	1.57	0.00186
Tape Recorder (R)	0.743	0.9596*	-0.2975	-0.0_412	0.2563	8.6	18.0	9.4	0.0273
Tape Recorder (3rd)	0.9596	0.9_451	-0.0412	-0.0_449	0.0411	18.0	27.4	9.4	0.00437
Digital Telemetry Unit (R)	0.969	0.9995	-0.0311	-0.0_350	0.0306	5.4	11.3	5.9	0.0062
Command Decoder (R)	0.976	0.9996*	-0.0244	-0.0_340	0.0240	1.4	3.0	1.6	0.0150
RF Switch (NR)	0.9992*	0.9_68	-0.00083	-0.0_619	0.00083	2.1	4.4	2.3	0.00036
Propulsion Subsystem									
Thruster Assemblies									
4 vs. 5 TH. + Serial Elements	0.9476	0.9704	-0.0539	-0.0300	0.0238	203.3	215.0	11.7	0.00203
Thruster Assemblies (R)									
5 vs. 6 TH. + Serial Elements	0.9704	0.9715*	-0.0300	-0.0289	0.0011	215.0	226.7	11.7	0.0_494
Hydrazine Tank & Feed System (NR)	0.9972*	---	-0.0028	---	---	6.0	---	---	---
Hydrazine Control Electronics (R)	---	.999*	---	---	---	---	1.5	---	---
Hydrazine Thruster Assembly (R)	---	.999*	---	---	---	---	0.55	---	---
Television + Gimbal System (NR)	0.9733	0.9993*	-0.0271	-0.0007	0.0264	6.5	13.7	7.2	0.00367

†R = Redundant, NR = Non-Redundant

* Reliability of proposed configurations

Table 8-2. Reliability Improvements Through Redundancy (Ranked by Sensitivity Coefficient $\Delta \ln R/\Delta W$

ELEMENT	$\frac{\Delta \ln R}{\Delta W}$	Stage REL	Δ Stage WT
Non-Redundant System	---	.296	0
Solar Array Drive Electronics	.1271	.280	0.314
Receiver	.0549	.318	2.61
Ranging Unit	.0520	.324	2.96
Control Processor	.0451	.381	7.16
Tape Recorder	.0273	.492	16.56
Sun Sensor Assembly	.0249	.532	25.91
Main Inverter	.0228	.558	28.01
Reaction Control Assembly	.0210	.593	30.83
Command Decoder	.0150	.607	32.43
Separation	.0127	.614	33.36
Control Electronics Assembly	.0097	.635	36.94
Deployment	.0097	.641	37.89
Star Sensor Assembly	.0084	.694	47.24
Inverter (1.2 KHz)	.0079	.706	49.44
3rd Receiver	.0075	.718	51.74
Buck Boost Regulator	.00679	.729	53.89
Command Distribution	.00659	.753	58.99
Rate Gyro Assembly	.00632	.766	61.59
Digital Telemetry Unit	.00520	.790	67.49
3rd Tape Recorder	.00437	.804	69.79
Television	.00367	.825	76.99
TWT & Power Supply	.00339	.840	82.36
Antenna Drive Assembly	.00326	.860	89.36
Power Source Logic	.00221	.892	105.86
Exciter	.00248	.893	106.80
Battery Charger	.00243	.899	109.30
5 Thrusters	.00203	.921	121.00
Buffer Storage Unit	.00186	.923	122.57
Battery	.00074	.951	162.57
6 Thrusters	.00009	.952	173.27

is a measure of the expected data return capability of the mission. In Figure 8-2 this is plotted as a function of redundancy weight W_{SR} and payload weight W_{PL}. We note that the maximum of the expected data return (175 kg) occurs at W_{SR} = 70 kg. The corresponding reliability is R_W = 0.81.

To achieve this result, the stage would have to be designed with the redundancy features above the broken line of Table 8-2, and none of those below the broken line.

It should be recognized that reliability and payload weight cannot be the only factors in the design of the redundancy complement. Various economical and engineering factors, in particular the required multi-mission compatibility of the stage, must also be taken into account. Therefore, it is not possible, or even desirable, to design the stage at

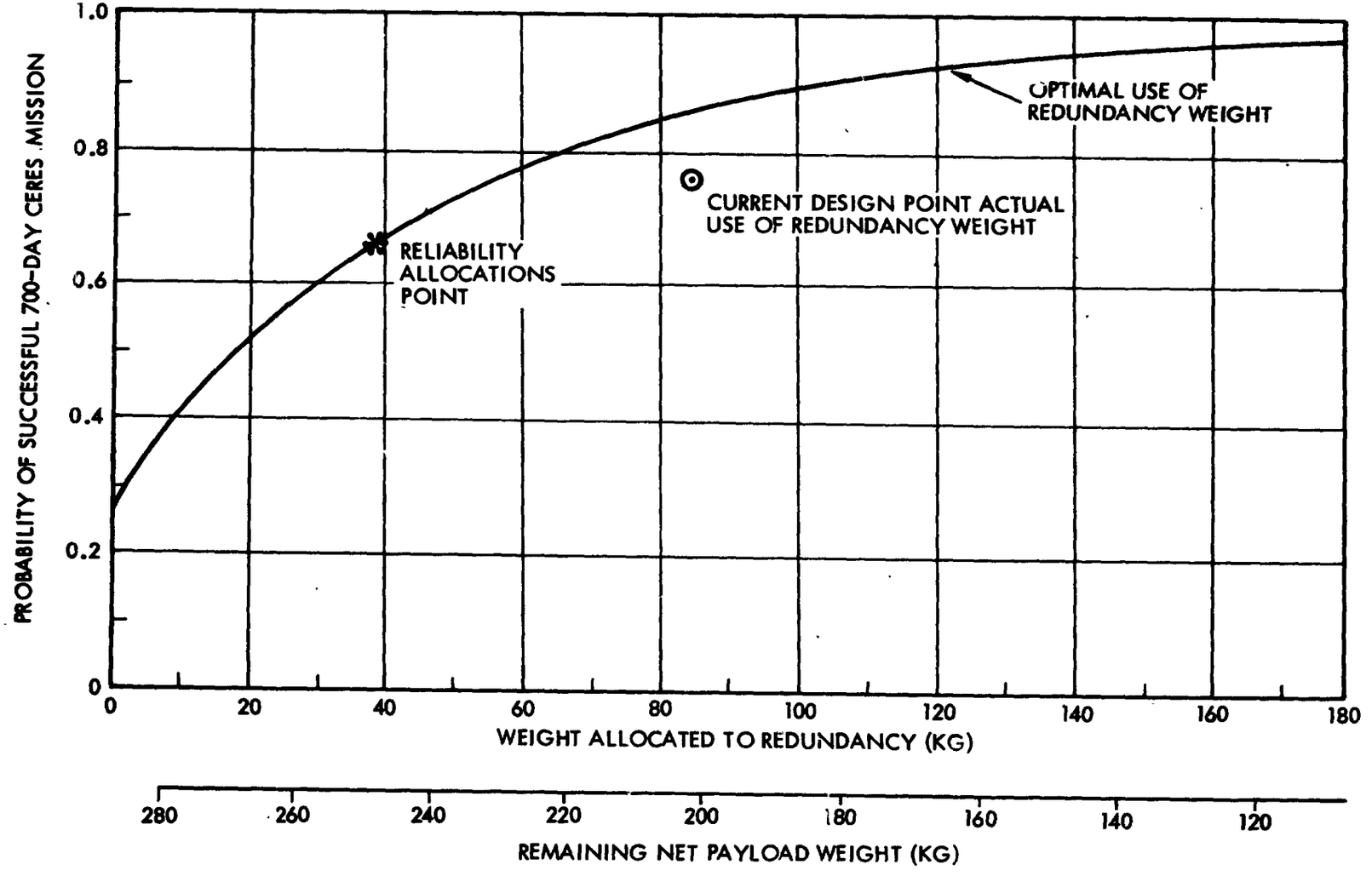

Figure 8-1. Probability of Success vs Redundancy Weight (700 Day Ceres Mission)

exactly the maximum expected value in Figure 8-2. Since the curve is quite flat in the region of the maximum expected value, a wide range of redundancy weight and reliability is available, permitting some latitude for other program-level tradeoffs. Thus any design which produces an expected data return within 10 percent of the maximum value (shaded region of Figure 8-2) would be acceptable.

The proposed configuration discussed here allocates 83 kg for redundancy weight, a reliability of 0.773 and therefore allows 203 kg of payload. (Design revisions made subsequent to this analysis modified the net payload weight to 188 kg, Section 6.14.) The expected data return is 157 kg.

8.3 RELIABILITY ALLOCATIONS

Tentative reliability allocations have been established for each unit, as shown in Table 8-3. The allocations are derived to give an overall spacecraft reliability of 0.65, which corresponds to the operating expected payload return value of 161 kg, or 92.5% of the maximum attainable. The point is marked with an asterisk in Figure 8-2.

This would be achievable with a redundancy weight allocation of only 40 rather than 70 kg and would thus permit 30 kg of payload increase from the nominal value. However, since the question of multi-mission compatibility must also be considered in the allocation of redundancy weight, the configuration initially selected will be left unchanged. The table merely serves to illustrate the reliability margin in various subsystems above the minimum values required to give an equivalent expected data return of 161 kg. This margin reflects the previously mentioned very flat maximum of the expected data return curve in Figure 8-2.

8.4 FAILURE MODES AND EFFECTS ANALYSIS

A unit level failure modes and effects analysis of the stage design is given in Table 8-4. The column labeled "Compensating Provisions" gives a good summary of the extent and philosophy of redundancy, conservatism and backup modes employed. At the unit level, consistent with this preliminary design, there are no identifiable electronic single-point failures which would cause catastrophic loss of the mission. Possible electro-mechanical failures are provided redundancy or work-around modes of operation.

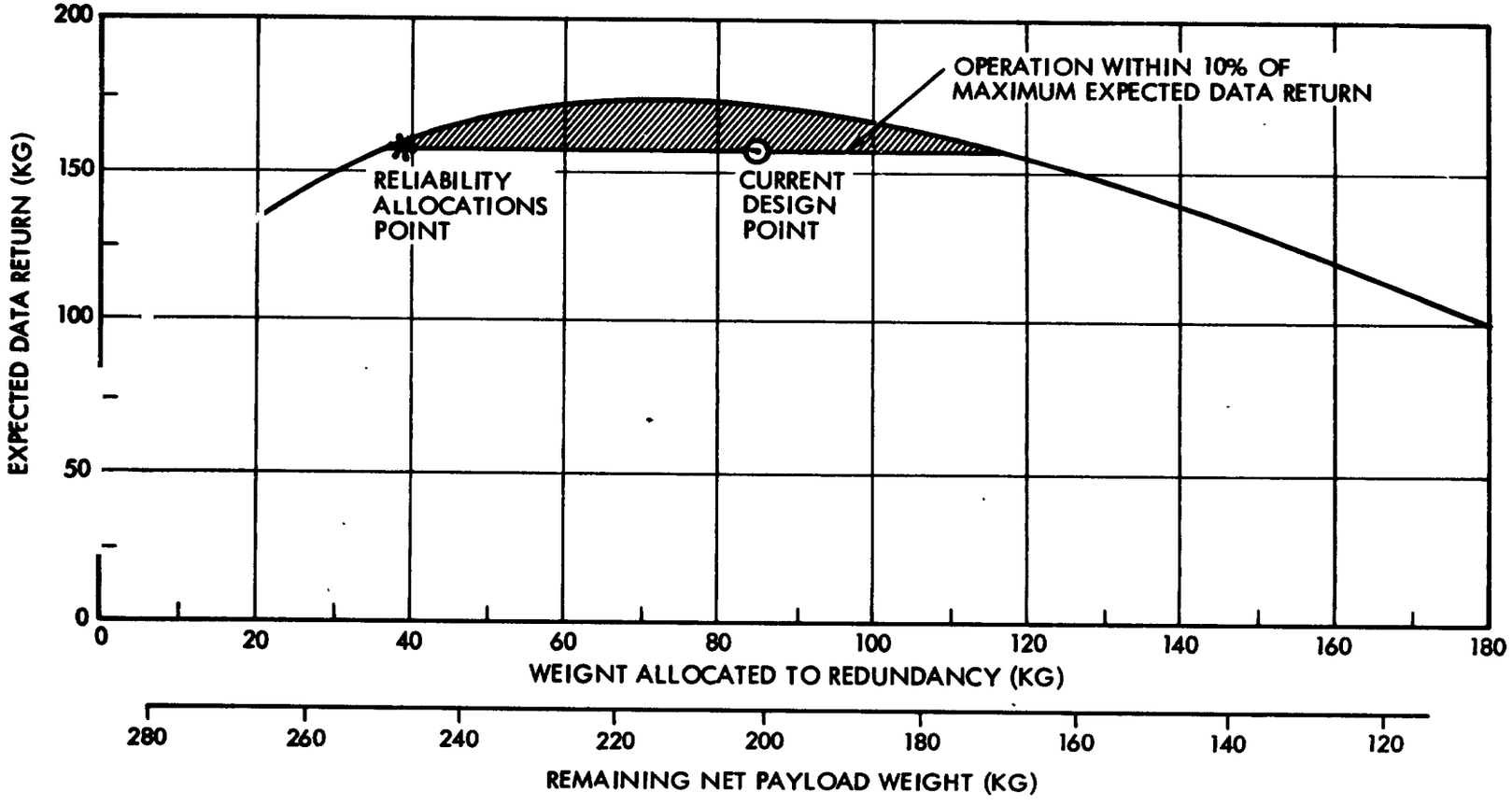

Figure 8-2. Expected Data Return vs Redundancy Weight (700 Day Ceres Mission)

Table 8-3. Reliability Allocations for Subsystem Units

UNIT	CURRENT RELIABILITY	ALLOCATION *
Structure Subsystem	.99	.98
Basic Structure	.999	.998
Separation Hardware	.998	.997
Deployment Hardware	.990	.984
Thermal Subsystem	.99	.98
Electrical Power Subsystem	.91	.86
Battery	.970	.952
Power Source Logic	.963	.941
Main Inverter Logic	.998	.997
Buck Boost Regulator	.999	.998
Inverter	.999	.998
Battery Charger	.994	.990
Solar Array	.994	.990
Solar Array Gimbal Drive Assy.	.994	.990
Solar Array Drive Electronics	.999	.998
Electrical Integration Subsystem	.99	.99
Command Distribution	.999	.998
Cables	.998	.997
Attitude Control Subsystem	.95	.92
Star Sensor Assembly	.996	.994
Sun Sensor Assembly	.999	.998
Antenna Drive Assembly	.977	.963
Rate Gyro Assembly	.999	.998
Control Processor Assembly	.979	.966
Control Electronics Assembly	.999	.998
Reaction Control Assembly	.998	.997
Communications & Data Handling Subsystem	.94	.90
TWT & Power Supply	.999	.998
Receiver	.982	.971
Ranging Unit	.999	.998
Exciter	.999	.998
Buffer Storage Unit	.999	.998
Tape Recorder	.960	.936
Digital Telemetry Unit	.999	.998
Command Decoder	.999	.998
RF Switch	.999	.998
Propulsion Subsystem	.97	.95
Ion Thruster Assemblies	.972	.955
Hydrazine Tank & Feed	.997	.995
Hydrazine Control Electronics	.999	.998
Hydrazine Thruster Assembly	.999	.998
Television & Gimbal System	.99	.98
System	.765**	.65

* with redundancy as shown in Table 8-1.
** Actually .772 when unit reliabilities are not arbitrarily truncated to three places as they are in this table.

FOLDOUT FRAME 1

Subsystem Component	Critical Failure Modes	Probability That Failure Modes Will Not Occur	Compensating Provisions
Structures			
Passive	Breakage or cracking	0.999	Conservative margins of safety, and/or extensive ground test strength verification
Separation events	Failure to separate	0.986	Redundant separation mechanisms
	Failure to activate required equipments		Activate equipments prior to launch Redundant activating mechanisms
Deployment events	Failure to deploy solar panels or antennas	0.986	Redundant deployment mechanism components Simplify deployment technique
Thermal			
Heaters	Failure "On"	0.994	Current limiting and on/off commands, then fuses are employed
Louver system	Failure to activate		Conservative design
Communications and Data Handling			
Transmitter and driver	Loss of transmitting capability		Redundant transmitters
Receiver	Loss of receiving capability	0.9818	Redundant receivers
Command demodulator	Failure to demodulate subcarrier signal		Redundant demodulators
	Failure to verify command		Redundant demodulators
Electrical Integration Ass'y	Loss of ability to process and distribute all commands		Redundant command processors
Ranging module (turnaround type)	Loss of signal generation capability	0.9998	Redundancy
			Ground station software to refine trajectory data and allow for accurate locating in case of ranging module failure
Buffer storage unit	Loss of data storage capability	0.9999	Redundant unit
			Real time transmission
Tape recorder	Loss of recording capability	0.9596	Redundant recorders
			Alternate mode using redundant buffer storage unit of realtime transmission
	Erroneous recording		Redundant recorders
Digital TLM unit	Loss of data formatting capability	0.9995	Redundant unit
Omniantenna systems	Structural failure	0.999	Conservative structural margin of safety
			High gain antenna provides backup
	Diplexer failure	0.999	Redundant diplexer or cross feeding circuits
			High gain antenna provides backup
High gain antenna system	Structural failure	0.999	Conservative margins of safety
			Good ground test verification
	Diplexer failure	0.999	Redundant diplexer
On-board Navigation (TV System)	Degraded optics	0.9993	Protective enclosure
	Electronic malfunction		Redundant unit
Gimbal drive	Mechnical malfunction	0.99	Safety margin in bearings/lubricants
	Electronics malfunction		Redundant unit
Electric Power			

[illegible]	Electronic malfunction	[illegible]	Redundant unit
Gimbal drive	Mechnical malfunction	0.99	Safety margin in bearings/lubricants
	Electronics malfunction		Redundant unit
Electric Power			
Stage power supply	Output shorted to ground		Internally redundant in critical circuits
Battery	Failure to store or supply power	0.97	Noncricital for primary mission
Buck boost regulator	Output shorted to ground	0.9998	Redundant unit
Battery charge control	Inability to unlock battery from discharge mode	0.9997	Backup command available
Inverters	Part failures resulting in loss of power		Redundant units
			Internal critical part redundancy
Solar Array	Open or short circuit cells	0.994	Highly redundant series parallel solar cell matrix
			Back diodes to shunt failed cells
	Micrometeroid damage		Conservative design margin
Solar array drive mechanism	Failure to orient array properly	0.999	Redundant drive circuits and actuators
Propulsion			
Thruster assembly (inc. isolator)	Short circuits		Redundant thrusters
			Series redundant isolators
Power processor	Part failures causing loss of power		Redundant units
			Internal critical part redundancy
Gimbal actuators	Mechanical failure	0.97_15	Conservative margins of safety
			Good ground test verification
	Electronics failure		Redundant circuits
Shutoff valve	Failure to function		Redundant valve coils and backup command available
			Redundant activating and arming circuits
Feed system	Structural failure		Conservative margins of safety
			Good ground test verification
	Leakage	0.9704	All welded or brazed system
			Good ground test verification
Vaporizer	Heater element failure		Redundant heater elements
			Redundant thrusters
	Plus "wetting"		Shutoff valves allow isolation of thruster and use of redundant thruster system
Chemical Propulsion			
Thruster	Failure to function	0.995	Conservative design
Valve and control assembly	Failure to function		Redundant unit
Feed system	Structural failure		Conservative margins of safety
			Good ground test verification
	Leakage		All welded or brazed system
			Good ground test verification
Attitude Control			
Sun sensor assembly	Sensor failure	0.9996	Redundant sensors
	Electronics failure		Redundant electronics
			Internal critical part redundancy

FOLDOUT FRAME 2

			of redundant thruster system
Chemical Propulsion			
Thruster	Failure to function	0.995	Conservative design
Valve and control assembly	Failure to function		Redundant unit
Feed system	Structural failure		Conservative margins of safety
			Good ground test verification
	Leakage		All welded or brazed system
			Good ground test verification
Attitude Control			
Sun sensor assembly	Sensor failure	0.9996	Redundant sensors
	Electronics failure		Redundant electronics
			Internal critical part redundancy
Canopus sensor assembly	Sensor failure	0.996	Redundant inertial reference
			Backup operating mode
	Electronics failure		Redundant electronics
			Internal critical part redundancy
			Ground command backup
Rate gyro assembly	Excessive drift	0.983	More frequent updating by star sensor
	Mechanical failure		Redundant unit
	Electronics failure		Redundant unit
Attitude control processor	Memory failure	0.979	Redundant unit
	Processor failure		Redundant unit and internal redundancy
Antenna control assembly	Mechanical failure	0.977	Redundant controls
			Point antennas by S/C maneuvering
	Electronics failure	0.9991	Redundant electronics
			Internal critical part redundancy
Power phase control electronics assembly	Thruster control	0.9993	Redundant assembly
			Internal critical part redundancy
			Ground command backup
Coast phase control electronics	ACS jets control failure		Redundant assembly
			Internal critical part redundancy
			Ground command backup
Reaction control engine system	Leakage	0.99802	Redundant seats
			Redundant activating circuits
			Redundant thrusters

The electric stage has a much greater weight capacity than the spacecraft previously considered in our reference study, SEMM-1. In the present design we have therefore allocated a larger weight increment W_{SR} to system redundancy. The following principal redundancy features, backup modes of operation and simplifying design features have been included:

- Roll control utilizes two gyros with weekly updating by the star sensor.
- If the star sensor fails mechanically, it can still be used in a stationary manner for a star reference signal.
- If the TV gimbals fail, navigation reference can still be attained by rotating the entire spacecraft until the target is in view.
- One sun sensor is located on the center body, and another is located on the solar array base. They are partially redundant and act as partial backup to each other.
- A hydrazine propulsion system is used for terminal guidance backup.
- Redundant computers are used for attitude control.
- Six thrusters are used to provide redundancy for even the most demanding mission, and to provide backup in the event of degraded performance in one or more of them. There are fewer moving parts in the thrust vector control mechanisms. The potential for frozen bearings is eliminated by the use of flexure pivots. Flexible feed lines and power cabling are simplified. Complex switching in the power processor unit is replaced by hard wiring one multiple-output section to each thruster.
- In missions with non-critical flight times, such as the out-of-ecliptic and solar probe missions, failure of a thruster can be compensated by extension of the total thrust time on other thrusters with a corresponding extension of total flight time.

There are other possible backup modes being considered for the stage design. The extent to which they might be incorporated will depend on future studies as the design progresses. They include the following provisions:

- Slow spinning about the roll axis can be instituted to alleviate a number of malfunctions, such as an emergency attitude control mode, assisting deployment of stowed appendices, and star referencing.

- If the high gain antenna drive fails, the entire vehicle may be rotated to effect proper pointing.

Certain mission requirements of the multi-mission stage are more demanding or complex than those considered in the SEMM-1 study. We have made the following design choices to meet these requirements or to alleviate their impact on mission success probability:

- A more demanding thrust phase is alleviated by the use of a highly redundant thruster module and a simple TVC system.

- The navigational and guidance requirements are achieved by using an on-board target sensor (TV) to augment ground-based navigation. In case of failure of the on-board system, DSIF interferometry techniques provide a less accurate but suitable navigational backup. Finally, an on-board hydrazine system is available to augment the low-thrust capability at 3 AU simplifying the mission profile.

- The effects of a more demanding vehicle orientation sequence are alleviated by providing for solar array reorientation. In the solar probe and mercury missions, the array is merely feathered, rather than requiring reorientation of the entire stage.

8.5 NEW TECHNOLOGY

Several system and subsystem design elements must be regarded as "new technology", and extra caution and consideration must be given to their design and test to assure a successful program. However, some of these design features are covered by redundancy and functional backup modes to alleviate the reliability impact.

- The solar array is a large, retractable device with an output voltage of 160 w. Rolled-up flexible arrays have been designed and tested but have not yet been operated in space. However the first such roll-up array will be test flown during this year.

- The 4.5 kw ion thrusters are not yet available. They must have a minimum operating life in the vicinity of 400 days. Test plans must be implemented to demonstrate this capability with acceptable confidence.

- The power processor's (PCU) SCR circuitry is still under development. Switching between some segments of the PPU and thrusters will be required.

- The feed system uses Xeolite absorption techniques for pressure regulation. These techniques are inherently simple and should be reliable.

- The orbit determination program has an inherent sensitivity to the effect of random perturbations due to changes in the thrust vector magnitude and orientation. The proposed mission profile minimizes this problem by providing repeated coasting periods during which time more accurate orbit determinations can be made.

- The on-board terminal navigation system will be proven on future Mariner, Viking and TOPS flights before the electric stage flies. A DSIF interferometry technique provides backup for this function.

- The 3-axis gimballed TVC system will be simple and reliable, but is only a conceptual development at the present time.

- Only the concept of rotating the star sensor is new for the SEMM-2 system. The optical system and electronics has been flown on Mariner. The system is redundant through use of a dual gyro reference updated by the star sensor.

9. ADVANCED TECHNOLOGY AND MISSION EVOLUTION

9.1 DESIRED ADVANCES IN TECHNOLOGY

Results of the system analysis and design studies indicate that the implementation of the electric stage program depends strongly on technology development not only in the field of solar-electric propulsion but other critical areas as well, e.g., attitude control of large flexible structures; guidance and navigation with respect to targets having a poorly defined ephemeris and being hard to detect, such as asteroids and comets; thermal control under extreme conditions; communication and data handling with wide variations of mission characteristics and constraints. Table 9-1 lists the principal areas identified in this study where technology advances are essential or desirable.

The technology of large, light-weight deployable solar arrays is only beginning to evolve. The first such array will be demonstrated in flight during the coming year. This will be a 1.5 kw two-boom rollout array developed by Hughes. The GE rollout array which has been under extensive laboratory development conforms better with our stage configuration and provides a larger power level, viz. 2.5 kw per panel. A major scale-up of this prototype array by more than a factor of 3 would be required. An increase in solar array voltage from the nominal 100 V level of the present design to 200 V used in the stage requires additional development and test. Other advances are required to assure adequate control of dynamic interaction with attitude control, torsional deflections and thermal distortion, and to assure cell and connector integrity under repeated retraction and deployment. Thermal protection in the case of the 0.1 AU solar probe, 0.38 AU Mercury mission and some comet missions also requires further development and test.

Power processors that use SCR technology and promise higher efficiency and reliability and a lower specific mass are now in advanced development but must still evolve into flight-readiness. The desirability of new circuitry for overload protection (fault-clearing switches) and maximum power sensing and flexible PPU module switching has been pointed out in the study.

Table 9-1. Advanced Technology Requirements

Technology Item	Advanced Technology Required/Desired	Area to Benefit from Improvement	Importance Rating*
Solar Array	• Increased size (17.5 kw)	Needed for stage implementation	A
	• Articulation joint	Mission feasibility in orbiter missions	A
	• Control of dynamic interactions	Pointing accuracy and stability	A
	• Medium array voltage (200 V)	Major weight savings, simplification	B
	• Thermal protection	Feasibility (solar probe, Mercury orbiter)	A
Power Processor	• SCR Type: Further development and test	System performance	B
	• Fault-clearing switch	Reliability	A
	• Maximum thrust point tracker	Performance and weight savings	B
	• PPU switch gear	Weight savings, reliability	C
Ion Thrusters	• High power rating (4.5 kw)	Weight savings, design simplification	A
	• Increased throttling range	Flexibility, reliability	C
	• I_{sp} reduction	Performance	B
	• Tankage and feed system	Simplification; weight savings	B
	• Increased mission life	Reliability, weight savings	A
Navigation and Guidance	• Improved DSIF navigation accuracy for low thrust missions	Guidance accuracy	B
	• Onboard terminal navigation capability	Mission success and scientific value	A
Attitude Control	• Rotatable star sensor	Design simplification; flexibility	B
	• TVC system	Simplicity, weight savings	B
	• Attitude control dynamic interaction	Accuracy; stability	A
	• Attitude control processor	Simplification; flexibility	B
Thermal Control	• Stage thermal protection	Survival	A
	• Solar array protection	Survival	A
	• Ion engine protection (inner solar system)	Performance and survival	A
Communications	• High-power solid state transmitter	Reliability; data rate capacity; cost savings in mission support	C
Mission Analysis	• Methodology and software	Efficient design process (cost savings)	B
	• New optimization criteria	System effectiveness and cost savings	C

*Key to importance ratings: A - Essential or of critical importance
B - Very desirable
C - Desirable

Advances in ion thruster technology are of principal concern. The study has shown the importance of high thruster power rating (4.5 kw) to keep the total number of active and redundant thrusters in a 15 kw vehicle within reasonable limits. Increased throttling capability (3:1) allows greater multi-mission flexibility and higher reliability, given a fixed number of thrusters. Reduction of specific impulse from the now achievable 3000 sec to 2500 sec with high efficiency would provide substantial payload gains in some missions. Improvement in thruster reliability to meet, and exceed, the specified 10^4-hr burn time objective will be essential to this program. This requires further component and design improvement, e.g., neutralizer arrangement.

The novel thrust vector control concept adopted in the stage design, and the novel pressure-regulated, thermally controlled Xeolite propellant feed system need further development and test. Our bladder support concept for a large tank with variable propellant loading also needs demonstration and test.

Electric thrust vectoring which is currently being developed under NASA contract should ultimately replace the mechanical TVC concept adopted in our stage design to permit a further reduction of weight, complexity and cost. The electric TVC approach is well suited because only small thrust angle deflections, not exceeding $\pm$ 10 degrees, are required in our stage design configuration.

Navigation and guidance of low thrust vehicles, requires further analytical study, hardware development and practical verification. New techniques being developed for conventional ballistic missions need adaptation to the electric stage. This includes accuracy improvement of DSIF based navigation techniques, such as the angle tracking method being developed by JPL for the Mariner Venus-Mercury shot, and on-board terminal navigation methods adapted to difficult targets such as comets.

Advances in mission analysis methodology are desirable to simplify or reduce iterations between initial performance calculations and preliminary vehicle design. As an example, the time-variability of solar array power due to solar radiation damage and micrometeoroid erosion

could be readily included inthe present simulation program and provisions made to use the initially allowed power margin for thrust purposes.

9.2 MISSION EVOLUTION

As a point of reference Figure 9-1 shows a tentative sequence of primary, alternate and growth missions beginning in 1976 with the Ceres rendezvous mission. The chart indicates that before all primary missions can be completed, using available launch opportunities, some alternate missions could begin in the late 1970's. The comet Halley rendezvous mission which requires about seven years via Jupiter swingby, if it is to be performed at all by the electric stage, would require launch as early as 1978-1979.

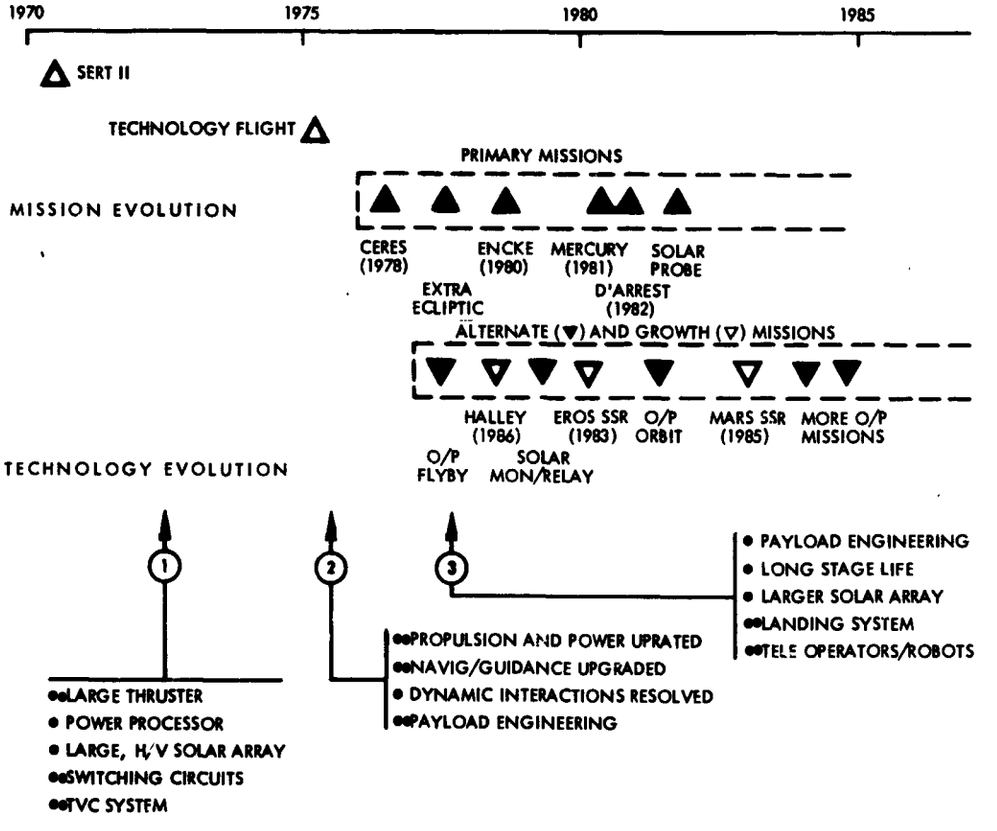

Figure 9-1. Technology Evolution and Projected Mission Sequence

A launch frequency of 1 to 2 flights per year is assumed in this schedule. Budget limitations may dictate a lower frequency. However the desired cost benefit of standardized vehicle production might be

lost if the stretchout led to interruption of assembly and test schedules. Also, a program extension beyond a 10 to 15 year-life span would increase the risk of obsolescence unless major technology advances can be incorporated as the program evolves. The prospect of solar-electric propulsion technology ultimately being displaced by nuclear-electric technology as the program is extended must also be taken into account.

The lower half of Figure 9-1 shows the technology evolution that is necessary to assure the growth from the pre-1970 state-of-the-art (SERT 2) through an intermediate level that would permit initiation of the first electric stage missions, to an advanced level required for more demanding later missions.

A technology flight around 1975 with a simpler mission profile than the Ceres rendezvous mission would be a very desirable first step by demonstrating solar-electric propulsion in a realistic mission environment. If the vehicle is equipped to return important scientific data an attractive dual-purpose mission can be achieved. Two mission concepts have been considered:

1) An asteroid belt fly-through with an out-of-plane component to determine the decrease of micrometeoroid flux with distance from the ecliptic and to find a safe route for future missions across the asteroid belt.

2) An out-of-ecliptic probe that includes significant solar distance variation to exhibit effects of propulsion power change. Flyby at earth at nodal crossings would provide an excellent demonstration of guidance and navigation capabilities.

The out-of-ecliptic mission analyzed among the five primary stage missions could conceivably be reformulated to include the technology flight objectives even at the risk of not achieving the desired full 45° orbit inclination.

10.0 PROGRAM PLAN

10.1 INTRODUCTION

The primary objectives of the planning effort were to gather and access data necessary to evaluate the solar electric upper stage design and to form the basis for stage and total program cost estimates. The stage, designed for multi-mission use, is developed during initial mission procurement and then used as a production article, with adaptations, for a series of missions outlined in the previous section. The total program encompasses all the missions and the necessary supporting elements to implement the sequence. The baseline stage development plan includes schedule and task descriptions that relate to the total program through the master schedule and interface definitions. The total program is expressed in the same elements in the plan and the cost estimate. Shown in the work breakdown structure in section 11.0 the elements are: Total program management and technical direction, payload projects for the twelve identified missions, the solar electric upper stage project, the launch vehicle, launch operations and mission operations.

The planning, done in conjunction with the cost estimates was performed in the following manner:

- Ground rules and assumptions were made that apply to all aspects of the planning and cost estimates.
- A work breakdown structure was defined to show how the stage is related to other elements of the program and to logically organize the cost estimates.
- The work breakdown was the basis for preliminary schedules to arrange and group the work in logical phases. This schedule was used as a guide by all planners and cost estimators.

The initial plans were layed out and then given to the participating subsystem engineers for refinement using the ground rules, master schedule, and planning work sheets. The data was then recombined and adjusted to form the final program plan. These data and the design data were used as the basis for the cost estimates.

The ground rules and assumptions from which the planning was derived are listed in Table 10-1. The work breakdown structure is defined in Section 11. The master schedule in its confirmed form is shown in Section 10.2.

Table 10-1. Solar Electric Upper Stage Program Planning Ground Rules

- The baseline plan includes all the activities required to design, develop, fly and operate the stage through the baseline mission, for example, the asteroid rendezvous mission.
- The baseline plan applies to the identified baseline stage design.
- The total program plan considers the effects of incremental configuration changes and stage quantities for the eleven other mission types identified.
- The plan identifies all elements that are required for the program.
- Maximum use of existing facilities is assumed. This applies to both contractor and Government facilities.
- Maximum application of proven implementation techniques and equipment is assumed.
- The schedule is based on current experience considering launch window opportunities, individual payload procurement, and regular production cycles for support elements.
- Ground test hardware required for the program will include engineering model units as required for new design, units for qualification test subsequently used in prototype stage testing, a combined structural and thermal model, a prototype stage, and selected spares.

10.2 SCHEDULES

10.2.1 Master Program Schedule

The schedule for a representative overall program, involving the programmatic sequence of missions identified in Section 9.0 is shown in Figure 10-1. This example includes the five primary missions

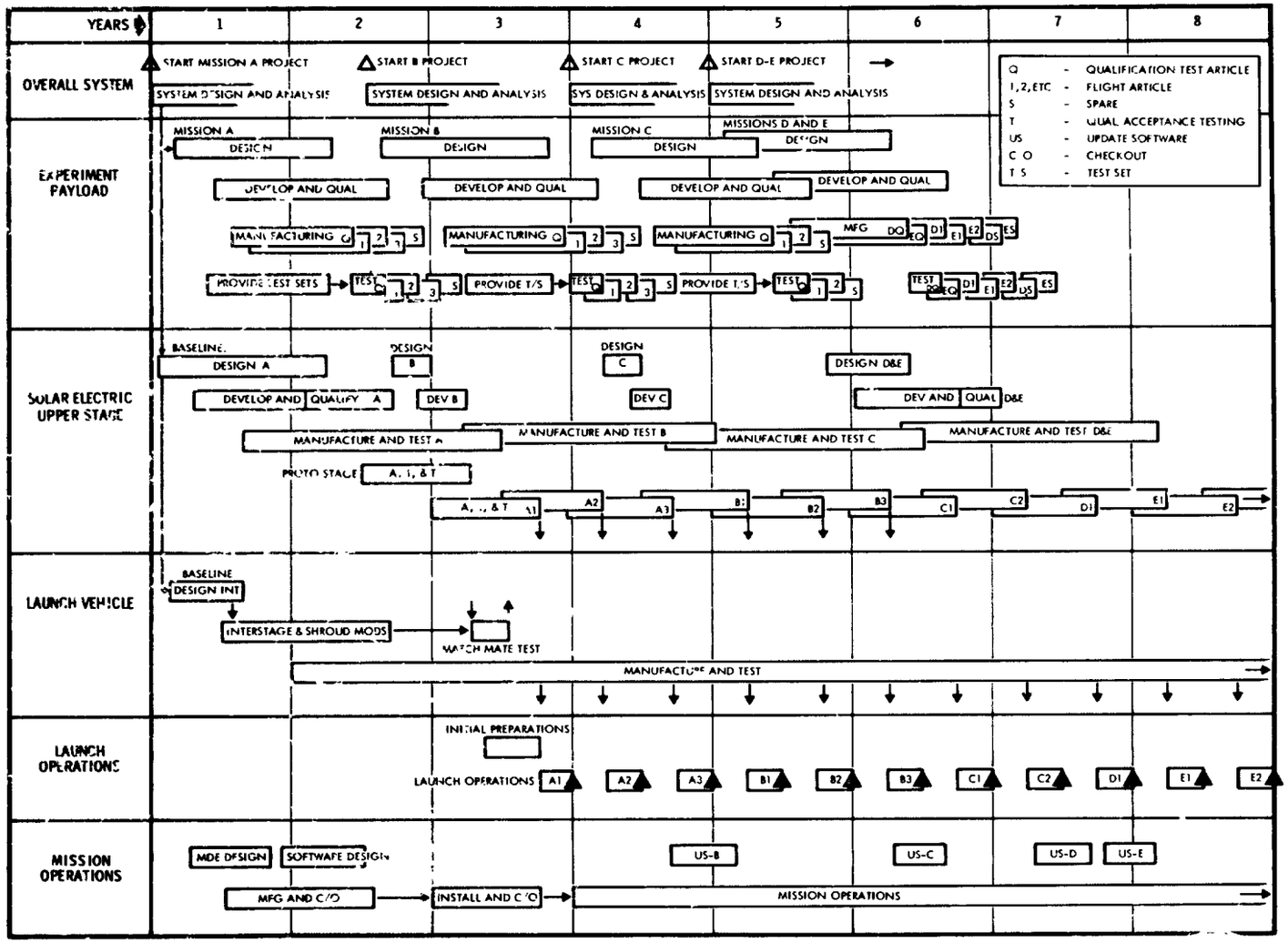

Figure 10-1. Master Program Schedule

and establishes a pattern that applies equally well to the secondary and growth missions. The five missions are: A) asteroid rendezvous (example baseline mission), B) comet rendezvous, C) out-of-ecliptic probe, D) Mercury orbiter, and E) solar probe. The letters correspond to those noted on the schedule.

The schedule is organized by major elements corresponding to those of the overall program work breakdown structure. These are the payload projects, the solar electric upper stage project, the launch vehicle, launch operations and mission operations. All of these elements are included to show the interrelated effects of launch rate on payload procurement and upper stage and launch vehicle production.

The schedule shows a launch rate of about two flights per year. This rate assumes that the payloads would be developed independently and would be started "new" for each mission by various contractors. The fact that the mission launch window requirements are not demanding permits a flexibility of launch rate that allows adjustments to realize an overall cost effective approach. Procured in this fashion, payload development is nearly insensitive to launch rate. By selecting a realistic and regular launch rate, effective cost savings can be realized in each of the other areas. A rate of two flights per year was chosen to maintain nearly constant man loading for the solar electric upper stage and launch vehicle production. The rate also affects the number of sets of equipment and special facilities required. In this case two system test sets are necessary during the prototype qualification period, therefore the stage production rate was subsequently adjusted to efficiently utilize these expensive items. Ultimately all other elements of the program should be planned to effectively use the facilities and not impose excessive "peaks" and "valleys" of activities or unnecessary duplication of expensive equipment or facilities. The rate chosen is not finally optimized and can be adjusted to more frequent launches with the use of additional support equipment. If the adjustment is for less frequent launches, a limit is realized when the rate is so slow as to cause "shut down" and "start-up" costs. Stock piling with adherence to regular production schedules can reduce these costs.

For the schedule shown each payload project is completed in approximately 24 months excluding payload/stage integration and launch support. Each type of payload is essentially sequential so that there is a possibility that flight data can influence future payload equipment design.

The solar electric upper stage is developed and flight qualified within the first 30 months and first flight is at the end of the 36th month. From this point on the stage is considered to be "in production" and only minor redevelopment effort is required to accommodate changing mission requirements and in no case is a complete requalification necessary. The existing prototype equipment can be updated and tested as required. The manufacturing, and assembly, integration and test operations appear to overlap slightly, but at a more detail level the operations performed during the overlap are dissimilar and only one set of support equipment is generally necessary. In the case of the stage system test equipment, two sets are necessary because they are used at the factory and the launch site at the same time.

The launch vehicle follows much the same pattern as the solar electric stage. There are initial one-time development and flight qualification efforts to adapt the electric stage to the launch vehicle including "match-mate" tests using the prototype stage. No further modifications are anticipated due to mission changes.

Launch operations are also repetitive after the first launch with mission-caused changes only being reflected in terms of launch vehicle control inputs and changes in payload launch preparation and checkout. Each payload project must provide for the latter changes.

The mission operations however are expected to change with each mission type. It was assumed that each payload would meet DSN interface requirements and because of this, the need for mission dependent equipment could be kept at a minimum. The updating of software to operate and monitor the stage/payload combination during transit is also considered to be minimal because the stage data handling subsystem is designed for flexibility and adequate capacity for all contemplated missions.

10.2.2 Stage Development Schedules

Stage development has been estimated and scheduled to the subsystem level in Figure 10-2. The design efforts shown are for both the subsystems and units. D indicates design completion or 100% release to manufacturing. P denotes initiation of procurement for items that are known to be independent of design changes and for long lead items. M signifies the beginning of the manufacturing effort and includes planning and tool design. Completion of engineering model tests are indicated by an E. The time phased use of major test articles, such as the structure model are shown and identified by test name. T indicates the beginning of formal unit qualification and acceptance testing. Completion of manufacturing and/or formal testing is indicated by the uncircled designators for each of the units required for ground test and flight. Deliveries of primary equipment to the prototype stage begin with the structure subsystem in the middle of the 17th month and are completed with the delivery of the communications equipment at the end of 20 months. The high-gain antenna is not required until the end of the 22nd month.

Figure 10-3 schedules the assembly integration and test of the prototype and first flight stage. Because of the modular design of the stage much of the build-up and checkout of the equipment can be done independently and concurrently. The payload assembly, equipment section, propulsion module, and solar arrays all fit this category. As much time as possible is allowed for payload buildup to give maximum assurance of satisfactory experiment function and calibration prior to stage build up.

The propulsion module can also be completely integrated prior to stage build-up with no need to break lines or disconnect wiring after completion of hot firing tests. The stage environmental tests are in sequence with the final assembly and integration of the complete stage.

The prototype stage schedule and the flight stage schedule differ primarily in the environmental test times and do not yet reflect application of the learning curve for the second article. Learning curve theory has been applied to the cost estimates however.

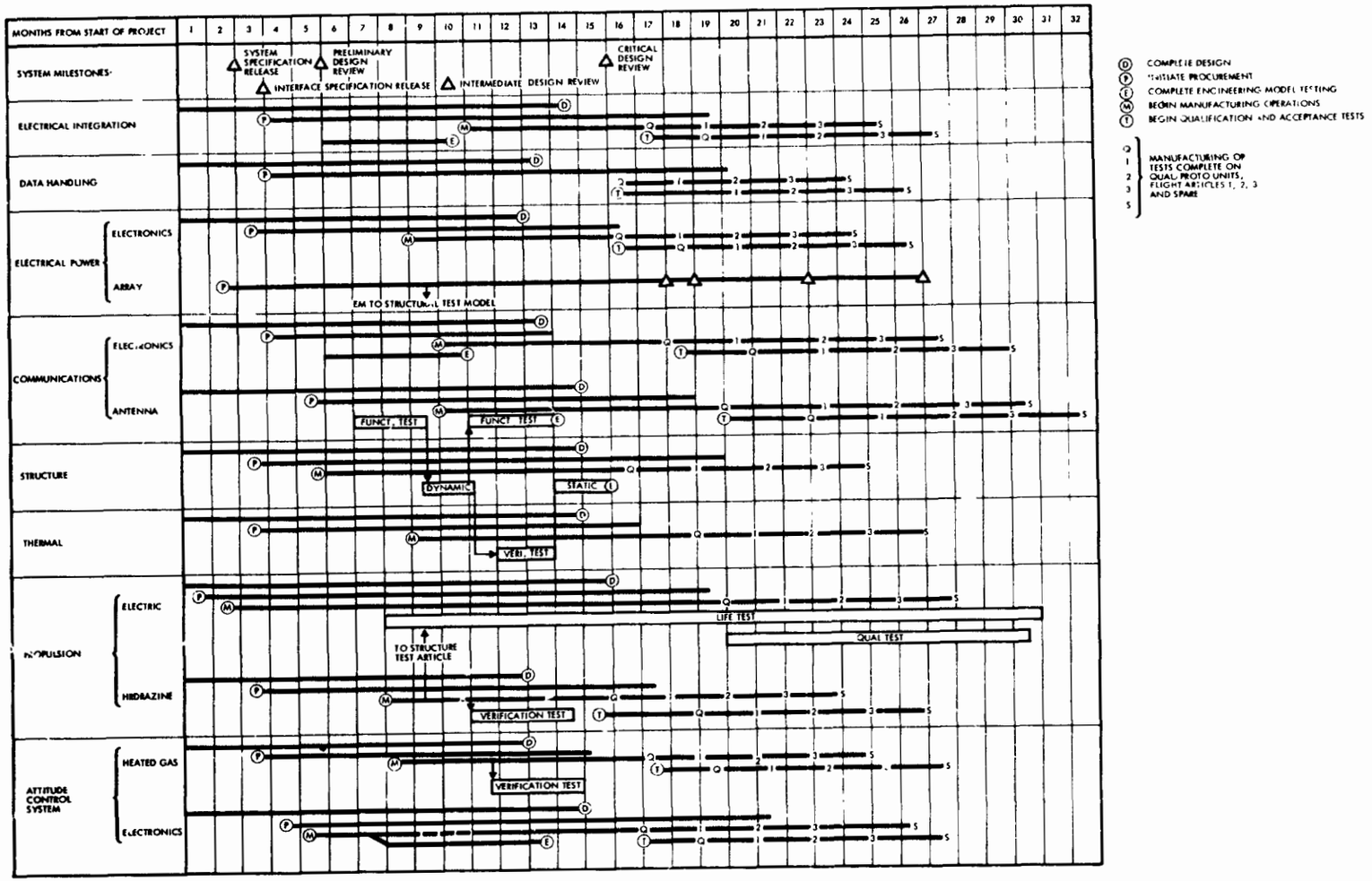

Figure 10-2. Baseline Subsystem Schedule For Design, Development, Manufacture and Qualification

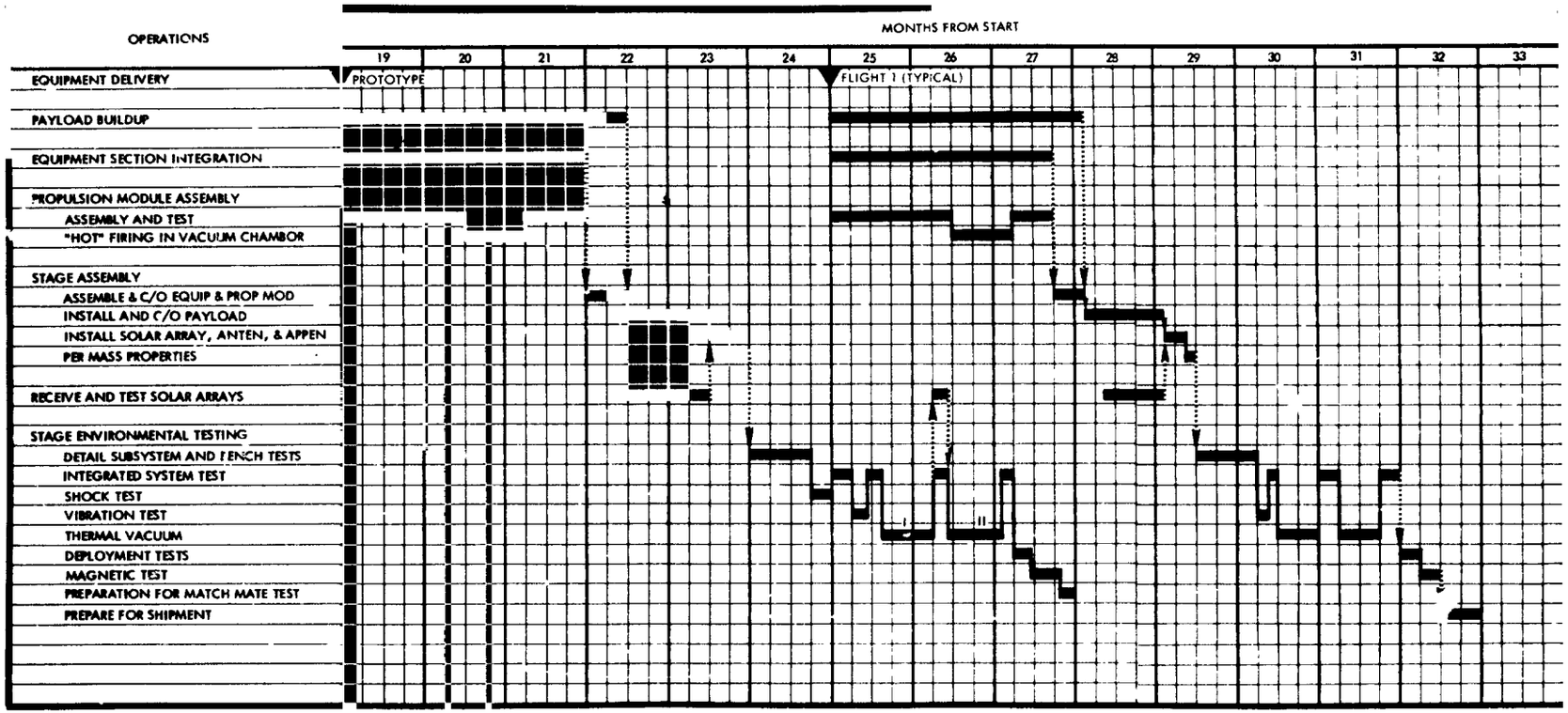

Figure 10-3. Stage Assembly, Integration and Test Schedule

Prototype build up begins with the receipt of structural hardware for the three sections. Actual equipment installation begins at the beginning of the 19th month. Prototype stage operations are complete at the end of the 27th month with completion of post-environmental functional tests and preparation for match-mate tests and storage.

First flight article build up starts after the completion of the assembly of the prototype stage using the same assembly station. The schedule allows for the first flight article to follow the prototype through assembly, integration and test without need for duplication of major facilities. The first flight article is delivered to the launch site at the end of the 33rd month permitting launch within 36 months.

These schedules are the baseline stage schedules and were used in estimating of the overall program schedule. Modification of a subsystem for different type missions will require roughly the same span times to design and qualify the new or modified units as shown in the subsystem schedules.

The major differences between the baseline schedule and other mission schedules are in that requalification of the complete stage is not required and that the majority of the effort is recurring, span times can be reduced because development is not required and learning curve theory is applicable. Therefore the span time required to prepare for a mission requiring a configuration change would be primarily dependent on the complexity of the modifications required. The remainder of effort (that of procurement and production of stage equipment) would fall within a twelve month period. The assembly integration and test time for the payload and stage would approximate that of the baseline schedule.

10.3 BASELINE DEVELOPMENT PLAN

This section describes the total program plan. The elements, other than the solar electric stage, are described sufficiently to show their relationship to the stage and help define the stage development plan. These elements correspond to those in the work breakdown structure and the cost estimates.

10.3.1 Overall Management

The overall program is managed by the Government. This portion of the program is responsible for the progressive and carefully timed procurement of the various other elements of the program. The overall management is vital in bringing about an orderly and cost effective accomplishment of the programmatic sequence of missions identified. The management effort is both financial and technical, interfacing with all other elements to achieve the exchange of data, provide primary mission analysis, and effect interface control that can allow a continuous program on which a multi-mission stage is so vitally dependent.

10.3.2 Experiment Payload

This element of the program is actually a number of separate and independent projects each managed and accomplished by contractors responsible for the design and integration of various mission dependent experiments into workable payloads. It includes the effort to coordinate the design of the experiments, meeting requirements dictated by the mission and interfacing equipment, and communication and data handling operations. Each mission type includes a separate experiment payload project. Twelve projects are assumed for completion of all twelve identified missions.

10.3.3 Solar Electric Stage Development

10.3.3.1 Project Management and System Engineering

The stage management discussed is internal contractor management. It includes the project manager and his staff, project planning and control, stage system engineering, control and experimenter liaison. The level of effort and emphasis of these activities is consistent with current NASA projects.

Project planning and control includes the support of cost control, schedule control, material coordination, contract property management, and project documentation.

System engineering and mission analysis include the mission-oriented functions of launch vehicle interface analysis, trajectory analysis, system test planning, and system design, specification and analysis.

Experimenter liaison encompasses documentation of experiment interface data, design specifications and data for experimenter use, definition of test requirements, and maintenance of the experimenter data book.

10.3.3.2 Product Integrity

This activity includes the quality assurance subproject; reliability work element, parts, materials, and processes work element; safety engineering and configuration control.

The quality assurance subproject includes quality engineering activities, quality assurance management and administration, and vendor quality assurance surveillance and management. Also included are quality assurance test observation engineering and inspection associated with subsystem development. Unit qualification and acceptance test quality assurance function are included as part of this element.

Reliability activities include design review support; life test support; unit, subsystem, and system reliability analysis; test survey, specifications and procedures review; vendor surveillance; failure reporting; and reliability management.

The parts, materials, and processes work element includes failure analysis, design review support, parts specification, material specification, support of parts applications, evaluation of parts and materials for magnetic properties, magnetic part inspection, and modification.

The configuration control includes document preparation and release, baseline data listing, verification data listing, and configuration management.

10.3.3.3 Subsystem Development

The subsystem development planning sheets express the typical activities that are required to provide the hardware. As an example Table 10-2 shows the structure subsystem development.

In brief outline, the planning sheet expresses anticipated subsystem development by indicating for each major step of DESIGN, DEVELOPMENT TESTING, MANUFACTURING, AND FORMAL TESTING the

Table 10-2. Structure Subsystem Development

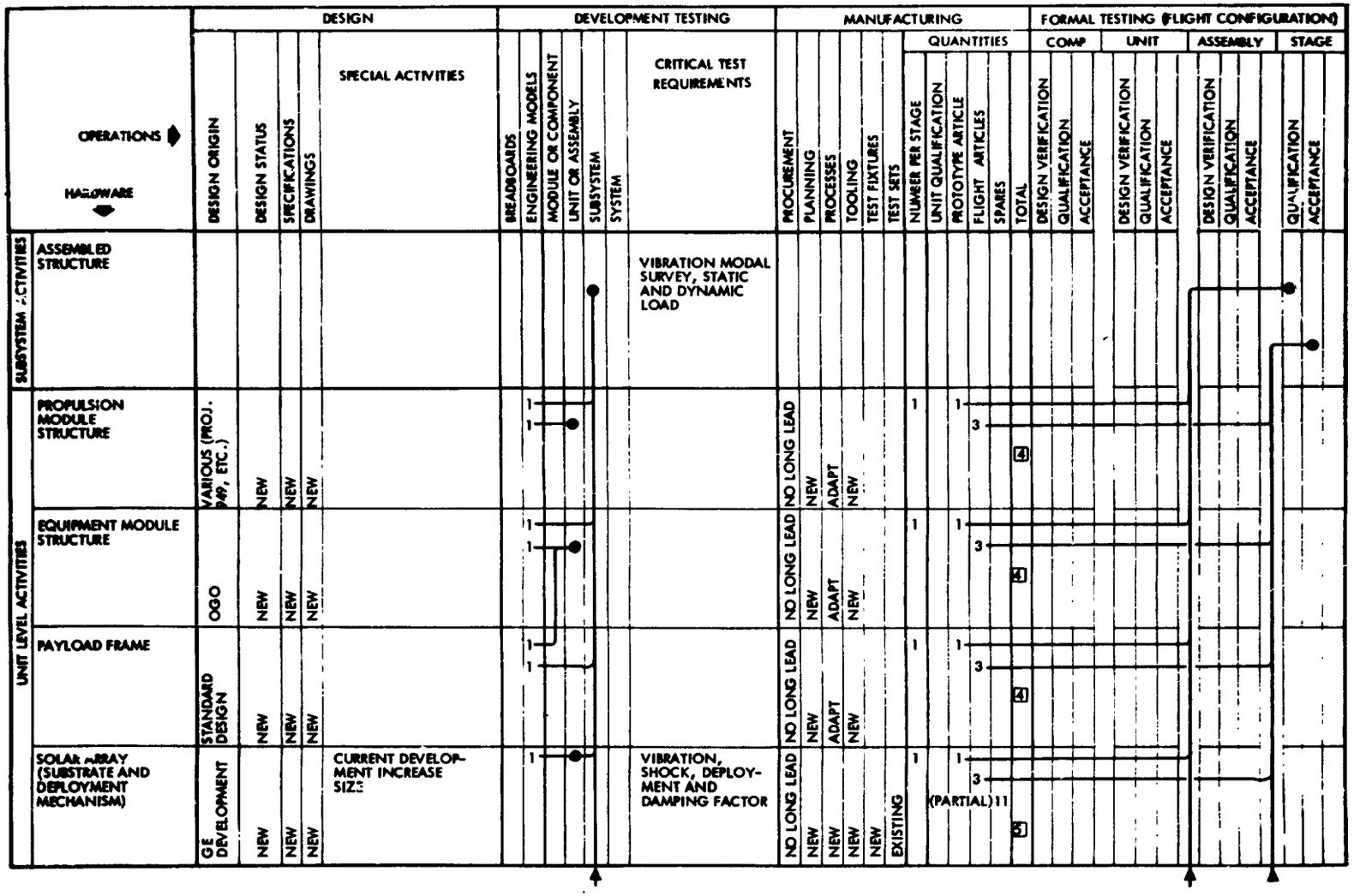

Table 10-2. Structure Subsystem Development (Continued)

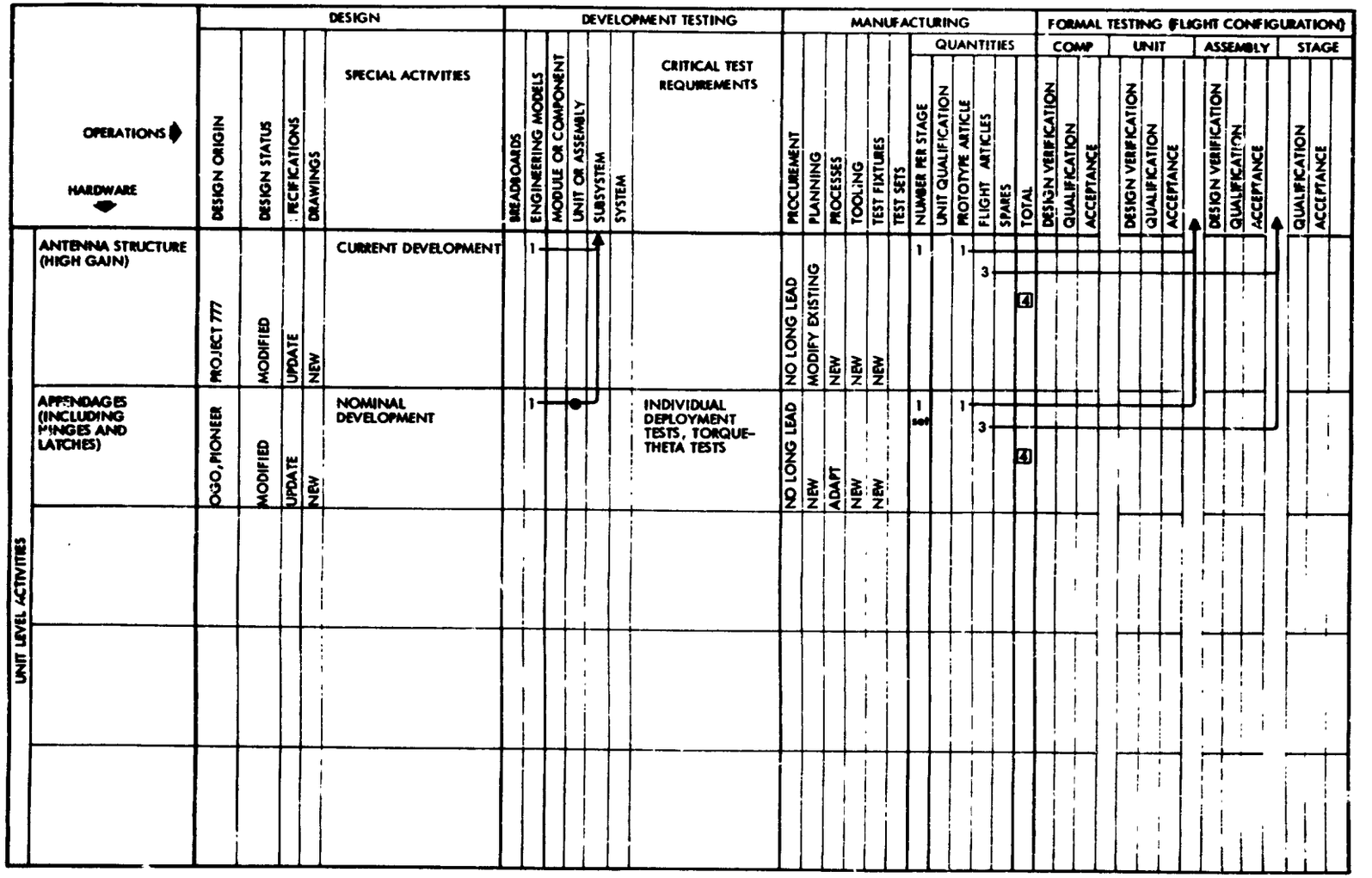

OPERATIONS / HARDWARE	DESIGN: DESIGN ORIGIN	DESIGN: DESIGN STATUS	DESIGN: SPECIFICATIONS	DESIGN: DRAWINGS	DESIGN: SPECIAL ACTIVITIES	DEVELOPMENT TESTING: BREADBOARDS	DEVELOPMENT TESTING: ENGINEERING MODELS	DEVELOPMENT TESTING: MODULE OR COMPONENT	DEVELOPMENT TESTING: UNIT OR ASSEMBLY	DEVELOPMENT TESTING: SUBSYSTEM	DEVELOPMENT TESTING: SYSTEM	DEVELOPMENT TESTING: CRITICAL TEST REQUIREMENTS	MANUFACTURING: PROCUREMENT	MANUFACTURING: PLANNING	MANUFACTURING: PROCESSES	MANUFACTURING: TOOLING	MANUFACTURING: TEST FIXTURES	MANUFACTURING: TEST SETS	MANUFACTURING: QUANTITIES: NUMBER PER STAGE	MANUFACTURING: QUANTITIES: UNIT QUALIFICATION	MANUFACTURING: QUANTITIES: PROTOTYPE ARTICLE	MANUFACTURING: QUANTITIES: FLIGHT ARTICLES	MANUFACTURING: QUANTITIES: SPARES	MANUFACTURING: QUANTITIES: TOTAL	FORMAL TESTING (FLIGHT CONFIGURATION): COMP: DESIGN VERIFICATION	FORMAL TESTING (FLIGHT CONFIGURATION): COMP: QUALIFICATION	FORMAL TESTING (FLIGHT CONFIGURATION): COMP: ACCEPTANCE	FORMAL TESTING (FLIGHT CONFIGURATION): UNIT: DESIGN VERIFICATION	FORMAL TESTING (FLIGHT CONFIGURATION): UNIT: QUALIFICATION	FORMAL TESTING (FLIGHT CONFIGURATION): UNIT: ACCEPTANCE	FORMAL TESTING (FLIGHT CONFIGURATION): ASSEMBLY: DESIGN VERIFICATION	FORMAL TESTING (FLIGHT CONFIGURATION): ASSEMBLY: QUALIFICATION	FORMAL TESTING (FLIGHT CONFIGURATION): ASSEMBLY: ACCEPTANCE	FORMAL TESTING (FLIGHT CONFIGURATION): STAGE: QUALIFICATION	FORMAL TESTING (FLIGHT CONFIGURATION): STAGE: ACCEPTANCE
UNIT LEVEL ACTIVITIES																																	
ANTENNA STRUCTURE (HIGH GAIN)	PROJECT 777	MODIFIED	UPDATE	NEW	CURRENT DEVELOPMENT		1						NO LONG LEAD	MODIFY EXISTING	NEW	NEW	NEW		1		1	3	[4]											
APPENDAGES (INCLUDING HINGES AND LATCHES)	2GO, PIONEER	MODIFIED	UPDATE	NEW	NOMINAL DEVELOPMENT		1					INDIVIDUAL DEPLOYMENT TESTS, TORQUE-THETA TESTS	NO LONG LEAD	NEW	ADAPT	NEW	NEW		1 (100)		1	3	[4]											

degree of similarity to current experience. Each hardware element that makes up the subsystem (including subsystem level functions) is listed on the left. Notation on the sheet indicates for each element: design derivation and status, necessary development testing by breadboard or engineering model at various levels at assembly, manufacturing background and quanties for ground and flight test, and test article utilization through formal-flight configuration testing. Space is available to make note in caption sentence form of special design and test activities. The intent is to express the development plan in terms to allow cost and schedule analysis by analogy with existing data.

Unit development tests for new design begin with breadboard testing for circuit verification. Engineering models are used for magnetic cleanliness testing and electromagnetic compatibility critical environment tests as well as for test set validation and performance testing.

The major subsystem development tests include the propulsion, structural, thermal, and a combined attitude control and propulsion module test. The propulsion tests include assembled engineering model testing, qualification test firing, and life testing. The structural tests include dynamic and static load tests, mass properties tests and appendage deployment verification. Launch vehicle compatibility and fit checks, and mechanical ground support handling and use verification are performed using full scale boiler plate models and then the prototype stage. The thermal subsystem tests verify the thermal control design under thermal-vacuum conditions simulating the worst case conditions for the mission. The combined attitude control and propulsion system tests check the performance and dynamic response of the three axis gimbal to control system operation.

Unit qualification and acceptance test are conventional for the electrical units. Qualification tests include shock, vibration, acoustics, thermal vacuum exposures with pre- and post-environment performance tests, EMC test, and magnetic properties test. Acceptance tests include vibration and thermal vacuum exposures with pre- and post-environmental performance tests and magnetic cleanliness tests. The qualification and acceptance test levels are based on the extremes of Titan 3E/Centaur launch environments.

10.3.3.4 Support Equipment Development

The electrical ground support equipment planned for use on the solar electric stage payload assembly, integration, and test consists of the consoles and racks listed in Table 10-3. Two of these system test sets are required for the baseline plan. The computer is assumed to be Government furnished.

The mechanical ground support equipment planned is listed in Table 10-4. It is typical of such spacecraft as OGO, HEAO and several equivalent current classified spacecraft.

Table 10-3. Electrical Ground Support Equipment

- RF Console
  - Narrowband receiver
  - Low power transmitter (exciter)
  - RF amplifier
  - Ramp generator
  - Command generator
- Digital Computer
  - Main frame
  - Paper tape punch
  - Card reader
  - Disc file
  - Typewriter
  - Line printer
- Recorder Console
  - 7-track
  - Mixed direct and FM
  - Tape transport servo
- Telemetry Data Console
  - Demodulator synchronizer
  - Computer buffer
  - Word select
  - Status display
  - D-A converters
  - Remote console driver/buffer
- Test Conductor Console
  - Remote display and callup
  - Remote CRT
- Ground Power Console
  - Solar array simulator
  - Stage power supply
- EGSE Peripheral
  - Ordnance/ACS test
  - ACS-simulator
  - Engine simulator
  - Hardline monitor
  - Sensor stimulators
  - Xenon array tester

Table 10-4. Mechanical Ground Support Equipment

- Stage work stand
- Rotation and vertical erection dolly
- Transporter (vertical)
- Propulsion module work stand
- Solar array holding and installation fixture
- Solar array deployment fixture
- Thruster assembly holding and installation fixture
- Thruster assembly alignment fixture
- High-gain antenna holding and installation fixture
- High-gain antenna alignment fixture
- Louver protective holder (three or four kinds)
- +X axis boom fixture
- Vibration test fixture
- Space simulation fixture
- Lifting slings
- Solar array storage containers
- Spacecraft shipping container
- Propellant loading/pressurization cart

10.3.3.5 Spacecraft Development

The prototype stage is used for initial system compatibility and performance tests and to verify system test set operations. The assembly integration, formal environmental testing for both the prototype and flight stages are shown in Figure 10-4. Build up and check out of the equipment section, propulsion module, payload equipment, and solar array assembly is done concurrently. The propulsion module, assembly is completed and a hot firing test is performed in a vacuum chamber prior to installation on the stage. All subsystems

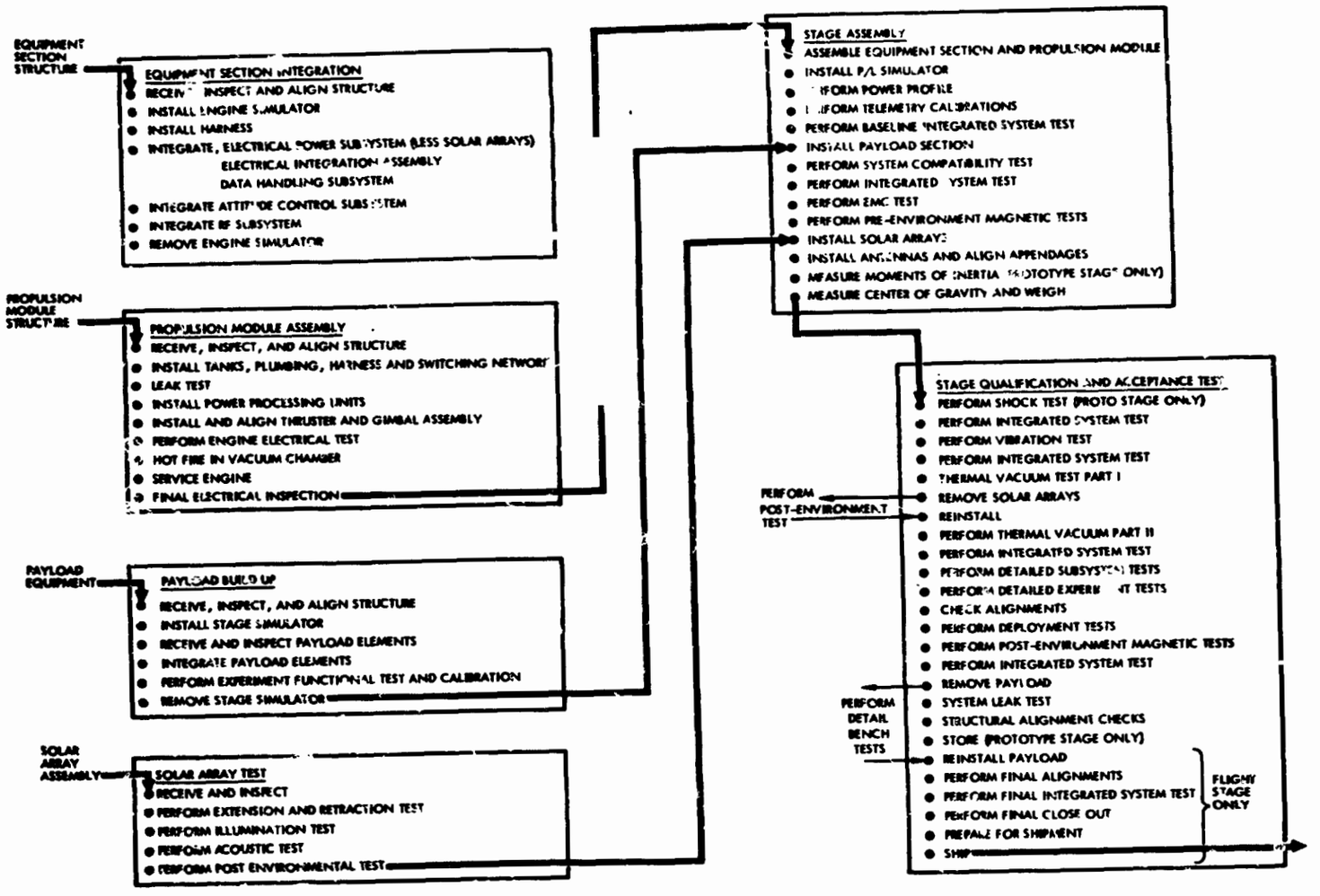

Figure 10-4. Stage Assembly, Integration and Test Tasks

can be integrated and checked on the equipment module, and the payload operated prior to propulsion module installation. The payload equipment can be tested using simulators with stage functions performed through hard lines to the equipment section. The solar array can be received and completely tested as an assembly. Each of these separate subassemblies are installed during stage assembly as complete modules, and each can be tested independently in detail following stage environmental tests.

Figure 10-5 shows a representative stage assembly and test area. An existing high bay of TRW building M-1 was used to check the facility application. All assembly and test operations, including deployment of the solar array wing can be accomplished in the area. The solar simulation chamber shown is used to test sections of the prototype stage for thermal characteristics that will subsequently be used for all up stage tests in the existing M-4 chamber.

10.4 BASELINE PRE-LAUNCH AND LAUNCH OPERATIONS

The launch operations include all operations for the launch complex, launch vehicle, solar electric upper stage and the payload. The launch complex support, (Government furnished) includes range support, base services, pre-and post-launch data reduction and analysis, the conduct of the countdown and launch, and pad-refurbishment. After the initial preparations, no modifications to procedures and operations are required except for payload differences and mission dictated loading and launch control procedures. The initial preparations include launch facilities modifications, for the stages and special launch equipment. It is assumed that each contractor, i.e., electric stage and payload contractors, will supply their own special launch support equipment. These include system test sets, mechanical handling equipment, propellant loading (mercury and hydrazine) and the maintenance and spares support. The launch vehicle system includes the stage, adapter to the solar electric upper stage, the shroud, propellant and boost vehicle contractor support.

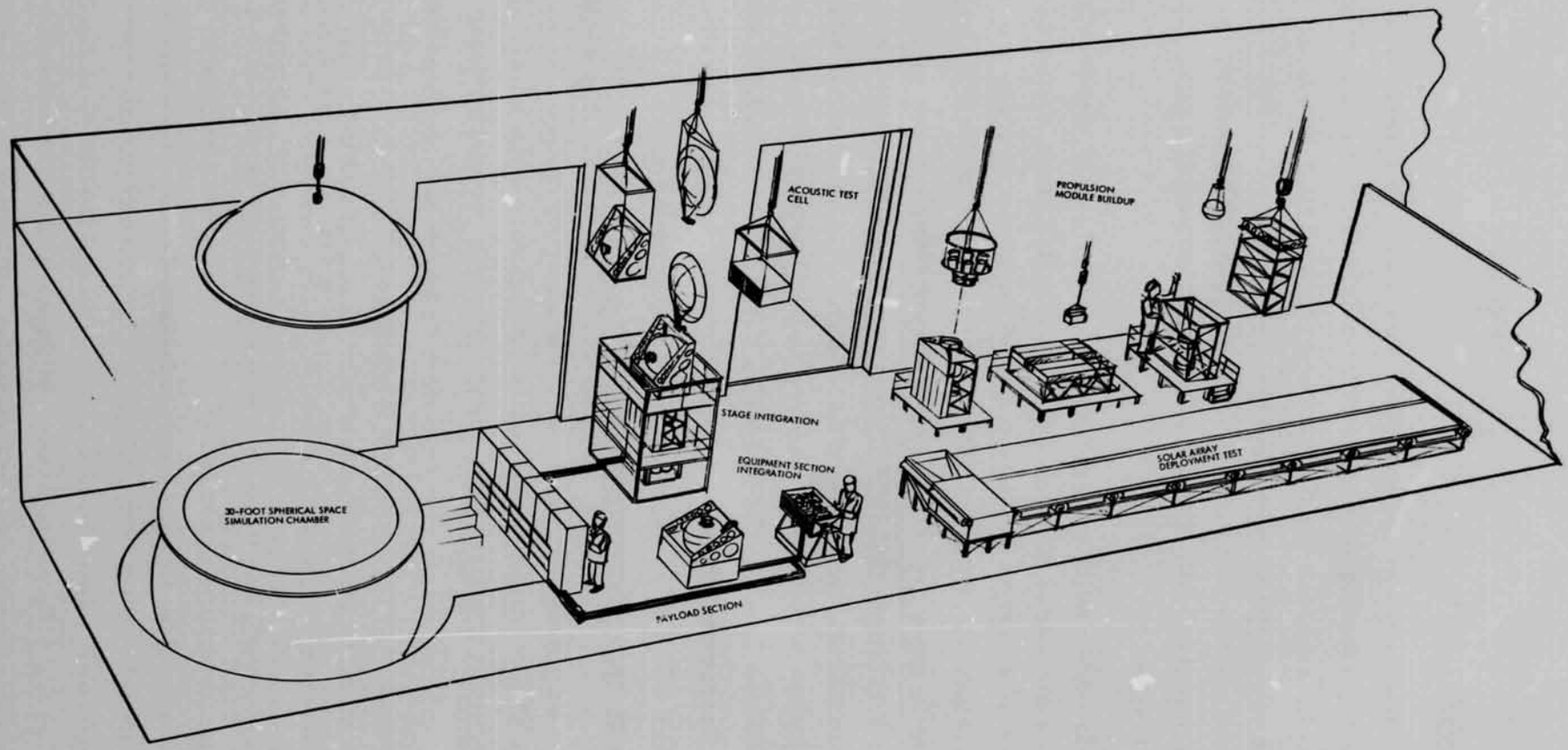

Figure 10-5. Representative Assembly Integration and Test (TRW Bldg. M-1 High Bay)

10.5 MISSION OPERATIONS

The stage-payload configuration as well as the payload are compatible with the existing Deep Space Network. The post-launch operation phase typically requires stage operation checks every five to seven days, using any of the 85-foot diameter DSIF antennas. Final data readout for the payload is considered dedicated and is usually through the 85-foot antenna, with limited use of the 210-foot diameter antenna on some missions.

At this point, no mission dependent equipment is identified. The preparations for initial mission operations will include design and development of software to operate the stage, process telemetry data, and transmit and verify commands. The prototype stage equipment section is to be used for DSIF-Stage-payload compatibility tests. A month before launch DSIF configuration verification tests are completed and software configuration is frozen. For subsequent mission launches, software is updated and verification tests are repeated for the configuration freeze. Mission operations are scheduled continuously for stages in transit. For the schedule shown, 3 to 4 stages can be in transit at one time.

10.6 INVENTORY REQUIREMENTS

Table 10-5 lists the stage equipment quantities required to support the twelve typical missions identified during the study. By accounting for each type of equipment applicable to each mission at the unit level, an idea of the true repetitive nature of the multi-mission stage design emerges. Individual units (black boxes) are applicable to many or all mission configurations even when stage and subsystem configurations vary from the baseline.

The table lists each mission in the proper programmatic sequence depending on priorities and complexity. The number of flights anticipated for each mission are shown. Stage configuration is expressed by units that make up each subsystem. Units that vary from baseline are shown also as line items. Quantities that make up the inventory of equipment are shown on the body of the table. Included are equivalent units required for development, unit qualification, system (or stage) qualification, and spares support.

INVENTORY REQUIREMENTS

MISSIONS				PRIMARY: BASELINE ASTEROID RENDEZVOUS	PRIMARY: COMET RENDEZVOUS	PRIMARY: OUT-OF ECLIPTIC	PRIMARY: MERCURY ORBITER	PRIMARY: SOLAR PROBE	SECONDARY: OUTER PLANET FLYBY (TOPS)	SECONDARY: OUTER PLANET ORBITER (TOPS)	SECONDARY: MARS/ VENUS ORBITER	SECONDARY: SOLAR MONITOR/ RELAY STATION	GROWTH: HALLEY'S COMET PROBE	GROWTH: ASTEROID SAMPLE RETURN	GROWTH: MARS SAMPLE RETURN	CUMULATIVE TOTALS: PRIMARY	CUMULATIVE TOTALS: PRIMARY AND SECONDARY	CUMULATIVE TOTALS: PRIMARY SECONDARY AND GROWTH
STAGE DESIGN CRITERIA																		
EXTREME THERMAL ENVIRONMENT					●		●	●					●					
HAZARDOUS ENVIRONMENT/MISSION					●			●					●	●	●			
DIFFICULT POWER AND THRUST REQUIREMENT					○	●	●			●			●	●	●			
COMPLEX MISSION SEQUENCE					●		●				○		●	●	●			
BULKY OR COMPLEX PAYLOAD						○		○	●	●		●		●	●			
SIGNIFICANT CHANGE OF CONFIGURATION								●							●			
DIFFICULT NAVIGATION AND GUIDANCE				●	●		●						●	●	●			
LONG MISSION LIFE (>2 YEARS)				○	○				●	●		●	●	●	●			
FLIGHTS PER MISSION				3	3	2	1	2	4	4	2	2	2	3	2	11	23	30
STAGE CONFIGURATION	*D	Q	S															
STRUCTURE:																		
PROPULSION MODULE	1	1		3	3	2	1	2	4	4	2	2	2	3	2	13	25	32
EQUIPMENT MODULE	1	1		3	3	2	1	2	4	4	2	2	2	3	2	13	25	32
PAYLOAD FRAME	1	1		3	3	2	1	2	4	4	2	2	2	3	2	13	25	32
SOLAR ARRAY SUPPORT STRUCTURE	1	1		3	3	2	1	2	4	4	2	2	2	3	2	13	25	32
HEAT SHIELD STRUCTURE	1	1				2										4	4	4
ANTENNA STRUCTURE	1	1		3	3	2	1	2	4	4	2	2	2	3	2	13	25	32
APPENDAGES, HINGES & LATCHES	1	1		3	3	2	1	2	4	4	2	2	2	3	2	13	25	32
THERMAL:																		
LOUVERS (SET)	1	2	1	3	3	2	1	2	4	4	2	2	2	3	2	15	27	34
INSULATION & RADIATOR PLATES	1	1		3	3	2	1	2	4	4	2	2	2	3	2	13	25	32
HEATERS (SET)	1	1	1	3	3	2	1	2	4	4	2	2	2	3	2	14	26	33
HEAT SHIELD	1	1						2								4	4	4
ELECTRIC PROPULSION:																		
ION THRUSTERS	2	13	(4)	18	18	12	6	12	24	24	12	12	12	18	12	85	157	199
BEAM AND ACCEL PPU	1	11	(3)	12	12	10	5	10	16	16	8	8	8	12	8	64	112	140
MULTIPLE OUTPUT PPU	1	13	(4)	18	18	12	6	12	24	24	12	12	12	18	12	84	156	198
PROPELLANT STORAGE & DIST.	2	4	(2)	3	3	2	1	2	4	4	2	2	2	3	2	19	31	38
SWITCHING NETWORK	2	4	(2)	3	3	2	1	2	4	4	2	2	2	3	2	19	31	38
THRUST VECTOR CONTROL	1	4	(2)	3	3	2	1	2	4	4	2	2	2	3	2	18	30	37
HYDRAZINE PROPULSION:																		
PROPELLANT TANK		1	1	3	3		1						2	3	2	9	9	16
FILL AND DRAIN VALVES		2	1	6	6		2						4	6	4	17	17	31
PRESSURE TRANSDUCER		1	1	3	3		1						2	3	2	9	9	16
FILTER		1		6	6		2						4	6	4	15	15	29
LINES AND FITTINGS		1		6	3		1						2	3	2	11	11	18
THRUST CHAMBER ASSEMBLY	1	1	1	6	6		2						4	6	4	17	17	31
ELECTRIC POWER:																		
BATTERY	6	2	1	3	3	2	2	2	4	4	4	2	2	3	4	21	35	44
STAGE POWER SUPPLY (PCU)	1	1	1	3	3	2	1	2	4	4	2	2	2	3	2	14	26	33
**SOLAR ARRAY 17.5 KW	1/4	1/4	1	3	3	2	1	2	4	4						12-1/2	20-1/2	20-1/2
SOLAR ARRAY 21.0 KW	1/4	1/4	1										2		2	1-1/2	1-1/2	5-1/2
SOLAR ARRAY 12.0 KW											2	2		3		0	4	7
ELECTRICAL INTEGRATION:																		
ELECT. INT. ASSEMBLY	1	1	1	3	3	2	1	2	4	4	2	2	2	3	2	14	26	33
HARNESS SET		1		3	3	2	1	2	4	4	2	2	2	3	2	13	25	32
ATTITUDE CONTROL SYSTEM: (ELECTRONICS)																		
COURSE SUN SENSORS		4	2	6	6	4	2	4	8	8	4	4	4	6	4	28	52	66
FINE SUN SENSORS		2	1	6	6	4	2	4	8	8	4	4	4	6	4	25	49	63
FINE SUN SENSOR ELECTRON.	2	1	1	3	3	2	1	2	4	4	2	2	2	3	2	15	27	34
STAR TRACKER		1	1	3	3	2	1	2	4	4	2	2	2	3	2	13	25	32
STAR TRACKER DRIVE (1-AXIS)		1	1	3	3	2	1	2	4	4	2	2	2	3	2	13	25	32
CONTROL PROCESSOR ASSY.		1	1	3	3	2	1	2	4	4	2	2	2	3	2	13	25	32
CONTROL ELECTRONICS ASSY	2	1	1	3	3	2	1	2	4	4	2	2	2	3	2	15	27	34
RATE GYRO ASSEMBLY		1	1	6	6	4	6	4	8	8	12	4	4	18	12	28	60	94
BI-AXIAL ANTENNADRIVE		1	1	3	3	2	1	2	4	4	4	2	2	3	2	13	27	34
TV CAMERA BI-AXIAL DRIVE		1	1	3	3		1				2	2	2	3	2	9	13	20
SOLAR ARRAY DRIVE ASSEMBLY		2	1	3	3	2	1	2	4	4	2	2	2	3	2	14	26	33
TV CAMERA		1	1	3	3		1				2	2	2	3	2	9	13	20
(PNEUMATICS)																		
NITROGEN TANKS	1	6	1	6	6	4	2	4	8	8	4	4	4	6	4	30	54	68
SOLENOID VALVES		13	3	36	36	24	12	24	48	48	24	24	24	36	24	148	292	376
NOZZLES	1	13	3	36	36	24	12	24	48	48	24	24	24	36	24	149	293	377
REGULATORS & RELIEF VALVES	1	2	1	6	6	4	2	4	8	8	4	4	4	6	4	28	50	64
PRESSURE TRANSDUCERS		4	2	12	12	8	4	7	16	16	8	8	8	12	8	50	98	126
CROSS CONNECT VALVES		2	1	6	6	4	2	4	8	8	4	4	4	6	4	25	49	63
ISOLATOR VALVES		2	1	6	6	4	2	4	8	8	4	4	4	6	4	25	49	63
FILL VALVES		2	1	6	6	4	2	4	8	8	4	4	4	6	4	25	49	63
LINES AND FITTINGS	1	1	1	3	3	2	1	2	4	4	2	2	2	3	2	14	26	33
TEMPERATURE TRANSDUCERS		2	1	6	6	4	2	4	8	8	4	4	4	6	4	25	49	63
COMMUNICATIONS:																		
COMMAND DEMODULATOR		1	1	3	3	2	1	2	4	4	2	2	2	3	2	13	25	32
RECEIVER	1	2	1	6	6	4	2	4	8	8	4	4	4	6	4	26	50	64
R-F SWITCHES		2	1	6	6	4	2	4	8	8	4	4	4	6	4	25	49	63
COUPLER DIPLEXER		1	1	3	3	2	1	2	4	4	2	2	2	3	2	13	25	32
DIPLEXER		1	1	3	3	2	1	2	4	4	2	2	2	3	2	13	25	32
TWTA	1	2	1	6	6	4	2	4	8	8	4	4	4	6	4	26	50	64
TWT DRIVER		2	1	6	6	4	2	4	8	8	4	4	4	6	4	25	49	63
S-BAND ANTENNA (8-FT)	1	1		3	3	2	1						2	3	2	11	11	18
S-BAND ANTENNA (4-FT)	1	1		3				2	4	4	2	2				7	19	19
OMNI-ANTENNA	1	2	1	6	6	4	2	4	8	8	4	4	4	6	4	26	50	64
DATA HANDLING:																		
TAPE RECORDERS	1	2	1	6	6	4	2	4	8	8	4	4	4	6	4	26	50	64
BUFFER STORAGE		2	1	6	6	4	2	4	8	8	4	4	4	6	4	25	49	63
DIGITAL TELEMETRY UNIT		1	1	3	3	2	1	2	4	4	2	2	2	3	2	13	25	32
BASE BAND ASSEMBLY		1	1	3	3	2	1	2	4	4	2	2	2	3	2	13	25	32

*D = DEVELOPMENT UNITS
Q = QUAL AND/OR PROTO UNITS
S = SPARE

● = CONDITION EXISTS IN ALL FLIGHTS
○ = CONDITION EXISTS IN SOME FLIGHTS

**SOLAR ARRAY CONSISTS OF TWO WING ASSEMBLIES OF 2 PANELS EACH

Table 10-5. Inventory Requirements

Cumulative totals for each unit are given for each of the three phases.

From these data, cost estimates can be made for various program plans. Figure 10-6 illustrates, in qualitative form, the effects of different approaches to procurement of the stages. Figure 10-6 shows cumulative totals of stages for each of the twelve missions identified. The quantities are shown for three different procurement plans. Plan A is the long range use of the multi-mission stage. Plan B reflects requalification at the beginning of each of the three phases. Plan C shows quantities required to requalify after each mission. Quantities include development, unit qualification, system qualification, and spares. Missions 4 and 5 (Mercury Orbiter and Solar Probe) share the same qualification testing.

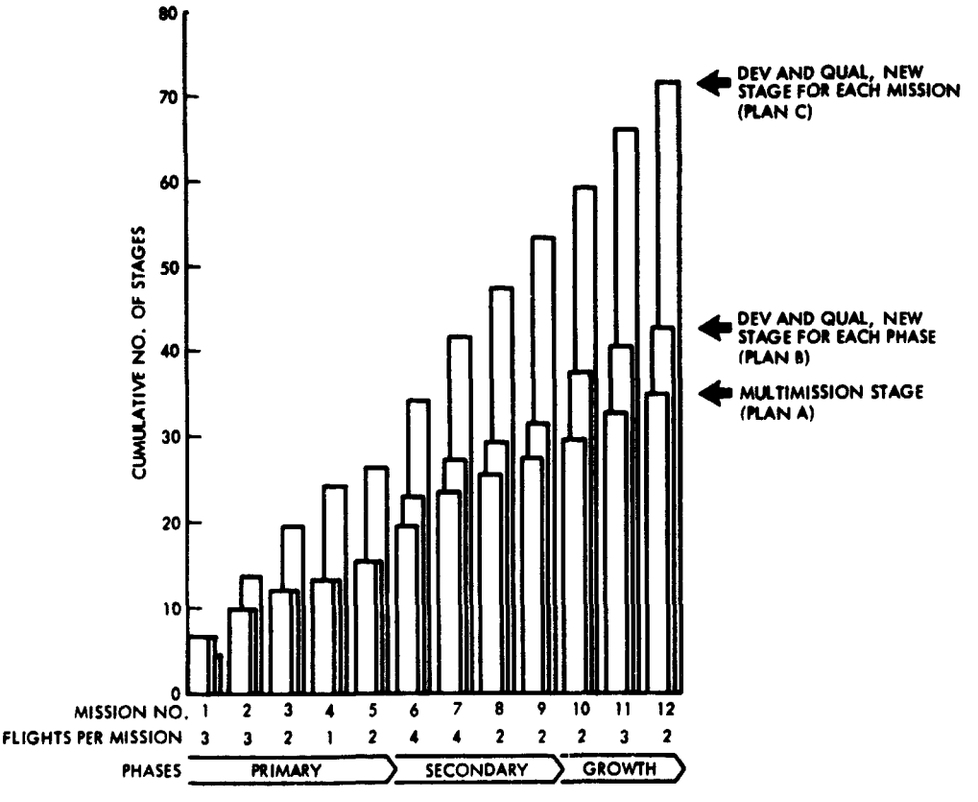

Figure 10-6. Comparison of Number of Stages Required for Multi-Mission Stage Approach and Individual Stage Approach

11. PROGRAM COST

11.1 COST ESTIMATES

This section provides representative cost data in support of resource planning for development and initial use of the baseline Solar Electric Upper Stage (SEUS), its payload, launch vehicle, mission and launch operations. The Work Breakdown Structure (WBS), Figure 11-1 outlines the overall program elements and their costs.

The total cost of three baseline SEUS vehicles, which reflects the system design, development, assembly and test amounts to $96.4 million. The largest individual cost items are the electrical power subsystem ($21.5 million), Electric Propulsion subsystem ($9.6 million), and the Attitude Control ($13.7 million), as would be expected in a vehicle of this type.

The total program cost of $126.4 million for three baseline missions is the summation of the cost estimates for each element shown on the WBS. This cost includes all project costs from design inception through life of mission operations of the third flight spacecraft. This covers a span of 6 years as shown in Figure 10-1, Overall Summary Schedule.

Government Engineering and Technical Direction costs includes the overall Government program management. TRW assumes these costs to be a factor of 8% of the total cost of all other program elements.

Representative cost estimates for the Solar Electric Upper Stage (SEUS) in the baseline configuration covers all costs of design, development, qualification and procurement of three flight spacecraft. Because of the importance of the SEUS cost accuracy to the total program cost model, TRW has concentrated its efforts in estimating the cost of this element.

The approach used to prepare cost estimates for the SEUS combined TRW recorded cost experience and "performer" management judgment to assure up-to-date application of the historical cost data. "Performer" refers to the organization that would accept responsibility

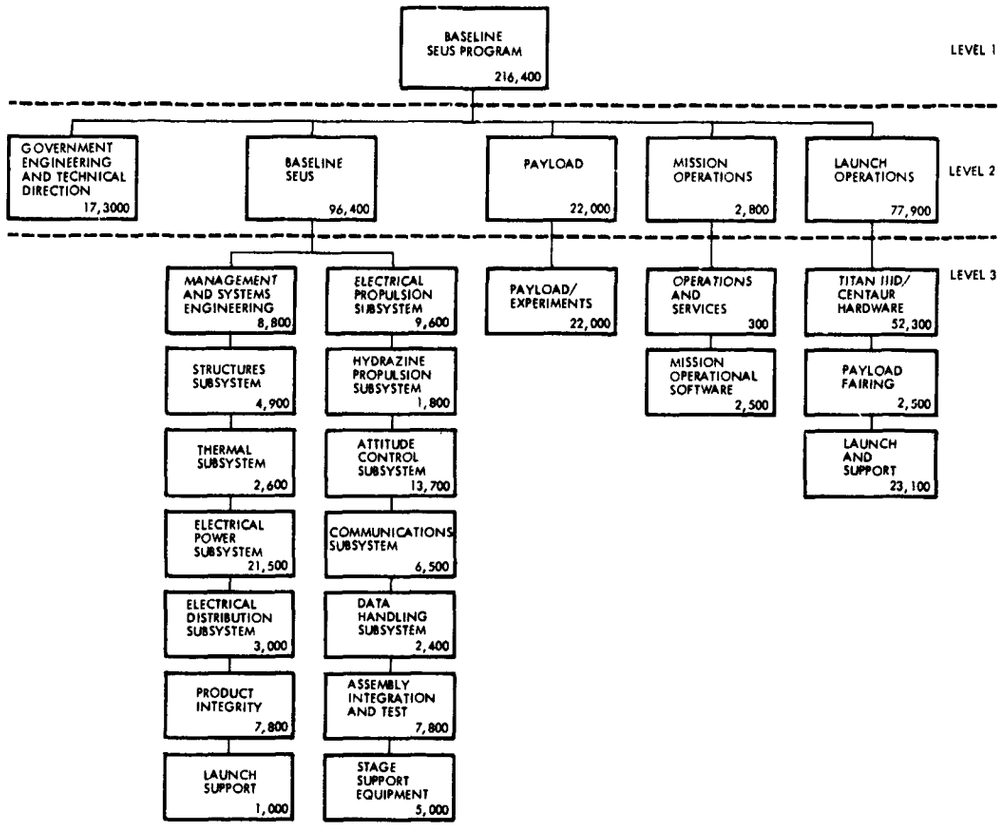

Figure 11-1. Baseline SEUS Program Elements and Cost (3 flights) ($K)

for the relevant work. Extensive use was made of the TRW cost data bank to develop comparisons between the SEUS cost elements and those of projects recorded in the data bank. Particularly useful data came from projects that resemble the SEUS such as OGO with its box structure, and Pioneer F and G with missions similar to that of the SEUS. DOD spacecraft experience was useful for up-to-date data at the unit level. Direct estimates were made in some cases where the cost data bank did not apply or where historical data did not exist.

The sequence of estimating and review is as follows. Each subsystem engineer involved in the design was required to complete "planning data sheets" (see Section 10.0). These contain such information as design status of the SEUS hardware, whether it is from current programs or new development, existing drawings and specifications, amount of development required for adaptation to the SEUS,

manufacturing information, and tests required. Planning data sheets were prepared to the black box level for each subsystem.

The TRW pricing organization used these data and the technical description of each subsystem as references when extracting data from the data bank. Data was adjusted to the SEUS by applying factors for complexity, quantity, and specific cost-sensitive characteristics.

For project level cost elements such as project management and system engineering, and product integrity, the SEUS project was compared to similar NASA Projects. Care was taken to ensure similarity of definition and content to analogous data.

All the data were reviewed by the pricing organization for compliance with current ratios for TRW projects. A composite result was then prepared for further review with "performer" management and cost adjustments made. A final senior management review assured that the estimates were realistic.

Payload/Experiments costs include the design, development and procurement of three flight payload systems in support of the baseline Asteroid Rendezvous mission. This also includes the launch support activities of the payload contractor(s). As this payload experiment package lacks as much definition as the SEUS itself, a gross cost estimate was made based on payload weight available.

Costs for Missions Operations are for program peculiar software and the training of operators in its use. No costs have been estimated for amortized use of existing facilities or operators.

Launch operations costs represent estimates for launch vehicles and launch services. Costs for launch vehicle hardware and its launch and support costs were obtained from Battelle Memo BMI-NLVP-IL-71-61 dated April 29, 1971. Cost estimates for the payload fairing are for the Viking fairing. (The Centaur D-1A fairing assumed in the design study would actually reduce this cost per vehicle flown by $300,000.00.)

11.2 COST SAVINGS BY ELECTRIC UPPER STAGE CONCEPT

Section 11.1 presented total program costs for the baseline Asteroid Rendezvous mission. This section will discuss some major

cost savings by utilization of the Solar Electric Upper Stage as a multi-mission vehicle.

Table 11-1, SEUS Costs for Primary, Secondary, and Growth Missions, shows a representative cost estimate for these further missions. These costs are grossly extended (i. e., at subsystem level, rounding to nearest 100, 000 dollars) on a learning curve projection (90%) of the baseline mission recurring costs. Adjustments of the estimates for each mission class include a 10% increment for production start up, "up-date" and any subsystem change required for the particular mission. Further cost reduction from that shown here would be possible by multiple procurements, or phased procurements which allow retention of orderly work flow. Figure 11-2 shows the resulting incremental and cumulative costs in a bar graph.

Figure 11-3, Cost Comparison of Multi-Mission Stage Approach and Individual Procurement, shows graphically the costs for three different procurement plans. Normalized cost is displayed in terms of cost of the first unit. More conservative ground rules were employed than in Figure 11-2. The learning curve was flattened after the 4th unit to a 95% learning curve and a more conservative qualification plan was introduced. Plan A is the long range use of the SEUS. Plan B reflects requalification at the beginning of each of the three phases. Plan C shows development and qualification of a new vehicle for each mission type. The total cost for Plan A shows a nearly 4:1 cost advantage compared to Plan C.

Another way to present the cost economy achievable by the multi-mission approach is to consider the recurrent cost per flight vehicle after the initial development cost for the first three units has been absorbed. This is shown in Figure 11-4 in terms of average cost per stage, by mission type. The cost of each of the three baseline vehicles is shown as $32.1 million. Vehicles for the subsequent flights average between $12 and $15 million each.

When viewed from the standpoint of overall cost effectiveness the stage cost, adding a net $12 to $15 million to the booster and launch support cost of $25 million per Titan 3D/Centaur booster, is reasonably low.

Table 11-1. Stage Cost Breakdown for Primary, Secondary and Growth Missions ($K)

Missions	Primary: Baseline Asteroid Rendez-vous	Comet Rendez-vous	Out-of-Ecliptic	Mercury Orbiter	Solar Probe	Secondary: Outer Planet Flyby (Tops)	Outer Planet Orbiter (Tops)	Mars/ Venus Orbiter	Solar Monitor Relay Station	Growth: Haley's Comet Probe	Asteroid Sample Return	Mars Sample Return	Cumulative Totals: Primary	Primary & Secondary	Primary, Secondary & Growth
Flights per Mission	3	3	2	1	2	4	4	2	2	2	3	2	11	23	30
STRUCTURE	4,900.	3,000.	1,900.	900.	1,800.	3,500.	3,300.	1,700.	1,600.	1,600.	2,400.	1,600.	12,500.	22,600.	28,200.
THERMAL	2,600.	1,500.	900.	500.	900.	1,700	1,700.	800.	800.	800.	1,200.	800.	6,400.	11,400.	14,200.
ELECTRIC POWER	21,500.	15,900.	10,000.	5,000.	9,600.	18,300.	17,600.	6,200.*	6,200.*	10,300.**	6,000.*	10,300.**	62,600.	110,300.	136,900.
ELECT. INTEGRATION	3,000.	600.	400.	200.	400.	700.	700.	300.	300.	300.	900.	300.	4,600.	6,600.	8,100.
PRODUCT INTEGRITY	7,800.	3,600.	2,300.	1,100.	2,200.	4,100.	4,000.	2,000.	2,000.	2,000.	2,900.	1,900.	17,000.	29,100.	35,900.
ELECTR. PROPULSION	9,600.	2,400.	1,500.	700.	1,500.	2,700.	2,600.	1,300.	1,300.	1,300.	1,900.	1,200.	15,700.	23,600	28,000
HYDRAZ. PROPULSION	1,800.	600.	400.	200.	400.	700.	700.	300.	300.	300.	900.	300.	3,400.	5,400.	6,900.
ATTITUDE CONTROL	13,700.	6,300.	4,000.	2,000.	3,800.	7,200.	7,000.	3,400.	3,400.	3,300.	5,000.	3,300.	29,800.	50,800	62,400.
COMMUNICATIONS	6,500.	2,100.	1,300.	700.	1,300.	2,400.	2,300.	1,100.	1,100.	1,100.	1,700.	1,100.	11,900.	18,800.	22,700.
DATA HANDLING	2,400.	900.	600.	300.	600.	1,000.	1,000.	500.	500.	500.	700.	500.	4,800.	7,800.	9,500.
ASSY,INTEG.& TEST	7,800.	3,000.	1,900.	900.	1,800.	3,500.	3,300.	1,700.	1,600.	1,600.	2,400.	1,600.	15,400.	25,500.	31,100.
LAUNCH SUPPORT	1,000.	900.	600.	300.	600.	1,000.	1,000.	500.	500.	500.	700.	500.	3,400.	6,400.	8,100.
STAGE SUPP.EQUIPMT.	5,000.	300.	200.	100.	200.	400.	400.	200.	200.	200.	300.	200.	5,800.	7,000.	7,700.
PRGM.MGMT/SYS.ENGR.	8,800.	4,500	2,800	1,400.	2,700.	5,200.	5,000.	2,500.	2,400.	2,400.	3,600.	2,400.	20,200	35,300.	43,700.
TOTALS ($000.)	96,400.	45,600.	28,800.	14,300.	27,800.	52,400.	50,600.	22,500.	22,200.	26,200.	30,600.	26,000.	212,900.	360,600.	443,400.
								* 12 KW Array	* 12 KW Array	** 21 KW Array	* 12 KW Array	** 21 KW Array			

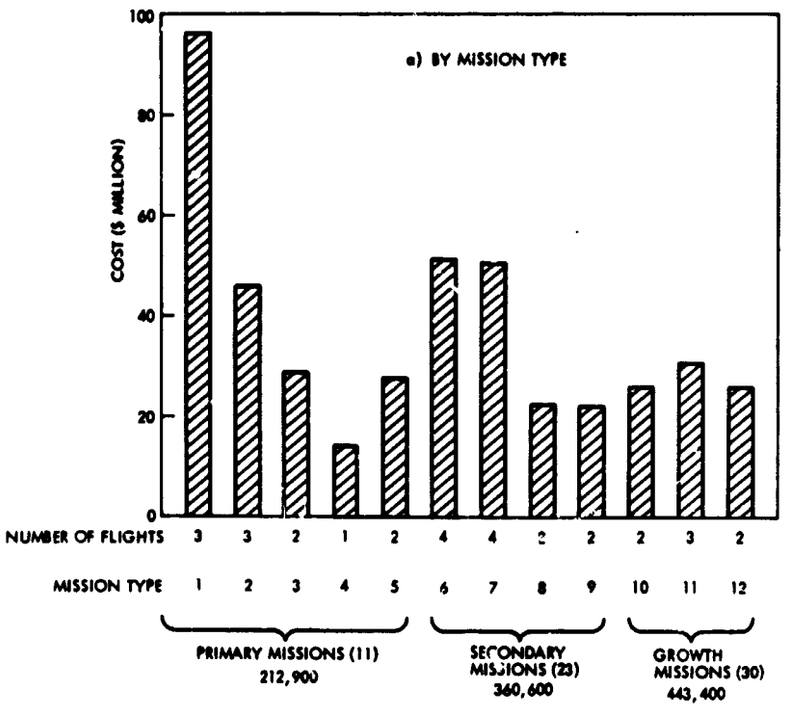

Figure 11-2a. Costs of Stage Procurement for Primary, Secondary and Growth Missions (By Mission Type)

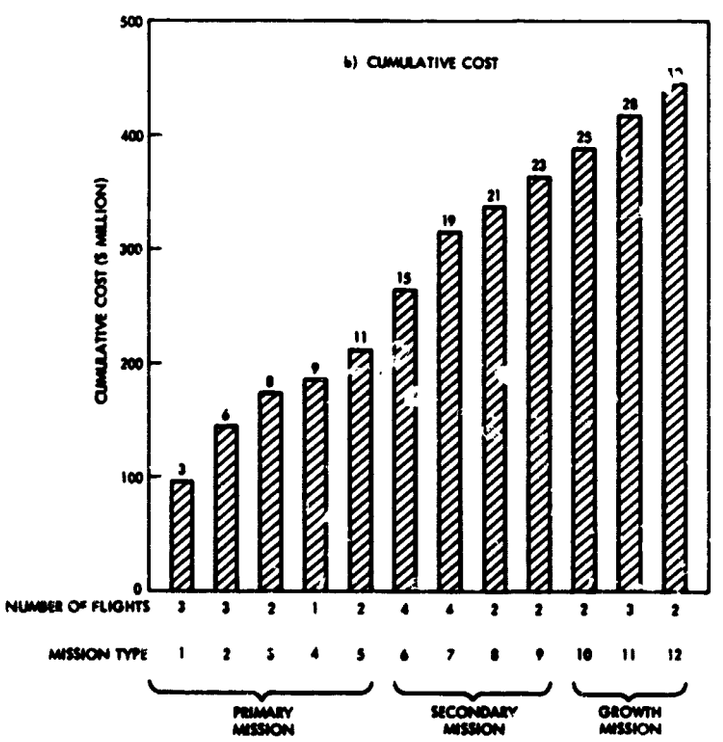

Figure 11-2b. Costs of Stage Procurement for Primary, Secondary and Growth Missions (Cumulative Cost)

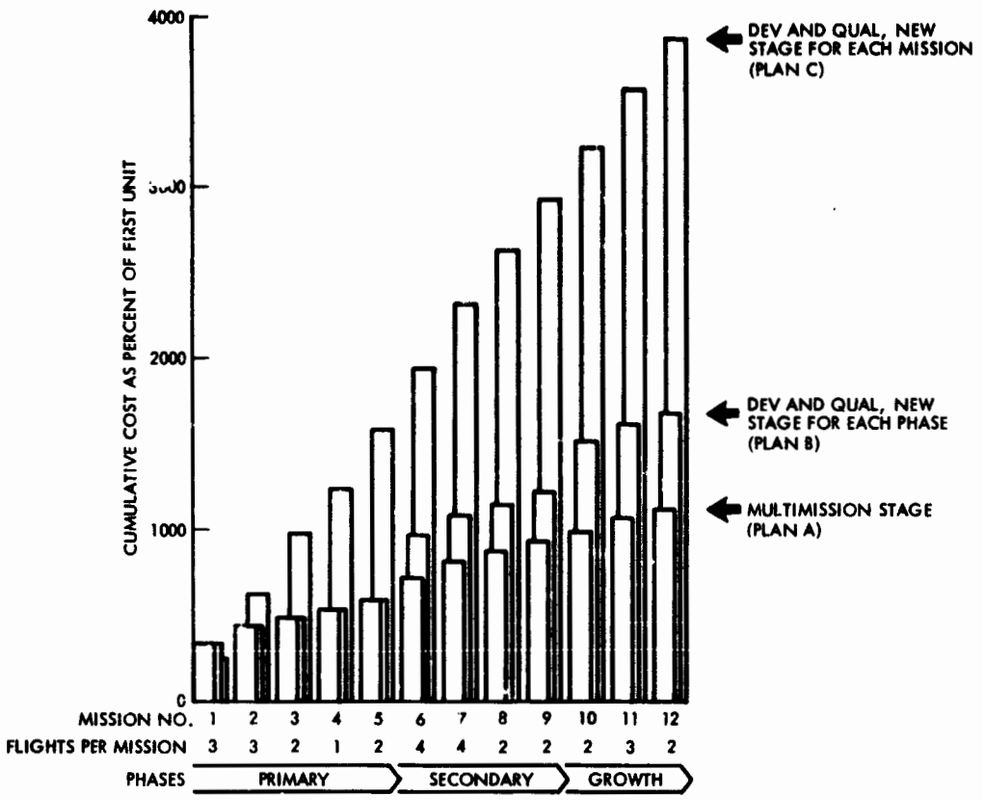

Figure 11-3. Cost Comparison of Multi-Mission Stage Approach and Individual Procurement

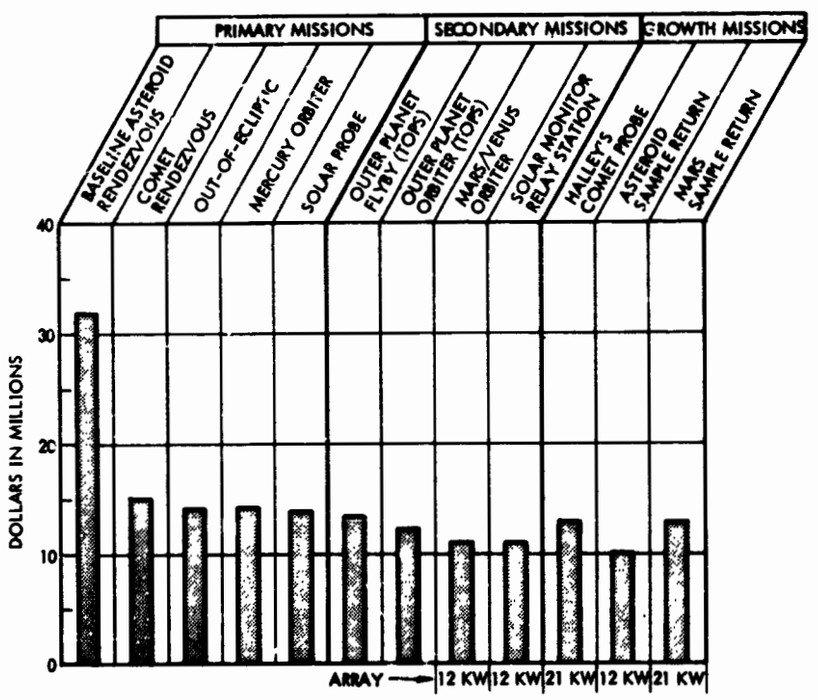

Figure 11-4. Average Cost of Electric Stage by Mission Type

One alternative to using electric propulsion in these missions would be to go beyond the Titan class of boosters into various Saturn class booster combinations at a cost increase that would be a multiple of the incremental stage cost. A second alternative would be the use of a space-storable high-energy chemical upper stage not as yet developed that would be capable of delivering the required large velocity impulse at destination in missions involving rendezvous with low gravity target bodies (i.e., asteroids or comets).

Specific cost saving approaches that we have identified during the study have been included in part in our stage design concept and help to keep the total program cost and the stage development and recurring cost elements within reasonable limits

These cost savings fall into the following three categories:

1) System Design

- Standardized propulsion module for all missions
- Reduced thrust time per thruster through extra spares (saves test program costs)
- Simplified thrust vector control hardware
- Increased solar cell cover glass thickness (6 mil)
- Allocation of spare power and telemetry capacity to payload usage

2) Mission Design and Support

- Infrequent telemetry periods
- Principal use of 85-foot DSIF antennas
- Reduced tracking time

3) Launch Cost

- Lower-cost booster (Titan 3D/Burner 2) applicable
- Tandem launch concept on Titan 3D/Centaur
- 10-foot Intelsat shroud instead of 14-foot Viking shroud

Although the individual cost savings achieved by each of these steps cannot be readily assessed, we estimate that in the aggregate a reduction of about 10 to and 20 percent of the program cost can be achieved by implementing these concepts. Of these concepts the use of the dual launch mode would provide by far the largest savings. However the acceptability of dual launch from the procurement and mission planning standpoint has not been established and additional tradeoff study is recommended.

12. SUMMARY OF TECHNICAL INNOVATIONS

The following list summarizes technical innovations in electric vehicle design, assembly, test and flight operations that were conceived under this study contract. This list is submitted in compliance with the New Technology Reporting Clause (May 1966) called out in the contract. A more complete discussion will be submitted by TRW Systems in a separate document.

The possibility of a transfer to the commercial sector of these innovations which are related specifically to solar-electric propulsion systems and interplanetary missions appears to be remote.

1) Protection of propellant expulsion bladder in an off-loaded standard size storage tank by filling the empty volume with a moldable solid, such as styrofoam. (Section 7. 2.)

2) Separation of thruster power processor modules into a Beam and Accelerator PPU Module and a Multiple-Output PPU Module, to achieve a significant weight saving and high reliability. (Section 7. 2.)

3) Use of a common thrust vector control system to provide TVC capability for ion engines and hydrazine thrusters mounted in the same assembly thus simplifying the design. (Section 6. 2.)

4) Use of a common shaft rotation drive assembly model in several different functions, e. g., biaxial antenna drive, star sensor rotation and solar array rotation, to save development cost. (Section 7. 3.)

5) Design of a removable payload mounting module for ease of assembly and test of scientific payload instruments. (Section 6. 2.)

6) Novel horizontal solar array deployment test facility suitable for long rollout array panels. (Section 10.)

7) Use of dual launch mode in missions that have compatible launch requirements to achieve large booster cost savings. (Section 5. 9.)

8) Use of the novel earth swingby mode to achieve compatibility of launch requirements in support of the dual launch mode for large cost savings. (Section 5. 9.)

9) Increase of electric stage payload capacity in some missions through off-loading of booster propellant or other means of reducing booster injection performance. (Section 5.10.)

10) Determination of unknown target range in rendezvous mission by a deliberate maneuver of the electric stage either through temporary interruption of the terminal thrust phase or by a lateral maneuver, i.e., adaptation of a technique known as maneuver-ranging in air-to-air combat. (Section 5.13.)

11) Use of a mother/daughter probe concept to enhance the scientific value of some missions by exploiting the large payload-carrying capacity of the electric stage. (Section 4.)

12) Use of repeated thrust phases to explore cometary tail regions in a criss-cross pattern exploiting the curvi-linear character of coast trajectories relative to the comet. (Section 5.11.)

13) Modification of thrust profile by including a sequence of brief coast phases to improve ground based tracking accuracy. (Section 5.13.)

14) Analytical approximation technique for simple determination of payload penalty when using an off-optimal thrust orientation. (Section 5.8 and Appendix C.)

REFERENCES

1-1 "Study of a Solar Electric Multi-Mission Spacecraft," JPL Contract No. 952394, Report 09451-6001-R0-03, TRW Systems, Redondo Beach, California, Volumes I and II, dtd 15 March 1970.

1-2 "Solar Electric Propulsion Asteroid Belt Mission Study," JPL Contract No. 952566, Report SD 70-21-1, North American Rockwell, Downey, California, Volumes I and II, January 1970.

1-3 "1975 Jupiter Flyby Mission Using a Solar Electric Spacecraft," ASD 760-18, JPL, Pasadena, California, March 1, 1968.

1-4 "Solar Powered Electric Spacecraft Study," Final Report, JPL Contract No. 951144, SSD 40094R, Hughes Aircraft Company, Space Systems Division, El Segundo, California, December 1965.

1-5 Wood, L. H., Dailey, C. C., Katz, L., and Vachon, R. I., "Planetary Photographic Exploration with Solar-Electric Propulsion," AIAA Electric Propulsion and Plasmadynamics Conference, Colorado Springs, Col., Report #67-712, Sept. 11-13, 1967.

1-6 Horsewood, J. L., Mann, F. I., and Flanagan, P. F., "Solar Electric Performance Data for Extra-Ecliptic and Solar Probes and Ceres, D'Arrest, and Encke Rendezvous Missions," Analytical Mechanics Associates, Inc., Report No. 70-47 under NASA Contract NAS5-20126, dtd. December 1970.

3-1 E. A. Willis, Jr., et al in "Prospects for a Multi-purpose Solar-Electric Propulsion Stage," NASA Technical Memorandum TMS-67801, Lewis Research Center, March 1971.

4-1 Alfven, H., and Arrhenius, G., "Mission to an Asteroid," Science, 167, 139, 1970.

4-2 Greenstadt, E. W., "Magnetic Interaction of Asteroid with the Solar Wind," TRW Report 99994-6065-R0-01, 21 September 1970, to be published in Icarus, 14, 1971.

4-3 Donn, B., and Alexander, W. M., "Discussion of Comet Probes," NASA GSFC Report X-613-62-52, July 1961.

4-4 Swings, P., "Possible Contributions of Space Experiments in the Field of Cometary Physics," Smithsonian Astrophysical Observatory Report, September 1962.

4-5 "Comet Intercept Study," Final Report, NASw-414, STL, Inc., (TRW Systems) March 1963.

REFERENCES (Continued)

4-6 Biermann, L., Browski, B., and Schmidt, H. U., "The Interaction of the Solar Wind with a Comet," Solar Physics, 1, 254, 1967.

4-7 Weidner, Don K., Editor, "Space Environment Criteria Guidelines for Use in Space Vehicle Development (1969 Revision)," NASA Tech. Memorandum TMX-53957, Marshall Space Flight Center, August 1970.

5-1 Long, James, E., "To the Outer Planets," JPL, Astronautics and Aeronautics, June 1969

5-2 Dixon, W. J., Wheeler, E. G., and Holtzclaw, R. W., "The Pioneer Spacecraft Flyby of Jupiter," Digest, IEEE 71 International Convention, March 22-25, 1971, New York, N. Y., p. 196.

5-3 Long, J. E., "Exploration of the Outer Planets," AIAA Paper No. 70-1246, presented at AIAA 7th Annual Meeting and Technical Display, Houston, Texas, October 19-22, 1970.

5-4 Horsewood, J. L., and Mann, F. I., "Solar Electric Interplanetary Trajectory and Performance Data for Sub-Optimal Powered Spacecraft," Analytical Mechanics Associates, Inc., under Contract NAS 5-11193 dtd. April 1970.

5-5 Bartz, D. R., and Horsewood, J. L., "Characteristics, Capabilities, and Costs of Solar Electric Spacecraft for Planetary Missions," AIAA Report No. 69-1103 presented at AIAA 6th Annual Meeting and Technical Display, Anaheim, California, October 20-24, 1969.

5-6 Horsewood, J. L., Mann, F. I., and Flanagan, P. F., "Solar Electric Performance Data for Extra-Ecliptic and Solar Probes and Ceres, D'Arrest, and Encke Rendezvous Missions," Analytical Mechanics Associates, Inc., Report No. 70-47 under Contract NAS5-20126 dated December 1970.

5-7 "Advanced Planetary Probe Study," Final Technical Report, JPL Contract 951311, Report No. 4547-6004-R0000, TRW Systems, Redondo Beach, California, Volume 1 to 3, 27 July 1966.

5-8 E. Stuhlinger, D. P. Hale, C. C. Dailey, and L. Katz, "The Versatility of Electrically Propelled Spacecraft for Planetary Missions," AIAA Paper No. 69-253, presented at AIAA 7th Electric Propulsion Conference, Williamsburg, Virginia, 3-5 March 1969.

5-9 "The First Panoramic Views of the Lunar Surface," NASA Report No. TT F-393, Presidium of the USSR Academy of Sciences, Moscow, 1966.

REFERENCES (Continued)

5-10 "Solar Electric Propulsion Capabilities for Mars Surface Sample Return Missions," Astro Sciences/IITRI, December 16, 1970.

5-11 "Comet Missions Study," IITRI, performed under JPL contract. Report in preparation (June 1971).

5-12 Mascy, A. C., and Niehoff, J., "Sample Return Missions to the Asteroid Eros," presented at IAU-Conference "Physical Studies of Minor Planets", Tucson, Ariz., Mar. 8, 1971.

5-13 Meissinger, H. F., and Greenstadt, E. W., "Design and Science Instrumentation of an Unmanned Vehicle for Sample Return from the Asteroid Eros," presented at IAU-Conference, "Physical Studies of Minor Planets", Tucson, Ariz, 8-10 Mar. 1971.

5-14 Michielsen, H. F., "A Rendezvous with Halley's Comet in 1985-1986," AIAA Paper No. 67-614, presented at AIAA Guidance, Control and Flight Dynamics Conference, Huntsville, Alabama/ August 14-16, 1967.

5-15 Roberts, David L., and Friedlander, Alan L., "Missions to the Comets," Joint National Meeting American Astronautical Society (15th Annual), Operations Research Society (35th National) June 17-20, 1969. Paper No. XA. 2.

5-16 Friedlander, A. L., Niehoff, J. C., and Waters, J. I., "Trajectory Requirements for Comet Rendezvous," AIAA Paper No. 70-1072, presented at AAS/AIAA Astrodynamics Conference, Santa Barbara, California, August 19-21, 1970.

5-17 "Comet Rendezvous Mission Study," Illinois Institute of Technology Research Institute, performed under JPL Contract, Final Report (in preparation), Chicago, Illinois, July 1971.

5-18 Jordan, J. F., "Orbit Determination for Powered Flight Space Vehicles on Deep Space Missions," Journal of Spacecraft and Rockets, Vol. 6, No. 5, May 1969.

5-19 Duxbury, T. C., "A Spacecraft-Based Navigation Instrument for Outer Planet Missions," AIAA Paper No. 69-902, presented at AIAA/AAS Astrodynamics Conference, Princeton, New Jersey, August 20-22, 1969.

6-1 "TOPS Outer-Planet Spacecraft," Astronautics and Aeronautics, September 1970.

REFERENCES (Continued)

7-1 Yasui, Robert K., Jet Propulsion Laboratory private communication.

7-2 Ross, R. G., Yasui, R. K., Jaworski, W., Wen, L., and Eleland, E. L., "Measured Performance of Silicon Solar Cell Assemblies Designed for Use at High Solar Intensities", JPL TM 33-473, March 1971.

7-3 Knobig, D., "Sonnenonde Optimierungsvorsclage and Systemanalysen", ERNO Brem 1968.

7-4 Barber, T. A., "1975 Jupiter Flyby Mission Using a Solar Electric Spacecraft", JPL Report ASD 760-18, March 1968.

7-5 Yasui, R. K., and Schmidt, L. W., "Performance Characteristics of Ti-Ag Contact N/P and P/N Silicon Solar Cells", Proceedings of 8th Energy Conversion Specialists Conference 1970.

7-6 Luft, W., "Silicon Solar Cells at Low Temperature", TRW Report 1968.

7-7 Luft, W., "Operations of Solar Cells at High Solar Intensities", TRW Report 1968.

7-8 Biess, J., "Multikilowatt Ion Thruster Power Processor", Final Report contract NAS 12-2183, June 1971.

7-9 J. M. Sellen, Jr., and Robert F. Kemp, "Operation of Solar Cell Arrays in Dilute Streaming Plasmas," Section III A, Final Report "Ion Beam Diagnostics," NASA CR-54692, TRW 4381-6017-R0000, February 10, 1966

7-10 W. R. Kerslake, D. C. Byers, et al, "Flight and Ground Performance on the SERT II Thrusters," AIAA Paper 70-1125.

7-11 R. T. Bechtel, B. A. Banks, T. W. Reynolds, "Effect of Facility Back Sputtered Material on Performance o Glass Coasted Accelerator Grids for Kaufman Thrusters,", AIAA Paper 71-156, January 1971.

7-12 "Feasibility Study for a Multi-Mission Electric Propulsion Spacecraft (Picneer Concept)," Final Report 18305-6001-R000, June 18, 1971.

7-13 J. H. Decanini, "Application of Sterographic Projections to the Solution of Field-of-View Gimballing and Trajectory Problems," TRW Memorandum 7236.7-8, 3 December 1969.

REFERENCES (Continued)

7-14 "Study of a Solar Electric Multi-Mission Spacecraft," Volume 1 B, page 299, TRW Report 09451-6001-R0-03.

7-15 DSN Standard Practice, Deep Space Network/Flight Project Interface Design Handbook, 810-5, Revision A, 1 October 1970.